CANADIAN THESES

THÈSES CANADIENNES

NOTICE

The quality of this microfiche is heavily dependent upon the quality of the original thesis submitted for microfilming. Every effort has been made to ensure the highest quality of reproduction possible.

If pages are missing, contact the university which granted the degree.

Some pages may have indistinct print especially if the original pages were typed with a poor typewriter ribbon or if the university sent us an inferior photocopy.

Previously copyrighted materials (journal articles, published tests, etc.) are not filmed.

Reproduction in full or in part of this film is governed by the Canadian Copyright Act, R.S.C. 1970, c. C-30.

AVIS

La qualité de cette microfiche dépend grandement de la qualité de la thèse soumise au microfilmage. Nous avons tout fait pour assurer une qualité supérieure de reproduction.

S'il manque des pages, veuillez communiquer avec l'université qui a conféré le grade.

La qualité d'impression de certaines pages peut laisser à désirer, surtout si les pages originales ont été dactylographiées à l'aide d'un ruban usé ou si l'université nous a fait parvenir une photocopie de qualité inférieure.

Les documents qui font déjà l'objet d'un droit d'auteur (articles de revue, examens publiés, etc.) ne sont pas microfilmés.

La reproduction, même partielle, de ce microfilm est soumise à la Loi canadienne sur le droit d'auteur, SRC 1970, c. C-30.

THIS DISSERTATION
HAS BEEN MICROFILMED
EXACTLY AS RECEIVED

LA THÈSE A ÉTÉ
MICROFILMÉE TELLE QUE
NOUS L'AVONS REÇUE

Canada

NL-339 (r. 86/06)

ISBN 0-315-33360-X

UNIVERSITÉ D'OTTAWA
UNIVERSITY OF OTTAWA

To Garnet

my extraordinarily patient and devoted fiancée

and my Parents

with gratitude for many years of encouragement and support

ABSTRACT

The implications of the Gouy-Chapman-Stern primitive model for the double layer at electrodes are considered with respect to the calculation of differential capacitance behaviour and the description of adsorption processes by isotherms taking account of dipolar discreteness effects without relying on dielectric continuum approximations.

On the basis of this structural model of the double layer, molecular polarization contributions to the interfacial potential profile and differential capacitance are evaluated according to three simple representations of the orientation of solvent dipoles at the electrode: the Watts-Tobin/BDM two-state model, the Fawcett three-state model and a Debye-Langevin-type continuum-of-orientations model.

The so-called Cooper-Harrison catastrophe, in which the induced polarization q_{dip} of the inner layer is calculated to exceed the surface charge density q_M of the electrode, is shown to arise for all models considered, and is therefore not, as previously supposed, a specific artifact of the two-state model with respect to which it was first noted. This polarization catastrophe is shown to arise from an oversimplified but frequently employed representation of the polarizing field as $E_1 = 4\pi q_M$. When the field assumed to act on the molecules in the polarization expressions is represented as $E_1 = \Delta\phi_1/d$ (where $\Delta\phi_1$ is the potential difference across the inner layer and d is its thickness), or as $E_1 = 4\pi(q_M - q_{dip})$, i.e. taking into account the reactive polarization of the inner layer, there result

implicit equations for q_{dip} and $\Delta\phi_1$ which provide self-consistent values of these quantities as a function of q_M or of electrode-solution potential difference V. Anomalous behaviour is then shown not to arise. These equations are shown to be formally consistent with conditions of continuity of potential and dielectric displacement, across the interfaces assumed to be present in the given model of the double layer.

These results are extended to consideration of the adsorption of neutral molecules, involving the displacement of polarized solvent molecules, by representing q_{dip} as the sum of polarization contributions due to solvent and adsorbate, appropriately weighted using the coverage fraction θ. This coverage fraction is defined by an isotherm containing electrostatic partition functions for the adsorbed species, which are defined in terms of the field $4\pi(q_M - q_{dip})$. The resulting expression for the differential capacitance of the interface in this situation simultaneously takes account of saturation polarization and change in inner-layer composition (i.e. "dielectric constant"), effects which were previously considered to be the basis for two fundamentally distinct treatments.

Using the conventional lattice model for the adsorbed monolayer, the calculation of nearest-neighbour free energies of interaction between adsorbed charges and dipoles is considered. Particular attention is given to the calculation of free energies of interaction among solvent dipoles and between adsorbed solvent dipoles and charges; both these effects are neglected in existing theories, which restrict attention to repulsion between adsorbed

charges, and assume that the co-adsorbed solvent molecules may be treated as a dielectric continuum. The resulting expressions for the pairwise interaction free energies occurring in a binary lattice of adsorbed charges and dipoles are combined, according to approximations of lattice-gas theory, to produce isotherms for a one-electron faradaic reaction resulting in the formation of a monolayer of partially discharged anions.

The potential distribution due to an adsorbed dipole of arbitrary orientation is determined, for several imaging situations, by the method of Fourier-Bessel integrals. By expansion of this expression and its derivatives, followed by summation over all lattice coordinates, expressions are derived for the dipolar discreteness field and potential, which were not considered in previous treatments of ionic adsorption. These are required in order to apply the so-called Mean Field Approximation, according to which interactions are assumed to be equivalent to an effective potential and field, with components proportional to θ (due to ions) and the reduced normal polarization $\langle s \rangle$ (due to dipoles). The effective potential and field are used to define thermodynamic functions for the adsorbed species. From consideration of the relationships which must be satisfied by q_M, q_{dip} and the adsorbed charge density q_{ion}, an expression is derived for the differential capacitance in the presence of ionic adsorption. Problems connected with the application of more accurate approximations of lattice-gas theory, and with the applicability of primitive model approaches to such phenomena, are briefly discussed.

PUBLICATIONS

1. B.E. Conway and S.L. Marshall
   "Relationship between treatments of solvent dipole orientation in the double layer and conditions giving rise to "catastrophe" behaviour in the capacitance"
   J. Electroanal. Chem. **178**: 185 (1984)

2. S.L. Marshall and B.E. Conway
   "Treatment of dipole orientation in the double layer at electrodes: Analysis of conditions giving rise to polarization catastrophes"
   J. Chem. Phys. **81**: 923 (1984)

3. B.E. Conway, K. Tellefsen and S. Marshall
   "Lattice models, interactions and solvent effects in electrochemical monolayer formation: Entropy and substitutional adsorption effects"
   Proceedings of the Symposium on the Chemistry and Physics of Electrocatalysis, The Electrochemical Society (1984), p. 15

4. Brian E. Conway and Simon Marshall
   "Some common problems concerning solvent polarization and dielectric behaviour at ions and electrodes"
   Aust. J. Chem. **36**: 2145 (1983)

5. B.E. Conway and S. Marshall
   "Consequences of partial charge transfer in lattice interactions among underpotential-deposited adatoms"
   Electrochim. Acta **28**: 1003 (1983)

ACKNOWLEDGEMENTS

I wish to express my sincere thanks to my thesis director, Professor B.E. Conway, first of all for providing me with an opportunity to do research on this interesting topic, but particularly for the many illuminating discussions which have occurred during his supervision of the work.

It is a pleasure to acknowledge also the valuable advice and encouragement I have received from Dr H. Angerstein-Kozlowska. Discussions with Dr Kozlowska were helpful in the early stages of the work, in defining some of the important questions to be considered, and in the later stages, in comparing predicted behaviour with experiment.

I am grateful to Dr D.F. Tessier for valuable assistance, not only in becoming "computer-literate", but in understanding the temperament of the PDP-11/34 computer on which most of the calculations were performed.

The social ambiance of the Electrochemistry research group has proved both congenial and stimulating, providing unlimited opportunities for discussions (or arguments) about virtually anything. However, I would especially like to thank those of my colleagues with whom I shared the office of Lab. 151 for providing such excellent company.

"For now we see through a glass, darkly;

Then, face to face:

Now I know in part, but then shall I know

Even as also I am known."

- I Corinthians 13: 12

TABLE OF CONTENTS

LIST OF IMPORTANT SYMBOLS

The following list includes the notation used in deriving the results of this thesis, and notation in frequently-quoted results due to other authors. Page numbers refer to the definitions of terms not in common use.

Symbol	Definition	Dimensions	Page
A	charge density in Gouy-Chapman theory $A = (\varepsilon kTn_0/2\pi)^{1/2}$	statC cm^{-2}	22
a_i	activity of species i	1	-
a_1, a_2	dipole self-image energies	erg	106
b	$r_0/2s$	1	89
b	Tafel slope	V^{-1}	130
b_1	ionic contribution to E_{eff}	statC cm^{-2}	190
b_2	dipolar contribution to E_{eff}	statC cm^{-2}	193
b_3	ionic contribution to V_{eff}	statC cm^{-1}	188
b_4	dipolar contribution to V_{eff}	statC cm^{-1}	192
C	double layer capacitance	F cm^{-2}	12
	pseudocapacitance (chapter 5 only)	F cm^{-2}	125
C_1	inner-layer capacitance	F cm^{-2}	21
C_2	diffuse-layer capacitance	F cm^{-2}	43
c_i	concentration of species i	mol/l	-
d	inner-layer thickness	cm	9
e_0	electronic charge	statC	3
E	inner-layer field	statC cm^{-2}	16
E_1	inner-layer field	statC cm^{-2}	24
E_2	field at outer Helmholtz plane	statC cm^{-2}	26
E	inner-layer field vector	statC cm^{-2}	89

E_{eff}	effective field, with components due to ions and dipoles	statC cm^{-2}	199
g	interaction parameter, Bragg-Williams isotherm	1	135
G	interaction parameter, Quasi-Chemical isotherm	1	138
k	reciprocal-space integration variable	1	91
kT	mean thermal energy	erg	-
K_{eq}	field-independent equilibrium constant $K_{eq} = \exp(-\Delta\mu^o/kT)$	1	65
K_+, K_-	equilibrium constants for electrode reaction according to two-state model	1	125
m	dipole moment	statC cm	16
$\langle m \rangle$	average dipole moment	statC cm	77
n_i	number density for ionic species i	cm^{-3}	3
n_i^o	bulk number density for ionic species i	cm^{-3}	3
N_w	inner-layer number density of H_2O(ads)	cm^{-3}	16
$n_{\pm}$	number densities of anions or cations at the outer Helmholtz plane	cm^{-3}	42
p	exp(mV/dkT)	1	125
$p_{\pm}$	anion/cation size factors	1	42
q_M	surface charge density	statC cm^{-2}	12
q_{dip}	inner-layer reactive polarization	statC cm^{-2}	13
q_{ion}	adsorbed ionic charge density	statC cm^{-2}	155
r_0	lattice parameter of the inner layer	cm	88
$\langle s \rangle$	reduced dipole moment $\langle s \rangle = \langle m \rangle / m$	1	84
s	radius of adsorbed ions	cm	88

U_+, U_+	residual orientational energies for the two-state model	erg	124
Uc	dipole-dipole interaction energy, according to BDM (ref. 11 of chapter 2)	erg	17
U_0	field-independent orientational energy difference	erg	63
V	electrode-solution potential difference	V or statV	9
V_r	reversible potential for surface electrode reaction	V or statV	129
V_{eff}	effective potential, with components due to ions and dipoles	statC cm^{-1}	199
x	number of H_2O(ads) displaced by adsorption of a neutral molecule	1	59
X	total field adjacent to an adsorbed charge	statC cm^{-2}	89
Y	dimensionless polarization $q_{dip}/N_w m$ according to BDM (ref.11 of chapter 2)	1	17
z	normal distance from the surface z = -s surface plane z = 0 inner Helmholtz plane $z = z_1$ outer Helmholtz plane	cm	3
z_a	electrostatic partition function for adsorbed charges $A_{(ads)}$	1	97
$z_b, z_{b,el}$	electrostatic partition function for adsorbed neutral molecules B(ads)	1	64
z_i	algebraic charge number for ions	1	3
$z_w, z_{w,el}$	electrostatic partition functions		

	for H_2O(ads)	1	63
z_{12}	partition function for isolated pair of H_2O(ads)	1	87
α, α_w	polarizability of H_2O(ads)	cm^3	60
α_b	polarizability of neutral molecules B(ads)	cm^3	60
β	depolarization factor $(\varepsilon-1)/(\varepsilon+1)$	1	91
β	symmetry factor	1	129
γ	electrosorption valency factor of charged adatoms A(ads)	1	78
γ	inner layer vacant space fraction	1	65
$\Delta\phi_1$	inner-layer potential difference	V or statV	9
$\Delta\phi_2$	diffuse-layer potential difference	V or statV	9
δ	$[1 + 4G\theta(1-\theta)]^{1/2}$	1	138
$\varepsilon, \varepsilon_2$	dielectric constant of diffuse layer	1	3
ε_{opt}	optical dielectric constant	1	16
ε_1	inner-layer dielectric constant	1	25
ε_{low}	saturation dielectric constant in BDM theory (ref. 11 chapter 2)	1	36
ζ_{12}	interaction partition function for an isolated pair of H_2O(ads)	1	87
ζ_{ww}	pairwise interaction partition function between H_2O(ads)	1	85
ζ_{aa}	pairwise interaction partition function between A(ads)	1	95
ζ_{aw}	pairwise interaction partition between A(ads) and H_2O(ads)	1	94

η	overpotential $V-V_r$	V or statV	-
Θ	coverage for adsorption reaction	1	60
θ	orientation angle with respect to the normal	radian	94
λ	Debye reciprocal length	cm^{-1}	3
μ_i	chemical potential of species i	erg	-
μ_i^o	standard chemical potential of species i	erg	-
ρ	radial distance, cylindrical polar coordinates	cm	
τ	ionic self-image potential	statV	91
ϕ	polar angle, cylindrical coordinates	radian	94
$\phi\dagger, \phi+$	fractions of H_2O(ads), two-state model	1	125
Φ	total image potential induced by adsorbed charges	statV	93
$\Phi^\dagger$	secondary image potential induced by adsorbed charges	statV	93
χ	diamagnetic susceptibility	cm^3	98
ψ	fraction of inner-layer sites occupied by hydration spheres of non-specifically adsorbed ions	1	43
Ψ	total image potential induced by adsorbed dipoles	statV	105
$\Psi^\dagger$	secondary image potential induced by adsorbed dipoles	statV	106
Ω	solid angle corresponding to dipole orientation coordinates	steradian	85

CHAPTER 1

GENERAL INTRODUCTION

1. Origins of the Present Work

In recent years, work originating from this laboratory [1] has involved the study of electrode reactions leading to the formation of chemisorbed monolayers of partially discharged halide or oxide species at noble metal electrodes. The two phenomena of most interest in the behaviour of such chemisorption processes are:

(a) Progress of the reactions *via* clearly defined intermediate stages, corresponding to definite values of sub-monolayer coverage;

(b) The occurrence of irreversible transformations in such monolayers, as manifested by hysteresis in their formation and reduction.

(c) Changes of solvation and interaction amongst the particles depending on their state of charge or adsorption.

Previous theories of electrochemical surface processes have been unsuccessful in providing satisfactory explanations for the first two of these phenomena, and the third as far as ion adsorption and solvent orientation are concerned. It was the original intention of the present work to construct a mechanistic theory of the behaviour of systems such as these. Inspection of the relevant literature, however, revealed important gaps in existing treatments of electrode reactions involving chemisorbed intermediates, notably, the neglect of energetic contributions arising from molecular polarization and interactions involving

solvent molecules, in the free energy balances proposed to apply to the reactions.

The emphasis of the investigation was therefore shifted from specific consideration of the surface reactivity of noble metal electrodes, and directed to more general questions concerning the analysis of molecular polarization and interaction effects at electrodes.

2. Double-Layer Models

By way of defining the terms of reference of the calculations and discussion in the following chapters, it is appropriate to consider at this point the various structural models which have formed the basis of existing theoretical treatments of charged interfaces.

These approaches may be broadly classified as "primitive" or "non-primitive", depending on the way in which polarization of solvent molecules is assumed to contribute to the interfacial potential profile, and on how the ion distribution is represented. Primitive models assume that the properties of the interface are determined by the manner in which the ions are distributed adjacent to the electrode, in a continuous medium having the bulk dielectric constant of the solvent. In non-primitive models, this dielectric continuum assumption is abandoned, and distribution functions are calculated for the solvent molecules as well as for the ions, as a function of distance from the electrode surface.

2.1 Primitive Models

(i) Gouy-Chapman Theory

The earliest important contributions to the theory of the double layer were those of Gouy [2] and Chapman [3], in which the potential ϕ in the interfacial region was assumed to be given by the Poisson-Boltzmann equation. For one-dimensional geometry this assumes the form

$$\partial^2\phi/\partial z^2 = -(4\pi/\varepsilon)\sum_i e_0 z_i n_i^\circ \exp[-z_i e_0\phi/kT] \qquad [1]$$

in which z_i is the (algebraic) charge number of ion i, with bulk number density n_i°, and ε is the dielectric constant of the solvent. An important modification of the theory due to Stern [4] recognized the existence of a plane of closest ionic approach, $z = z_1$, which is at potential $\Delta\phi_2$ with respect to the bulk of the solution.

The solution of the Poisson-Boltzmann equation for a 1:1-electrolyte (containing n_0 ions per cm^3) in this situation is [5]

$$\phi = (4kT/e_0)\tanh^{-1}[e^{-\lambda(z-z_1)}\tanh(e_0\Delta\phi_2/4kT)] \qquad [2]$$

where

$$\lambda = (8\pi n_0 e_0^2/\varepsilon kT)^{1/2}$$

is the Debye reciprocal length.

Since the capacitance behaviour predicted by the Gouy-Chapman theory bears limited resemblance to experiment only in dilute electrolytes, most of the subsequent developments of primitive double-layer theories have sought to explain the experimental behaviour of charged electrode interfaces(e.g., as manifested by the variation of capacitance as a function of potential) in terms of the properties of the region between the plane of closest approach $z = z_1$ and the electrode surface ($z = -s$). Thus, the interface is, in effect, treated as being divided into "compact" or "inner" ($z < z_1$) and "diffuse" ($z \geq z_1$)

regions, with the Gouy-Chapman theory being retained to describe the behaviour of the latter.

Improvements have, however, been proposed for the Poisson-Boltzmann equation. These include corrections for the finite sizes of ions (i.e. their volume fractions) [6-8], and the dielectric saturation effect caused by locally high ionic concentrations [9,10].

(ii) Statistical-Mechanical Treatments of the Diffuse Layer

Another class of primitive models comprises those which concentrate on improving the treatment of the ionic distribution, without necessarily assuming the properties of the compact region (e.g. the dielectric constant) to be fundamentally different from those of the diffuse region. Thus, the self-consistent definition of the potential ϕ in terms of the local charge density ρ is supplemented by the inclusion of interaction effects via consideration of the relationship between the potential of mean force and the ionic distribution functions.

Early work along these lines was carried out by Stillinger and Kirkwood [11], who derived the hierarchy of integral equations satisfied by ionic distribution functions of successively higher orders. Subsequent work has investigated the implications of the various approximations which may be used in order to determine these distribution functions, for example the Hypernetted-Chain theory [12] and Mean-Spherical Approximation [13]. Space does not permit a detailed examination of these approaches here, but a recent review by Henderson [14] discusses not only the relationship between the various approximations but

also the comparison of their predictions with Monte-Carlo simulations of the primitive model.

2.2 Non-Primitive Models

The common feature of treatments of this type is the explicit inclusion of the bound charge density (arising from solvent polarization) in the expression defining the field as a function of distance. These treatments are much less numerous than those discussed in the previous sections; again, however, it is possible to distinguish two types of approach.

(i) Integral Equations

The integral equation of the Mean-Spherical Approximation appropriate for a system composed of ions and point dipoles was solved by Carnie and Chan [15] and Blum and Henderson [16]. The result is, however, exceedingly complicated. A general feature of this problem is that the ion-ion interactions are much stronger, because they are no longer attenuated by the factor $1/\varepsilon$ occurring in primitive models; this complicates the solution of the equations by rendering inapplicable certain approximations valid for small interaction energies.

(ii) Lattice-Gas Theories

Integral equations of the type just described still retain the approximate description of the solvent molecule as a point dipole. The implications of finite size of dipoles have been considered in recent work by Macdonald and co-workers [17,18]. The interface is modelled by these authors as a lattice gas, composed of layers of ions and such finite dipoles; the free- and bound-charge densities are related self-consistently to the local field, which is determined as a function of distance.

Since these non-primitive approaches are very recent, detailed comparison of their predictions with experiment has not yet appeared. However, more insight into the physical reasonableness of a given statistical-mechanical approach is to be obtained by comparison with Monte-Carlo simulations, which permit the characteristics of the physical model to be decoupled from the approximations necessary to solve the equations.

3. Scope and Objectives

In the previous section, the various structural models which have been proposed to describe charged interfaces were discussed. The most popular of these is that described in Section 2.1 (i), viz. the Gouy-Chapman-Stern approximation. There exists, however, a great diversity of treatments even within this class, some of which are based on approximations which are more accurate than those used by others. It is thus difficult, from examination of these approaches as a group, to draw general conclusions as to their physical realism and experimental verisimilitude.

It is the purpose of the present work to consider certain general questions connected with the construction of such primitive models, when applied to the analysis of several selected aspects of the behaviour of electrode-solution interfaces. The specific aims may be summarized as follows.

The first problem arising in the application of a primitive model to the simulation of a given system is that of reconciling the electrical behaviour of the compact and diffuse regions of the double layer. As shown in Chapter 2, this reduces to consideration of the manner in which the polarization of the

inner layer is calculated as a function of the relevant electrical variables. This point is of quite general interest in the light of previous speculation in the literature [13] that the primitive model itself is reponsible for the prediction of physically unrealistic behaviour, e.g. negative capacitance.

Chapter 3 considers the implications of the results of Chapter 2 with respect to the description of the adsorption of non-polar, neutral molecules at electrodes. The specific problem treated is the combination of the thermodynamics of adsorption (as expressed by the isotherm) with the self-consistent treatment of the polarization contributions due to adsorbate and solvent in the compact region.

Consideration of adsorption reactions involving the deposition of polar species at electrodes requires adequate treatment of the interactions existing between the occupants of the adsorbed layer. In order to discard the approximate treatment of co-adsorbed solvent molecules as a dielectric continuum, which forms the basis of existing theories, account must be taken of the interactions between solvent molecules and adsorbed species, and among the solvent molecules themselves. For solvent molecules of freely variable orientation, these interactions are evidently related to the extent of orientational polarization and hence to the field; the calculation of the various possible interaction energies between adsorbed charges and dipoles is considered in Chapter 4, in terms of the lattice model generally assumed to describe the compact region of the interface.

The calculation of polarization and interaction components of the free energy change of a surface electrode reaction is

considered in Chapter 5, with respect to a one-electron electrodeposition reaction which has been proposed as a model for processes occurring at the noble-metal electrodes studied currently in this laboratory and elsewhere. Here, the interaction energies are combined according to the various approximations of lattice-gas theory, in order to obtain the adsorption isotherm.

The final problem, considered in Chapter 6, is that of ionic adsorption at electrodes. The major additional factors which must be considered in this case are the long-range coulombic energies of interaction between ions and dipoles, which, according to the mean-field approximation, may be considered as components of an effective potential (determining the energy of ions) and field (determining the energy of dipoles). The effective field and potential are then used to define thermodynamic functions for the adsorbed species. Calculation of the differential capacitance behaviour in this case requires consideration of the relationship between the metal surface charge density and the charge densities associated with ionic adsorption and dipole polarization.

The analysis to be presented in the following chapters is proposed to apply to a primitive model of the Gouy-Chapman-Stern type, with the metal surface assumed to behave as a perfect conductor. The compact region is assumed to consist of adsorbed water molecules (represented as point dipoles) located on the points of a lattice, which may be displaced by adsorption processes of one kind or another. The potential distribution within the compact layer is assumed to be linear (this is equivalent to neglecting the contribution of higher multipole

moments to the total polarization) and that in the diffuse region is assumed to be given by eqn. 2. This situation is represented schematically in Fig. 1, which also serves to define the notation to be used subsequently.

The introductory remarks and references relevant to each problem will be included in the respective chapters.

Fig.1: Assumed interfacial potential profile, according to the primitive model, in the absence of appreciable ionic specific adsorption.

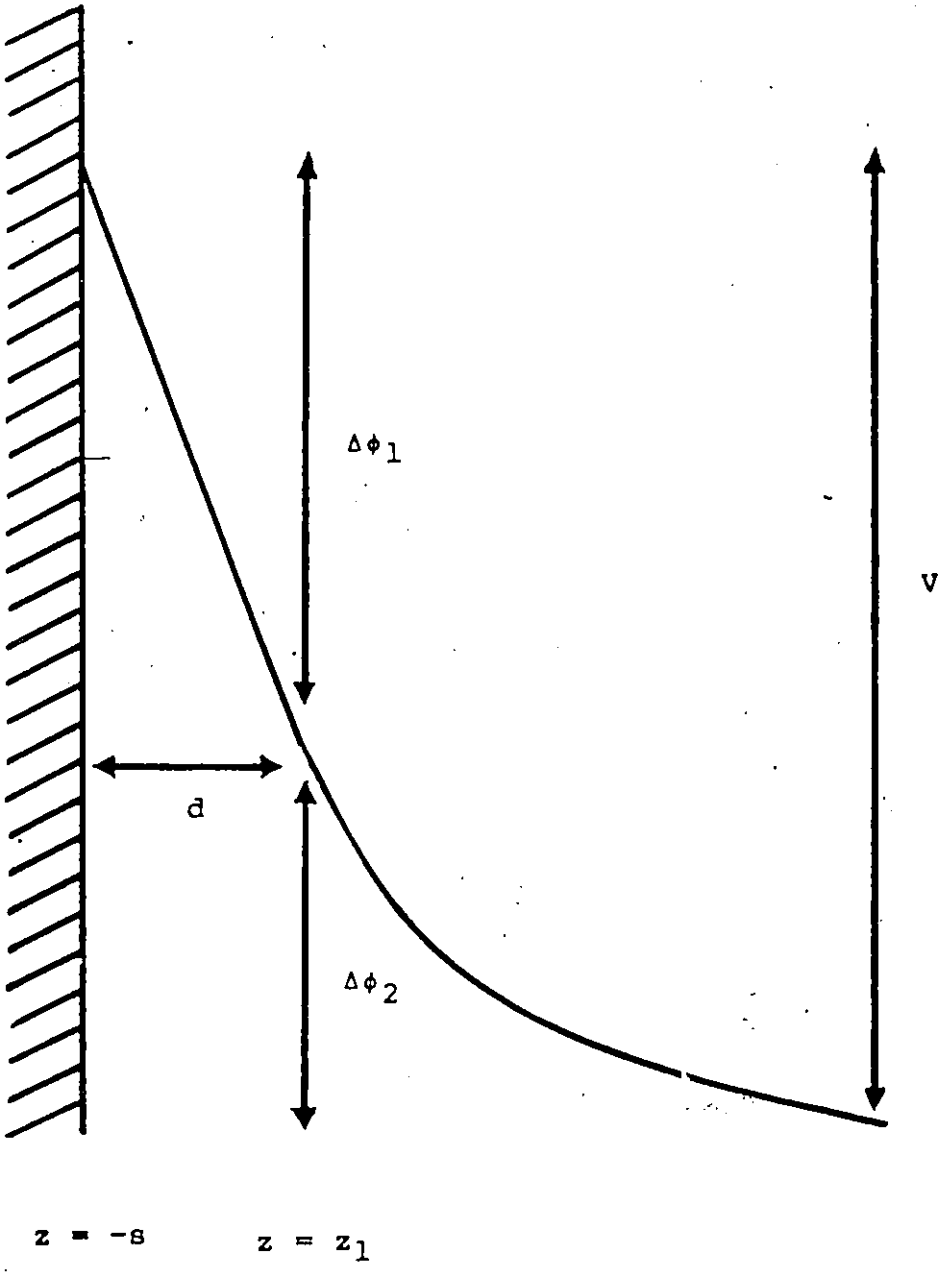

References

1. B.E. Conway and H.A. Kozlowska

   Acc. Chem. Res. **14**: 49 (1981)

2. G. Gouy

   J. Chim. Phys. (Paris) **29**: 145 (1903)

3. D.L. Chapman

   Phil. Mag. **25**: 475 (1913)

4. O. Stern

   Z. Elektrochem. **30**: 508 (1924)

5. D.C. Grahame

   Chem. Revs. **41**: 441 (1947)

6. T.B. Grimley

   Proc. Roy. Soc. Lond. **A201**: 40 (1950)

7. V. Freise

   Z. Elektrochem. **56**: 822 (1952)

8. S. Levine

   Proc. Phys. Soc. (London) **A66**: 365 (1953)

9. B.E. Conway, J.O'M. Bockris and I.A. Ammar

   Trans. Faraday Soc. **47**: 756 (1951)

10. H. Brodowsky and H. Strehlow

    Z. Elektrochem. **63**: 262 (1959)

11. F.H. Stillinger, jr. and J.G. Kirkwood

    J. Chem. Phys. **33**: 1282 (1960)

12. S.L. Carnie, D.Y.C. Chan, D.J. Mitchell and B. Ninham

    J. Chem. Phys. **74**: 1472 (1981)

13. L. Blum

    J. Phys. Chem. **81**: 136 (1977)

14. D. Henderson

Prog. Surf. Sci. 13: 197 (1983)

15. S.L. Carnie and D.Y.C. Chan
J. Chem. Phys. 73: 2949 (1980)

16. L. Blum and D. Henderson
J. Chem. Phys. 74: 1902 (1981)

17. J.R. Macdonald and S.W. Kenkel
J. Chem. Phys. 80: 2168 (1984)

18. S.W. Kenkel and J.R. Macdonald
J. Chem. Phys. 81: 3215 (1984)

CHAPTER 2

TREATMENT OF DIPOLE ORIENTATION IN THE DOUBLE LAYER AT ELECTRODES: ANALYSIS OF CONDITIONS LEADING TO POLARIZATION CATASTROPHES

1. Introduction

Most of the existing experimental work on the double layer capacitance (C) behaviour of electrodes has been interpreted in terms of primitive models, and has centred on the significance of the inner-layer capacitance as a function of the overall metal-solution potential difference (V) or surface charge (q_M) [1-4], electrode metal [5,6] and nature of the solvent [7,8]. Theories of the inner-layer capacitance have assumed various molecular models for the solvent orientational polarization, e.g. an Ising-type two-state model [9,10,11], a three-state model [12], and cluster [3] and continuous orientation models [13,14]. These have been, to varying degrees, successful in predicting on a semi-empirical basis (cf. refs. 1,3,11,15): a) the capacitance as a function of V or q_M; b) the related adsorption behaviour of simple organic molecules as a function of V or q_M [11,15] and c) the Esin and Markov derivative $(\partial V/\partial \ln c)_q$ for shift of electrode potential with changing chemical potential of a simple non-ionic organic adsorbate [15] which adsorbs by solvent dipole displacement [11] in the inner-layer.

While various theories of the dipole orientation and associated inner-layer capacitance have given [1-3,11,15] plausible accounts of C(V) and of the adsorption behaviour of organic molecules at Hg, attention was directed by Cooper and Harrison [16] to a serious and interesting paradox (the so-called

"Cooper-Harrison catastrophe" [17]) which arises in the two-state treatments of solvent dipole polarization and derived capacitance behaviour. These authors pointed out two interesting features of the two-state model: a) that this model predicts physically impossible negative values of the differential capacitance for certain conditions, depending on choice of values of the relevant parameters; and b) that a spontaneous antiferroelectric orientation of solvent dipoles would arise at the potential of zero charge, (cf. the orientational and librational entropy [19,20]) which is not indicated. Point (a) corresponds to a situation where the charge density, q_{dip}, at one side of the oriented solvent layer can exceed that, q_M, on the surface of the metal electrode which causes the induction of the solvent polarization. Correspondingly [18], the effective dielectric constant of the inner-layer can become negative.

By considering components of the electrode double-layer capacitance, Parsons [17] suggested that the origin of the paradox lies in the unrealities of the two-state model for the orientational polarization of solvent at electrodes, viz. that at the potential of zero charge, the dipoles would have a lower energy when aligned in a fashion parallel (→) to the electrode surface than in the "antiferroelectric" orientation (↑↓↑↓↑↓↑↓); the former alignment would therefore probably be preferred apart from the probably important effects of H-bonding with molecules in the bulk solvent. The participation of dipoles oriented parallel to the electrode surface was embodied in Fawcett's [12] three-state treatment of the inner-layer polarization and associated

capacitance behaviour. The possibility of such a parallel configuration [17] also, of course, avoids the problem [16] of spontaneous antiferroelectric orientation.

It should be mentioned that on the basis of the two-state model treated by Bockris, Devanathan and Mueller ("BDM" [11]), prediction of a catastrophe depends on the value chosen for the parameter [Uc/kT in ref. 11] representing pairwise lateral repulsive interaction energy between oriented dipoles. An appreciable value of Uc/kT diminishes the rate of increase of orientational polarization (below the saturation limit) with increasing q_M or field E, so the paradox will not necessarily arise. This point is treated later in a quantitative way. Similarly, it can be shown that the prediction of a polarization catastrophe by a three-state model depends on the value chosen for the relative energy of the third (parallel) state, as well as on the parameters characterising the strength of interactions. It is obvious, however, that the selection of suitable values of parameters does not provide a fundamental basis for disposing of the problem.

In recent work on double-layer structure involving integral equations and computer simulations, Henderson and Blum [21,22,23] infer that the polarization catastrophe arises from intrinsic unrealities of primitive models, as manifested, e.g., in the consequent division of the double-layer capacitance into "compact" and "diffuse" components. However, these authors give no calculations or analytical proof that this is so. Admittedly, non-primitive approaches are more theoretically appealing and probably closer to the truth than primitive ones, but the latter

still provide reasonably good agreement with experiment in many cases, in addition to a convenient basis for the semi-quantitative theoretical interpretation of various electrode processes.

The subject of this chapter is the basis of electrostatic treatments of such primitive models, inasmuch as they are reasonable as first approximations to the actual structure of the double-layer. Specifically, the question which is considered is the relationship between the field exerted by the charged electrode and the resulting polarization of molecules adjacent to it. It is shown that an approach to the calculation of the latter quantity can be made which is completely free of "catastrophic" behaviour; by way of illustration, the capacitance of electrodes according to several simple models for the compact double-layer is calculated, in the absence of ionic contact-adsorption and field-independent orientational preferences of solvent dipoles.

2. Behaviour of Various Models in Relation to the Paradox

(i) Continuous Orientation Model

The most general polarization model for the inner-layer is one in which all dipole orientations are possible but are distributed according to their energy in the interfacial field according to a Langevin function (cf. ref. 25). A similar model was used by Macdonald and Barlow [14], but as will be discussed later, their treatment avoids the catastrophe.

In order to explore the behaviour of this model, the field E due to a surface charge density q_M is written first as

$$E = 4\pi q_M \qquad [1]$$

following previous usage in the literature [9,10,11,14,24]. (As noted by Fawcett [12], it is convenient to use the unrationalised form of the electrostatic equations, owing to some confusion which exists regarding the definition of polarizability in SI units.) The resulting polarization in the interphase, due to dipoles of moment m, may be identified with an equivalent surface charge density q_{dip}, opposing the free charge density q_M. Then

$$q_{dip} = N_{dip} m \, L(4\pi q_M m/kT) \qquad [2]$$

where N_{dip} is the number density of solvent dipoles in the inner-layer at the electrode interface, and the Langevin function $L(x) = \coth x - 1/x$. Note that q_{dip} becomes evaluated as charge cm^{-2}.

By way of illustration, consider a case where $q_M = 5.0 \times 10^{-6}$ C $cm^{-2} = 1.5 \times 10^4$ statcoulomb cm^{-2}. For water (w), with $m = 1.8 \times 10^{-18}$ statcoulomb cm, and taking $N_{dip} = N_w = 3.34 \times 10^{22}$ cm^{-3} and $kT = 4.12 \times 10^{-14}$ erg at 298 K, q_{dip} is readily calculated to be 5.3×10^4 statcoulomb cm^{-2}, which is seen to be more than three times the charge density q_M assumed to "cause" the polarization. The continuous orientation model is therefore seen to give rise to precisely the same kind of paradox as that noted by Cooper and Harrison for the two-state model.

In treatments of the orientational polarization of the inner-layer, the field $4\pi q_M$ has sometimes been written as attenuated by the factor $1/\varepsilon_{opt}$ which reflects the atomic and/or electronic polarization. (In ref. 11, this was referred to as ε_{low}, and proposed to have a value between 2 and 6.) If this is done here, the expression for q_{dip} becomes

$$q_{dip} = N_{dip} m \, L(4\pi q_M m/\varepsilon_{opt} kT) \qquad [3]$$

That the paradox can also arise with eqn. 3 can easily be

demonstrated by examining the value of q_M relative to the saturation value of q_{dip}, viz. for H_2O, $N_w m = 6.02 \times 10^4$ statcoulomb cm^{-2}. In Fig. 1, $q_M/N_w m$ is plotted with the right hand side of eqn. 3 as a function of q_M for various values of ε_{opt}. The difference between the inducing charge q_M and the induced charge q_{dip} is seen to decrease with increasing ε_{opt}, but it is evident that an unrealistically large value would be required to ensure that q_{dip} would always be less than q_M. This value may be obtained from the low-field approximation to the Langevin function in eqn. 3, viz.

$$q_{dip} = q_M \cdot (4\pi N_w m^2 / 3\varepsilon_{opt} kT) \qquad [4]$$

For the coefficient of q_M to be less than unity, it is easily verified that ε_{opt} must be at least 12, an impossibly large value for the optical dielectric constant of a small molecule. Similar, but less pronounced effects can be observed when graphs similar to Fig. 1 are plotted for temperatures greater than 298 K.

(ii) Two-State Watts-Tobin/BDM Model

The prediction of anomalous behaviour by this model has been the subject of considerable discussion [16,17]. The point of interest here is the relationship of such behaviour to the strength of interactions assumed to exist between the molecules.

According to the BDM theory [11], the dimensionless polarization $Y = q_{dip}/N_w m$ is given by the solution of the equation

$$Y = \tanh(4\pi q_M m/\varepsilon_{opt} kT - UcY/kT) \qquad [5]$$

where U is the pairwise lateral interaction energy and 2c is the two-dimensional coordination number for the dipoles. The function

Fig. 1 Reduced polarization $q_{dip}/N_w m$ calculated from eqn. (3) for various values of ε_{opt}. kT = 4.116 x 10^{-14} erg at 298 K; m = 1.8 x 10^{-18} statcoulomb cm (= 6.0 x 10^{-30} C m); N_w = 6.649 x 10^{22} cm^{-3}.

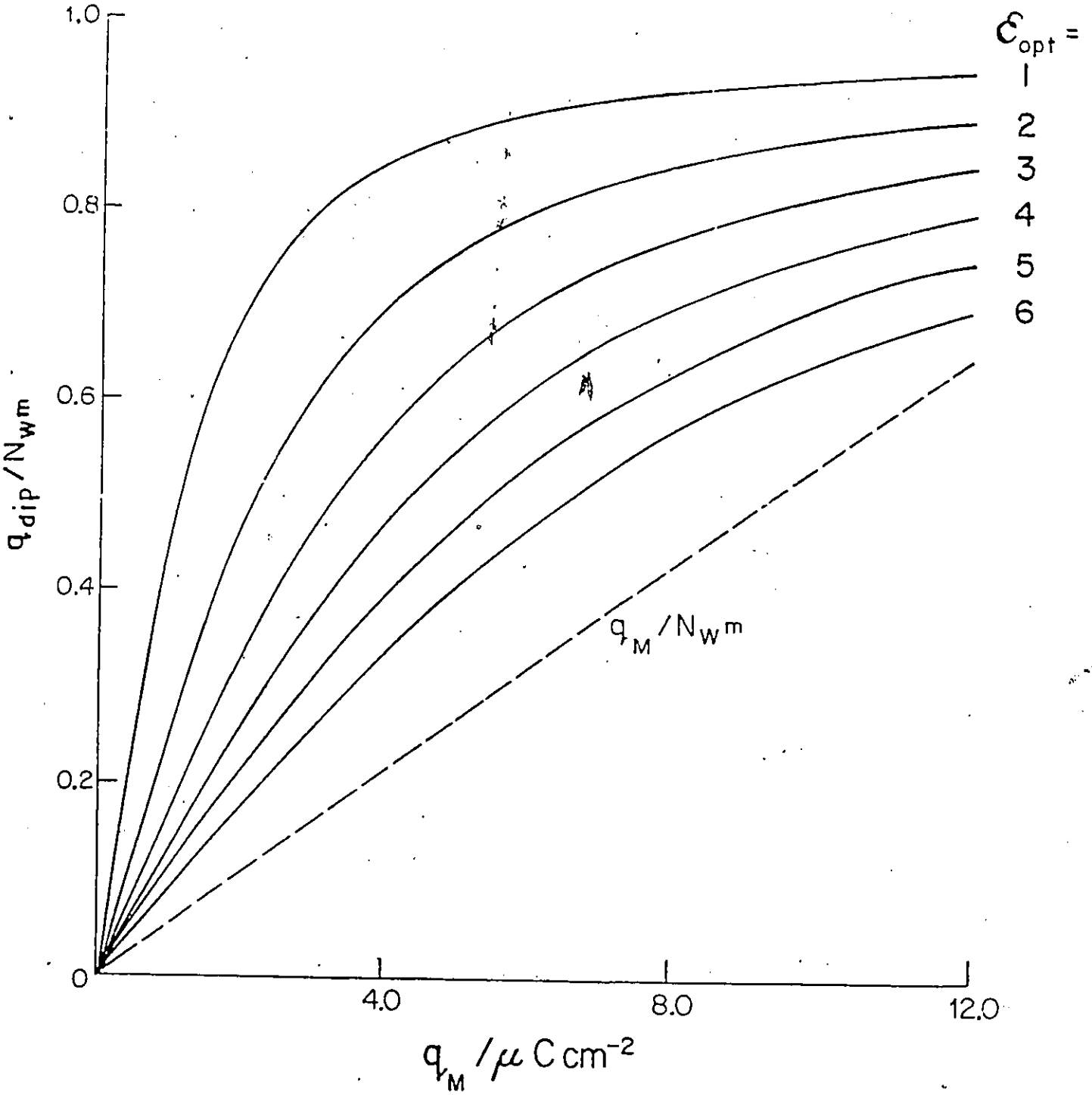

Y is plotted in Fig. 2 as a function of q_M, for various values of Uc/kT, taking $\varepsilon_{opt} = 1$. It is seen that only if Uc/kT is sufficiently large is the paradox relieved.

The value of Uc/kT for which this is so can be obtained by linearizing the tanh function for small values of its argument, and solving for Y:

$$Y = 4\pi q_M m/\varepsilon_{opt} kT - UcY/kT \qquad [6]$$

$$Y = (4\pi q_M m/\varepsilon_{opt} kT)/(1 + Uc/kT) \qquad [7]$$

whence

$$q_{dip} = q_M.(4\pi N_w m^2/\varepsilon_{opt} kT)/(1 + Uc/kT) \qquad [8]$$

The use of eqn. 8 in estimating the "critical" value of Uc/kT requires specification of N_w and ε_{opt}. Depending on the electrode potential [13,18] and ionic composition of the double layer [27], N_w can lie between the bulk number density 3.34×10^{22} cm^{-3} and the close-packed value 6.47×10^{22} cm^{-3} (for spheres of radius 1.35×10^{-8} cm). From the previous section, ε_{opt} can be taken as 1 (corresponding to the vacuum field) or between 2 and 6 (as in ref. 11).

With $N_w = 6.47 \times 10^{22}$ cm^{-3} and $\varepsilon_{opt} = 1$, the lower limit of Uc/kT is 63.0, whilst with $N_w = 3.34 \times 10^{22}$ cm^{-3} and $\varepsilon_{opt} = 6$ (cf. ref. 11), it is 5.2. These values are, of course, arbitrary, despite the fact that the second is more reasonable than the first. Interestingly, the value 5.2 corresponds roughly with that of 3 - 4 inferred by Conway and Dhar [15] from measurements of the Esin-Markov derivative for adsorption behaviour at mercury, using the flat non-dipolar molecule 1,4-pyrazine as a probe for water dipole orientation as a function of q_M.

It was also noted by Levi et al. [6] that the paradox could

Fig.2: Orientation fraction $Y = q_{dip}/N_w m$ calculated according to the BDM theory [eqn. (5)] with $E = 4\pi q_M/\varepsilon_{opt}$ ($\varepsilon_{opt} = 1$). Molecular parameters as for Fig. 1.

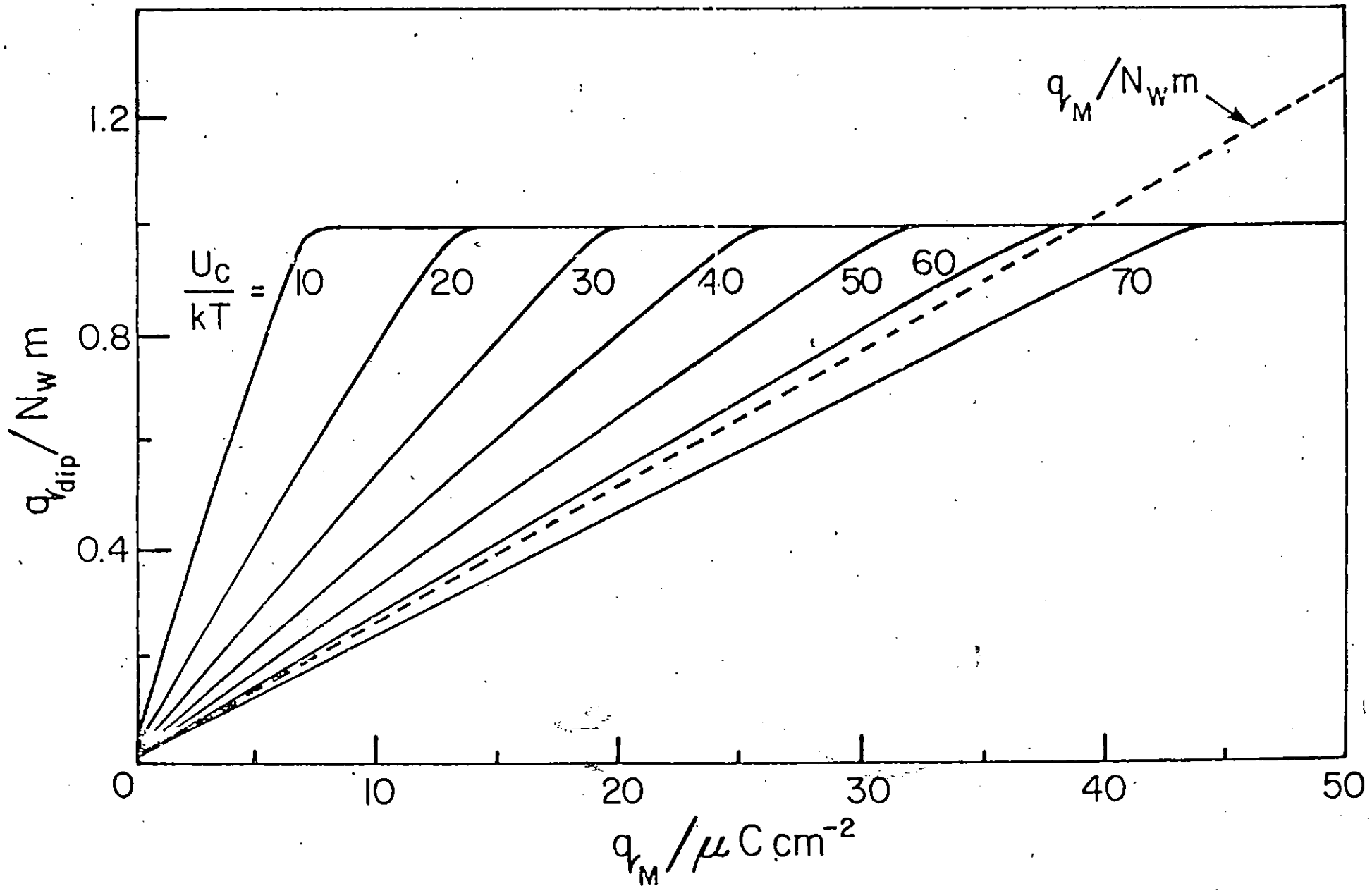
$q_M / N_W m$
1.2
0.8
0.4
$\frac{U_c}{kT}$ = 10
20
30
40
50
60
70
$q_{dip} / N_W m$
0
10
20
30
40
50
$q_M / \mu C\,cm^{-2}$

be removed by considering interaction effects, but these authors did not deduce the required value for Uc/kT.

(iii) Fawcett Three-State Model

In the light of the suggestion by Parsons [17] that the cause of the catastrophe could be the neglect of the most stable configuration of the dipoles (i.e. parallel to the electrode surface), it is of interest to examine the polarization behaviour predicted by the Fawcett three-state model [12]. According to this approach, molecular polarization is due to an effective field which includes contributions from neighbouring dipoles, similar to that proposed in the two-state treatment of Levine, Bell and Smith [24]. With the inclusion of the third (parallel) state of relative energy U, the equations given by Fawcett can be expressed in the form

$$q_{dip}/N_w m = Y = 2 \sinh(mE/kT)/[2 \cosh(mE/kT) + \exp(-U/kT)] \quad [9]$$

where E is the effective field given by

$$E = 4\pi q_M(1 - c\alpha/Bd^3) - cmY/Bd^3, \text{ and } B = 1 + c\alpha/d^3.$$

The dipoles are assumed to have an effective coordination number c, polarizability α and diameter d. In the absence of interactions, an explicit equation for Y in terms of q_M is recovered; this is plotted in Fig. 3a for various values of U. It is seen that even for the relatively large value of U = -10 kT, the dimensionless polarization rapidly exceeds its maximum permissible value given by the straight line. The use of appreciably large values of U is also seen to result in a second inflexion point, so it is predicted that the total polarization curve will exhibit a plateau. Such a plateau was also observed in

a recent computer simulation by Schmickler [26] who considers it to be an unsatisfactory characteristic of this model, when applied to H_2O.

The inclusion of interaction effects in the above equation results, as expected, in a less rapid variation of Y with q_M, as shown in Fig. 3b. It is also evident from the calculations that for a value of U more negative than about -3 kT, the paradox is avoided. Once again, however, there is no a priori reason why this value should be selected for U. Therefore, it appears that the inclusion of a third state does not, in principle, avoid the paradox.

3. Relationship Between Field and Polarization

(i) Representation of the Field in the Inner-Layer

It has been seen that the paradox is manifested as an over-compensation of the polarization in relation to the charge density on the electrode. From the above arguments, it appears that, apart from the arbitrary assignment of the values of model-dependent parameters, the explanation for this over-compensation is that the electrostatic energy of the dipoles in the electrode's field is over-estimated with respect to kT. This in turn suggests that the field which is used in the above polarization expressions is not represented correctly. This section discusses the representation of the field, and its relationship to the polarization which it induces. Since it has been shown above that the inclusion of interactions does not necessarily eliminate prediction of anomalous behaviour, it is assumed first for simplicity that the dipoles can independently orient themselves in the electrode's field. Admittedly, this is

Fig.3a: Reduced polarization calculated according to the Fawcett theory for no interactions. Parameters of Fig. 1.

b: Reduced polarization calculated according to the Fawcett theory, with an effective coordination number of 6. Parameters of Fig. 1.

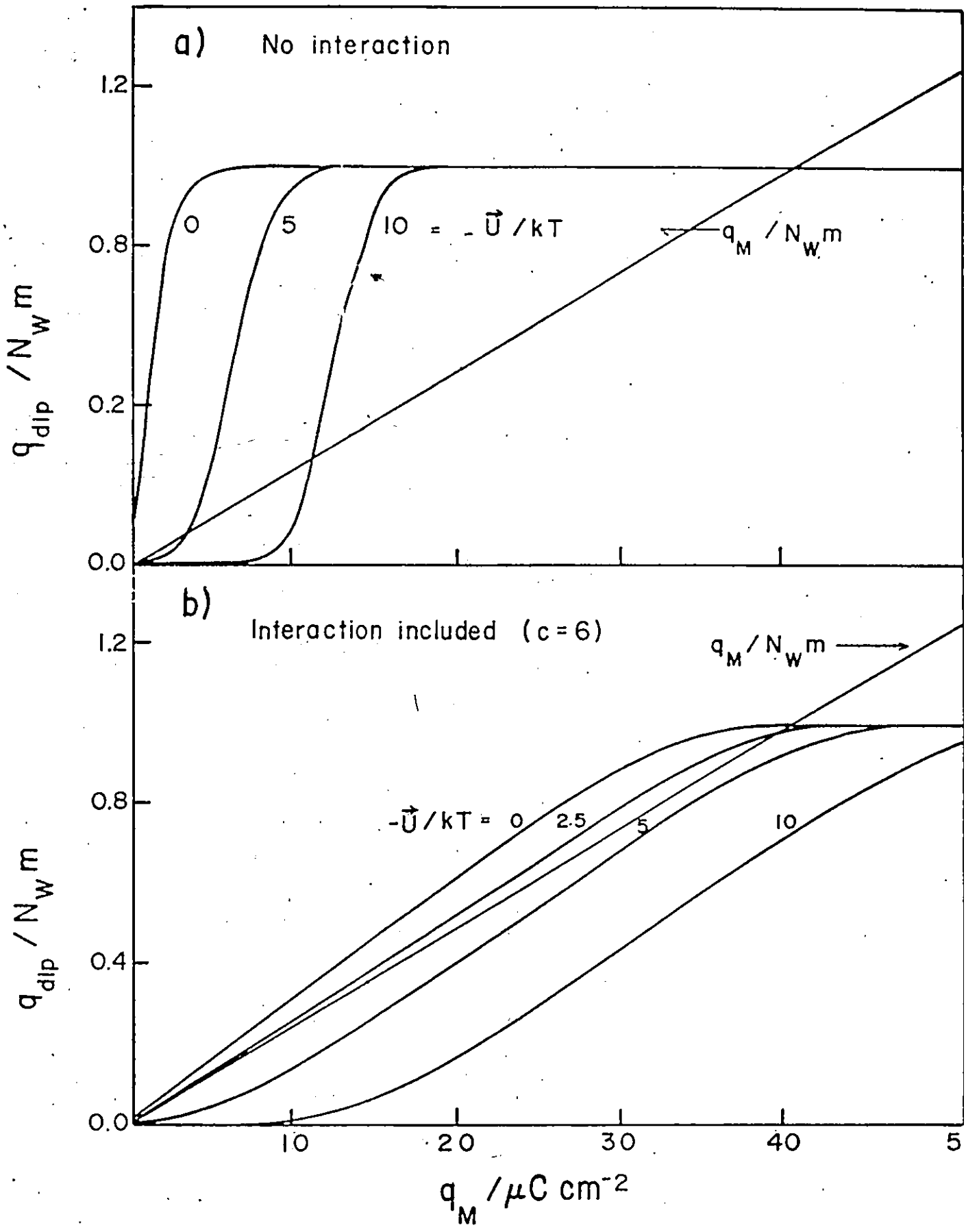
a) No interaction
1.2
0.8
0.2
0.0
0
5
10 = - U / kT
q_M / N_W m
q_dip / N_W m
b) Interaction included (c = 6)
q_M / N_W m
1.2
0.8
0.4
0.0
-U / kT = 0
2.5
5
10
q_dip / N_W m
10
20
30
40
5
q_M / μC cm^-2

impossible for a polar condensed phase; the inclusion of intermolecular interactions with the aid of one or other statistical-mechanical approximation will result in modified polarization functions, to which, however, the following arguments may be readily extended.

The starting point of the analysis of the inner-layer solvent polarization, originally presented by Mott and Watts-Tobin [9], is an equation for the surface charge density q_M in terms of the inner-layer potential drop, $\Delta\phi_1$, which, apart from minor changes in notation, may be written as follows:

$$q_M = \Delta\phi_1/4\pi d + N_w m \tanh(m\Delta\phi_1/dkT) \qquad [10]$$

assuming that the saturation dielectric constant of the layer is unity. Throughout their paper, Mott and Watts-Tobin consider that the potential drop $\Delta\phi_1$ is approximately equal to the electrode-solution potential drop V; thus, it is possible to obtain the following expression for the differential capacitance:

$$C \approx C_1 = [1 + (4\pi N_w m^2/kT)\ \mathrm{sech}^2(m\Delta\phi_1/dkT)]/4\pi d \qquad [11]$$

This is evidently of the form expected for a differential capacitance, viz. an effective differential dielectric constant divided by $4\pi d$. Furthermore, C according to eqn. 11 is clearly non-negative and hence has no trace of "catastrophic" behaviour. The most important difference between the orientational polarization term in eqn. 10 and the expressions given in the previous sections of this chapter is that the field acting on the dipoles is <u>not</u> taken as the vacuum field $4\pi q_M$, or its equivalent in BDM [11], but as $\Delta\phi_1/d$ - this is obviously the resultant of the field $4\pi q_M$ and the polarization which opposes it, since by

hypothesis there are no other species in the compact region. Therefore, the reason for the paradox may be identified as the inconsistency between the representation of the field in the inner-layer and the resulting polarization. In other words, use of the resultant field $\Delta\phi_1/d$ in the tanh term of eqn. 10 predicts sensible behaviour, whilst use of $4\pi q_M$ does not, as shown in the previous sections.

(ii) Components of the Electrode-Solution Potential Drop

Eqn. 10 was used by Mott and Watts-Tobin to evaluate q_M explicitly as a function of $\Delta\phi_1$. Alternatively, it can be regarded as an implicit relation for $\Delta\phi_1$ in terms of q_M. In general, however, the approximation $\Delta\phi_1 \simeq V$ is not an accurate one; rather, $\Delta\phi_1$ must be calculated from the experimental variation of q_M with V. In order to do this, q_M must be related to the remaining potential drop $V - \Delta\phi_1$ in the solution. Using the standard result from the theory of the diffuse double layer [32],

$$q_M = 2A \sinh[(V - \Delta\phi_1)e_0/2kT] \qquad [12]$$

where $A = (\varepsilon_2 kTn_0/2\pi)^{1/2}$, ε_2 is the bulk dielectric constant of the solvent and n_0 is the number of ions per cm^3 for a 1:1-valent electrolyte. By equating the two expressions 10 and 12 for q_M, one obtains an equation from which $\Delta\phi_1$ may be determined:

$$2A.\sinh[(V - \Delta\phi_1)e_0/2kT] - \Delta\phi_1/4\pi d - N_w m.\tanh(m\Delta\phi_1/dkT) = 0 \qquad [13]$$

Alternatively, for the continuous-orientation model,

$$2A.\sinh[(V - \Delta\phi_1)e_0/2kT] - \Delta\phi_1/4\pi d - N_w m.L(m\Delta\phi_1/dkT) = 0 \qquad [14]$$

The solution of eqn. 14 is shown in Fig. 4a for various ionic concentrations. It is seen that the calculated values of $\Delta\phi_1$ are always less than V, but that the approximation $\Delta\phi_1 \simeq V$ becomes

Fig.4a: Potential drop $\Delta\phi_1$ across the compact double layer from eqn. (14), for various values of ionic concentration. $N_w = 3.342 \times 10^{22}$ cm^{-3}; other parameters as for Fig. 1.

b: Potential drop $\Delta\phi_1$ across the compact double layer, using the continuous orientation [curve (1)] and two-state [curve (2)] models, for c = 0.001 mol dm^{-3}. $N_w = 3.342 \times 10^{22}$ cm^{-3}; other parameters as for Fig. 1.

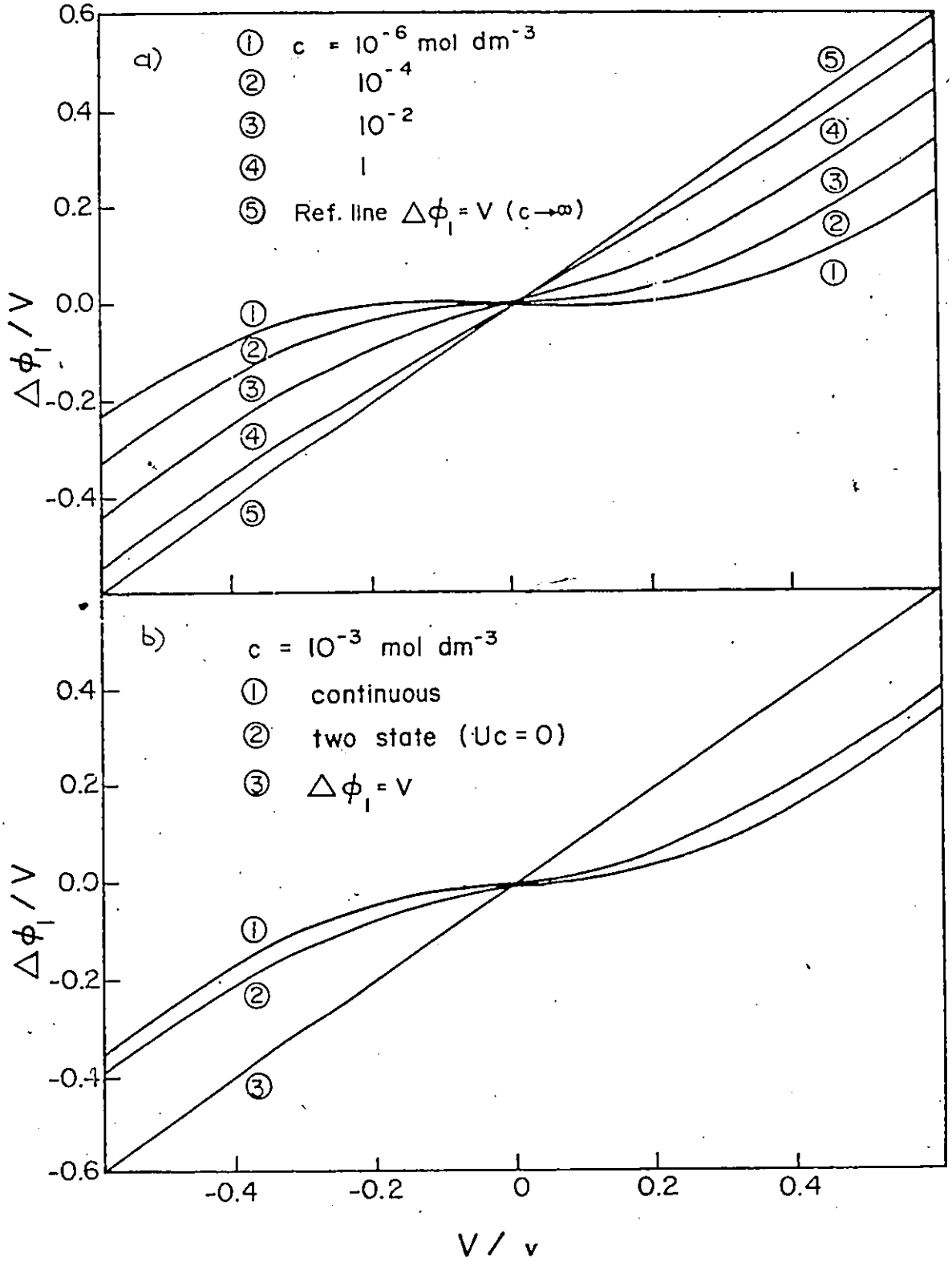
a)
① c = 10⁻⁶ mol dm⁻³
② 10⁻⁴
③ 10⁻²
④ 1
⑤ Ref. line Δφ₁ = V (c→∞)
b)
c = 10⁻³ mol dm⁻³
① continuous
② two state (Uc = 0)
③ Δφ₁ = V
Δφ₁ / V
V / v
0.6
0.4
0.2
0.0
-0.2
-0.4
-0.6
-0.4
-0.2
0
0.2
0.4

progressively worse with decreasing concentration, as expected. In Fig. 4b, the solution of eqn. 14 is compared with that of eqn. 13 for c = 0.001 mol dm^{-3}; the behaviour is qualitatively similar but the two-state model leads to a rather sharper variation of $\Delta\phi_1$ with V. This section has treated, for completeness, the general case where the diffuse-layer potential drop is not necessarily negligible. However, it must be mentioned that the inclusion of the diffuse-layer p.d. and its relation to q_M (eqn. 12) does not have any effect on whether or not the Cooper-Harrison catastrophe arises, as is seen in section (iii) which follows.

As observed above, the Cooper-Harrison catastrophe consists of an over-compensation of q_{dip} in relation to q_M. Evidently, this can also be regarded as a discontinuity in the potential at the boundary of the compact and diffuse regions of the double layer. However, the introduction of the electroneutrality condition 12, has ensured continuity of potential between the two regions. Furthermore, the procedure which has just been described shows that the use of a primitive model for the double layer does not, in fact, require the assumption of negative capacities for the inner region, as stated by Blum [23].

(iii) Determination of the Polarization

An alternative approach to the problem is suggested by the earlier statement that the field $\Delta\phi_1/d$ in eqn. 10 is the resultant of that due to q_M and to q_{dip}. Accordingly, the effect of orientation of dipoles in the inner-layer could be represented in terms of a reduction of the field from its in vacuo value $4\pi q_M$

by 4π times the polarization q_{dip}, i.e.

$$E_1 = \Delta\phi_1/d = 4\pi(q_M - q_{dip}) \qquad [15]$$

as in the classical representation of the field and polarization in a bulk dielectric [29,30,31] where $E = E_{vac} - 4\pi P$. The use of this alternative representation of the field results in an implicit equation for q_{dip} in terms of q_M; for each of the two simple models being considered, such an equation has the following respective forms:

$$q_{dip} = N_w m \tanh[4\pi(q_M - q_{dip})m/kT] \quad \text{(two-state)} \qquad [16a]$$

$$q_{dip} = N_w m \, L[4\pi(q_M - q_{dip})m/kT] \quad \text{(continuous)} \qquad [16b]$$

The tanh and Langevin functions may clearly be replaced with the polarization expression appropriate for any other model being considered. It is readily verified that the determination of q_{dip} by solution of eqn. 16a is equivalent to the determination of $\Delta\phi_1$ by solution of Watts-Tobin's eqn. 10. For, from eqn. 15, $\Delta\phi_1 = 4\pi d(q_M - q_{dip})$, and on substitution of this into eqn. 10 one recovers eqn. 16a.

The inner-layer capacitance may now be expressed in terms of the derivative of q_{dip} with respect to q_M. This is obtained by implicit differentiation of eqn. 16a:

$$dq_{dip}/dq_M = \frac{(4\pi N_w m^2/kT)\,\mathrm{sech}^2[4\pi(q_M - q_{dip})m/kT]}{1 + (4\pi N_w m^2/kT)\,\mathrm{sech}^2[4\pi(q_M - q_{dip})m/kT]} \qquad [17]$$

By definition, the reciprocal inner-layer capacitance is, from eqn. 15,

$$1/C_1 = d\Delta\phi_1/dq_M = 4\pi d(1 - dq_{dip}/dq_M) \qquad [18]$$

so that

$$C_1 = [1 + (4\pi N_w m^2/kT)\,\mathrm{sech}^2[4\pi(q_M - q_{dip})m/kT]]/4\pi d \qquad [19]$$

which is seen to be identical to 11, derived from Watts-Tobin's eqn. 10, on substituting for $\Delta\phi_1$.

For eqns. 17-19 to give sensible results one must, of course, have that $q_{dip} \leq q_M$. This may be shown, as before, in the low-field limit by linearizing the expressions 16 and solving for q_{dip}:

$$q_{dip} \simeq q_M.(4\pi N_w m^2/kT)/[1 + 4\pi N_w m^2/kT] \text{ (two-state)} \quad [20a]$$

$$q_{dip} \simeq q_M.(4\pi N_w m^2/3kT)/[1 + 4\pi N_w m^2/3kT] \text{ (continuous)} \quad [20b]$$

In both cases, it is seen that $q_{dip} \leq q_M$, so that no paradox arises; it further follows that q_{dip} is always less than q_M, since tanh x and L(x) are bounded from above by their respective approximations x and x/3. This is more clearly shown by Fig. 5a, where the solution of eqn. 16b is plotted as a function of q_M.

Non-orientational polarizability of the molecules may, of course, be included in the calculations; in this case, the equation for q_{dip} is, e.g.

$$q_{dip} = 4\pi N_w \alpha (q_M - q_{dip}) + N_w m L[4\pi(q_M - q_{dip})m/kT] \quad [21]$$

and the corresponding capacitance expression is

$$C_1 = [1 + 4\pi N_w \alpha + (4\pi N_w m^2/kT)L'[4\pi(q_M - q_{dip})m/kT]]/4\pi d \quad [22]$$

where $L'(x) = 1/x^2 - \text{cosech}^2 x$ is the derivative of the Langevin function $L(x) = \coth x - 1/x$. The solution of eqn. 21 does not exhibit the saturation behaviour observed for $\alpha = 0$ for reasons which are obvious.

(iv) Dielectric Constant of the Inner Layer

In the light of the above discussion, an effective dielectric constant of the inner-layer may be represented as (e.g. for the two-state model)

$$\varepsilon_1 = 1 + 4\pi q_{dip}/4\pi(q_M - q_{dip}) = q_M/(q_M - q_{dip}) \quad [23]$$

Fig.5a: Reduced polarization for the continuous-orientation model, calculated by solution of eqn. (20b), with the parameters of Fig. 1.

b: Dielectric Constant of the inner layer as a function of q_M, for the continuous-orientation model. Curve 1: with field $E = 4\pi(q_M - q_{dip})$ [eqn. (20b)]; Curve 2: with field $E = 4\pi q_M$. Parameters as for Fig. 1.

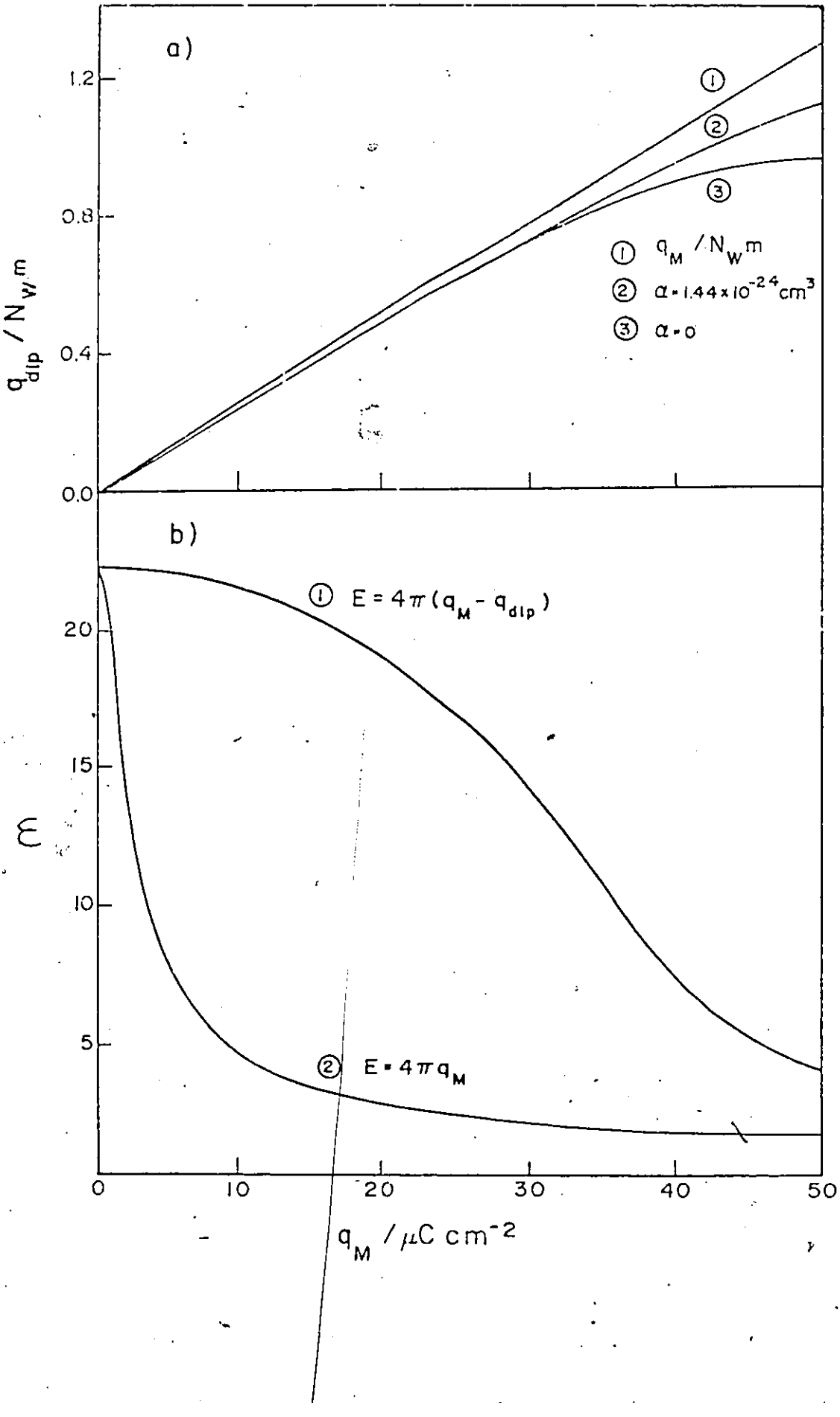
a)
1.2
0.8
0.4
0.0
$q_{dip} / N_W m$
① $q_M / N_W m$
② $\alpha = 1.44 \times 10^{-24} cm^3$
③ $\alpha = 0$
b)
20
15
10
5
ε
① $E = 4\pi (q_M - q_{dip})$
② $E = 4\pi q_M$
0
10
20
30
40
50
$q_M / \mu C\ cm^{-2}$

where q_{dip} is the solution of eqn. 16a or as

$$\varepsilon_1 = 1 + 4\pi N_w m \tanh(m\Delta\phi_1/dkT)/(\Delta\phi_1/d) \quad [24]$$

where $\Delta\phi_1$ is the solution of eqn. 10.

Eqn. 23 also follows from equating the dielectric displacement at the electrode surface (where $\varepsilon = 1$ and $E = 4\pi q_M$) to that within the layer [where $\varepsilon = \varepsilon_1$ and $E = 4\pi(q_M - q_{dip})$]:

$$4\pi q_M . 1 = 4\pi(q_M - q_{dip}).\varepsilon_1 \quad [25]$$

Interestingly, this means that the field can also be represented as $E_1 = 4\pi q_M/\varepsilon_1$ where ε_1 is given by eqn. (23), rather than being taken as constant as in the BDM treatment [11].

Attention is now directed to the continuity of the displacement across the inner-layer/solution interface. The diffuse-layer field, obtained by a first integration of the Poisson-Boltzmann equation, is

$$E_2 = (32\pi n_0 kT/\varepsilon_2)^{1/2} \sinh(\phi e_0/2kT) \quad [26]$$

where ϕ is the potential at a distance x from the boundary of the solution and ε_2 is the bulk dielectric constant of the solvent. At $x = 0$, $\phi = V - \Delta\phi_1$, so that the displacement is

$$\varepsilon_2 E_2 = (32\pi n_0 kT\varepsilon_2)^{1/2} \sinh[(V-\Delta\phi_1)e_0/2kT] \quad [27]$$

$$= 4\pi . 2A \sinh[(V-\Delta\phi_1)e_0/2kT] \quad [28]$$

with A as previously defined. Equating this with $\varepsilon_1 E_1$ evaluated from eqn. 24, one obtains

$$\Delta\phi_1/d + 4\pi N_w m \tanh(m\Delta\phi_1/dkT) = 4\pi . 2A \sinh[(V-\Delta\phi_1)e_0/2kT] \quad [29]$$

which is simply eqn. 10 multiplied throughout by 4π.

The solutions of eqn. 16a for q_{dip} and eqn. 10 for $\Delta\phi_1$ are therefore seen to be equivalent to applying the displacement continuity condition to the electrode/inner-layer- and inner-

layer/solution-interfaces, respectively.

Dielectric displacement continuity conditions were used in the treatment of Macdonald and Barlow [14], which avoids the Cooper-Harrison catastrophe, the dielectric constant ε_1 varying with E_1. The calculations of these authors were very detailed, and the procedure relating E_1, q_M and V was less direct than that described here. The importance acquired in the literature by the catastrophe since publication of ref. 16 suggests that Cooper and Harrison and subsequent authors were unaware of the purport of the earlier work of Macdonald and Barlow [14].

(v) Interim Summary

The procedure described above for calculation of the inner-layer polarization q_{dip} or potential drop $\Delta\phi_1$ is consistent with, or derivable from, the following electrostatic constraints which must be satisfied by the given structural model of the double layer:

(a) Dielectric displacement continuity across the electrode/inner-layer interface;

(b) Dielectric displacement continuity across the inner-layer/solution interface;

(c) Continuity of potential between inner-layer and solution.

It is further evident from the discussion so far that the conventional representations of the field as $E_1 = 4\pi q_M$ or as $E_1 = 4\pi q_M/\varepsilon$ (with ε constant) lead to the prediction of anomalous polarization behaviour, irrespective of the particular molecular model being considered, which is, in turn, equivalent to the non-satisfaction of these constraints.

The behaviour of the models considered in section 2, when

they are modified using the above representations of the field, will now be considered.

4.Dielectric Behaviour of Modified Polarization Functions

While detailed consideration of non-primitive approaches is beyond the scope of the present chapter, it is nevertheless interesting to examine the fundamental differences between them and the arguments of the above section. In general, the field and polarization are not uniform as has been assumed, but are determined as a function of distance by the Poisson equation,

$$\mathrm{div}\mathbf{E} = 4\pi(\rho - \mathrm{div}\mathbf{P})$$

in which ρ is the free (ionic) charge density, and $-\mathrm{div}\mathbf{P}$ is the bound (dipolar) charge density, which both depend on distance through the potential and field respectively. The solution of this equation requires the substitution of suitable statistical-mechanical expressions for ρ and divP, so that the field is defined implicitly in terms of itself.

The field $4\pi(q_M - q_{dip})$ is equivalent in classical dielectric theory to the inclusion of a screening effect due to induced polarization at the boundaries of the dielectric. The use of this field in the eqns. 20 implies that the dipoles are screening themselves from polarization by the electrode, which in itself seems "paradoxical", if the field and its polarization component are interpreted in a strictly macroscopic sense. Rather, these quantities should be regarded, as has just been stated, as being functions of distance from the electrode, which are assumed here to be approximately constant over the molecular diameter d. Thus, eqns. 20 may in turn be regarded as (crude)

difference approximations to Poisson's equation, with very simple expressions for the ionic and dipolar charge densities, with the added approximation that the polarization component of the field may be neglected beyond the first monolayer.

Schmickler [26,28] has, in fact, suggested that the Cooper-Harrison catastrophe arises from the fundamental inapplicability of dielectric theory to systems of molecular dimensions. As has just been shown, formal application of the classical results seems to provide a sensible description, but the fields and polarizations involved are best regarded as short-range approximations to the position-dependent quantities defined by Poisson's equation.

With these observations in mind, it is evident that the physical significance of the dielectric constant is elusive. However, it is of interest to compare the polarization behaviour predicted by the various molecular models being considered, by calculating an effective dielectric constant in the inner-layer, in terms of the approximate values of the field and polarization determined by equations of the type 20.

(i) Continuous-Orientation Model

It has already been demonstrated that when the field 15 is used in the Langevin function, this predicts sensible values of the polarization. With the low-field approximation for q_{dip}, eqn. 20b, it is possible to obtain a corresponding estimate of the effective dielectric constant, since

$$q_M - q_{dip} = q_M/(1 + 4\pi N_w m^2/3kT); \qquad [30]$$

substitution of this into eqn. 23 gives

$$\varepsilon_1 = 1 + 4\pi N_w m^2/3kT \qquad [31]$$

This is the result usually quoted for the dielectric constant of a substance containing non-polarizable, independently-orienting dipoles of moment m. Eqn. 23 is, of course, valid for all finite values of q_M; a graph of effective dielectric constant as a function of q_M is shown in Fig. 5b. It is seen that, as expected, saturation occurs much less readily than it does if $E = 4\pi q_M$ is used.

(ii) Watts-Tobin/BDM Two-State Model

When the field applied to the dipoles in eqn. 5 is taken to be given by eqn. 15, Y is given implicitly by the equation

$$Y = \tanh[4\pi q_M m/kT - (Uc/kT + 4\pi N_w m^2/kT)Y] \qquad [32]$$

As seen in Fig. 6a, the solution of this equation is consistent with q_M for values of Uc/kT which otherwise give "catastrophic" behaviour (cf. Fig. 2). The effect of increasing this parameter is qualitatively similar but less pronounced.

By the usual linearization procedure, one obtains the low-field expression for the effective dielectric constant according to this model:

$$\epsilon_1 = 1 + (4\pi N_w m^2/kT)/[1 + Uc/kT] \qquad [33]$$

This may be compared with the approach used by Levine et al [24]. Neglecting electronic polarization and field-independent orientational preferences of dipoles, the potential difference across the dipole layer was written as

$$\Delta\phi_1 = 4\pi d(q_M - N_w mY) \qquad [34]$$

which, when combined with

$$\Delta\phi_1/d = 4\pi q_M/\epsilon_1 \qquad [35]$$

gives the following expression for ϵ_1:

Fig.6a: Reduced polarization according to the BDM theory, with $E = 4\pi(q_M - q_{dip})$, parameters as in Fig. 1.

b: Dielectric constant according to the BDM theory with $E = 4\pi(q_M - q_{dip})$, parameters as in Fig. 1.

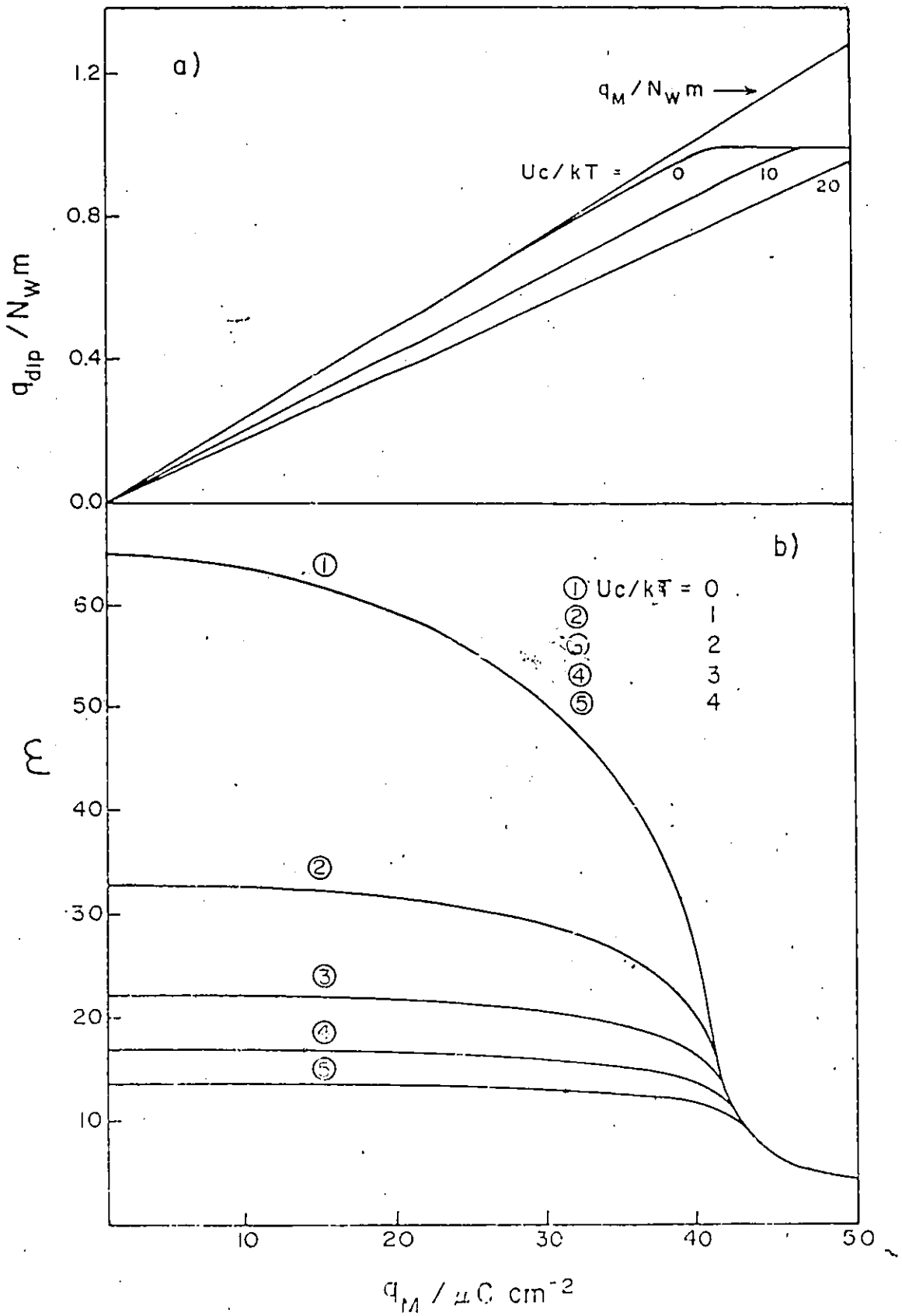
a)
b)
$q_M / N_W m$
Uc/kT = 0
10
20
$q_{dip} / N_W m$
1.2
0.8
0.4
0.0
① Uc/kT = 0
② 1
③ 2
④ 3
⑤ 4
ε
60
50
40
30
20
10
10
20
30
40
50
$q_M / \mu C\ cm^{-2}$

$$\varepsilon_1 = 1/(1 - N_w mY/q_M) \qquad [36]$$

Taking into account mutual depolarization of dipoles in parallel orientation gives [24]

$$\varepsilon_1 = 1/[1 - N_w mY/(1 + \alpha c/d^3)q_M] \qquad [37]$$

(using the notation employed earlier in section 2(iii)). Eqn. 36 or its modified form 37 encounters problems when Y is related to q_M through a polarization function using a field $E = 4\pi q_M$, since the ratio $N_w mY/q_M$ is appreciably greater than unity even when $Uc/kT \simeq 3$ (the value indicated by experiment [15]). Then ε_1 is negative, corresponding to the polarization catastrophe, for exactly the same reasons as those pointed out by Cooper and Harrison for the capacitance behaviour and discussed in the previous section.

By combining eqns. 32 and 23, the effective dielectric constant can be evaluated as a function of q_M, and this is shown in Fig. 6b. The decrease in ε_1 for large values of Uc/kT is also reflected by the approximation 33 and the corresponding decrease in the slopes of the polarization curves (Fig. 6a).

(iii) Fawcett Three-State Model

The replacement of $E = 4\pi q_M$ by $E = 4\pi(q_M - q_{dip})$ in the equations defining Y according to this model results in polarization curves exemplified by Fig. 7a, calculated for the case of the absence of interactions. Once again, the polarization catastrophe is avoided, but the curves still exhibit the second inflexion point observed earlier, and the inclusion of interactions also causes the saturation limit to be reached at higher fields.

In the low-field limit, the polarization behaves quite

Fig.7a: Reduced polarization according to the Fawcett model, with $E = 4\pi(q_M - q_{dip})$, no interactions. Parameters of Fig.1.

b: Dielectric constant according to the Fawcett model with $E = 4\pi(q_M - q_{dip})$, no interactions, parameters of Fig. 1.

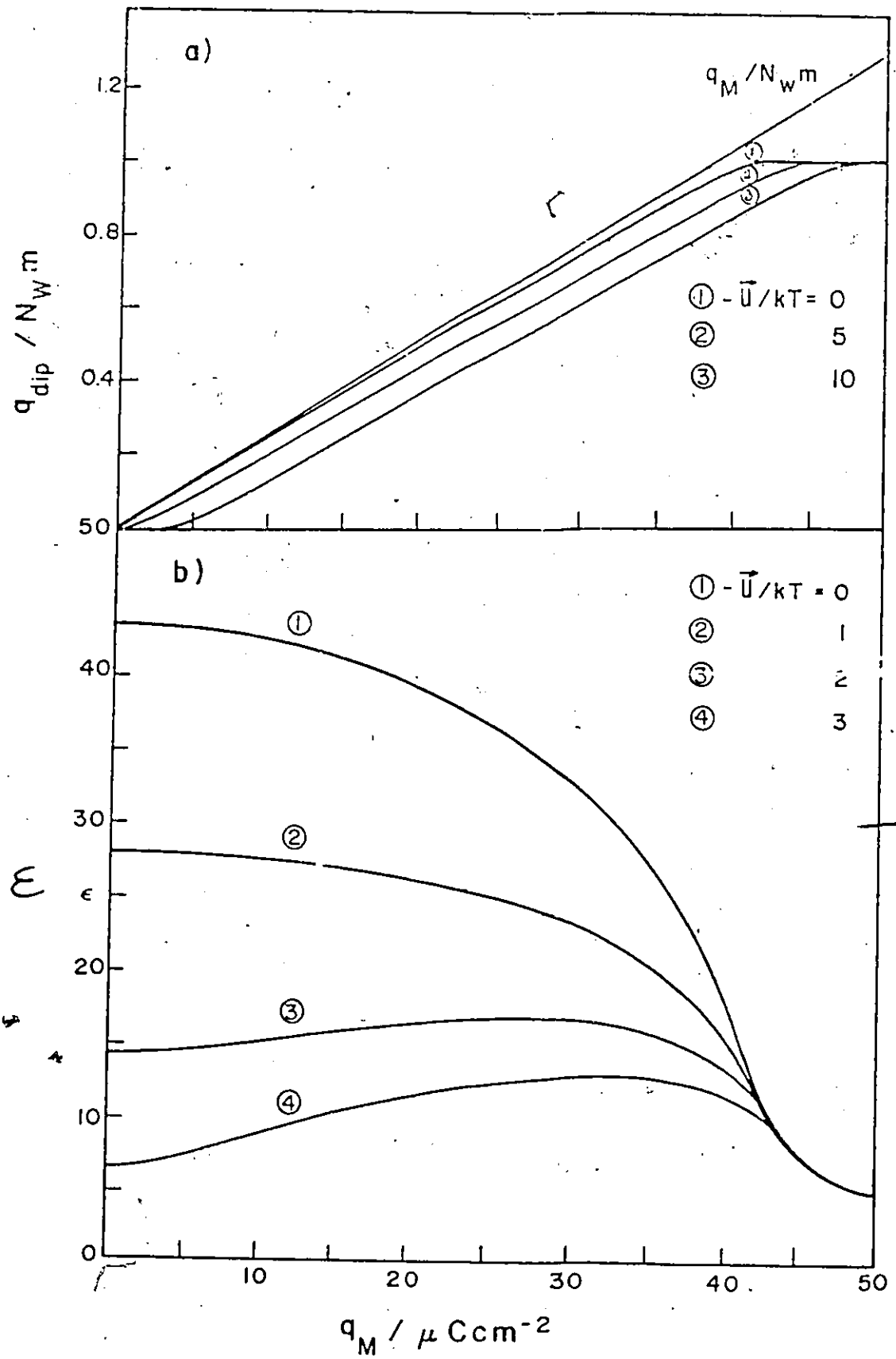
a)
$q_M / N_w m$
$q_{dip} / N_w m$
1.2
0.8
0.4
50
① - $\vec{U}/kT$ = 0
② 5
③ 10
b)
① - $\vec{U}/kT$ = 0
② 1
③ 2
④ 3
40
30
20
10
0
10
20
30
40
50
ϵ
$q_M / \mu C cm^{-2}$

differently from that according to other models. Specifically, for a finite value of U, the limiting slope of the curve of q_{dip} vs. q_M is not constant as $q_M = 0$ is approached; this corresponds to the intrinsic energy U being larger than the electrostatic energy of dipoles in the other configurations. In this limit, the effective dielectric constant is

$$\varepsilon_1 = 1 + \frac{(1 - c\alpha/Bd^3)8\pi N_w m^2/kT}{2 + 2m^2c/Bd^3kT + \exp(-U/kT)} \qquad [38]$$

In the absence of interactions, and with U = 0, this expression reduces to

$$\varepsilon_1 = 1 + (4\pi N_w m^2/kT).2/3 \qquad [39]$$

The factor of 2/3 is simply the fraction of dipoles in "polarizable" states, in the limit of zero field. For this special case, the polarization function is very similar to the Brillouin function of order 1, describing the magnetic polarization of a paramagnetic salt in which the dipoles can assume 3 = 2 x 1 + 1 orientations with respect to the field. It is easily shown that the expression may be written as

$$q_{dip} = N_w m[(3/2)\coth(3mE/2kT) - (1/2)\coth(mE/2kT)] \qquad [40]$$

With the approximation $\coth x \approx 1/x + x/3$, this gives

$$q_{dip} = (2N_w m^2/3kT)E \qquad [41]$$

Therefore

$$q_{dip} = (8\pi N_w m^2/3kT)/(1 + 8\pi N_w m^2/3kT) \qquad [42]$$

from which follows the above result on substitution into eqn. 23. As expected from the shape of the polarization curves for the three-state model, the effective dielectric constant initially increases with increasing field (i.e. q_M) for sufficiently large

values of U, as shown in Fig. 7b.

5. Calculation of Capacitance Behaviour

(i) General

The double layer capacitance may be calculated, as usual, as a function of q_M or of V. For a given value of q_M, the polarization q_{dip} (and hence its derivative dq_{dip}/dq_M) must be obtained by solution of implicit equations of the type 16. If V be specified, the problem can be considered as the determination of $\Delta\phi_1$ by solving an equation of type 10. An alternative but equivalent procedure involves combination of the implicit equation for q_{dip} with the inverse of the equation representing q_M in terms of the diffuse-layer potential drop $V - \Delta\phi_1$, viz. [32]

$$V = 4\pi d(q_M - q_{dip}) + (2kT/e_0)\sinh^{-1}(q_M/2A) \qquad [43]$$

The simultaneous solution of eqn. 43 and, e.g. 16a, 16b, or 32 is found to converge more rapidly than the solution of equations of the type 10.

As observed before, the differential capacitance of the inner-layer may be expressed in terms of the derivative dq_{dip}/dq_M. The inverse of the total differential capacitance may be obtained by differentiating equation 43 with respect to q_M:

$$1/C = 4\pi d(1 - dq_{dip}/dq_M) + (kT/e_0A)/[1 + (q_M/2A)^2]^{1/2} \qquad [44]$$

The inverse capacitance expressions for the inner-layer, appropriate for each of the models which are being considered, are as follows (for brevity, the interaction effects will be included as components of an effective field, following Cooper and Harrison [16] and Levine et al [24]):

$$1/C_1(\text{continuous}) = 4\pi d/[1 + (4\pi N_w m^2/kT)L'(mE/kT)] \quad [45a]$$

where $E = 4\pi(q_M - q_{dip})$;

$$1/C_1\ (\text{BDM}) = 4\pi d \frac{1 + (Uc/kT)\,\text{sech}^2(mE/kT)}{1 + (Uc/kT + 4\pi N_w m^2/kT)\,\text{sech}^2(mE/kT)} \quad [45b]$$

where $E = 4\pi(q_M - q_{dip}) - (q_{dip}/N_w m^2)Uc$; and

$$1/C_1\ (\text{Fawcett}) = 4\pi d \frac{4 + 2\exp(-U/kT)\cosh(mE/kT)}{[2\cosh(mE/kT)\exp(-U/kT)]^2} \quad [45c]$$

where $E = 4\pi(q_M - q_{dip})(1 - \alpha c/Bd^3) - (cm/Bd^3)q_{dip}/N_w m$.

(ii) Continuous-Orientation Model

In Fig. 8a, the total differential capacitance for the continuous-orientation model is shown for various concentrations c of 1:1-valent electrolyte. As expected, the "fine structure" due to the diffuse-layer contribution vanishes for large c. The curves are completely symmetrical and tend to a low limit with large positive or negative potentials, in contrast with experiment; this is because the simple model which is being used does not take into account e.g. asymmetrical dependence of N_w on the potential [13,18] or ionic composition of the double layer [27]. Here the main intention is to predict qualitatively the effect of dielectric saturation on the capacitance.

The importance of N_w in determining the value of the inner-layer capacitance is shown in Fig. 9a, where the inner-layer component is shown separately as a function of q_M. The values of C_1 are not exactly proportional to N_w, owing to the implicit nature of the equations defining q_{dip}, but it is easy to see how an appreciable unidirectional variation of N_w with q_M could give rise to a pronounced asymmetry in the curves, about the potential

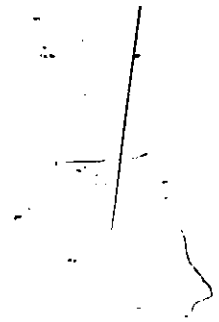

Fig.8a: Differential capacitance for continous-orientation model, with $N_w = 3.342 \times 10^{22}$ cm^{-3}, other parameters as in Fig.1.

b: Differential capacitance for modified BDM model (eqn. 45b) with $N_w = 3.342 \times 10^{22}$ cm^{-3}, other parameters as in Fig. 1.

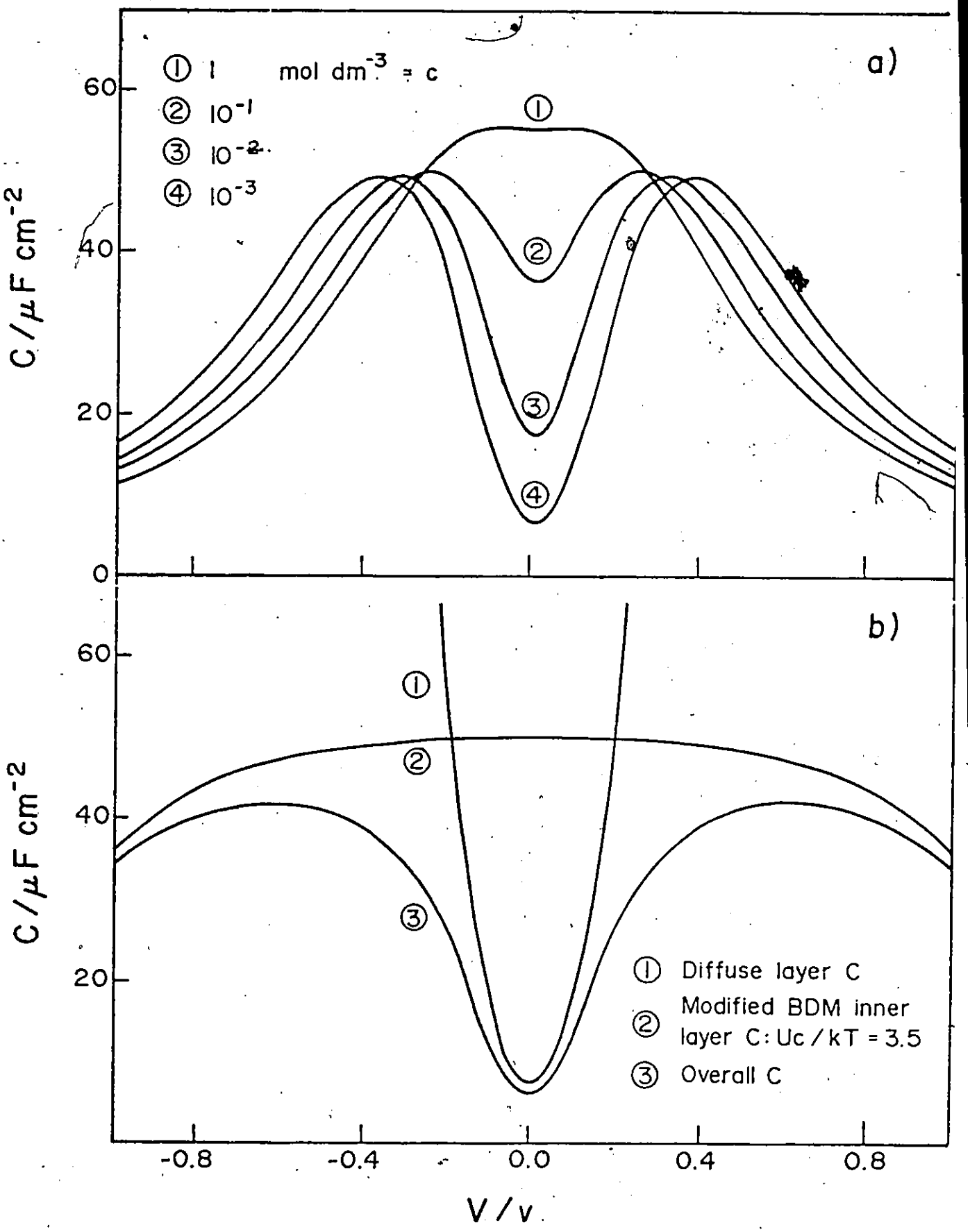
a)
① 1 mol dm^{-3} = c
② 10^{-1}
③ 10^{-2}
④ 10^{-3}
C / μF cm^{-2}
60
40
20
0
b)
C / μF cm^{-2}
60
40
20
① Diffuse layer C
② Modified BDM inner layer C: Uc / kT = 3.5
③ Overall C
-0.8
-0.4
0.0
0.4
0.8
V / v

Fig.9a: Inner-layer capacitance for continuous-orientation model.

b: Inner-layer capacitance for BDM model, with $N_w = 3.342 \times 10^{22}$ cm^{-3}.

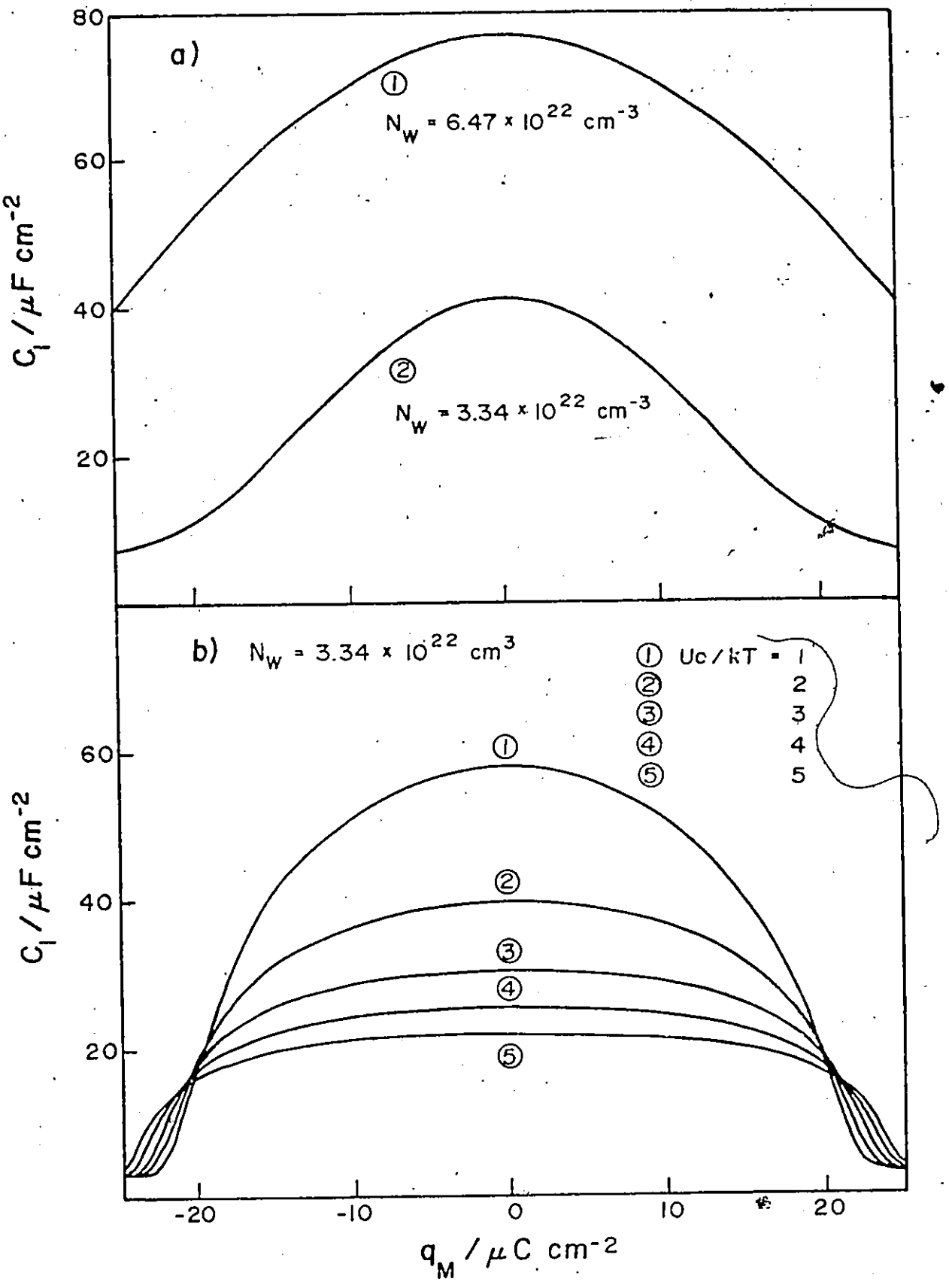
a)
① $N_w = 6.47 \times 10^{22}$ cm^{-3}
② $N_w = 3.34 \times 10^{22}$ cm^{-3}
C_1 / μF cm^{-2}
80
60
40
20
b) $N_w = 3.34 \times 10^{22}$ cm^3
① Uc / kT = 1
② 2
③ 3
④ 4
⑤ 5
C_1 / μF cm^{-2}
60
40
20
-20
-10
0
10
20
q_M / μC cm^{-2}

Fig.10a: Inner-layer capacitance as a function of q_M. Curve 1: BDM theory with U = 0; Curve 2: continuous-orientation model; Curve 3: Dipole capacity according to ref. 11. $N_w = 3.342 \times 10^{22}$ cm^{-3}.

b: Inner-layer capacity according to the Fawcett model, with no interactions and $N_w = 3.342 \times 10^{22}$ cm^{-3}.

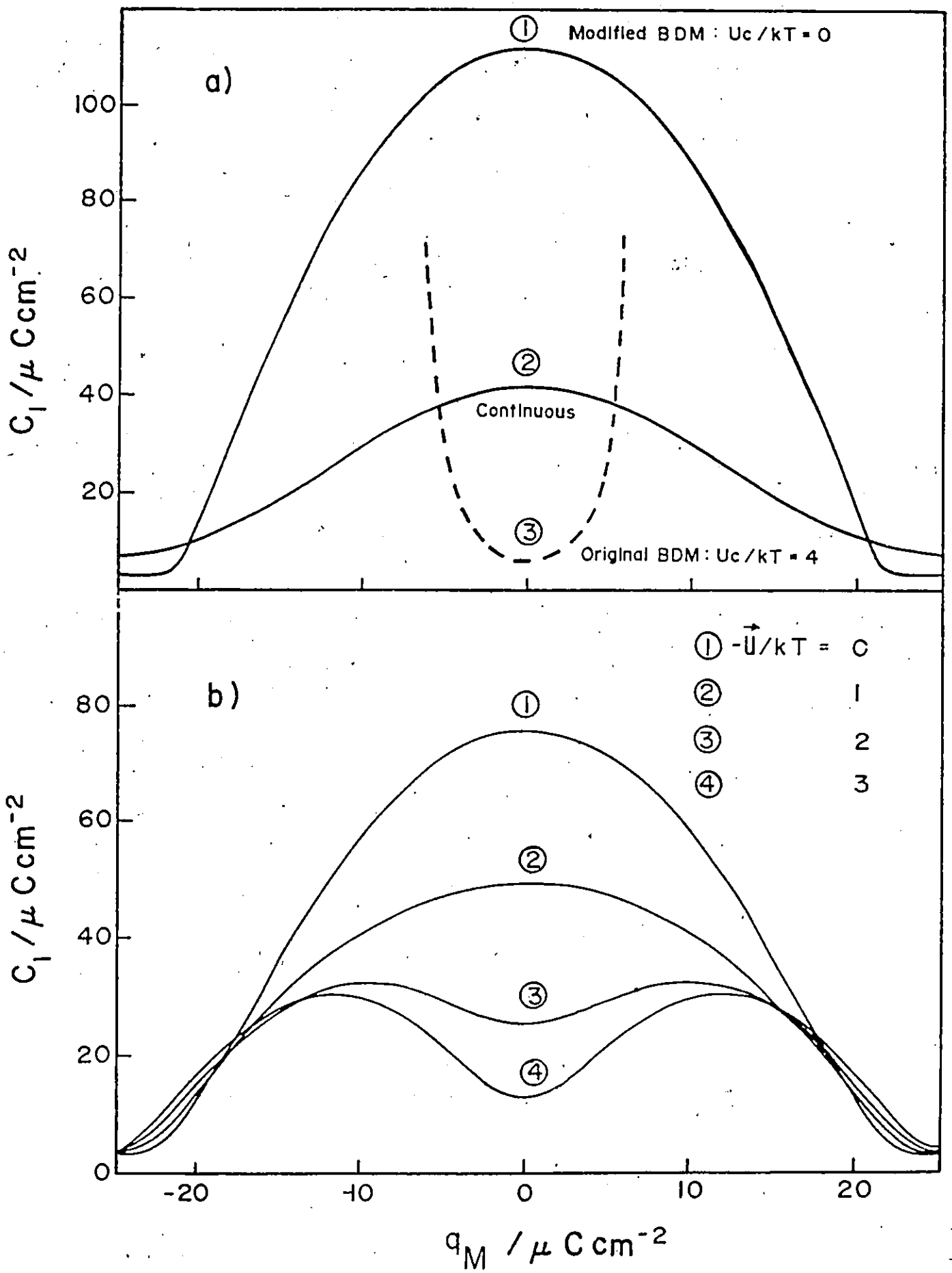
a)
① Modified BDM : Uc / kT = 0
②
Continuous
③
Original BDM : Uc / kT = 4
100
80
60
40
20
$C_1 / \mu C cm^{-2}$
b)
① $-\vec{U}/kT$ = 0
② 1
③ 2
④ 3
80
60
40
20
0
-20
-10
0
10
20
$q_M / \mu C cm^{-2}$

of zero charge.

(iii) Two-State Model: Comparison with BDM's Capacity Calculations

The capacitance components for this model, according to eqn. (45b), are shown as a function of V in Fig. 8b for c = 0.001 mol dm^{-3}, and the inner-layer component separately in Fig. 9b as a function of q_M. From the latter, it is seen that the saturation behaviour is sensitive to the value of Uc/kT; this corresponds to the dependence of the slope of the polarization curves given earlier on the value of this parameter. From Fig. 10a, it is seen that for Uc/kT = 0 the capacitance is very much larger than the corresponding capacitance for the continuous-orientation model, which reflects the more rapid variation of the tanh function with its argument than that of the L function.

It is evident that the inner-layer capacitance curves calculated according to the above procedure are both qualitatively and quantitatively different from those presented by BDM in their paper of 1963 [11]. This is because they treat a "triple layer" model in which a dipole layer capacitance is independent of an ionic Helmholtz layer capacitance (but each is a function of q_M) and in series with it rather than regarding, as is implicit in our modified BDM treatment and Watts-Tobin's work, the dipole layer as the dielectric of variable polarization within the Helmholtz layer itself.

Specifically, the curves presented here show that the capacitance decreases, eventually to a limiting value, with increasing positive or negative values of q_M (which is what would be expected as a result of dielectric saturation and is also

qualitatively in agreement with the semi-empirical calculations of refs. 1,2,3 and 12), whilst those of BDM increase to infinity with increasing q_M. This discrepancy can be traced to the way in which the dipole potential is calculated in terms of the orientation fraction Y (cf., apart from minor changes in notation, eqns. 34 and 35 of ref. 11), viz.

$$\Delta\phi_{dip} = 4\pi N_T m Y/\varepsilon_{low} \qquad [46]$$

in which N_T is the number of molecules per unit area and ε_{low} is taken as <u>constant</u> (= 6). Accordingly, they obtain the dipole capacitance by differentiating eqn. 46 with respect to q_M, resulting in

$$1/C_{dip} = (N_T/kT).(4\pi m/\varepsilon_{low})^2(1-Y^2)/[1 + (1\mathrm{?}Y^2)Uc/kT] \qquad [47]$$

from which it is seen that for large values of q_M, $Y^2 \to 1$, so that C_{dip} tends to infinity. This situation seems physically unreasonable since, using the analogy of a parallel-plate condenser, an increasingly large capacitance means that a vanishingly small potential drop is required to sustain a given charge on the plates. On the contrary, the effect of dielectric saturation should be to require an increasingly large potential drop to sustain such a charge density. However, BDM regard the C_{dip} to be in a series relation with (i) a supposed contact-adsorption capacitance associated wih ionic contact-adsorption, and with (ii) the diffuse-layer (the "triple layer" model [11]); by contrast, in Watts-Tobin's treatment, the dipole orientation corresponds to polarization of the solvent layer acting as the dielectric of the double layer "metal to OHP" rather than as a separate region. The above anomaly would not arise in the actual BDM treatment, since if $C_{dip} \to \infty$, $C_1 \to C_{contact\ ads.}$ (cf. Bockris

and Reddy in Ref. 11). A further problem seems nevertheless to arise insofar as BDM only treat the case of specific adsorption (using Grahame's results for aq. KCl) without referring to the case of aq. NaF solutions, with virtual absence of contact adsorption, for which, however, "capacitance hump" behaviour is still clearly manifested. Thus, the BDM treatment, while having some ideas in common with the Watts-Tobin treatment, offers a fundamentally different basis for the explanation of the capacitance hump, yet one which may not be applicable to cases (such as aq. NaF) where ionic specific adsorption is unimportant.

The problem of the prediction of increasing dipole-layer capacitance with increasing q_M that follows from eqn. 47, does not arise in the approach used in the present chapter, where the potential drop is expressed in terms of the field $4\pi(q_M - q_{dip})$ and not simply in terms of q_{dip} alone as implied by eqn. 46. In other words, it is necessary to include in $\Delta\phi_1$ the contribution arising from the charge density itself, as in ref. 9. The inner-layer capacitance, given by inverting eqn. 45b, correctly tends to $1/4\pi d$ for large q_M, implying (as it must) a limiting value of ε of unity in the absence of electronic polarization contributions, as assumed here.

A further important point is as follows: presuming that this deduction about the significance of BDM's calculation of the dipole layer capacitance is correct, it means that their conclusion that C_1, being usually [11] much larger than other (so-called contact adsorption) capacitance components of the double layer except that of the diffuse layer, does not determine

the overall capacitance behaviour, is incorrect. This appears to have been the implicit conclusion reached by several authors of subsequent papers [1,3,12,24] but without there being given any explicit basis of the kind presented here. In fact, post-BDM calculations on inner-layer capacitance have concentrated on explaining the results from Grahame's well-known [32] data for aqueous NaF at Hg in terms of the dipole-layer properties rather than (cf. ref. 11) in terms of ionic contact adsorption with negligible contribution from a BDM-type dipole capacitance component.

In the light of the results presented in this section, it is of interest to consider the approach used by Cooper and Harrison themselves in their treatment of the inner-layer capacitance. The "effective field" to which they refer is the sum of the vacuum field q_M/ϵ_0 (= $4\pi q_M$ in the notation of this chapter) and a field corresponding to the total interaction energy experienced by a given dipole amongst its neighbours. The ensemble average of this quantity gives the field which is used in their implicit definition of the polarization fraction R (which is referred to here as Y); cf. eqns. 7, 13 and 14 of ref. 16. This equation is of essentially the same form as eqn. 5 of the present chapter. When they come to calculate the differential capacitance, Cooper and Harrison invoke an electrostatic equation equivalent to eqn. 15 above in order to define the "total" electric field E_t in the inner-layer. This field is then converted into a potential difference by multiplying by the layer thickness, and differentiated implicitly with respect to q_M to obtain the inverse of the capacitance component. Since Cooper and Harrison's

E_t is essentially identical to the field which has been used here, it may be concluded that the resulting catastrophic behaviour arises because they evidently use the vacuum field (proportional to q_M - see p. 94 of ref. 16) and not E_t in their equation 18 for R (Y). In other words, as pointed out in sections 2 and 3, it seems that the catastrophe which arises in their treatment may be attributed to an inconsistency between the field assumed to orient the dipoles and the field which determines the potential drop across the inner-layer.

(iv) Fawcett Three-State Model

The inner-layer capacitance component calculated from eqn. 45c is shown in Fig. 10b. For small values of the third-state energy U, the curves are qualitatively similar to those for the other two models, but a minimum appears for sufficiently large U, corresponding to the intrinsic energy of the third state being greater than the electrostatic energy of the parallel/antiparallel states. This minimum is evidently predicted for the same reason as the increase in effective dielectric constant with increasing q_M, shown in Fig. 8b, and the corresponding plateaux in the polarization curves of Fig. 7a. Fig. 10b is in agreement with capacitance curves calculated by Fawcett [12], who has used this model to interpret capacitance curves measured in electrolytes with aspherical solvent molecules.

The general form of Fig. 10b is also similar to the differential capacitance curves measured in the presence of adsorbing organic molecules, in that it exhibits a minimum at the

point of zero charge. The minima in such capacitance curves are generally interpreted [33] in terms of a reduction of the effective dielectric constant of the inner region due to replacement of water molecules by those of the adsorbate. In the absence of adsorbing molecules, the polarization of solvent according to the Fawcett model can be interpreted similarly, as a "replacement" of molecules in polarizable states by those in the third, non-polarizable state. The calculation of capacitance curves in the presence of organic adsorbates will be dealt with in Chapter 2.

In recent papers of Badiali et al [34] and Schmickler [35], the effects of potential-dependent electron overspill on double-layer capacitance behaviour have been examined. Physically, the tail of the electron distribution extends significantly beyond the metal "surface" and so can be expected to exert some polarization influence on the solvent dipoles in this region. The effect of introducing a finite jellium polarizability is to increase the height of the capacitance maximum around $q_M = 0$. However, the profiles of capacitance as a function of q_M remain essentially symmetrical. Since it has been shown in earlier sections of this chapter that the Cooper-Harrison paradox arises from the electrostatic treatment of the inner-layer solvent polarization, including the consideration of lateral interactions, it does not seem that the introduction of the jellium polarizability will have more than a slight perturbing effect on the dipole polarization vs. q_M relation in the BDM treatment, which predicts paradoxical behaviour for small values of Uc/kT.

6. Some Refinements of the Primitive Model

The calculations presented so far have been based on a deliberately simplified specific model for the interface, but one which is, withal, essentially the same as that used in most existing theoretical treatments of double-layer capacitance behaviour. One of the most important simplifications, apart from the neglect of interactions, is that the number density of polarizable species in the compact double layer is constant. The earliest treatment to incorporate a possible variation of N_w was that of Macdonald and Barlow [14], which did so by considering the electrostrictive effect of the interfacial field on the pressure in the inner layer, and hence the number density. More recent work by Conway [18,27] has concentrated on the related problem of overlap between ionic hydration co-spheres in solution and at electrodes. In the present section, some consequences of each of these effects will be considered, in the light of the results discussed in the preceding sections.

(i) Influence of Diffuse-Layer Ions on Inner-Layer Polarization

The dimensions of the compact double layer assumed in the calculations so far are such that the distance of closest ionic approach to the electrode is at least equal to the molecular diameter. If the ions are hydrated, this implies that the are some water molecules which are located in the inner layer, but, by virtue of their strong attachment to ions, do not contribute to the inner-layer polarization of the electrode. This situation will evidently result in the following:

(a) Potential-dependence of the dipolar number density N_w

(b) Dependence of the polarization behaviour on the size of the hydrated ions, viz. on the number of inner-layer lattice sites occupied by members of the hydration spheres of ions located at the outer Helmholtz plane

(c) A purely "mechanical" interdependence of the compact and diffuse-layer capacitance components.

A detailed consideration of the implications of "specific" ionic adsorption (in which ions are supposed to occupy the inner layer) will be given in Chapter 6; in anticipation of this later discussion, it is therefore of interest to consider the qualitative implications of "non-specific" effects of ions, such as those considered here, with regard to the predicted capacitance behaviour.

According to the Gouy-Chapman theory, the charge-balance condition to be satisfied by the interface is given by eqn. 12; in terms of the inner-layer field E_1, this may be written

$$q_M = 2A \sinh[(V-E_1 d)e_0/2kT] \qquad [48]$$

The numbers of cations and anions in the plane where the potential is $V-E_1 d$ are respectively

$$n_+ = n_0 \exp[-(V-E_1 d)e_0/kT] \qquad [49a]$$

$$n_- = n_0 \exp[(V-E_1 d)e_0/kT] \qquad [49b]$$

so that the total number of ions in this plane is

$$n_+ + n_- = 2n_0 \cosh[(V-E_1 d)e_0/kT] \qquad [50]$$

If it be now supposed that each cation and anion occupy p_+ and p_- sites in the inner layer respectively, the total number of sites thus occupied (i.e., polarizable water molecules excluded) is

$$p_+n_+ + p_-n_- = n_0(p_+ \exp[-(V-E_1 d)e_0/kT)] + p_- \exp[(V-E_1 d)e_0/kT]) \qquad [51]$$

so that the departure of the number density N_w from its normal

value N_w^0 may be expressed by the equation

$$N_w = N_w^0(1 - \psi) \qquad [52]$$

where

$$\psi = (p_+\exp[-(V-E_1d)e_0/kT] + p_-\exp[(V-E_1d)e_0/kT])n_0/N_w^0 \qquad [53]$$

In the absence of specific adsorption, the charge density on the electrode may also be written as, e.g.

$$q_M = E_1/4\pi + N_w m.L(mE_1/kT) \qquad [54]$$

and as before, equating these two expressions for q_M permits the determination of E_1, by the solution of the equation

$$E_1/4\pi + N_w^0(1-\psi)L(mE_1/kT) = 2A \sinh[(V-E_1d)e_0/2kT] \qquad [55]$$

where the potential-dependence of ψ is given by eqn. 52.

The inner-layer capacitance requires the derivative dq_{dip}/dq_M, which in this case is given by

$$dq_{dip}/dq_M = (N_w^0m^2/dkT)(1-\psi)L'(mE_1/kT).d\Delta\phi_1/d_M - N_w^0m\ L(mE_1/kT).d\psi/dq_M \qquad [56]$$

where

$$d\psi/dq_M = (n_0/N_w^0)(p_-\exp[(V-E_1d)e_0/kT] - p_+\exp[-(V-E_1d)e_0/kT]) \times (e_0/kT).d\Delta\phi_2/dq_M \qquad [57]$$

Identifying the derivatives of the two potential drops with the corresponding reciprocal capacitance components, one obtains the followng equation for C_1:

$$1/C_1 = 4\pi d(1 - dq_{dip}/dq_M)$$

$$= 4\pi d[1 - (N_w^0m^2/dkT)(1-\psi)L'(mE_1/kT).1/C_1 - N_w^0m\ L(mE_1/kT)(n_0/N_w^0)(p_-\exp[(V-E_1d)e_0/kT] - p_+\exp[-(V-E_1d)e_0/kT]) \times (e_0/kT).1/C_2 \qquad [58]$$

whence

$$C_1 =$$

Fig.11: Total capacitance as a function of V, with consideration of the non-specific ionic effects of the diffuse layer. $c = 0.1$ mol/l, $N_w^0 = 3.342 \times 10^{22}$ cm^{-3}.

Curve 1: $p_+ = 1$, $p_- = 2$

Curve 2: $p_+ = 2$, $p_- = 1$

Curve 3: $p_+ = 0$, $p_- = 0$

V - p.z.c./V

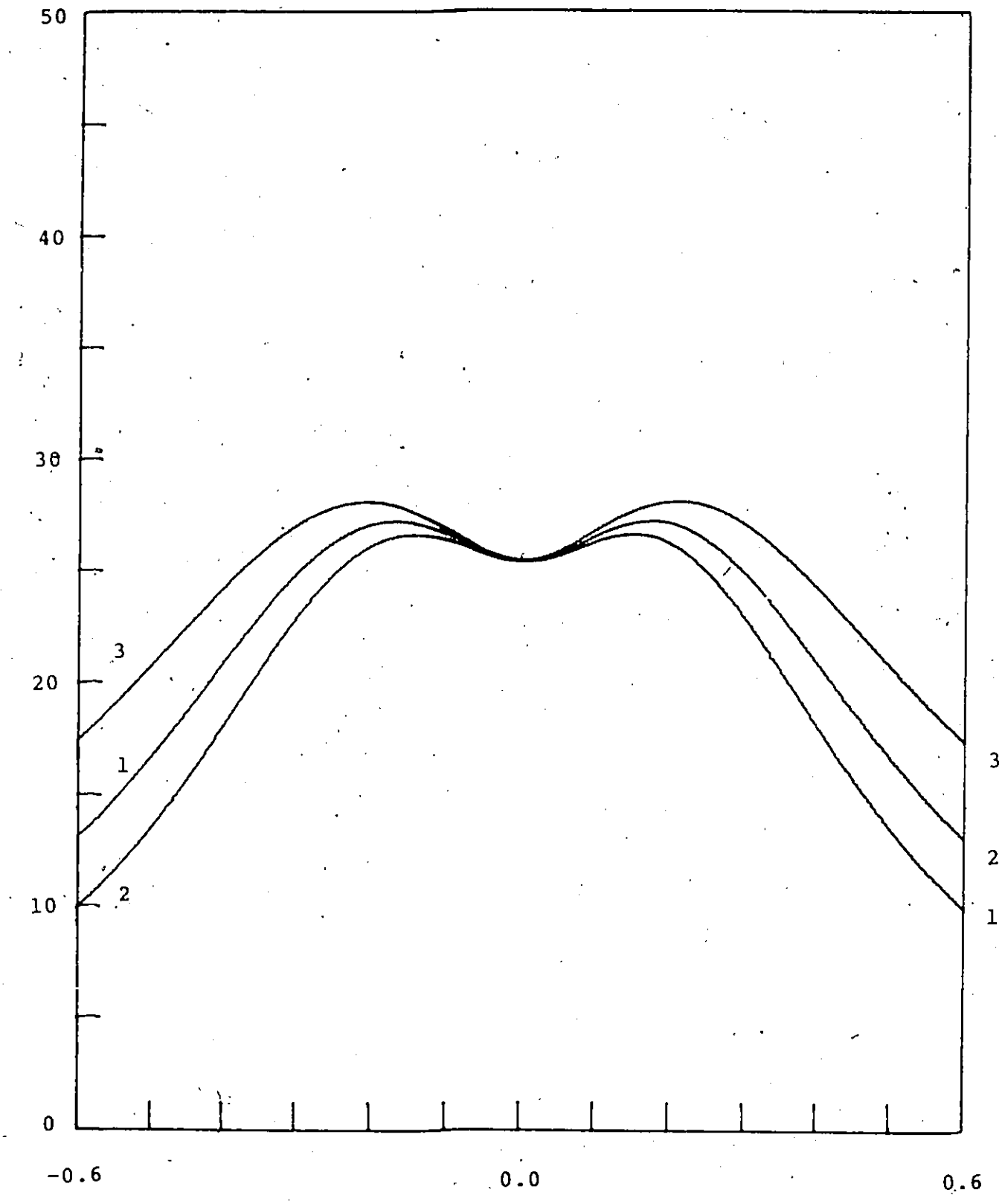
10^6C/F cm^{-2}
50
40
30
20
10
0
3
1
2
3
2
1
-0.6
0.0
0.6
V/V

$$1 + (4\pi N_w^0 m^2/kT).(1-\psi)L'(mE_1/kT)$$

$$4\pi d[1 - (me_0n_0/kT)(p_-exp[(V-E_1d)e_0/kT] - P_+exp[-(V-E_1)e_0/kT])]/C_2 \quad [59]$$

This clearly reduces to the previous expression for the continuous-orientation when $\psi = 0$; from the form of eqn. 59, it is evident that the differential dielectric constant implied in this capacitance is dependent on C_2 not only in an indirect fashion, via the electrical boundary conditions, but also directly in the potential-dependent denominator expressing the non-specific ionic effect.

Fig. 11 shows the total capacity $C = C_1C_2/(C_1+C_2)$ as a function of potential, for the particular case of c = 0.1 mol/l. The effect is to reduce the capacity (i.e. the dominant inner-layer component), as suggested by eqn. 59. It thus seems that this effect is small, both qualitatively and quantitatively, especially considering the assumptions made in the calculation. Nevertheless, the above argument is of interest in that it demonstrates how an interdependence of C_1 and C_2 may arise in a manner not previously noted in the literature.

(ii) Relationship Between Number Density and Polarization Energy

The double-layer calculations of Macdonald and Barlow [14] incorporated electrostriction effects by representing the density of water as a function of pressure by using an empirical equation of state, and identifying the pressure with electrostrictive pressure associated with the inner-layer field. While it is almost a truism to observe that these results are strictly true only for continuous media, since precisely the same can be said

of the electrostatic equations used in the preceding calculations, it is nevertheless evident that some macroscopic quantities lend themselves more readily than others to a microscopic interpretation. Thus, rather than introducing the electrostriction effect indirectly through the attribution of a "pressure" to a polarized monolayer, it seems preferable to consider the problem directly in terms of molecular polarization free energies.

As noted earlier, the number density of bulk, un-electrostricted H_2O is only about half that corresponding to a close-packed monolayer. In order to consider the consequences of a variation of N_w such as that referred in Section 5 (ii), it may be supposed that N_w be given by an equation of the form

$$N_w = N_{w,0} + \gamma(N_{w,1} - N_{w,0}) \qquad [60]$$

where

$$N_{w,0} = 3.342 \times 10^{22} \text{ cm}^{-3} \text{ (bulk)}$$

$$N_{w,1} = 6.469 \times 10^{22} \text{ cm}^{-3} \text{ (close-packed)}$$

(the latter figure being based on an assumed molecular diameter of 2.7×10^{-8} cm), and γ is a fraction describing the amount of free space in the surface layer. The problem of determining γ is formally identical to that of determining the coverage fraction θ in a Langmuir adsorption isotherm. Thus, it is possible to write

$$\gamma/(1-\gamma) = \exp(-\Delta\mu_w^0/RT) \qquad [61]$$

where

$$\Delta\mu_w^0 = -RT \ln(z_w) - RT \ln(z_w^0)$$

and z_w, z_w^0 are the electrical and non-electrical partition functions, respectively. $\Delta\mu_w^0$ is thus the free energy change of transferring one mole of water molecules from the diffuse layer

(where, according to the primitive model, their polarization free energy may be neglected) to the adsorbed layer, where it is polarized by the electrode and acted upon by field-independent forces. From statistical mechanics [25,29], the electrical partition function of a dipole, polarized by a field E_1 with respect to which it can assume continuous range of orientations, is

$$z_w = 4\pi\exp(\alpha E_1^2/2kT).\sinh(mE_1/kT)/(mE_1/kT) \qquad [62]$$

The "isotherm", eqn. 61, may readily be solved:

$$\gamma = z_w^0 z_w/(1 + z_w^0 z_w) \qquad [63]$$

In order to calculate the effects of such a variation of N_w on the predicted capacitance behaviour, one again starts from the definition of q_{dip}, which is identical to eqn. 21, but with N_w given by eqn. 60. Differentiating, one has

$$dq_{dip}/dq_M = (1 - dq_{dip}/dq_M) \times [(N_{w,0} + \gamma(N_{w,1}-N_{w,0}))f_2 + \gamma(1-\gamma)(N_{w,1}-N_{w,0})f_1] \qquad [64]$$

where

$$f_1 = (4\pi/kT)[\alpha E_1 + mL(mE_1/kT)]$$

$$f_2 = 4\pi[\alpha + (m^2/kT)L'(mE_1/kT)]$$

and use has been made of the result

$$dN_w/dq_M = \gamma(1-\gamma).\partial\ln(z_w)/\partial E_1, 4\pi(1-dq_{dip}/dq_M)(N_{w,1}-N_{w,0}) \qquad [65]$$

Solving for dq_{dip}/dq_M,

$$dq_{dip}/dq_M = \frac{[N_{w,0} + \gamma(N_{w,1}-N_{w,0})]f_2 + \gamma(1-\gamma)(N_{w,1}-N_{w,0})}{1 + [N_{w,0} + \gamma(N_{w,1}-N_{w,0})]f_2 + \gamma(1-\gamma)(N_{w,1}-N_{w,0})f_1} \qquad [66]$$

so that

$$C_1 = [1 + [N_{w,0} + \gamma(N_{w,1}-N_{w,0})]f_2 + \gamma(1-\gamma)(N_{w,1}-N_{w,0})f_1]/4\pi d$$

The expression for the differential dielectric constant in this case is thus seen to reduce to eqn. 22 in the limiting cases when $\gamma = 0$ or 1.

It is evident that the prediction of an effect of this type would be dependent on the relative values of the electrical and non-electrical factors of the partition function for the adsorbed water molecules, to say nothing of their interactions with neighbours; if the field-independent terms were very large, the fraction γ would be effectively unity, even in the vicinity of the p.z.c., so that the overall variation of the number density in this manner would be negligible. Also, the nature of this variation is evidently dependent on the form of the field-dependence of the partition functions; z_w as given by eqn. 62 is obviously an even function of its argument, so that the variation of γ would be symmetrical about the p.z.c.. and therefore incapable of explaining, by itself, the asymmetry in experimental capacitance behaviour. A slight asymmetry would result if a field-independent orientational energy difference of the dipoles were incorporated into the model, but the strong field-dependence of the partition functions would dominate this for potentials appreciably removed from the p.z.c.

This particular calculation, of course, neglects interaction effects, but the method described above could still, in principle, be employed to describe the electrostriction effects with the inclusion of interactions. The question of interactions between dipoles is considered in detail in Chapters

4 and 5. Application of the approximations of lattice-gas theory to describe these electrostriction effects in this manner would result in an "isotherm" for γ which would no longer be of the Langmuir-form, but would be an implicit function of γ. Alternatively, one would have to abandon the lattice formulation, and express the thermodynamic functions for the adsorbed dipoles in terms of two-dimensional radial distribution functions; most treatments of primitive models are based on lattices, since these are more tractable than two-dimensional fluids. From a physical point of view, it is conceivable that a lattice might indeed be the more appropriate physical description, e.g. if the adsorption energy were high enough and the surface were crystalline, permitting epitaxial adsorption. If this were the case, however, the value of γ would be virtually equal to 1.

One physical effect which has not hitherto been considered is the possibility of an electronic interaction between adsorbed species and the excess charge density q_M; this energy would vary in an asymmetric fashion about the p.z.c. and could, in principle, give rise to a unidirectional variation of N_w.

(iii) Consideration of a Second Polarized Layer

The solution of eqn. 16b determines not only q_{dip} for given q_M, but also the field within the layer of molecules. Since q_{dip} has been shown to be less than q_M, this field has a finite value, and will operate on the next layer of molecules; in an analogous fashion, it is possible to determine the polarization of this second layer. Clearly, it is less realistic to assume the existence of a second ion-free layer of water molecules, but it is nevertheless of interest to investigate the qualitative effect

of inclusion of such a second layer on the predicted capacitance, neglecting non-orientational polarizability contributions.

The potential drop is in this case represented as the sum of three potential drops:

$$V = \Delta\phi_1 + \Delta\phi_2 + \Delta\phi_3 \qquad [68]$$

which are defined as follows in terms of the relevant charge densities:

$$E_1 = 4\pi(q_M - q_{dip,1}) = \Delta\phi_1/d \qquad [69]$$

$$E_2 = 4\pi(q_M - q_{dip,1} - q_{dip,2}) = \Delta\phi_2/d \qquad [70]$$

$$\Delta\phi_3 = (2kT/e_0)\sinh^{-1}(q_M/2A) \qquad [71]$$

The polarizations in each layer satisfy the equations

$$q_{dip,1} = N_w m\, L(mE_1/kT) \qquad [72]$$

$$q_{dip,2} = N_w m\, L(mE_2/kT) \qquad [73]$$

In calculating the capacitance, one has to take account of the effect of the first potential drop on the second:

$$1/C = d\Delta\phi_1/dq_M + d\Delta\phi_2/dq_M + d\Delta\phi_3/dq_M \qquad [74]$$

From earlier working

$$d\Delta\phi_1/dq_M = 4\pi/[1 + (4\pi N_w m^2/kT)L'(mE_1/kT)] \qquad [75]$$

$$d\Delta\phi_2/dq_M = 4\pi d[1 - dq_{dip,1}/dq_M - dq_{dip,2}/dq_M] \qquad [76]$$

where

$$dq_{dip,1}/dq_M = \frac{(4\pi N_w m^2/kT)L'(mE_1/kT)}{1 + (4\pi N_w m^2/kT)L'(mE_1/kT)}$$

$$dq_{dip,2}/dq_M = \frac{(4\pi N_w m^2/kT)L'(mE_2/kT)}{[1 + (4\pi N_w m^2/kT)L'(mE_1/kT)][1 + (4\pi N_w m^2/kT)L'(mE_2/kT)]}$$

Therefore the total inverse capacitance due to dipole

polarization is

$$d\Delta\phi_1/dq_M + d\Delta\phi_2/dq_M =$$

$$\left[\frac{4\pi d}{1 + (4\pi N_w m^2/kT)L'(mE_1/kT)}\right]\cdot\left[1 + \frac{1}{1 + (4\pi N_w m^2/kT)L'(mE_2/kT)}\right] \qquad [77]$$

and as before

$$d\Delta\phi_3/dq_M = (kT/e_0A)/[1 + (q_M/2A)^2]^{1/2} \qquad [78]$$

The differential capacitance of this "triple layer" is shown Fig. 12, with the corresponding capacity calculated for consideration of only one polarized layer. It seen that, interestingly, the second polarized layer makes only a minor difference to the predicted capacitance. The resultant polarization in both layers would, of course, be less with the inclusion of interactions <u>via</u> the Mean Field Approximation, but the above procedure for calculating the corresponding capacitances could still be used, taking account of the extra dependence of the effective fields on q_{dip}.

The division of the interface into a series of polarized layers is the basis of some very recent work by Macdonald and co-workers [36,37]. The most important difference between their work and that discussed in the present chapter is the treatment of the water dipoles as finite, rather than as infinitesimal. As a result of this abandonment of the usual point-dipole assumption, some very interesting mathematical results arise in the definition of the bound charge density as a function of distance. Nevertheless, the self-consistent definition of the free- and bound-charge densities in terms of the local electric field is

Fig. 12: Total capacitance as a function of V, for one [curve (1)] and two [curve (2)] dipole layers; c = 10^{-3} mol/l.

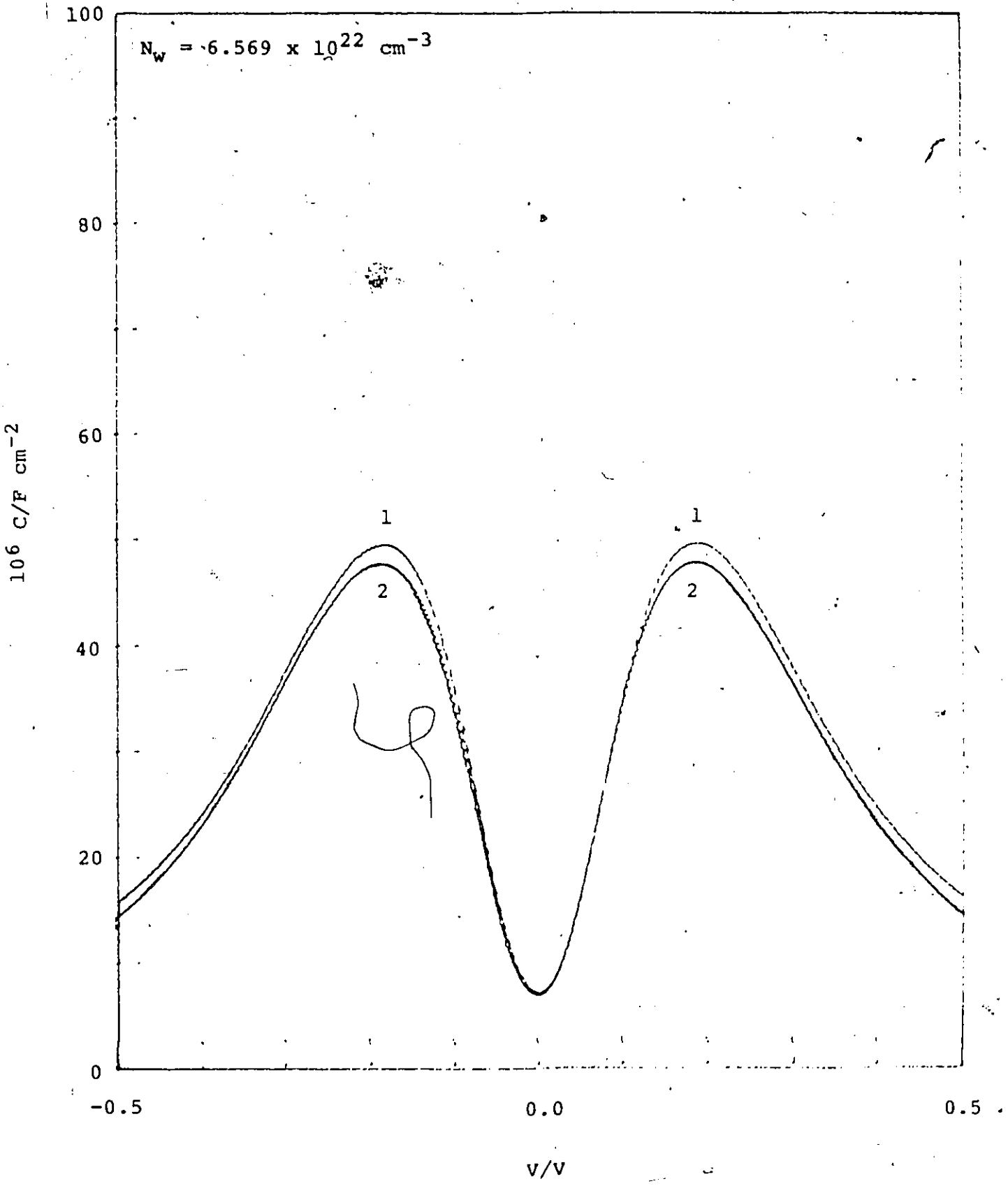

fundamentally similar to that which has been used, for the simple case of one polarized layer (eqn. 15), throughout the present work. The behaviour of this model, however, appears to be radically different from the point-dipole model, in that very little dielectric saturation is predicted.

7. Conclusions

Calculations of solvent dipole polarization in the inner region of the double layer are compared on the basis of three simple approaches: the Watts-Tobin/BDM two-state model, the Fawcett three-state model and a Debye-Langevin-type continuum-of-orientations model. The Cooper-Harrison paradox, in which the surface charge density q_M is exceeded by the induced charge density q_{dip}, arises in all treatments which assume that $E_1 \propto q_M$, and so is not a specific artefact of the two-state model. Also, the problem is unconnected with any metal-dependent preferred orientations of solvent dipoles. Whether or not this paradox arises is dependent, however, on the arbitrary assignment of the values of the model-dependent parameters.

The origin of the Cooper-Harrison paradox is traced to the way in which the field E, associated with the electrode surface charge which "causes" the polarization, is represented. When E is represented as $\Delta\phi_1/d$ (Watts-Tobin) or equivalently as $4\pi(q_M - q_{dip})$, instead of as $4\pi q_M$ or $4\pi q_M/\varepsilon_{low}$ (BDM), the paradox does not arise with any model.

The consequences of this difference in the representation of E are investigated with respect to the behaviour of the effective dielectric constant of the inner-layer and the corresponding component of the differential capacitance, as a function of field

or q_M.

The conclusion reached here that the origin of the paradox is in the way the electrostatic treatment of the orientational polarization has been given, rather than resulting from the intrinsic unrealities of the two-state model, is not in conflict with Parsons' deduction that the most stable configuration of dipoles at the p.z.c. is parallel to the surface. Physically, such an arrangement is probably correct, but this is a question separate from the problem of electrostatics addressed in the present chapter.

The implications of a variation in the number density of polarizable species in the inner-layer are examined briefly. The two possible mechanisms considered for this variation are a) occupation of space in the inner-layer by the hydration shells of non-specifically adsorbed ions, and b) electrostriction. The latter effect is interpreted in terms of the molecular free energy of polarization by the field E_1, influencing the tendency of solvent molecules to reside in the diffuse or compact double-layer regions.

The procedures described enable a comparison to be made of the predicted capacitance behaviour of several molecular models for the solvent polarization of the inner-layer. Subsequent work will examine their extension to the analysis of neutral molecule adsorption and dipole-displacement effects in electrode kinetics.

8.Acknowledgement

The writer gratefully acknowledges helpful comments by Dr J.R. Macdonald on some of the points discussed in the present chapter.

References

1. B.B. Damaskin and A.N. Frumkin
Electrochim. Acta **19**: 173 (1974)

2. B.B. Damaskin
Elektrokhimiya **1**: 63 (1965); see also
B.B. Damaskin
J. Electroanal. Chem. **75**: 359 (1975)

3. R. Parsons
J. Electroanal. Chem. **59**: 229 (1975)

4. B.E. Conway
Advances in Colloid and Interface Science **8**: 91 (1977)

5. S. Trasatti
J. Chem. Soc., Faraday Trans. I **68**: 229 (1972);
J. Electroanal. Chem. **39**: 163 (1972); **44**: 367 (1973); **54**: 437 (1974); **64**: 128 (1975)

6. M.D. Levi, A.V. Shlepakov, B.B. Damaskin and I.A. Bagotskaya
J. Electroanal. Chem. **1**: 138 (1962)

7. R. Parsons
quoted in ref. 4; see e.g. Electrochim. Acta, **21**: 681 (1976)

8. R.Payne
Advances in Electrochemistry and Electrochemical Engineering **7**: 1 (1970)

9. N.F. Mott and R.J. Watts-Tobin
Electrochim. Acta **4**: 79 (1961)

10. R.J. Watts-Tobin
Phil. Mag. **6**: 133 (1961)

11. J.O'M. Bockris, M.A.V. Devanathan and K. Mueller
Proc. Roy. Soc. Lond. **A274**: 55 (1963); see also

J.O'M. Bockris and A.K.N. Reddy

"Modern Electrochemistry" pp. 779-790, Plenum N.Y. (1972)

12. W.R. Fawcett

J. Phys. Chem. **82**: 1385 (1978); see also

W.R. Fawcett and M.D. Mackey

J. Chem. Soc. Faraday Trans. I **69**: 634 (1974)

W.R. Fawcett

Isr. J. Chem. **18**: 3 (1979)

13. J.R. Macdonald

J. Chem. Phys. **22**: 1857 (1954); see also

J. Chem. Phys. **22**: 763, 1317 (1954)

14. J.R. Macdonald and C.A. Barlow

J. Chem. Phys. **36**: 3062 (1962)

15. B.E. Conway and H.P. Dhar

Croat. Chim. Acta **45**: 173 (1973); see also

B.E. Conway, J.G.Mathieson and H.P. Dhar

J. Phys. Chem. **78**: 1226 (1974)

16. I.L. Cooper and J.A. Harrison

J. Electroanal. Chem. **66**: 85 (1975)

17. R. Parsons

J. Electroanal. Chem. **109**: 369 (1980); see also

Trans. SAEST (India) **13**: 239 (1978)

18. B.E. Conway and S. Marshall

Austr. J. Chem. **36**: 2145 (1983)

19. B.E. Conway and L.G.M. Gordon

J. Phys. Chem. **73**: 3609 (1969)

20. D.D. Eley and M.G. Evans

Trans. Faraday Soc. **34**: 1093 (1938)

21. D. Henderson and L. Blum

J. Electroanal. Chem. **132**: 1 (1982)

22. D. Henderson

Prog. Surf. Sci. **13**: 197 (1983)

23. L. Blum

J. Phys. Chem. **81**: 136 (1977)

24. S. Levine, G.M. Bell and A.L. Smith

J. Phys. Chem. **73**: 3534 (1969)

25. P. Debye

"Polar Molecules", Chemical Catalogue Company, N.Y. (1929);

Physik. Zeit. **13**: 97 (1912)

26. W. Schmickler

J. Electroanal. Chem. **157**: 1 (1983)

27. B.E. Conway

J. Electroanal. Chem. **81**: 123 (1981)

28. W. Schmickler

J. Electroanal. Chem. **149**: 15 (1983)

29. C.J.F. Boettcher

"Theory of Electric Polarization", 2ed., v.1, Elsevier, Amsterdam (1972)

30. J.B. Hasted

"Aqueous Dielectrics", Chapman and Hall, (1973)

31. H. Froehlich

"The Theory of Dielectrics", O.U.P. (1949)

32. D.C. Grahame

Chem. Revs. **41**: 441 (1947)

33. A.N. Frumkin

"Potentsialy Nulevogo Zaryada", Izdatel'stvo "Nauka" (1979), chapter 6.

34. J.-P. Badiali, M.-L. Rosinberg and J. Goodisman
J. Electroanal. Chem. **150**: 25 (1983)

35. W. Schmickler
J. Electroanal. Chem. **150**: 19 (1983)

36. J.R. Macdonald and S.W. Kenkel
J. Chem. Phys. **80**: 2168 (1984)

37. S.W. Kenkel and J.R. Macdonald
J. Chem. Phys. **81**: 3215 (1984)

CHAPTER 3

NEUTRAL MOLECULE ADSORPTION ISOTHERMS AND CAPACITANCE EXPRESSIONS

The present chapter examines the application of the results and conclusions of Chapter 2 to the description of neutral molecule adsorption at electrodes. This area of interfacial electrochemistry is interesting because the development of molecular models requires the consideration of two intimately related aspects:

(i) Configurational - the problem of determining the spatial distribution of molecules of different sizes at an interface;

(ii) Electrostatic - the calculation of the favourable configurations as a function of the electrical boundary conditions, and hence the net polarization.

These two components of the problem are evidently inter-related; (ii) depends on (i) because the various possible adsorption configurations will determine the extent of polarization at the interface, and (i) depends on (ii) because the various configurations will differ in electrical energy.

For the specific case of adsorption of neutral, non-polar molecules from aqueous solution, the water molecules will play a double role: their free energy of polarization will contribute to the overall free energy change for the process, and the number of them remaining in the adsorbed layer at equilibrium will (largely) determine the charge sustainable at the metal for a given potential and electrolyte concentration. The main difference between the situation considered here and that

considered earlier is that the number density of H_2O(ads) will be variable by virtue of the adsorption process; in other words, the "dielectric" of the inner layer is of variable composition. The resulting expression for the differential capacitance will therefore need to take account of this variation in a self-consistent manner.

The existing theoretical considerations of neutral molecule adsorption reactions may be divided into two groups, according to whether the process is viewed thermodynamically as a replacement of polarized solvent molecules [1-3] or as a change of inner-layer dielectric constant with coverage of adsorbate [4,5] (the "parallel capacitors" model of Frumkin, Damaskin and co-workers). The adherents of the molecular-replacement view have concentrated on the ability of various specific models to reproduce the experimentally observed variation of coverage with electrical variables, whilst the parallel-capacitors model has been principally applied to the interpretation of differential capacitance behaviour (in which it seems to have been moderately successful at a semi-empirical level).

Inspection of a recent monograph [6] shows that capacitance measurement is the major experimental technique employed by workers of the Soviet school for the investigation of neutral molecule adsorption. This appears not to be so in other literature; consequently, the theoretical interpretation of capacitance curves in the presence of neutral molecule adsorption has not been given much attention in the light of the molecular-replacement approach. The principal objective of the present

chapter is the calculation of the capacitance behaviour predicted for a reaction of the form

$$B(aq) + xH_2O(ads) = B(ads) + xH_2O(aq) \qquad [1]$$

in order to determine the extent to which the primitive model of the double layer is capable of accounting for experimental behaviour. (In the equations which follow, quantities pertaining to adsorbed B and H_2O molecules will be designated by the subscripts b and w respectively.)

There has been considerable discussion (reviewed by Rangarajan [7]) on whether adsorption isotherms for processes represented by eqn. 1 should be more properly represented with potential V or surface charge q_M as the independent variable. The theoretical approaches to this question have generally centred around which of the parameters in common empirical theories should be considered functions of the electrical variables. Evidently, however, it should not matter which of the electrical variables is used, so long as they bear the correct relationship to each other. Thus, the question of whether a given isotherm is congruent with repect to V or q_M reduces to the calculation of q_M as a function of V (as in the previous chapter), or vice versa. From an experimental point of view, the natural independent variable is evidently the applied potential V; the problem considered is therefore the determination of q_M, q_{dip}, and θ as a function of V.

2. Inter-relation of Field, Polarization and Potential

The electrode surface is supposed to be covered with a monolayer, with a fraction θ of sites occupied by non-polar adsorbate molecules of polarizability α_b. The remaining fraction

$1-\theta$ of the sites are occupied by water molecules with polarizability α_w and permanent dipole moment m. Each adsorbate molecule is assumed to occupy x lattice sites, whilst each water molecule occupies only one; the number density of adsorption sites per unit volume is taken to be that corresponding to the number of water molecules per unit volume, N_w (see Chapter 2, Section 2 (i)). As in Chapter 2, the total reactive polarization q_{dip} of the adsorbed layer may be written

$$q_{dip} = N_w(\theta.\alpha_b E_1/x + (1-\theta).[\alpha_w E_1 + mL(mE_1/kT)]) \quad [2]$$

This simply states that the polarization corresponding to a coverage fraction θ is equal to its values in the limits $\theta = 0$ and $\theta = 1$, weighted by the appropriate fractions θ and $1-\theta$. The factor $1/x$ in the induced polarization due to adsorbate is necessary to express the number density of adsorbate molecules in terms of the number density of solvent molecules, recalling that the ratio of areas occupied by the two species is x, which is required in turn to be consistent with the stoicheiometry of eqn. 1. As before, the interfacial field may be represented in the form $E_1 = 4\pi(q_M - q_{dip})$, so that eqn. 2 contains two variables. The second equation which must be simultaneously satisfied by these two variables is that of potential continuity, viz. that the sum of the potential differences across the two regions of the double layer is equal to the applied electrode-solution potential difference V:

$$V = E_1.d + (kT/e_0)\sinh^{-1}(q_M/2A);\ A = (\varepsilon kTn_0/2\pi)^{1/2} \quad [3]$$

where n_0 is the number density of ions per unit volume, for the 1:1-valent electrolyte, and ε is the bulk dielectric constant of

the solvent. In writing this equation, it is assumed that there are no contact-adsorbed ions, and that the Gouy-Chapman theory is valid. Ionic adsorption will be considered in more detail in Chapter 6, and there are more accurate expressions for the diffuse charge density, as a function of potential, but this latter refinement is not important to the present argument.

The special case where $\theta = 0$ has been considered in Chapter 2; otherwise, the dependence of θ on E_1, as expressed by the adsorption isotherm, must be considered.

3. Adsorption Isotherm

The extent to which the electrode under consideration will be covered with adsorbate will be determined by:

(a) the relative strengths of interaction of the molecules b and w with the metal surface;

(b) the relative free energies of the molecules in the field exerted by the electrode;

(c) the resultant of the attractive and repulsive forces existing between similar and different adsorbed species;

(d) the relative free energies of the species in the adsorbed layer and in the solution, just adjacent to the surface.

Factor (a) includes not only the "chemical" or field-independent interactions, such as those arising from dispersion forces and donor-acceptor interactions, but also the interactions between the adsorbed species and the image dipoles induced by them in the metal; (a) and (b) are thus not strictly independent. Likewise, inter-molecular attractions and repulsions will influence the extent to which molecules can be polarized by the electrode, implying an interdependence of (b) and (c).

The problem of calculating the interaction energies of adsorbed species with the electrode surface and with each other (factors (a) and (c)) will be considered in the next chapter. The intention here is to consider the relationship between the polarization components due to adsorbate and solvent molecules, and the type of capacitance behaviour which this implies; therefore, attention is restricted to factor (b) in the construction of the isotherms. The neglect of factor (d) is a common feature of primitive models in general; in addition to considering the effect of the ions on each other in the diffuse layer, one also would have to consider the effect of these ions on the solubility (and hence the free energy) of the adsorbate, in this anisotropic situation. The literature of solution chemistry contains treatments of the ionic-strength dependence of the solubility of non-electrolytes [8], but the corresponding phenomena have not been considered in the interfacial context; since the overall purpose of this thesis is to examine the implications of primitive double-layer models, these effects are neglected in the present treatment.

Since the thermodynamic quantity of central importance in determining the position of an equilibrium is the chemical potential, the starting point in the analysis of the molecular adsorption model under consideration is the partition function for N_1 solvent molecules and N_2 adsorbate molecules adsorbed on a lattice containing a total of $N = N_1 + N_2$ sites:

$$Z = W(N_1,N_2).z_1^{N_1}.z_2^{N_2}/W_1(N_1)W_2(N_2) \qquad [4]$$

where $W(N_1,N_2)$ is the total number of configurations for

adsorption of all molecules among the adsorption sites, and $W_1(N_1)$ and $W_2(N_2)$ are the respective numbers of ways of distributing the solvent and adsorbate molecules among the sites occupied by them. The molecular partition functions for the solvent and adsorbate are denoted by z_1 and z_2 respectively. Adopting Flory-Huggins statistics in order to calculate the degeneracies W, W_1 and W_2, the results for the chemical potentials of adsorbed species are as follows [9-12]:

$$\mu_b = -kT \ln(z_b) + kT \ln[\theta/e^{(x-1)(1-\theta)}] \quad [5]$$

$$\mu_w = -kT \ln(z_w) + kT \ln[(1-\theta)/e^{\theta(1/x-1)}] \quad [6]$$

The molecular partition functions z are themselves the product of several factors, of which the most important (for present purposes) is the electrical partition function $z_{w,el}$, containing the Boltzmann factors for each possible value of the dipole-field potential energy. For the two-state model originally proposed by Mott and Watts-Tobin [13] and Bockris, Devanathan and Mueller [3], inclusion of orientational and distortional polarization energies gives for $z_{w,el}$

$$z_{w,el} = 2 \cosh(mE_1/kT)\exp(\alpha_w E_1^2/2kT) \quad [7]$$

whilst for a continuous range of possible orientations with respect to the field, the classical theory of molecular dielectrics yields the result (see, e.g., ref. 14)

$$z_{w,el} = \exp(\alpha_w E_1^2/2kT).4\pi \sinh(mE_1/kT)/(mE_1/kT) \quad [8]$$

Inclusion of a field-independent orientational energy difference U_0 (i.e., the difference in potential energy between orientations at angles 0 and π with respect to the normal) results in the similar expression

$$z_{w,el} = \exp[(\alpha_w E_1^2+U_0)/2kT].4\pi\sinh(mE_1/kT+U_0/2kT)/(mE_1/kT+U_0/2kT)$$

[8a]

In Chapter 4, it will be shown that the interactions experienced by polarized dipoles may be accounted for by a field-dependent factor of the electrical partition function, the form of which is derived from a Monte-Carlo simulation of the polarization behaviour of a plane dipole lattice.

Since the adsorbate has no permanent dipole moment, its electrical partition function is simply

$$z_{b,el} = \exp(\alpha_b E_l^2/2kT) \qquad [9]$$

The field-independent factors z^o of the partition functions may be identified with the standard chemical potentials of the adsorbed species: $\mu^o = -kT \ln(z^o)$; it is therefore possible to write

$$\mu_b = \mu_b^o - kT \ln(z_{b,el}) + kT \ln[(1-\theta)/e^{(x-1)(1-\theta)}] \qquad [10]$$

and

$$\mu_w = \mu_w^o - kT \ln(z_{w,el}) + kT \ln[(1-\theta)/e^{\theta(1/x-1)}]. \qquad [11]$$

Since the field independent terms are now all included in μ^o, the subscript "el" will be omitted henceforth from the partition functions z.

The condition of equilibrium for the process 1 is that the sum of the chemical potentials of the reactants be equal to the sum of the chemical potentials of the products:

$$\mu_B^o + RT\ln(a_B) + x\mu_w^o - xRT\ln(z_w) + xRT\ln[(1-\theta)/e^{\theta(1/x-1)}]$$
$$= x\mu_{H2O}^o + xRT\ln(a_{H2O}) + \mu_b^o - RT\ln(z_b) + RT\ln[\theta/e^{(x-1)(1-\theta)}] \qquad [12]$$

which readily rearranges to the isotherm:

$$\theta/e^{(x-1)}(1-\theta)^x = K_{eq}(a_B/a_{H2O}^x).z_b(E_1)/z_w(E_1)^x \qquad [13]$$

$$= K_{eq} c_B . z_b(E_I)/z_w(E_I)^x$$

in which the standard chemical potentials have been incorporated into the equilibrium constant K_{eq}, and c denotes molar concentration. The molecular chemical potentials have been multiplied by Avogadro's number to make them consistent with the molar units employed for the species in the solution phase.

The isotherm eqn. 13 must be solved for θ, for each pair of values of q_M and q_{dip} arising in the iterative solution of the polarization eqn. 2.

4. Calculation of Coverage as a Function of Potential

(i) Influence of Reaction Stoicheiometry

The most obvious factor determining the shapes of the adsorption curves calculated from eqn. 13 is the number x of H_2O(ads.) displaced by adsorption of one B molecule. Comparison of curves calculated for different reaction stoicheiometry requires that the field-independent equilibrium constant be adjusted accordingly. This can be done by noting that the equilibrium constant can be written in the form

$$K_{eq} = \exp[-(\mu_b^o - \mu_B^o)/RT] . (\exp[+(\mu_w^o - \mu_{H2O}^o)/RT])^x \qquad [14]$$

A hypothetical case is considered in which both exponential terms are equal to 10, and c_B = 1 mol/l.

The results of this series of calculations are shown in Fig. 1, from which it is evident that as the number of displaced water molecules x increases, the coverage fraction θ becomes more strongly dependent on V. Such bell-shaped adsorption curves are observed experimentally, but in practice they are asymmetric about the point of maximum adsorption. This asymmetry is generally attributed [15] to a field-independent orientational

Fig. 1: Coverage-potential curve for the adsorption reaction

$B(aq) + xH_2O(ads) = B(ads) + xH_2O(aq)$

for various values of x.

$T = 298$ K, $m = 1.8 \times 10^{-18}$ statC cm, $N_w = 6.469 \times 10^{22}$ cm^{-3}, $c_B = 1.0$ mol/l = electrolyte concentration.

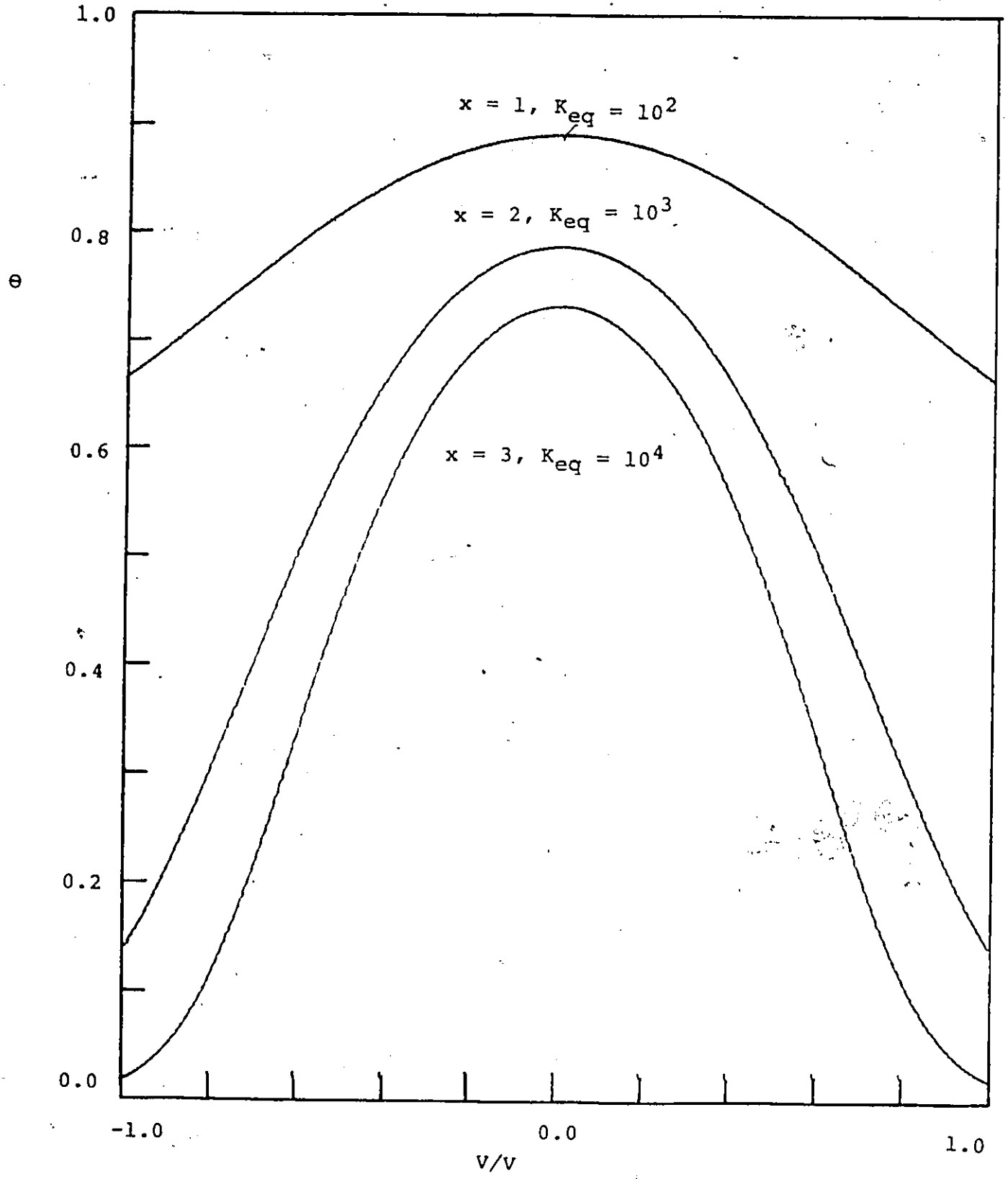
1.0
0.8
0.6
0.4
0.2
0.0
θ
x = 1, $K_{eq} = 10^2$
x = 2, $K_{eq} = 10^3$
x = 3, $K_{eq} = 10^4$
-1.0
0.0
1.0
V/V

energy difference, which was assumed to be zero in these calculations. In addition, the experimental curves are generally not as wide as those of Fig. 1; for example, the coverage-potential curve given by Bockris et al. [3] for n-butyl alcohol with a bulk concentration of 0.05 mol/l has a width of about 0.8 V at half the maximum coverage.

(ii) Electrochemical Contribution to the Adsorption Free Energy

This is given by the difference in the logarithms of the partition functions of the polarized species, with the appropriate value of x; it is plotted, in the dimensionless form

$$\Delta\mu_{el}/RT = x\ln(z_w) - \ln(z_b) \qquad [15]$$

as a function of V in Fig. 2. The maximum in the coverage corresponds to the minimum in this quantity, as expected. The large value of this energy difference at both ends of the potential scale is reflected in the correspondingly small values of θ. These results are consistent with the well-known physical interpretation [1-3,15] that the displacement of water molecules from the surface is easiest when the polarization of these species is minimal, i.e. at the potential of zero charge (p.z.c.). The bell-shaped coverage curves are also obtainable from existing theories, e.g., that of Bockris et al. [3]; the dependent variable is almost invariably q_M, however. Of course, the coverage in eqn. 2 could equally well be obtained by specifying q_M, and solving the equation for q_{dip} in the manner described in Chapter 2. The point of interest here is the simultaneous determination of q_M and q_{dip} as a function of V.

(iii) Influence of Electrolyte Concentration

Fig. 2: Electrochemical free energy change (eqn. 15) as a function of potential V, for the values of x, K_{eq} and other parameters in Fig. 1.

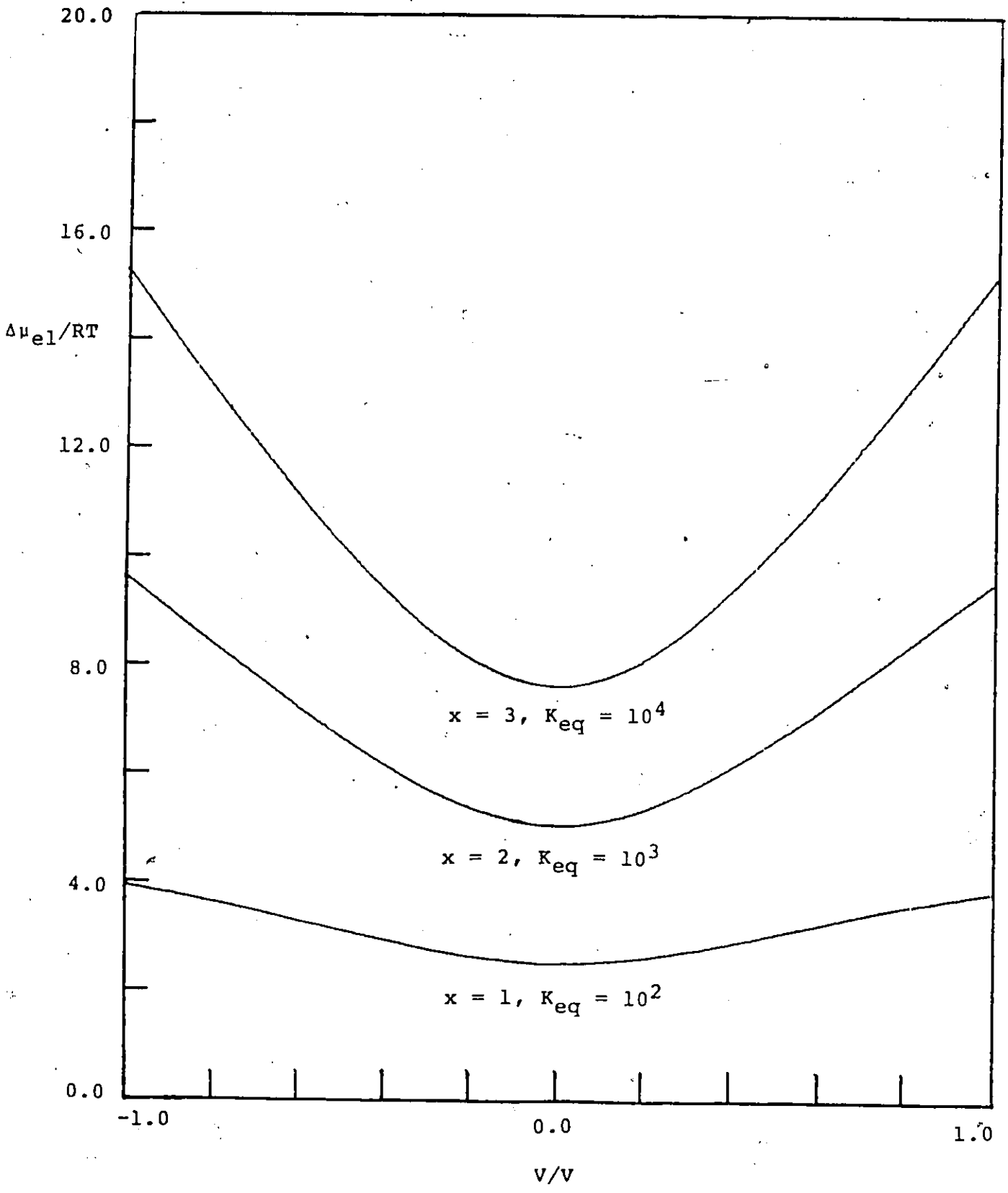

Since the ability of the electrode to sustain a charge density at a given potential V depends on whether this can be balanced by a diffuse layer of ionic charge in the solution, one could expect a difference between curves calculated for various values of the supporting electrolyte concentrations. Specifically, the constant A in the second term of eqn. 3 depends on the square root of the ionic concentration. The effect turns out to be small, as shown in Fig. 3, where the coverage for a reaction with x = 3 is calculated for ionic concentrations from 10^{-3} to 1 mol/l. The curves coincide at the point of zero charge; elsewhere, the coverage at a given potential is reduced by increasing ionic concentration, since the higher charge which is permitted to accumulate results in higher fields and therefore higher values of the electrochemical free energy change.

The calculations presented thus far are in qualitative agreement with experimental behaviour; considering the simplicity of the model considered, however, one should not expect much better agreement. For example, in addition to affecting the electrode charge, an increase in the electrolyte concentration could significantly alter the activity of the adsorbate close to the electrode. This could in turn give rise to salting-out effects as noted by Frumkin [4], as well as micelle formation [16] and deviations from monolayer coverage [17]; these effects are likely to be particularly pronounced for adsorbates very much larger than the solvent molecules. In addition, for large molecules, it is less likely that the adsorption could be represented by a single reaction of the form 1. For example, the adsorption of, say, a 5-carbon primary amine or alcohol could be

Fig. 3: Effect of electrolyte concentration on coverage-potential curves. $x = 2$, $K_{eq} = 10^2$.

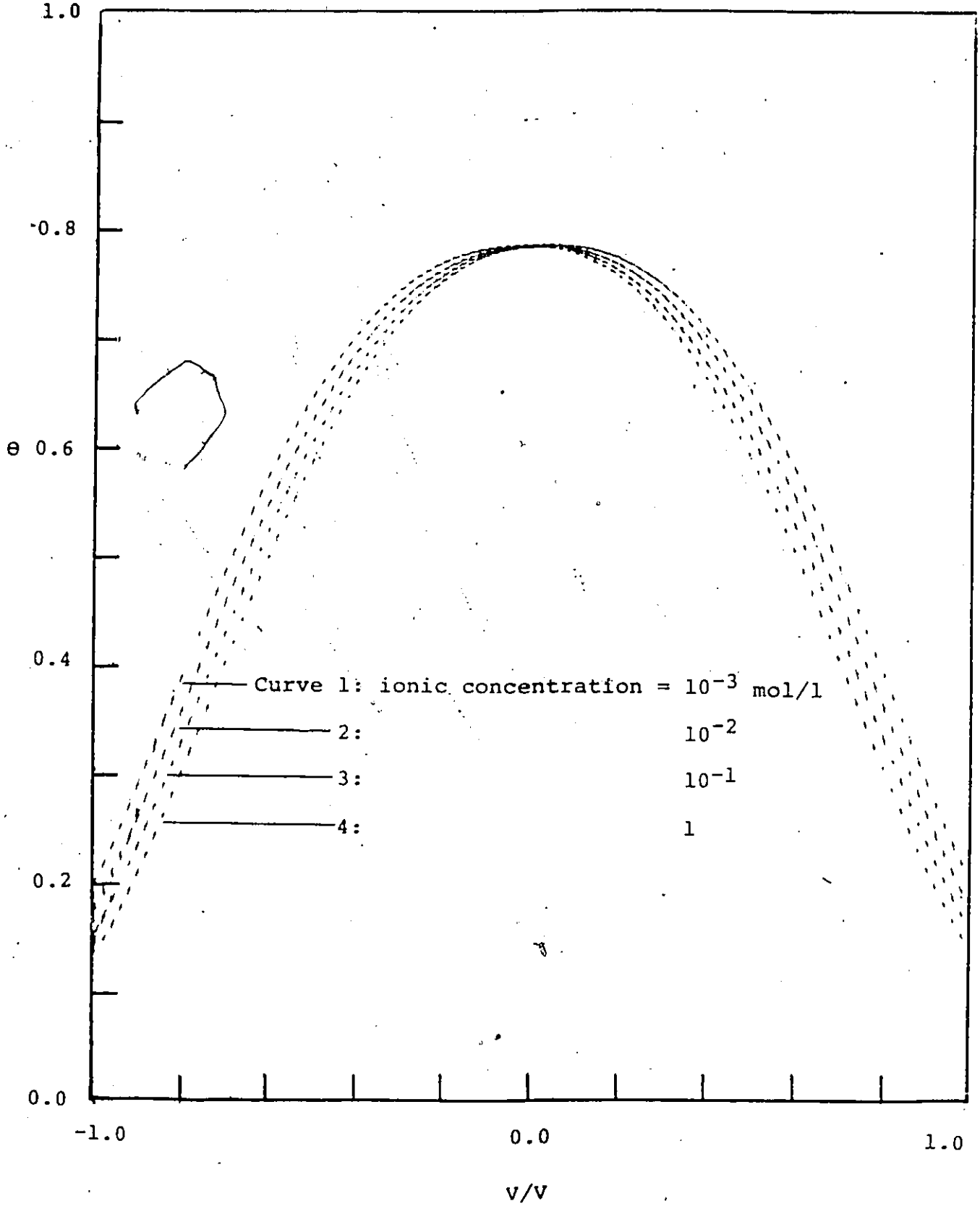

the resultant of several processes of the type 1, with x = 1,2,3 and 4. The simulation of this phenomenon would require the total coverage to be broken down into fractions corresponding to occupation of groups of 1, 2, 3 and 4 contiguous sites by each adsorbate molecule in various conformations.

5. Differential Capacitance

The inverse differential capacitance of the electrode is obtained, as in Chapter 2, by differentiation of the overall electrode-solution potential difference V with respect to q_M. The reciprocal of the inner-layer capacitance is then given by

$$d\Delta\phi_1/dq_M = 4\pi d(1 - dq_{dip}/dq_M) \qquad [16]$$

where q_{dip} is given by the solution of eqn. 2. Performing the indicated differentiations

$$dq_{dip}/dq_M = (f_1 + f_2.\partial\theta/\partial q_M)[1 - dq_{dip}/dq_M] \qquad [17]$$

where

$$f_1 = \theta.4\pi N_w\alpha_b/x + (1-\theta).4\pi N_w[\alpha_w + (m^2/kT)L'(mE_1/kT)]$$

and

$$f_2 = N_w[(\alpha_b/x - \alpha_w)E_1 - mL(mE_1/kT)]$$

The partial derivative of θ with respect to q_M is obtained by taking the logarithms of the isotherm and differentiating implicitly; writing

$$\theta/(1-\theta)^x = K \qquad [18]$$

where K represents the right-hand member of eqn. 13, including the factor of e^{x-1}, one has

$$[1/\theta + x/(1-\theta)].\partial\theta/\partial q_M = \partial \ln K/\partial q_M \qquad [19]$$

i.e.

$$\partial\theta/\partial q_M = (4\pi/kT)[(\alpha_b - x\alpha_w)E_1 - xmL(mE_1/kT)]$$

$$x\,\theta(1-\theta)/[1 + (x-1)\theta] \qquad [20]$$

The polarization functions in this expression result from the logarithmic differentiation of the partition functions in the isotherm, eqn. 13.

Solving eqn. 17 for dq_{dip}/dq_M provides

$$dq_{dip}/dq_M = (f_1 + f_2.\partial\theta/\partial q_M)/[1 + f_1 + f_2.\partial\theta/\partial q_M] \qquad [21]$$

The expression for the reciprocal inner-layer capacitance is therefore

$$1/C_1 = 4\pi d/[1 + f_1 + f_2.\partial\theta/\partial q_M] \qquad [22]$$

As in Chapter 2, the inner-layer capacitance is formally similar to a normal capacitance, being equivalent to a "dielectric constant" divided by $4\pi d$. From the definitions of f_1 and f_2, however, it is evident that the susceptibility implied in this dielectric constant is a differential susceptibility, i.e. the derivative of the polarization with respect to the applied field, rather than an integral one, as in the usual definition, defined with the ratio of the field and polarization. This, of course, corresponds to the use of a differential capacitance rather than the more normal integral capacitance.

As in Chapter 2, the reciprocal differential capacitance of the diffuse layer is given by

$$1/C_2 = (kT/e_0).(1/2A)/[1 + (q_M/2A)^2]^{1/2} \qquad [23]$$

and the overall differential capacitance of the interface is

$$C = C_1C_2/(C_1 + C_2) \qquad [24]$$

The values of θ and C for a reaction of type 1 with $x = 3$ are shown in Figs. 4 and 5, for various values of U_0/kT. The use of non-zero values of U_0 has the predictable effect of displacing the potential of maximum adsorption, but, interestingly, does not

Fig. 4: Coverage-potential curves, for various values of field-independent orientational energy difference U_0. x = 3, $K_{eq} = 10^5$, c_B = 1 mol/l

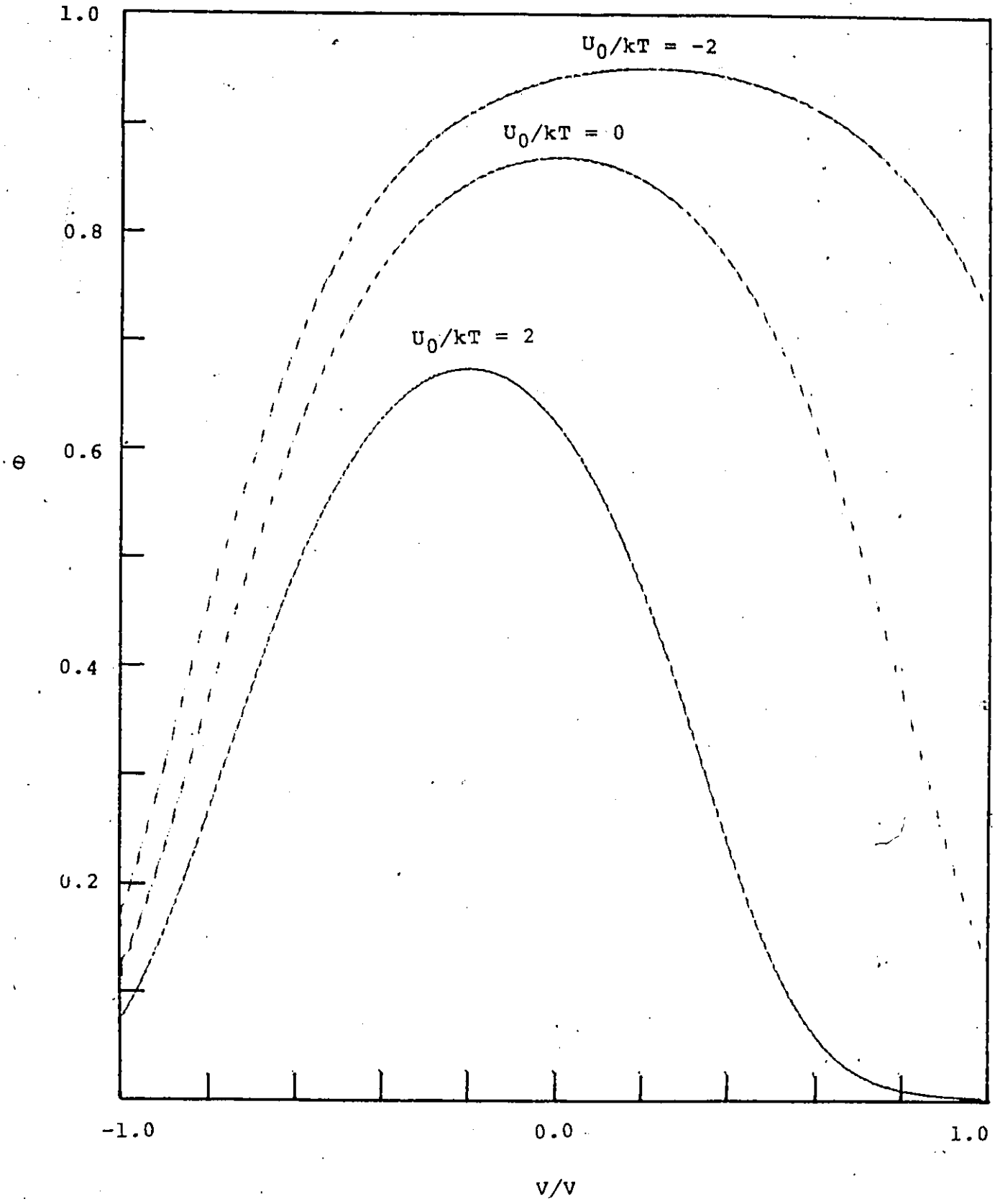

Fig. 5: Capacitance-potential curves corresponding to Fig. 4.

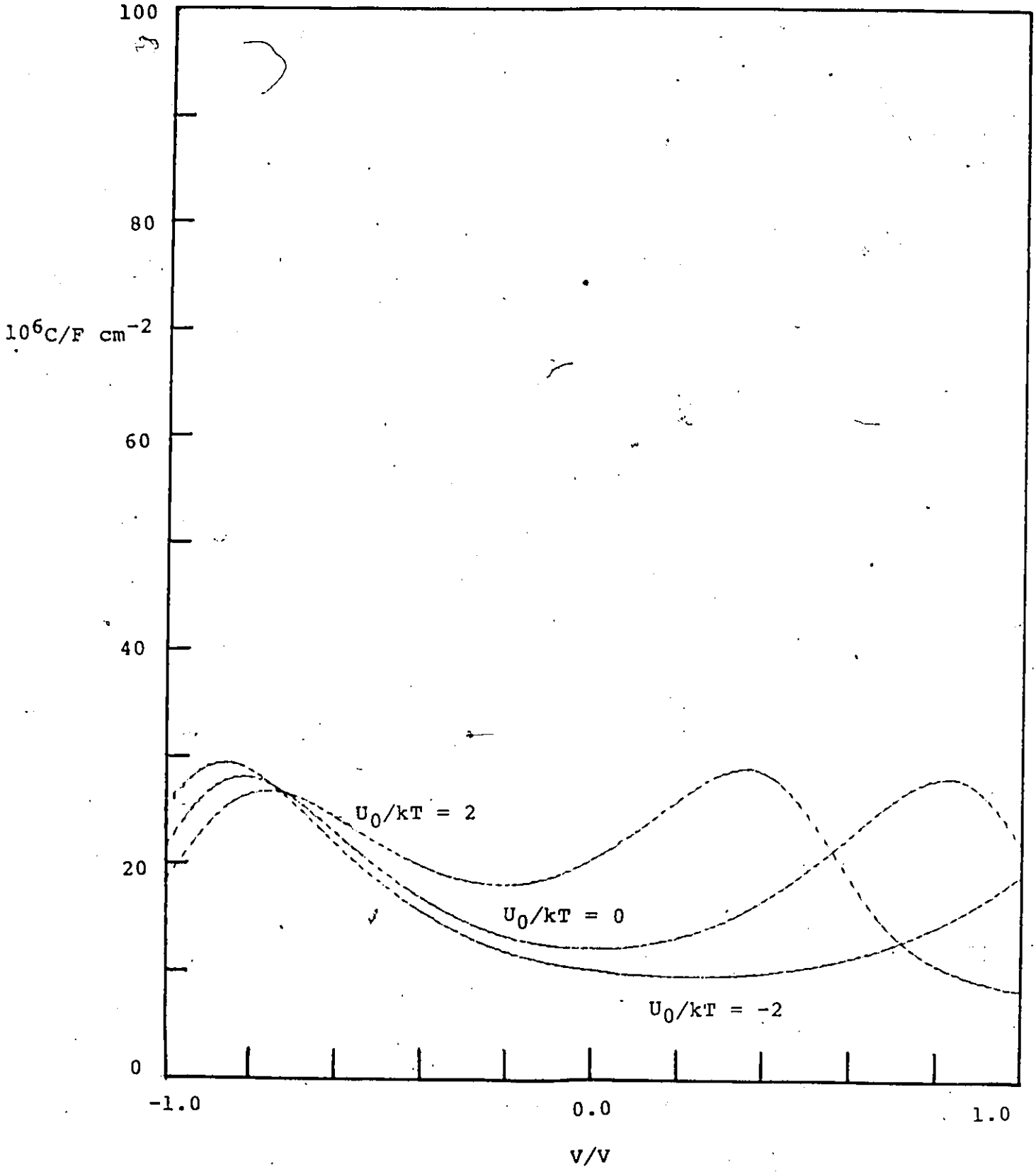

also cause an asymmetry of the θ - V curve of the type observed experimentally. The capacitance curves have two widely spaced peaks, in which respect they are similar to experimental C - V curves; the peaks of the latter are however, considerably sharper than those in Fig. 5, and not as far apart on the potential scale. Again, these discrepancies are hardly surprising in view of the simplicity of the model, e.g. in neglecting interactions. On the basis of the parallel-capacitors model, Frumkin [6] has attributed the sharpness of the peaks to the existence of attractive interactions between adsorbate molecules.

6. Comparison with the Parallel-Capacitors Model

In work originating from the Soviet School, the charge density on the electrode surface is expressed in terms of its values in the limiting cases $\theta = 0$ and $\theta = 1$:

$$q_M = q_{M,0} \cdot (1-\theta) + q_{M,1} \cdot \theta \qquad [25]$$

This is to be contrasted with the approach used in the present work, which is equivalent to writing

$$q_{dip} = q_{dip,0} \cdot (1-\theta) + q_{dip,1}\theta \qquad [26]$$

(where $q_{dip,0}$ and $q_{dip,1}$ are the values of q_{dip} corresponding to $\theta = 0$ and 1 respectively) and determining q_M and q_{dip} by solving eqns. 2, 3 and 13 for each value of V. The manner in which the adsorption free energy is represented is completely different, however. The Frumkin-Damaskin model equates the free energy of adsorption to the work of charging a parallel-plate capacitor filled with a dielectric of variable composition, dependent on the extent of adsorption. This work is expressed by the classical formula

$$W = C'V^2/2 \qquad [27]$$

The capacitance C' is in turn proposed to vary in a linear manner with θ as well as the charge density:

$$C' = C_0'.(1-\theta) + C_1'.\theta \qquad [28]$$

The physical basis of this theory is fundamentally different from that of the molecular-replacement approach used here, since the formula $W = C'V^2/2$ is valid only if the capacitance is constant with q_M during the charging process. In other words, saturation effects of the type considered here and in Chapter 2 cannot be incorporated; the only non-constancy of C' allowed for in the parallel-capacitors model is that arising from the replacement of adsorbed solvent by adsorbate. In the present approach, however, both composition- and saturation-effects are included automatically.

7. Comparison with the Treatment of Bockris et al.

Apart from the representation of the interfacial field as proportional to q_M (the implications of which have been discussed in Chapter 2), the most obvious respects in which the approach used here differs from that employed by Bockris et al. [3] are as follows:

(i) Inclusion of Dipole-Dipole Interactions

The solvent molecules are proposed to be described by a two-state polarization model, which incorporates the effect of dipole-dipole interactions by use of the mean-field approximation, as discussed earlier. An obvious error arises in this treatment when applied to the consideration of neutral-molecule adsorption; the mean field proposed to act on the molecules is still given by $4\pi q_M/\varepsilon_{low} - UcY/m$, where the notation

is defined in Chapter 2, even in the presence of appreciable adsorption. For a significant value of θ, a corresponding fraction of the nearest-neighbours of a given dipole will be adsorbate molecules, which by hypothesis do not exert a dipole field. Therefore, the dipolar interaction term UcY should itself be weighted by the factor $1-\theta$, so that the total field acting on the adsorbed species is $4\pi q_M/\varepsilon_{low} - UcY(1-\theta)/m$.

(ii) Free Energy of Adsorption

In their formulation of the free energy changes for displacement of molecules of H_2O(ads), oriented at angles of 0 or π with respect to the normal, the contribution of the nearest neighbours is a field proportional to the reduced polarization $Y = q_{dip}/N_w m$; thus, it is not a free energy in the strict statistical-mechanical sense. The free-energy of displacement of the H_2O(ads) should be expressed in terms of the partition function, which is in turn defined in terms of the fields exerted by the surface charge density and the neighbours. This automatically takes account of the entropic effect associated with electrostatic polarization; evidently, the free energy of adsorption (that is, taking into account the contributions of all polarization states), should be an even function of the charge q_M. If the free energy is defined in terms of Y, then this is not so, since Y is an odd function.

8. Conclusion

In the present chapter, it has been shown that the molecular-replacement approach to the description of adsorption of neutral molecules at charged interfaces, proposed originally

by Butler et al. [1,2] and developed subsequently by Bockris et al. [3], is capable of accounting for the main features of the experimental variation of the differential capacitance and coverage with potential. The specific model used in the calculations is simple, but relations of the form 21, used to define the capacitance, must always be satisfied. The extent of this agreement with experiment, however, probably depends significantly on how sensitively the electrical partition function and associated polarization depend on the field in terms of which they are defined. The calculation of dipolar discreteness contributions to the effective field acting on adsorbed species is considered in Chapter 6.

The construction of a molecular model which quantitatively agrees with experiment, e.g. with respect to capacitance behaviour as a function of V or q_M, would be much more difficult to achieve in the presence of neutral molecule adsorption than in the absence, because of the assumptions which must be made in order to render the problem tractable. Some of these assumptions have been enumerated above; the most important and interesting of these are connected with the problems of dealing with molecules of different sizes. Similar problems arise, however, in the consideration of simpler systems, in which it is desired to interpret the differential capacitance behaviour of aspherical molecules. In such cases, if one adopts a lattice-layer formulation of the interface, the space occupied in one layer by a molecule might be different for each possible orientation with respect to the field. As stated by Rangarajan [7], such effects have not been considered in the electrochemical context, and

offer interesting possibilities for future work.

REFERENCES

1. J.A.V. Butler

   Proc. Roy. Soc. Lond. **A122**: 399 (1929)

2. J.A.V. Butler and C. Ockrent

   J. Phys. Chem. **34**: 2286 (1934)

3. J.O'M. Bockris, M.A.V. Devanathan and K. Mueller

   Proc. Roy. Soc. Lond. **A274**: 55 (1963)

4. A.N. Frumkin

   Modern Aspects of Electrochemistry **3**:

5. A.N. Frumkin

   Z. Physik **35**: 792 (1926)

6. A.N. Frumkin

   "Potentsialy Nulevogo Zaryada", Izdatel'stvo "Nauka" (1979)

7. S.K. Rangarajan

   Chem. Soc. Spec. Periodical Reports **7**: 203 (1980)

8. E.L. McBain and E.C. Hutchinson

   "Solubilization and Related Phenomena", Academic Press N.Y. (1955)

9. P.J. Flory

   J. Chem. Phys. **10**: 51 (1942)

10. M.L. Huggins

    Ann. N.Y. Acad. Sci. **43**: 1 (1942)

11. E.A. Guggenheim

    "Mixtures", Oxford University Press (1952)

12. H.P. Dhar, B.E. Conway and K.M. Joshi

    Electrochim. Acta **18**: 789 (1973)

13. N.F. Mott and R.J. Watts-Tobin

Electrochim. Acta **4**: 79 (1961)

14. T.L. Hill

"An Introduction to Statistical Thermodynamics", Addison-Wesley (1962)

15. J.O'M. Bockris and A.K.N. Reddy

"Modern Electrochemistry", Plenum N.Y. (1972), v.2 Chapter 7

16. A.N. Frumkin, A. Gorodetskaya and P. Chugunov

Acta Physicochimica U.R.S.S. 1: 12 (1934)

17. V.I. Melik-Gaikazyan

Zh. Fiz. Khim. **26**: 1184 (1952)

CHAPTER 4

ANALYSIS OF PAIRWISE INTERACTIONS BETWEEN POLAR SPECIES ADSORBED AT ELECTRODES

1. Introduction

The electrical behaviour of isotropic polar media has been moderately well explained [1] by models which assume the molecules of interest to be surrounded by a dielectric continuum of constant permittivity. These quasi-macroscopic models, however, are fundamentally inapplicable to the analysis of dipolar interactions at electrode-solution interfaces, since the very high field strengths present make it quite unrealistic to assume linear dielectric behaviour.

Most of the approaches to this problem have been made within the framework of the "primitive" model of the double layer, described in Chapter 1, thus explicitly considering only the first monolayer of solvent dipoles adjacent to the electrode, and describing the behaviour of the remaining species using the Poisson-Boltzmann law. The lateral interactions between the molecules occupying the inner layer are generally assumed to be equivalent to a mean field, the magnitude of which is proportional to the ensemble average dipole moment, $\langle m \rangle$. This results in implicit equations for this quantity as a function of the electrode's field, represented as proportional to the surface charge density q_M [2] or as the potential drop $\Delta\phi_1$ across the inner layer divided by its thickness, d [3]. Recently, Schmickler has presented more accurate alternatives to the mean-field approximation, involving explicit calculation of nearest-

neighbour interactions [4], and a computer simulation of the polarization of a monolayer of point-dipoles, assuming a continuous range of orientations and calculating interactions using the exact dipole-dipole interaction potential energy. In its treatment of dipole-dipole interactions, the latter work is probably the most accurate version of the primitive model to have appeared thus far.

The underlying objective of most of the above work has been the interpretation of the capacitance behaviour of various electrode-solution interfaces, as a function of q_M or electrode-solution potential difference, V. Another area of electrochemistry in which the analysis of dipolar interactions is of importance is the theory of ionic specific adsorption, and the related phenomenon of electrochemical formation of monolayers of discharged, or partially discharged, ions. Here again, one observes a considerable diversity of treatments, but it is nevertheless possible to identify the two essential (and to some extent interdependent) questions which must be addressed by all of them:

(a) What is a reasonable electrostatic model for the adsorbed species?

(b) How is the chemical potential of the adsorbed species related to its coverage, reflecting the existence of interactions?

The simplest answers to question (a) have proposed that the adsorbed ions function as simple charges, or charges plus single or multiple images [5], being thus equivalent to surface dipoles. Ions may exist in partially discharged states characterized by the electrosorption valency factor, γ [6,19]. The interaction energy

between a given adsorbed species and its neighbours is usually expressed in terms of the so-called micropotential or discreteness-of-charge potential, which is defined [7] as the total coulombic potential acting at the site of the species under consideration, minus the (infinite) contribution due to the species itself. This micropotential may be distinguished from the macropotential, which is the average potential resulting from the spatial distribution of charges and dipoles.

The calculation of the micropotential is a difficult problem, to which much attention has been devoted by numerous authors over the years. A more detailed examination of these treatments will be given in Chapter 6; for present purposes, it may be observed that the most popular model assumed is that of a regular lattice of charges, separated by a dielectric continuum. Important contributions of this type have been made by Macdonald and Barlow [7,8,9], Levine, Bell and Calvert [10] and authors of the Soviet school [11,12]. The treatments differ in the number of dielectric interfaces assumed to be present (which determines the nature and extent of imaging to be expected), and in the approximations used in summing the potential contributions due to the charges and their images. The alternative treatments do not assume a lattice arrangement, but attempt to calculate distribution functions in terms of cluster integrals [13] or, more recently, by solution of integral equations [14]. The dielectric constant of the adsorbed layer is generally assumed, constant.

Approaches to the configurational component of the problem,

expressed by question (b), have been of two types: (i) a mean field approximation resulting in a linear variation of chemical potential with coverage, i.e. $\mu = \mu^0 + g\theta$ (the Frumkin isotherm [16]) and (ii) the estimation of interaction energy in terms of the mean distance between adsorbed species, resulting in chemical potentials varying with some power of $\theta^{1/2}$ [5,17]. Treatments of type (i) are the more numerous, and the implications of possible dependence of the g-parameter on electrical variables or even on θ have been considered - see, for example, a recent review by Rangarajan [18].

The use of a dielectric continuum approximation to describe solvent behaviour in the above treatments is to be contrasted with approaches to the interpretation of capacitance behaviour in the (assumed) absence of ionic contact-adsorption, in which the molecular nature of the solvent, according to whatever specific model, is of central importance.

The significance of the dielectric constants used in these treatments is in their determination of the strength of ion-ion interactions; an obvious refinement would be to assume a variable dielectric constant, with a value determined as a function of the electrical boundary conditions, as in the work of Macdonald and Barlow [20]. This would also be equivalent to the self-consistent determination of the bound charge density of the inner layer, as has been shown elsewhere [33]. For the purpose of constructing adsorption isotherms, however, such a description of solvent molecules would still neglect the contribution of their polarization and interaction energies to the chemical potential balance defining the coverage fraction.

It is the purpose of the present chapter to consider the calculation of pairwise interaction free energies between charges and dipoles; subsequently, it will be shown how these can be combined, according to well-defined statistical-mechanical approximations, to produce estimates of the chemical potential of each component of the adsorbed layer. Ultimately, it is hoped to use these results to construct a consistent picture of the implications of the primitive model, with respect to the simultaneous adsorption of ions and dipoles at electrodes.

2. Interactions Between Solvent Dipoles

Two alternatives to the mean field approximation were recently described by Schmickler [21]: (a) the Bethe approximation, according to which interactions between the central dipole and its nearest neighbours are treated explicitly and interactions of these neighbours with the remaining molecules using the mean field approximation, and (b) a periodic cluster approach, involving calculation of the energies of all the polarization states in a small group of dipoles which is assumed to repeat itself periodically. The Bethe approximation is criticised as giving too much emphasis to central dipole/nearest neighbour interactions, and neglecting short-range order in the treatment of interactions between the neighbouring dipoles. The periodic cluster approach is preferable, because it can be readily used to set up a Monte Carlo simulation of the polarization behaviour of a dipole lattice. Such a simulation would provide information on the implications of a particular molecular model, which is free of the limitations imposed by

approximations inherent in analytical treatments.

In Schmickler's application [4] of the periodic cluster method to a lattice of dipoles which can assume a continuous range of orientations, the nearest-neighbour interactions experienced by each member of the lattice are calculated explicitly using the dipole-dipole interaction energy formula, whilst the interactions with the remaining dipoles are treated using the mean field approximation. The resulting variation of the average polarization <m> with applied field is qualitatively similar to that expressed by the Langevin function appropriate for non-interacting dipoles, but as expected, much higher values of the field are required to approach the limit of saturation polarization.

The use of the mean field approximation for the non-nearest neighbour interactions allows the calculation of the polarization which would be expected with consideration of only nearest-neighbour interactions. To see how this may be done, it may be observed that, in the earlier treatments of dipole-dipole interactions using the mean field approximation (for example, those examined in Chapter 2), <m> is given by the solution of an implicit equation of the form

$$\langle m \rangle = f(E - c\langle m \rangle) \qquad [1]$$

where E is the applied field, and c is a constant depending on the effective coordination number and the field exerted at a neighbouring site by one such dipole. The polarization function f appropriate for the given molecular model can therefore be considered to operate on an effective field given by

$$E_{eff} = E - c\langle m \rangle \qquad [2]$$

The results of such calculations usually show <m> as a function of the applied field E. If <m> be plotted as a function of E_{eff} instead of E, the graph of <m> corresponding to the absence of interactions will be recovered. The result of applying the transformation expressed by eqn. 2 will thus be a "compression" of the graph of <m>, i.e. the saturation limit will be approached with lower fields. This procedure will now be applied to the results of ref. 4.

For the hexagonal lattice assumed in the calculations, the total effective coordination number was taken to be 10.962 (rather than the value of 11.035 calculated by Topping [36] - further discussion of this is given in Chapter 6). Therefore, the effective coordination number for the non-nearest-neighbour dipoles is 10.962 - 6 = 4.962. In other words, the combined field of all non-nearest neighbour dipoles is equal to 4.962 times the field exerted at the origin by one such dipole at distance r_0. Taking m = 1.835×10^{-18} statcoulomb cm and the dipole-dipole distance r = 3.0×10^{-8} cm, the coefficient of <m>/m (referred to as <s> in Schmickler's paper) is c = $4.962 \times (1.835 \times 10^{-18})/(3.0 \times 10^{-8})^3 = 3.372 \times 10^5$ statvolt cm^{-1}. By way of illustration, consider the first value <s> = 0.039, corresponding to an applied field of 3.767×10^4 statvolt cm^{-1}. Applying eqn. 2, it is found that the effective field for this point is $3.767 \times 10^4 - 0.039 \times (3.372 \times 10^5) = 2.452 \times 10^4$ statvolt cm^{-1}. The results of proceeding similarly for the remaining values of <s> estimated from Fig. 3 of ref. 4, are shown in Fig. 1, with the original uncorrected values of <s> and the corresponding values of the

Langevin function included for comparison.

For the purposes of the present discussion, the quantity of interest is the average component of the chemical potential per molecule, which results from nearest-neighbour interactions. This information is contained in the difference between curve 1 of Fig. 1 (calculated for non-interacting dipoles) and curve 2 (calculated for nearest-neighbour interactions). More specifically, the total electrical partition function z for each member of the lattice is required; the factor of this due to the interactions can be obtained by dividing by the partition function appropriate for non-interacting dipoles polarized by a field E, viz. [22]

$$z_w = 4\pi\exp(\alpha E^2/2kT)\sinh(mE/kT)/(mE/kT) \qquad [3]$$

where α is the polarizability. (Schmickler's calculation did not consider the non-orientational contribution to the polarization, i.e. it was assumed that $\alpha=0$. Throughout the present work, the interactions involving the field-induced dipole moments are neglected.)

In general, it is impossible to calculate the partition function directly by Monte Carlo simulation [23]; it is necessary to obtain z by integration of the internal energy as a function of temperature. For a system of dipoles, z can also be obtained by integration of the molecular polarization as a function of field, since the statistical-mechanical definition of the average dipole moment is [22]

$$\langle m\rangle = kT\,\partial\ln(z)/\partial E \qquad [4]$$

Thus, one has for the total electrical partition function

$$z = \exp(\int_0^E \langle m\rangle dE'/kT) \qquad [5]$$

Fig. 1: Polarization curves as a function of mE/kT

Curve 1: L(mE/kT)

Curve 2: polarization curve from ref. 4 calculated for nearest-neighbour interactions

Curve 3: Original data from ref. 4

$m = 1.835 \times 10^{-18}$ statC cm, $r_0 = 3.0 \times 10^{-8}$ cm, T = 293 K ($kT = 4.045 \times 10^{-14}$ erg)

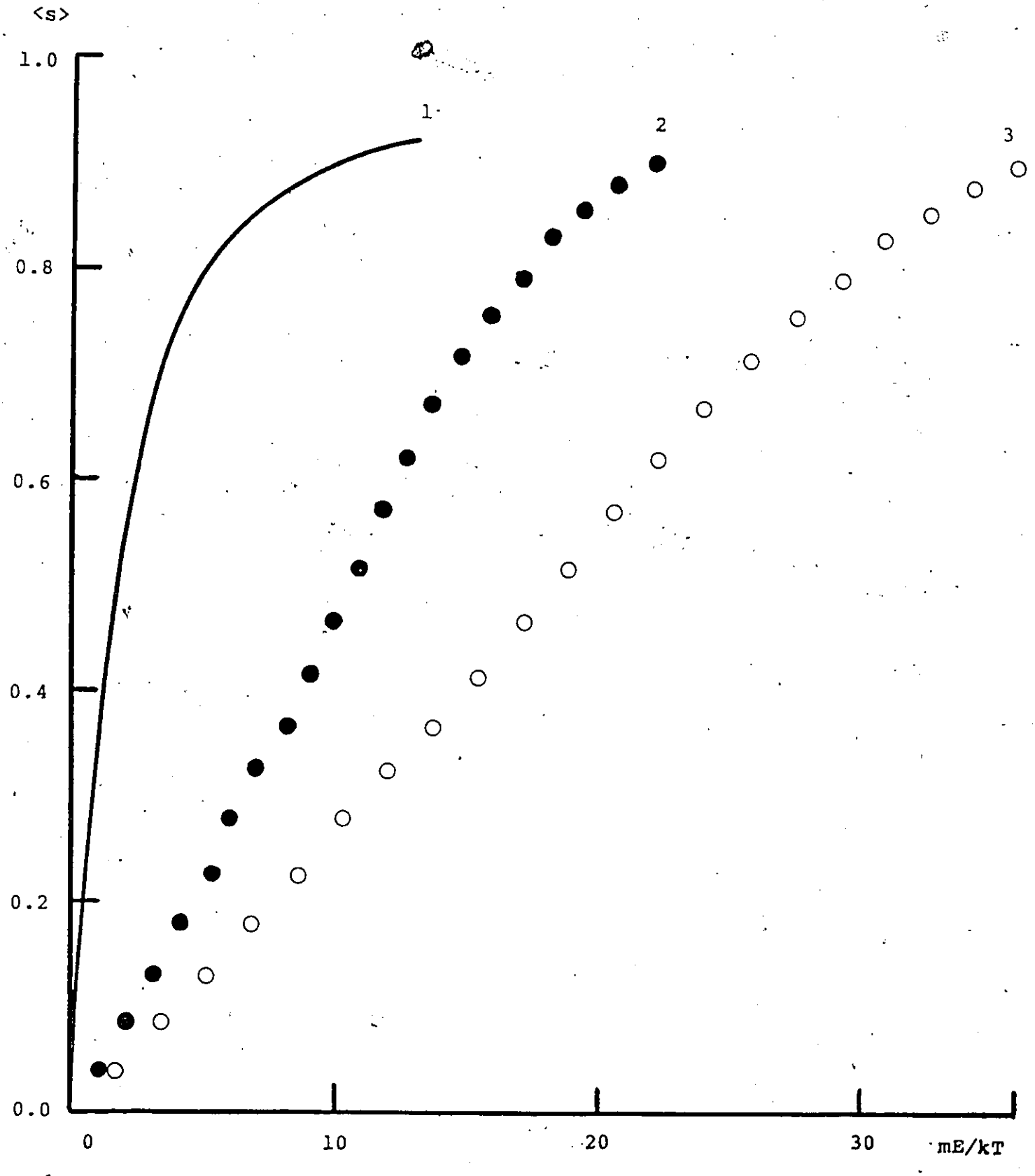
<s>
1.0
0.8
0.6
0.4
0.2
0.0
0
10
20
30
mE/kT
1
2
3

The molecular partition function for each member of an hexagonal lattice with nearest-neighbour pairwise interaction energy u_{ww} is [22]

$$z = z'\exp(-3u_{ww}/kT) \qquad [6]$$

where z' represents the partition function for non-interacting molecules, and the factor of 3 results from dividing the coordination number of 6 by 2, to avoid counting interactions twice. For the case under consideration, with $z' = z_w$, the interaction energy for a given value of E will depend in a rather complex way on the relative orientations of the neighbouring dipoles, so u_{ww} in eqn. 6 should be interpreted as the potential of mean force averaged (at least in principle) over all possible values of the angular coordinates of the neighbouring dipoles. With this definition, u_{ww} may be identified as a free energy of interaction, which in turn corresponds to a factor ζ_{ww} of the partition function such that $u_{ww} = -kT\ \ln(\zeta_{ww})$. Substituting this into eqn. 5, one obtains

$$z_w\zeta_{ww}^3 = \exp(\int_0^E \langle m\rangle dE'/kT) \qquad [7]$$

so that the partition function ζ_{ww} for pairwise interaction of solvent dipoles is

$$\zeta_{ww} = [\exp(\int_0^E \langle m\rangle dE'/kT)/z_w]^{1/3} \qquad [8]$$

The pairwise chemical potential of interaction, defined by $u_{ww}/kT = -\ln(\zeta_{ww})$ and obtained by integration of curve 2 in Fig. 1, is shown in Fig. 2, as a function of mE/kT. The behaviour of this function seems intuitively reasonable in that for large values of mE/kT, the interaction energy tends to a limiting value, characteristic of a completely polarized lattice.

Fig. 2: Reduced effective pairwise interaction free energy $u_{ww}/kT = -\ln(\zeta_{ww})$ as a function of mE/kT, calculated using the least-squares constants fitting the data of ref. 4. Other parameters as in Fig. 1.

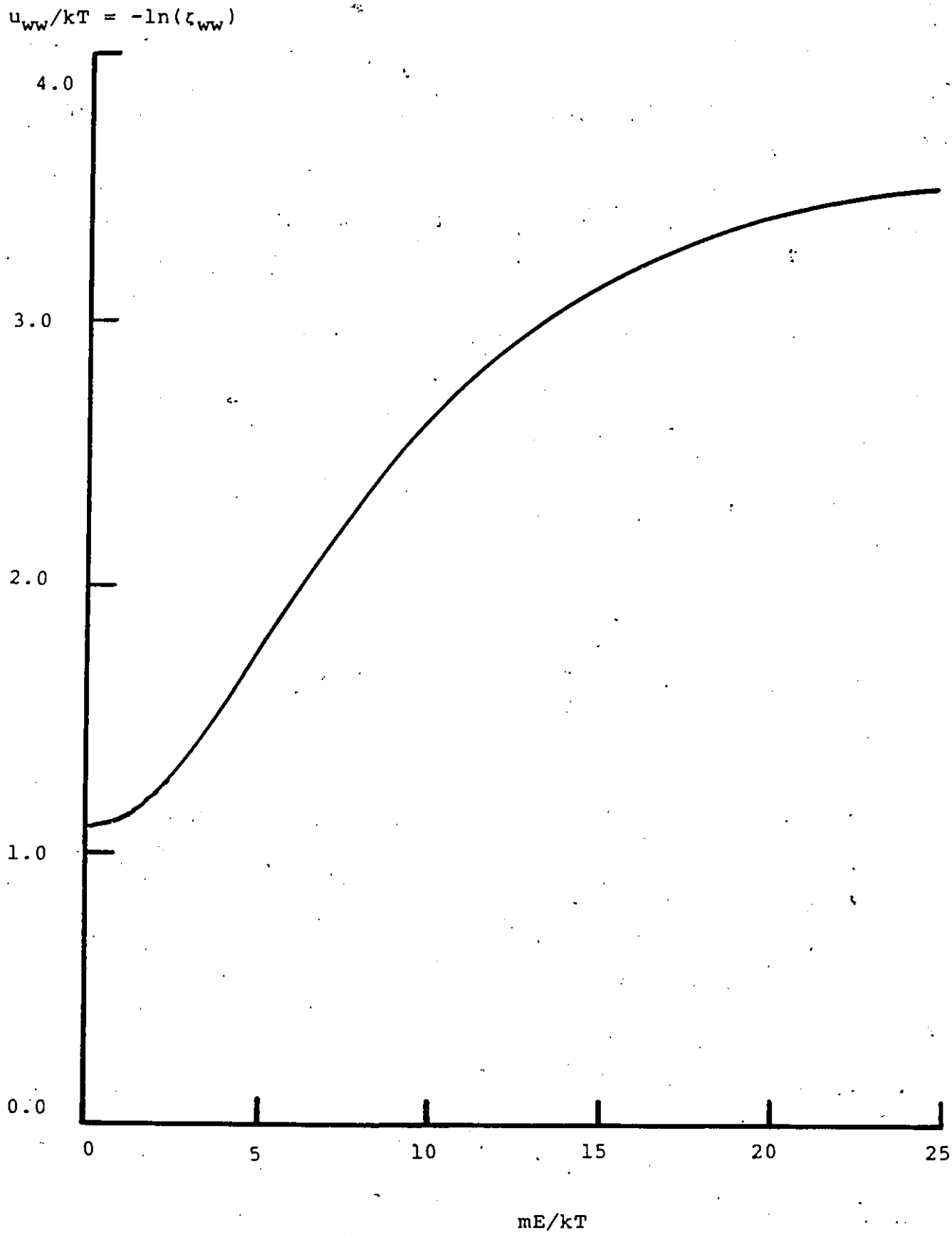
$u_{ww}/kT = -\ln(\zeta_{ww})$
4.0
3.0
2.0
1.0
0.0
0
5
10
15
20
25
mE/kT

An empirical representation of u_{ww} as a function of E is

$$u_{ww} = a - 1/(c_1 + c_2(mE/kT)^2 + c_3(mE/kT)^4) \qquad [9]$$

for values of mE/kT less than about 25, so that

$$\zeta_{ww} = \exp[1/(c_1 + c_2(mE/kT)^2 + c_3(mE/kT)^4) - a] \qquad [10]$$

The least-squares values of these constants fitting Schmickler's MC data, which were used in plotting Fig. 2, are a = 4.0905, c_1 = 0.3356, $c_2 = 3.7269 \times 10^{-3}$ and $c_3 = -2.4977 \times 10^{-6}$. Physically, the constant a should be equal to m^2/r^3kT; with the values of m, r and T (293 K) used in Schmickler's calculations, $m^2/r^3kT = 3.083$.

The difference between this and the least-squares value of a probably results from the cumulative errors in the calculations, such as the graphical interpolation used in the integration, the graphical method used to obtain <s> from ref. 4 and the original scatter present in these values. The value of a is, nevertheless, comparable to m^2/r^3kT. It is to be observed, however, that u_{ww} as defined above is an apparent pairwise free energy of interaction. The Monte-Carlo simulation from which it was extracted automatically takes account of the local order propagated throughout the lattice, even though only the nearest-neighbour interactions were calculated exactly. Such a propagation of order is likely to be less important for the continuous-orientation model than for the two-state model, since there are infinitely many more accessible configurations. A consequence of this is that the free energy u_{ww} is more reliably estimated from a Monte-Carlo simulation, as just described, than it would be by evaluating the partition function for a central dipole and its nearest neighbours.

It is nevertheless of interest to determine to what extent the effective pairwise interaction energy u_{ww} differs from that calculated for an isolated pair of adjacent dipoles. In order to do this, the total partition function for the pair is considered; this is given by

$$z_{12} = \int_0^{\pi}\int_0^{2\pi}\int_0^{\pi}\int_0^{2\pi}\exp[(\cos\theta_1+\cos\theta_2)mE/kT-U_{12}/kT]d\Omega_1 d\Omega_2 \quad [11]$$

where $d\Omega_1$ and $d\Omega_2$ are the solid angle elements for the angles $\theta_1,\phi_1,\theta_2,\phi_2$ describing the orientation of each of the dipoles 1 and 2:

$$d\Omega_1 = \sin\theta_1 d\theta_1 d\phi_1,\ d\Omega_2 = \sin\theta_2 d\theta_2 d\phi_2$$
$$\mathbf{m}_1 = m(\sin\theta_1\cos\phi_1,\ \sin\theta_1\sin\phi_1,\ \cos\theta_1)$$
$$\mathbf{m}_2 = m(\sin\theta_2\cos\phi_2,\ \sin\theta_2\sin\phi_2,\ \cos\theta_2) \quad [12]$$

and U_{12} is the classical electrostatic interaction energy for two ideal dipoles, separated by a distance $r = |\mathbf{r}|$:

$$U_{12}=\mathbf{m}_1.\mathbf{m}_2/r^3-3(\mathbf{m}_1.\mathbf{r})(\mathbf{m}_2.\mathbf{r})/r^5 \quad [13]$$

As in the previous derivation of ζ_{ww}, it is necessary to divide by the orientational partition function for the non-interacting dipoles, viz. eqn. (3) with $\alpha = 0$:

$$\zeta_{12} = z_{12}(E)/z_w(E)^2 \quad [14]$$

The results of such a calculation are shown in Fig.3, with u_{ww} plotted for comparison. It is seen that the difference between the free energies u_{ww} and $u_{12} = -kT\ln(\zeta_{12})$ can vary from about 2kT to -kT depending on the field E. More importantly, however, consideration of only a pair of interacting dipoles leads to a net attraction, i.e. a negative potential energy of interaction, whilst the effective pairwise free energy of interaction u_{ww} is always positive, corresponding to a repulsion.

Fig. 3: Comparison of reduced interaction free energies u_{ww}/kT (curve 1, cf. eqn.10) and u_{12}/kT (curve 2, cf. eqn.11) as a function of mE/kT.

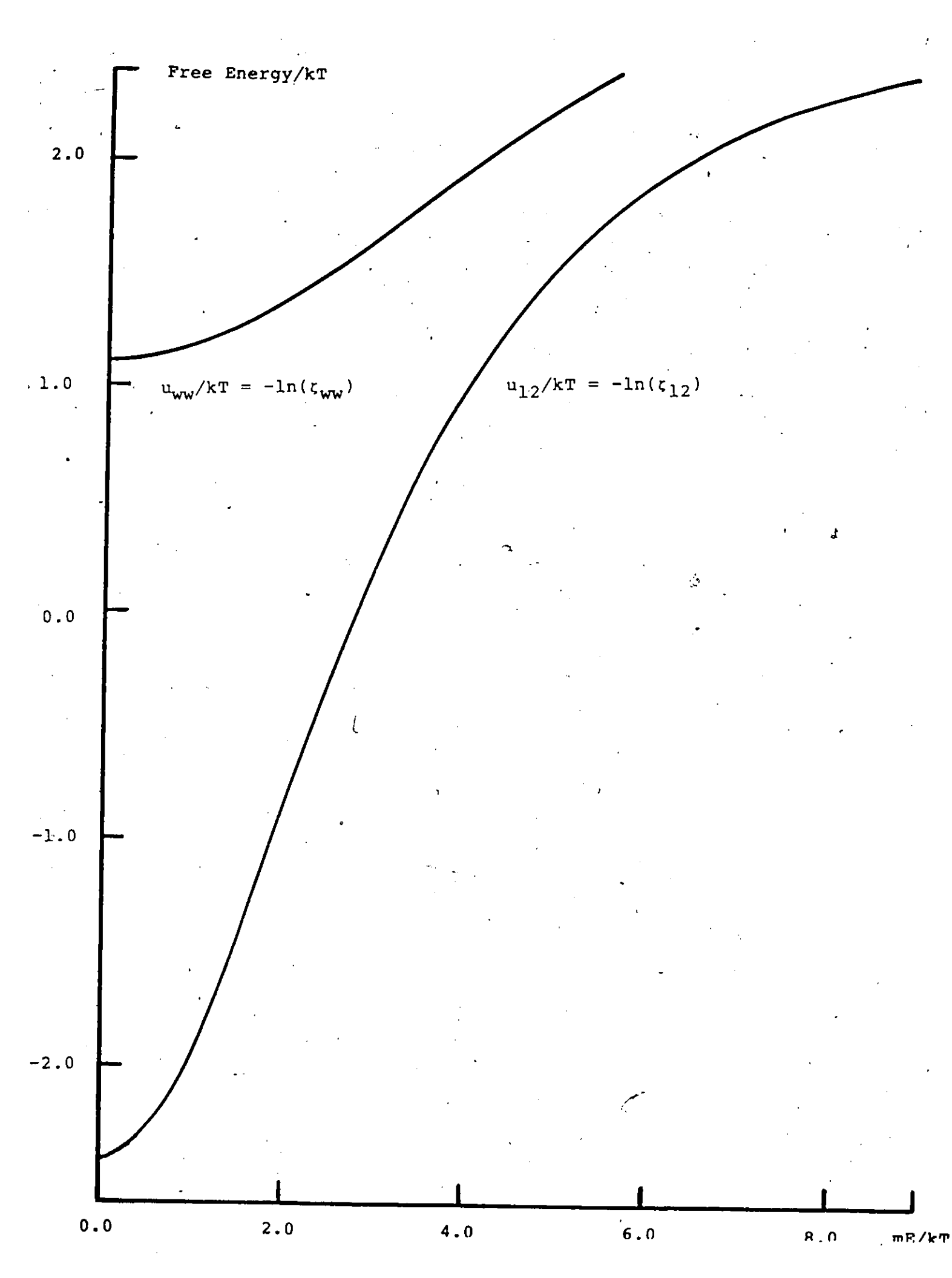
Free Energy/kT
2.0
1.0
0.0
-1.0
-2.0
$u_{ww}/kT = -\ln(\zeta_{ww})$
$u_{12}/kT = -\ln(\zeta_{12})$
0.0
2.0
4.0
6.0
8.0
mR/kT

u_{12} is then clearly unsuitable as an approximation to the free energy of interaction for a collection of dipoles, even though it exhibits qualitatively the same variation with E as ζ_{ww}. The calculation thus serves to illustrate the cooperative nature of dipole-dipole interactions in such an array.

3. Interactions Between Adatoms and Solvent Molecules

The calculation of the free energy of interaction between an adatom and an adsorbed solvent molecule is simplified, to some extent, by the fact that the former species is of fixed orientation. However, it is less accurate to approximate the behaviour of the adatoms by point dipoles, as assumed in the previous section (and as assumed in this section) for the solvent molecules. Such finite-size effects, as will be shown, complicate the angular dependence of the interaction energy between the adatom and an adjacent solvent molecule.

It is assumed that the adatom or adsorbed ion can be considered to be a uniform spherical distribution of negative charge of total magnitude γe_0, where e_0 is the electronic charge and γ is the electrosorption valency factor (which lies between 0 and 1) centred a distance s from the surface. By a standard result from field theory, originally due to Newton (see, for example, ref. 24), the resulting field intensity at a point outside the sphere is equivalent to that of a point charge of equal magnitude, located at the centre. This charge will induce an image located an equal distance from the other side of the surface plane. In order to calculate the interaction energy experienced by a point solvent dipole located at a point P, a horizontal distance r from the negative charge, it is required to

calculate the total field acting at this point: this will be the resultant of the fields exerted by the adatom charge, its image and the electrode. The geometrical disposition of the charges and the directions of the corresponding field vectors are shown in Figs. 4a and 4b.

The field exerted at the point (x,y,z) by a charge q located at the point (x_1,y_1,z_1) is

$$q(x-x_1,y-y_1,z-z_1)/[(x-x_1)^2+(y-y_1)^2+(z-z_1)^2]^{3/2} \qquad [15]$$

For the charges themselves, $q=-\gamma e_0$, $x_1=-r_0$, $y_1=0$, $z_1=0$ (since only two coordinates are required, the direction y=0 is arbitrarily chosen), so that the field at the origin (0,0,0) due to the adatom is

$$E_1 = (-\gamma e_0/r_0^2,0,0) \qquad [16]$$

For the images, $q = \gamma e_0$, $x_1 = -r_0$, $y_1=0$ and $z_1=-2s$, so that the field at the origin due to the images is

$$E_2 = \gamma e_0(r_0,0,2s)/[r_0^2+4s^2]^{3/2} \qquad [17]$$

The vector sum of these two fields is

$$E_3 = (\gamma e_0 r_0/[r_0^2+4s^2]^{3/2} - \gamma e_0/r_0^2,\ 0,\ \gamma e_0.2s/[r_0^2+4s^2]^{3/2}) \qquad [18]$$

which becomes, on introducing the dimensionless parameter $b = r_0/2s$,

$$E_3 = ([b^3/(1+b^2)^{3/2}-1]\gamma e_0/r_0^2,\ 0,\ (\gamma e_0/r_0^2).b^2/(1+b^2)^{3/2}) \qquad [19]$$

$$= (-.6464\gamma e_0/r_0^2,\ 0,\ .3536\gamma e_0/r_0^2)$$

when b=1. The total field acting at the origin is given by the vector sum of E_3 and E=(0,0,E):

$$X=([b^3/(1+b^2)^{3/2}-1]\gamma e_0/r_0^2,\ 0,\ E+(\gamma e_0/r_0^2).b^2/(1+b^2)^{3/2}) \qquad [20]$$

Fig. 4a: Arrangement of adsorbed charges and primary images.

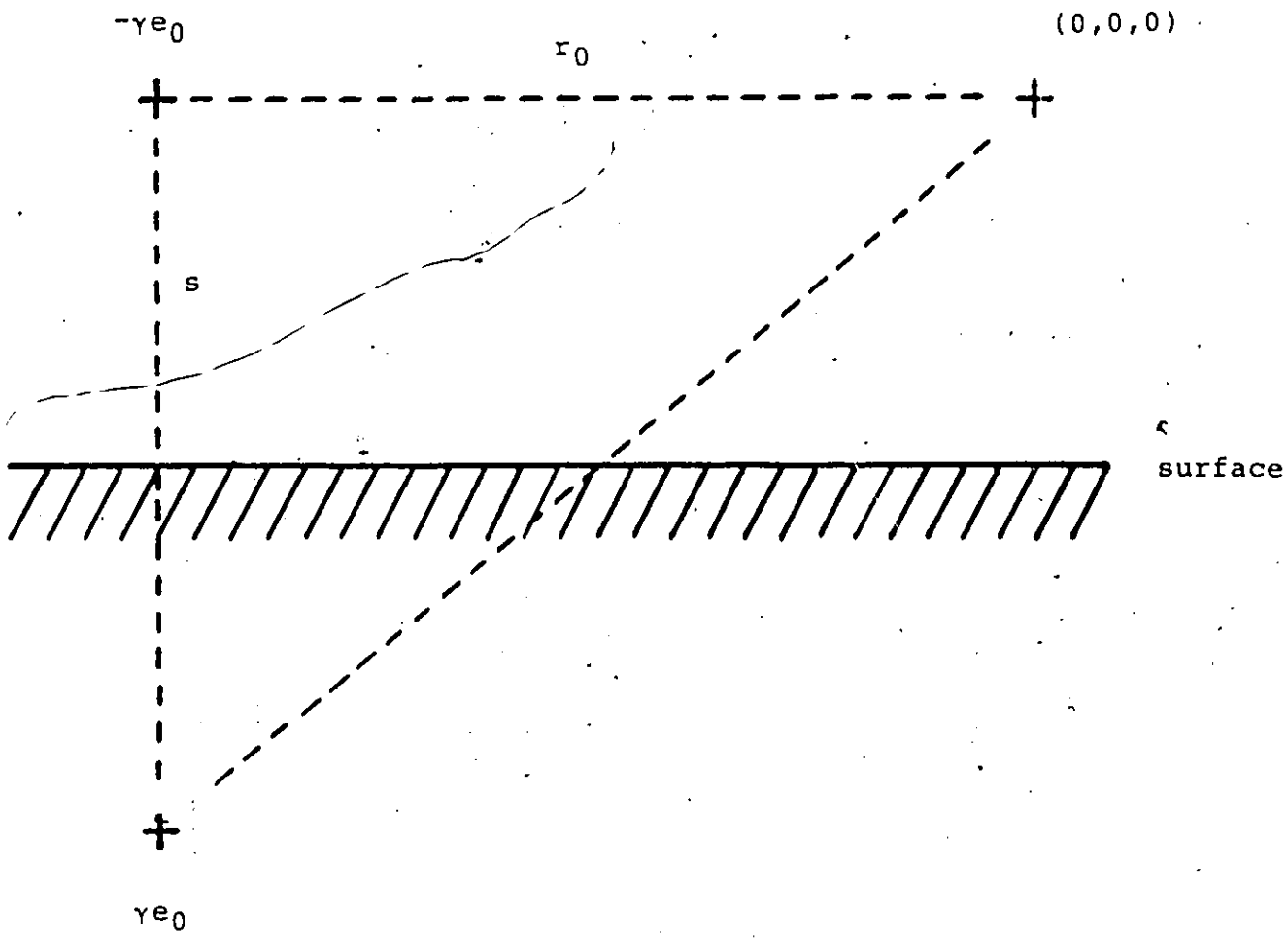

Fig. 4b: Definition of Field vectors associated with adsorbed charges and primary images.

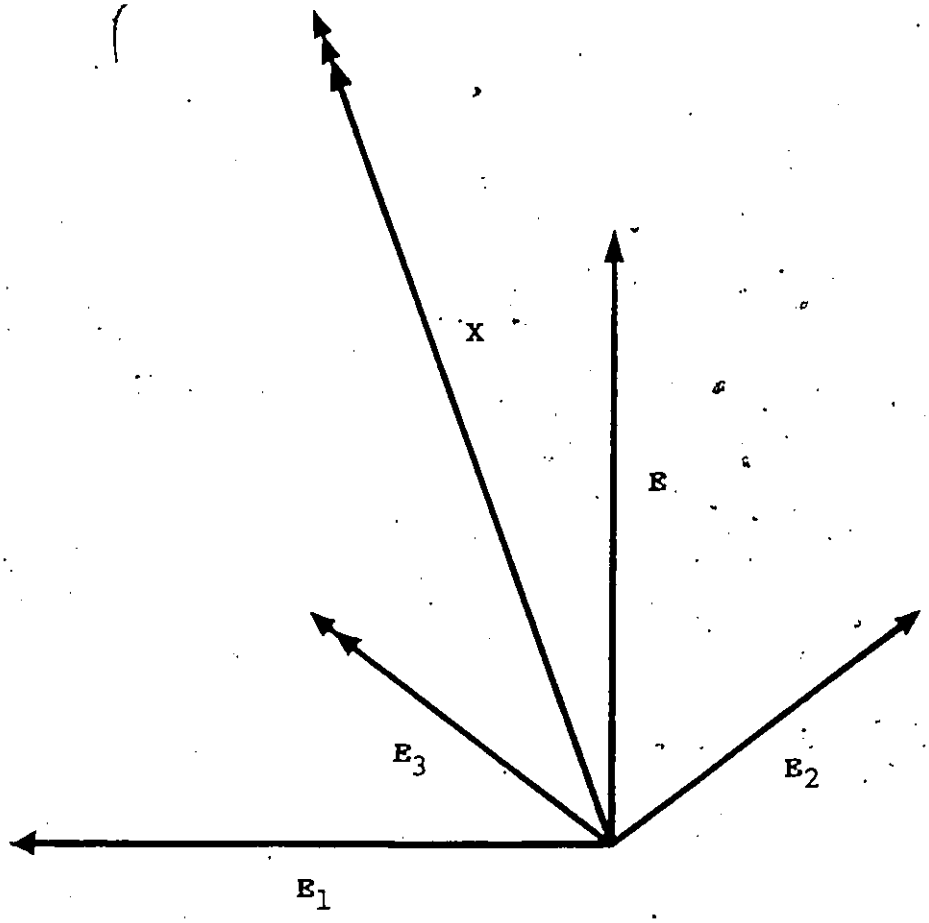

In addition to the single images induced in the metal (which will be referred to as primary images), the adatom will induce images in the diffuse double layer, which according to the primitive model is treated as a semi-infinite continuum with the bulk dielectric constant of water, $\varepsilon_2 = 78$. The interface is thus proposed to include two parallel dielectric boundaries; it is well known [25] that in such circumstances point charges will induce an infinite series of images, in both dielectrics. These will be referred to as secondary images.

In order to calculate the contribution of these extra images induced in the diffuse double layer and in the metal, to the energy of the adatom, it is necessary to solve the boundary value problem for the potential in the inner layer (region 1) and the diffuse layer (region 2), assuming that the metal is a perfect conductor. This calculation has formed the basis of numerous treatments of ionic adsorption, which will be considered in more detail in Chapter 6. Such approaches may be broadly classified according to whether the diffuse layer is assumed to be a dielectric continuum, or a perfect or imperfect conductor. The treatment of the diffuse layer as an imperfect conductor was first carried out by Kir'yanov [37], who assumed the potential distribution in the diffuse layer to be given by the linearized Poisson-Boltzmann equation.

The limiting case of this solution, when the reciprocal screening length $\lambda \to 0$, is formally equivalent to the case where the diffuse layer is modelled as a dielectric continuum; this latter potential problem was first solved by Buff and Stillinger [38]. More recently, it also formed the basis of a theory of

ionic adsorption presented by Bockris and Habib [15] using a dielectric continuum approximation for both regions. For the total energy of a charge $-\gamma e_0$, located in the plane z = 0, in the inner layer of dielectric constant ε_1 bounded by the electrode surface (z = -s) and the outer Helmholtz plane (z = z_1), these authors obtained the result

$$((\gamma e_0)^2/\varepsilon_1)[\int_0^\infty -e^{-2sk}dk - \beta\int_0^\infty dk\ e^{-2kz_1}(1-e^{-2sk})^2/[1-\beta e^{-2k(z_1+s)}]] = -e_0\gamma T \qquad [21]$$

where $\beta = (\varepsilon_1-\varepsilon_2)/(\varepsilon_1+\varepsilon_2)$ and the notation has been changed to conform to that used in the present chapter. The first integral has the value -1/2s, so that the first term in this expression is immediately recognized as the interaction energy between a charge and its primary image, which would be expected from the above discussion. The second term thus represents the contribution of secondary imaging in both the metal and the solution. In order to evaluate this for the interface model considered here, ε_1 is taken as 1 (since the dipole polarization is to be considered explicitly), ε_2=78 and $z_1 = s = 1.5\times10^{-8}$ cm. With these constants, the second integral in the expression 21 has the value 3.190×10^7 cm^{-1}, which is seen to be comparable to that of the first integral ($1/2s = 3.333 \times 10^7$ cm^{-1}).

In order to obtain the above result, it was necessary to calculate the potential in the inner layer, in cylindrical coordinates (ρ,ϕ,z), due to the charge system located on the z-axis. (In this coordinate system, ρ represents the radial distance from the origin of the plane z = 0, parallel to the electrode surface, and ϕ specifies the direction of this radius

vector within the plane.) According to Bockris and Habib, the potential is assumed to have the following forms:

$$-s<z<z_1: \quad V_1 = -e_0\gamma\int_0^\infty e^{-k|z|}J_0(k\rho)dk + \Phi \qquad [22]$$

where

$$\Phi \equiv -\gamma e_0\int_0^\infty J_0(k\rho)[e^{kz}f_1(k)+e^{-kz}f_2(k)]dk$$

is the total potential due to induced polarization;

$$z_1<z<\infty: \quad V_2 = -e_0\gamma\int_0^\infty J_0(k\rho)f_3(k)e^{-kz}dk \qquad [23]$$

$J_0(x)$ is the Bessel function of the first kind, of order zero. The functions f_1 and f_2, which vanish at the electrode surface and satisfy the conditions of continuity of potential and dielectric displacement between regions (1) and (2), are

$$f_1(k) = \beta e^{-2kz_1}(1-e^{-2ks})/[1-\beta e^{-2k(s+z_1)}] \qquad [24a]$$

$$f_2(k) = [-e^{-2sk} + \beta e^{-2k(z_1+s)}]/[1-\beta e^{2k(s+z_1)}] \qquad [24b]$$

The solution to the boundary value problem considered by Kir'yanov [37] is, within region (1), identical in form to that given by eqns. 24a and 24b, but in this case

$$\beta = [\varepsilon_2 - k/(k^2+\lambda^2)^{1/2}]/[\varepsilon_2 + k/(k^2+\lambda^2)^{1/2}] \qquad [24c]$$

The corresponding ionic image energy will be different, depending on the values of the dielectric constant and screening length of the diffuse layer. For zero ionic strength, $\beta \approx 0.975$; the effect of a non-zero value of λ will be to increase β, but in the limit $\lambda \to \infty$, $\beta \to 1$. Thus, for large values of the diffuse layer dielectric constant as that used here, $0.975... < \beta < 1$, so that β can be considered as approximately constant. Physically, this means that the potential exerted in region (1) by the ions in region (2) is masked by the high value of the dielectric constant.

The contribution to the potential due to the secondary

imaging may therefore be identified as

$$\phi^{\dagger}(\rho,z) = -\gamma e_0 \int_0^{\infty} J_0(k\rho)[e^{kz}f_1(k) + e^{-kz}f_2(k) + e^{-k(z+2s)}]dk \qquad [25]$$

and the corresponding field components in the radial and normal directions are given by

$$-\partial\phi^{\dagger}/\partial\rho = -\gamma e_0 \int_0^{\infty} kJ_1(k\rho)[e^{kz}f_1(k) + e^{-kz}f_2(k) + e^{-k(2s+z)}]dk \qquad [26a]$$

$$-\partial\phi^{\dagger}/\partial z = \gamma e_0 \int_0^{\infty} kJ_0(k\rho)[-e^{kz}f_1(k) + e^{-kz}f_2(k) + e^{-k(z+2s)}]dk \qquad [26b]$$

To include the effect of secondary imaging due to a neighbouring charged adatom, the radius vector ρ is assumed to join the origin and the lattice point; the effective field **X** should now include these expressions, evaluated at $\rho = r_0$ and $z = 0$, so that

$$X_x = [b^3/(1+b^2)^{3/2} - 1]\gamma e_0/r_0^2 - \partial\phi^{\dagger}/\partial\rho|_{r_0,0} \qquad [27a]$$

$$X_y = 0 \qquad [27b]$$

$$X_z = E + (\gamma e_0/r_0^2).b^2/(1+b^2)^{3/2} - \partial\phi^{\dagger}/\partial z|_{r_0,0} \qquad [27c]$$

Evaluation of the two extra terms using $s = 1.5\times10^{-8}$ cm and $z_1 = s$ gives $\partial\phi^{\dagger}/\partial\rho = -1.833 \times 10^5\gamma$ statcoulomb cm^{-2}, $\partial\phi^{\dagger}/\partial z = 5.983 \times 10^4\gamma$ statcoulomb cm^{-2}. The ratio E/X is plotted in Figs. 5a and 5b, which were calculated with the consideration of primary and primary plus secondary imaging, respectively. The secondary imaging contribution has the interesting effect of making X vary more "symmetrically" with E.

To calculate the free energy of interaction between the adatom-image species and the adjacent solvent dipole, of vector moment **m**, it is necessary to integrate the Boltzmann factor of

Fig. 5a: Ratio E/X, with consideration of primary images only (cf. eqn. 20).

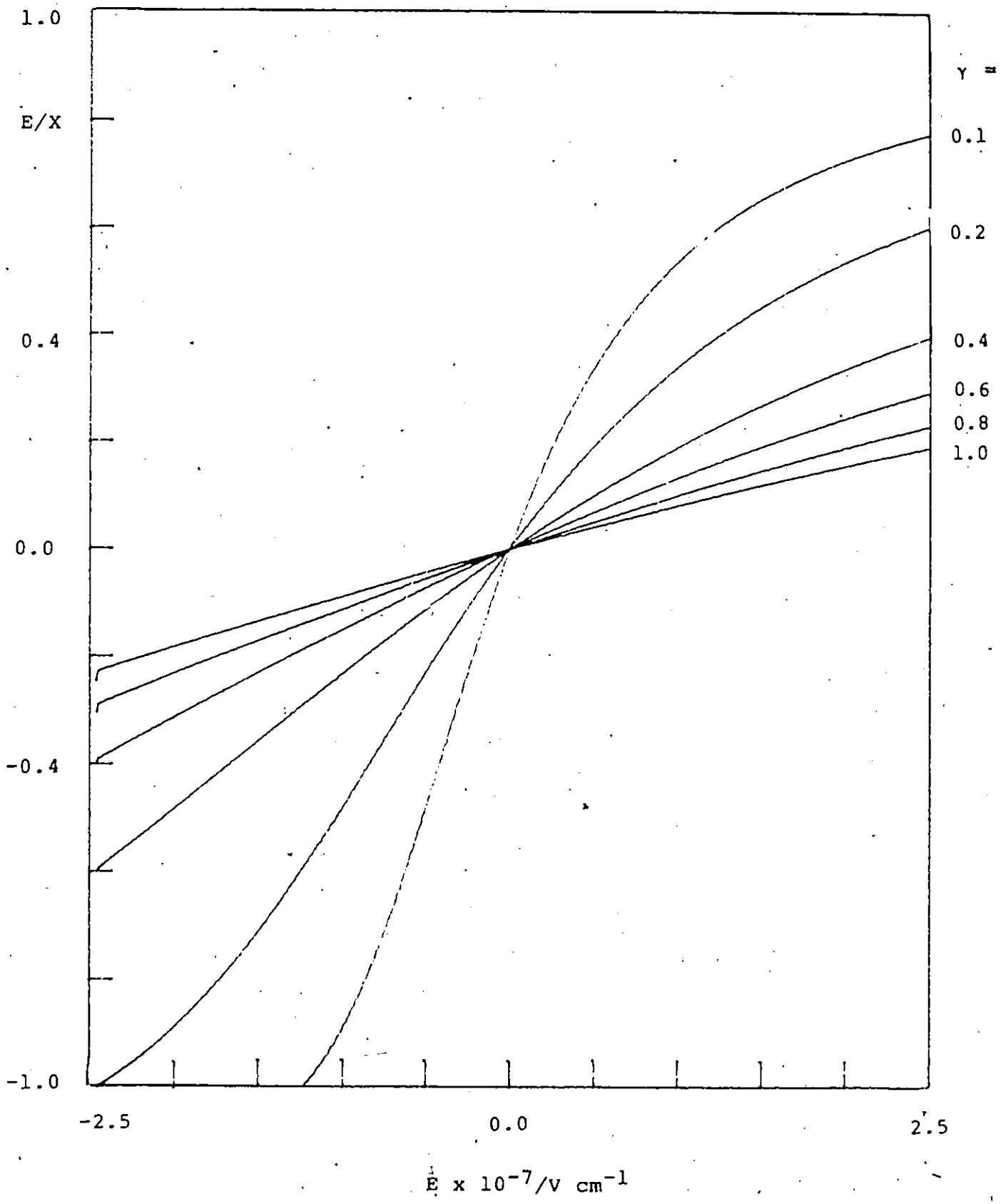

Fig. 5b: Ratio E/X, with consideration of primary and secondary images (cf. eqns. 27a - 27b).

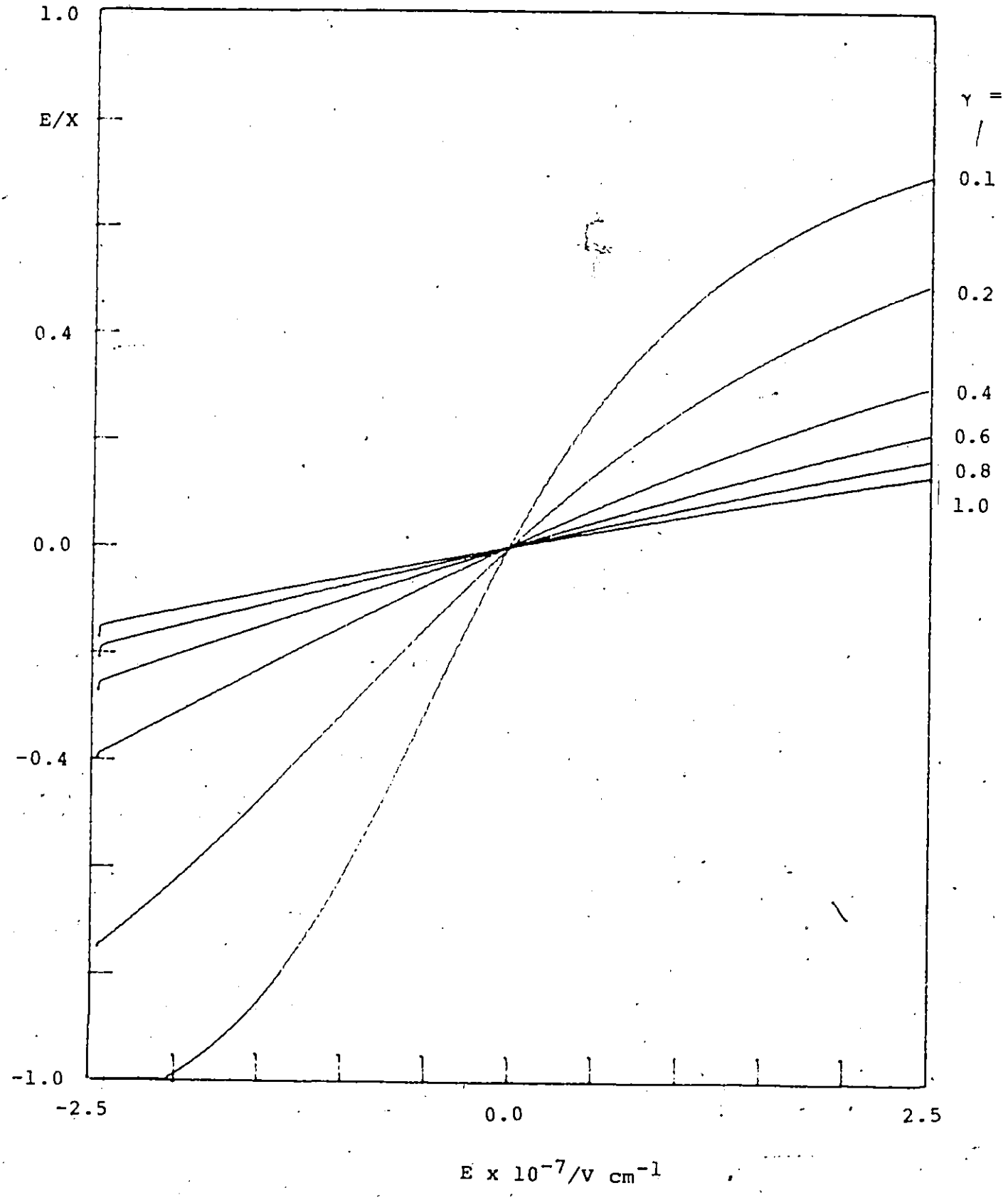

the interaction energy $-\mathbf{m}.\mathbf{X}$ over all possible values of the angular coordinates of $\mathbf{m}$, which are

$$\mathbf{m} = m(\sin\theta\cos\phi,\ \sin\theta\sin\phi,\ \cos\theta) \qquad [28]$$

where the angles are defined in Fig.6. Abbreviating $\mathbf{X}$ by writing $\mathbf{X}=(X_x,0,X_z)$, the interaction energy becomes

$$-\mathbf{m}.\mathbf{X} = -m(X_x,\ 0,\ X_z).(\sin\theta\cos\phi,\ \sin\theta\sin\phi,\ \cos\theta) \qquad [29]$$

$$= -mX_x\sin\theta\cos\phi - mX_z\cos\theta \qquad [30]$$

The partition function for the polarization of $\mathbf{m}$ by $\mathbf{X}$ is defined by

$$\exp(\alpha X^2/2kT)\int_0^{\pi}\int_0^{2\pi}\exp[m(X_x\sin\theta\cos\phi + X_z\cos\theta)/kT]\sin\theta\,d\theta\,d\phi \qquad [31]$$

The integral over ϕ is [26]

$$\int_0^{2\pi}\exp[mX_z\sin\theta\cos\phi/kT]d\phi = 2\pi.I_0(mX_x\sin\theta/kT) \qquad [32]$$

where $I_0(x)$ is the modified Bessel function of the first kind, of order zero, with power series expansion

$$I_0(x) = J_0(ix) = 1 + (x/2)^2 + (x/2)^4/(2!)^2 + \ldots.$$

The integral in eqn. 31 therefore reduces to

$$\int_0^{\pi}\exp(mX_z\cos\theta/kT).I_0(mX_x\sin\theta/kT).2\pi\sin\theta\,d\theta \qquad [33]$$

The field $\mathbf{X}$, defined by eqn. 27, contains a contribution from the electrode's field $\mathbf{E}$. Thus, in order to extract from this integral the contribution due to the field-dependent interaction between $\mathbf{m}$ and the adatom, it is necessary to divide by the partition function for polarization of the solvent dipole by the field E, defined by eqn. 3. The final result for the partition function for the solvent dipole-adatom pair is therefore

$$\zeta_{aw} = \frac{\int_0^{\pi}I_0(mX_z\sin\theta/kT)\exp(mX_x\cos\theta/kT)\sin\theta\,d\theta}{2\sinh(mE/kT)/(mE/kT)}$$

Fig. 6: Definition of geometrical variables.

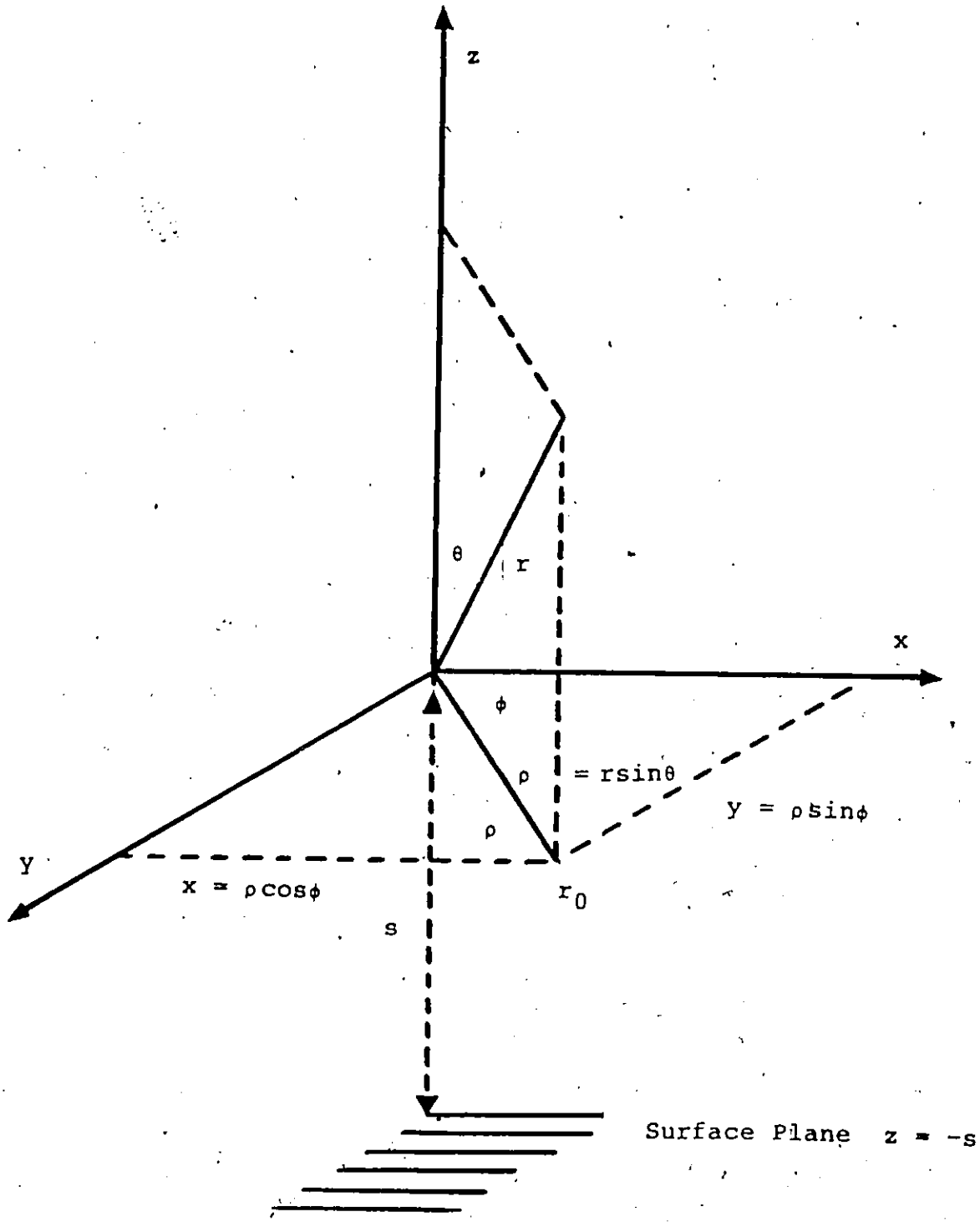

$$x \exp[\alpha(X^2 - E^2)/2kT] \qquad [34]$$

and as before, the corresponding free energy of interaction is

$$u_{aw} = -kT \ln(\zeta_{aw}) \qquad [35]$$

With this definition of ζ_{aw}, it is seen that in the special case $\gamma = 0$, the numerator of the expression 34 becomes equal to the denominator, so that $u_{aw} = 0$, which is to be expected for interaction of a dipole with an uncharged, non-polarizable species.

In Figs. 7a and 7b, u_{aw}/kT is plotted as a function of the electrode field strength E, with the same values of γ used in Figs. 5a and 5b, with consideration of primary and primary plus secondary imaging respectively.

To include long-range coulombic effects, the field **E** in the definition of **X** must be replaced with an effective field $\mathbf{E}_{eff}$, including contributions proportional to Θ (due to the charges) and $\langle s \rangle = \langle m \rangle / m$ (due to the dipoles). The determination of these contributions will be considered in detail in Chapter 6.

4. Interactions Between Adatoms

The energy of interaction between two neighbouring adatoms may be readily calculated using the results of the previous section; this is simply the charge times the potential due to the neighbouring species, evaluated at z=0:

$$u_{aa} = -\gamma e_0 V_1 \qquad [36]$$

$$= (\gamma e_0)^2 [1/r_0 - 1/(r_0^2+4s^2)^{1/2} - \phi^\dagger]$$

$$\zeta_{aa} = \exp(-u_{aa}/kT)$$

With $r_0 = 2s = 3.0 \times 10^{-8}$ cm, $e_0 = 4.803 \times 10^{-10}$ statcoulomb and $kT = 4.045 \times 10^{-14}$ erg, one has the following numerical value

$$u_{aa}/kT = 177.4\gamma^2 \qquad [37]$$

Fig. 7a: Adatom-dipole interaction free energy (cf. eqn. 34), with consideration of primary images only.

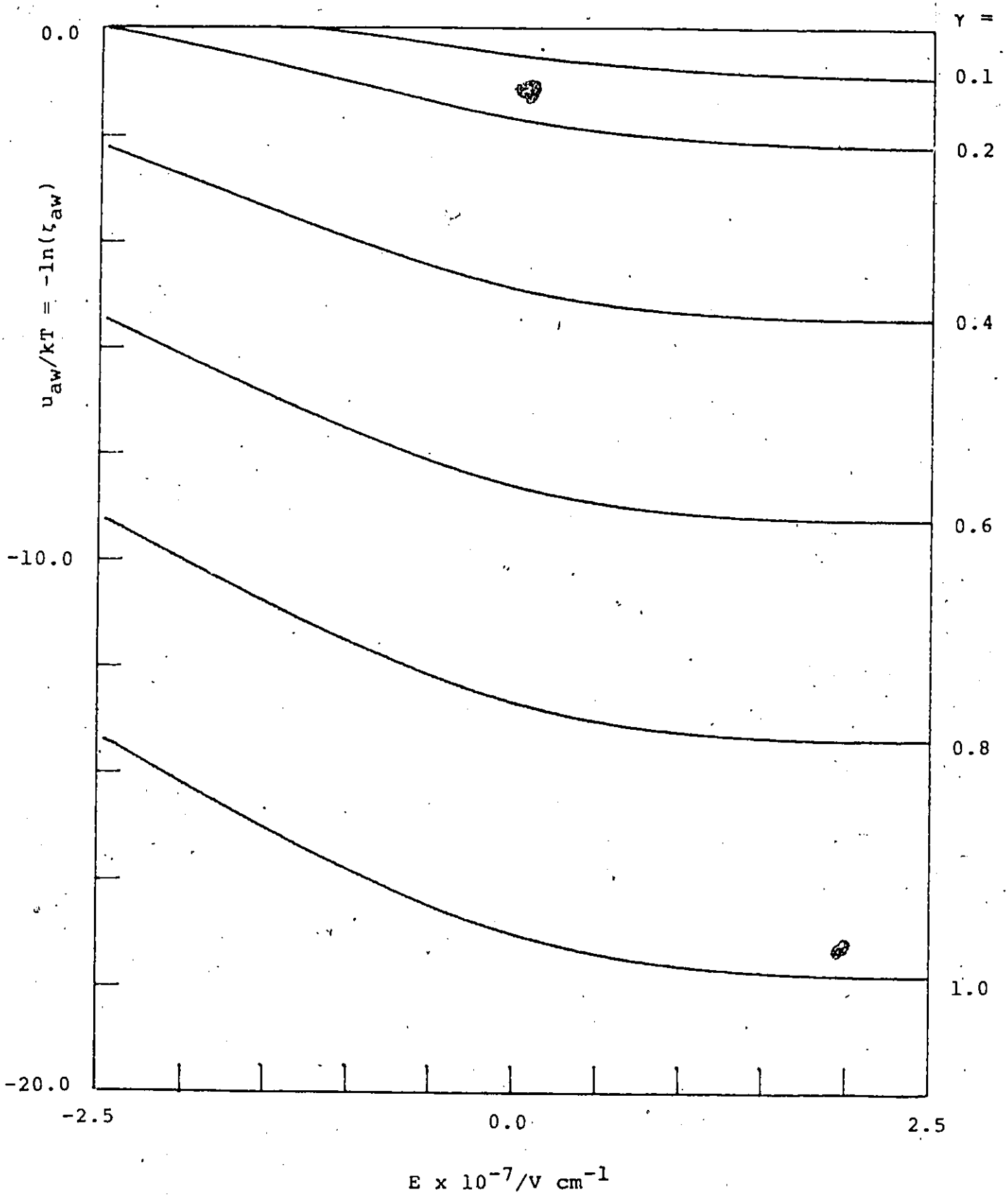

Fig. 7b: Adatom-dipole interaction free energy (cf. eqn. 34), with consideration of primary and secondary images.

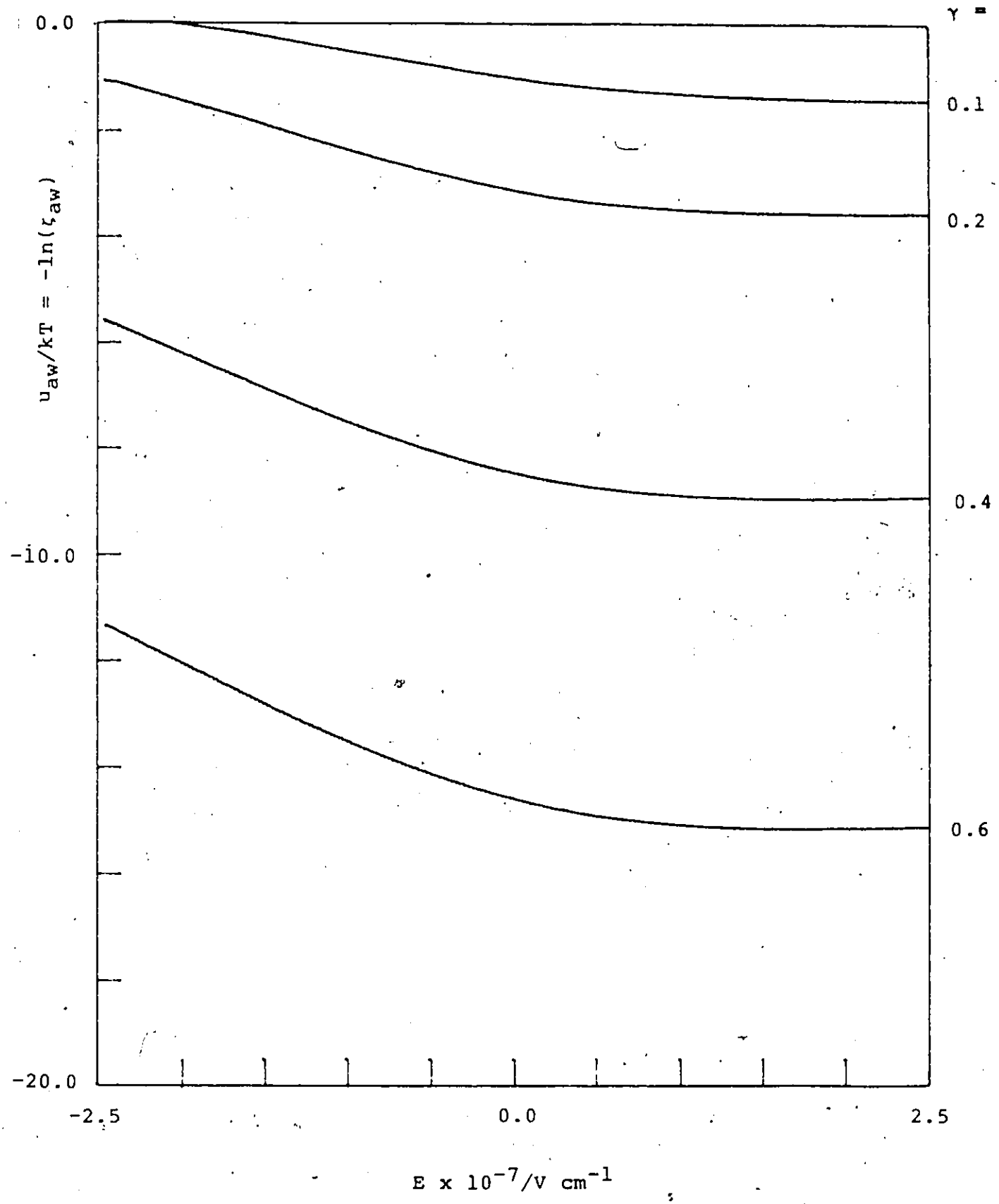

As has recently been shown [19], the "$\theta^{1/2}$"-type isotherm appropriate for the electrodeposition of a charged species on a surface (neglecting images) leads to anomalous behaviour of the reaction pseudocapacitance as a function of potential. This problem, as will be demonstrated subsequently, results from the configurational component of the model rather than the physically unrealistic assumption that the induced charges can be ignored. Of course, for the enormous values of interaction energy given by eqn. 33 with large γ, the assumption that only nearest-neighbour interactions need be considered is quite unrealistic. The use of the mean field approximation to account for non-nearest-neighbour interactions will be discussed in more detail in connexion with the construction of ionic adsorption isotherms; the results of the present chapter are proposed to apply only to surface species bearing relatively small charges. Attention will first be restricted to the consideration of nearest-neighbour pairwise interactions, which, using the results of Chapter 5, will provide a basis for the interpretation of more realistic treatments incorporating mean-field effects.

In order to calculate the electrical energy of the adatoms in the double layer, it is necessary to consider the potential profile; since the micropotential contribution is implicitly neglected by considering only nearest-neighbour interactions, the potential distribution in the double layer may be taken to be the macropotential, which varies linearly as shown in Fig. 1 of Chapter 1. The electrical energy of the adatoms is that experienced by their charge, $-\gamma e_0$, at the midpoint of the compact

double layer, where the potential is V/2, assuming that the diffuse-layer potential drop is negligible. To this must be added the potential energy of interaction between the charge and the image which it induces in the metal, which is given by eqn. 21. One therefore has for the electrical partition function

$$z_a = \exp[\gamma e_0 (V/2+T)/kT] \qquad [38]$$

In the more general treatment including long-range coulombic interactions, the term V/2 in this expression will be replaced with the effective potential V_{eff} corresponding to the field E_{eff} mentioned above. In addition to V/2, this contains the micropotential contributions due to charges and dipoles.

5. Interactions Between Solvent Molecules and the Electrode

The various recent theoretical treatments of the interactions of water molecules with metal surfaces are quite difficult to compare, because they are based on different assumptions. Indeed, the problem itself is more difficult, because a realistic treatment requires a consideration of the electronic structure of the metal surface as well as that of the adsorbed molecules, and hence the rejection of the simple classical model of the electrode surface as that of a perfect conductor, with the surface charge density ideally localised in one plane. Only in the most recent treatments of interfacial polarization is allowance made for the non-ideality of the electrode surface charge distribution [27].

As yet, there exists no strictly quantum-mechanical treatment of molecular interactions with charged metal surfaces, although attempts have been made [28] to treat the problem of interaction of H_2O molecules with metal clusters of various

sizes. A detailed calculation, taking into account the finite separation of the charged components of an adsorbed water molecule, was made by Gonzales Maroto et al. [29]. This retained a classical model for the surface and considered the interaction energy as a function of distance from the metal as well as angular orientation, but was restricted to the case $q_M=0$.

(i) Dispersion Energies

Within the limits of the primitive model, the dispersion contribution to the interaction energy of an adsorbed species with a metal surface has usually been calculated using the Kirkwood-Mueller equation [30], viz.

$$U_{disp} = Nm_0c^2\alpha_1\alpha_2/r_0^3(\alpha_1/\chi_1 + \alpha_2/\chi_2) \qquad [39]$$

where N is the number of substrate atoms per cm^3, m_0 is the mass of an electron, c is the velocity of light, r_0 is the distance between the centres of the the adsorbed molecules (1) and the substrate atoms (2), and α_1, χ_1 and α_2, χ_2 are the respective polarizabilities and diamagnetic susceptibilities. Using values of these parameters appropriate for H_2O ($\alpha_1 = 1.44\times10^{-24}cm^3$, $\chi_1 = -2.16\times10^{-29}cm^3$) and Hg ($\alpha_2 = 5.05\times10^{-24}cm^3$, $\chi_2 = -5.61\times10^{-29}cm^3$) and T = 293K, there results $U_{disp} = 4.65kT$, which is certainly not negligible, as frequently assumed.

This formula is based on the assumption of a localized interaction between the molecule and a single atom of substrate. In view of the delocalized electronic structure of metallic surfaces, it is possible that not all the electrons in the metal atoms may necessarily contribute to the dispersion interaction, so that eqn. 39 might tend to overestimate its magnitude; also,

no account is taken of an electronic interaction between molecular orbitals and the variable excess surface charge density of the metal. The various approximate treatments of dispersion interactions and their possible relevance to anisotropic systems have been discussed in a recent monograph by Nicholson and Parsonage [31]. For present purposes, dispersion energies are assumed to be included in the intrinsic adsorption energies of each species, and hence in the field-independent factors of the corresponding partition functions.

(ii) Field-Independent Orientational Preference

Treatments of dipole orientation in the compact double layer generally incorporate the possibility of an intrinsic energetic preference of one orientation over another. In the simple two-state model described by Bockris, Devanathan and Mueller (BDM) in 1963 [2], this energy difference was attributed to the non-coincidence of the dipole with the centre of the molecule, such that when the oxygen is closest to the metal, the image energy is slightly more negative. With a displacement of 5×10^{-10} cm of the dipole from the centre, the energy difference is given by these authors (in the notation of the present chapter) as

$$\Delta U = 3m^2 d / 2r_0^4 \qquad [40]$$

which for T = 293K amounts to 0.780 kT.

In the treatment of Macdonald and Barlow [20], a continuous-orientation model was used, and the field dependent orientational preference was assumed to vary with cos θ, being given by $-U_0(1 + \cos\theta)/2$, which is $-U_0$ when $\theta = 0$ and 0 when $\theta = \pi$. The energy difference is thus equivalent to a field $U_0/2m$, which is termed the "natural" field by these authors. Although detailed molecular

arguments as to its value were not presented, the existence of such an orientational preference was attributed to the combined influence of orbital overlap with metal atoms and hydrogen bonding with solvent molecules in the adjacent layer of the electrolyte.

Several investigators (reviewed in ref. 39) have attempted to infer a value of the intrinsic energy difference by analysis of experimental differential capacity-charge curves in terms of various molecular models. The charge density required to minimize the capacity is then taken to be that which balances the "natural" field which is equivalent to the energy difference. For example, in BDM [2], the influence of the energy difference given by eqn. 40 is stated to be equivalent to that of a charge density of $-2\ \mu C\ cm^{-2}$. This is correct, however, only if the equivalent field energy mE/kT is calculated using $E = 4\pi q_M/\epsilon$, where ϵ is constant and equal to 6; with these values, one obtains $mE/kT = 0.579$. It has been shown, however, that the use of this representation of the field gives inconsistent results [32,33]. The reliability of energetic differences estimated in this way is therefore suspect.

An additional factor, which seems not to have been discussed in the literature, is the influence of the surface dipole moment of the metal, which in turn arises from the "overspill" of the electron density. The origin of this effect is quantum-mechanical, and it does not readily lend itself to a classical interpretation. A related effect, mentioned in Chapter 2, is the possibility of interaction between the excess surface charge

density and adsorbed species; the result of this would be to introduce asymmetry into the variation of the partition function, whilst the surface dipole moment, being an intrinsic property of the metal, would be expected to exert a constant influence on the energy of the adsorbed species.

Several factors, then, have been proposed to contribute to the field-independent orientational energy difference for an adsorbed water molecule. Unfortunately, it is not possible to reliably estimate any of them from an ab initio model, or to unambiguously determine them from experimental results. The existence of such preferences is, however, supported by considerable experimental evidence [2,34,35]. In subsequent work on ionic adsorption isotherms, the procedure of Macdonald and Barlow will be followed, in accounting for such effects by the expression $U_0(1+\cos\theta)/2$, but acknowledging that the value of U_0 is probably determined by several different factors.

When this angular potential energy is superimposed on the energies resulting from permanent and induced dipole moments, the electrical partition function becomes

$$z_w = 2\pi\exp(\alpha E^2/2kT)\int_0^{\pi}\exp(mE\cos\theta/kT + U_0(1+\cos\theta)/2kT)\sin\theta d\theta$$

$$= 4\pi\exp(U_0/2kT+\alpha E^2/2kT)\sinh(mE/kT+U_0/2kT)/(mE/kT+U_0/2kT) \quad [41]$$

On taking the logarithmic derivative, the extra factor of $\exp(U_0/2kT)$ disappears and the Langevin function, of argument $mE/kT+U_0/2kT$, results.

(iii) Image Interactions Involving Dipoles

The treatment of Macdonald and Barlow assumed the following form for the variation of the orientational potential energy with θ:

$$U(\theta) = -mE\cos\theta - U_0(1+\cos\theta)/2 - (a_1+a_2\cos^2\theta) \qquad [42]$$

The third term on the right is the energy of interaction of the dipole with the images induced by it in the metal and in the diffuse double layer. The values of the constants a_1 and a_2 depend on whether single or multiple images are considered. Considering first that single images are induced in the metal by the dipoles, the interaction energy is then given by eqn. 13, with $\vec{m}_1 = m(\sin\theta, 0, \cos\theta)$ located at the origin, and $m_2 = m(-\sin\theta, 0, \cos\theta)$ located at the point (0, 0, -2s), so that r = (0, 0, 2s) and $r = |r| = 2s$:

$$U_{image} = m^2(\cos^2\theta - \sin^2\theta)/8s^3 - 24s^3m^2\cos^2\theta/8s^3 \qquad [43]$$
$$= -(1 + \cos^2\theta)m^2/8s^3$$

The constants a_1 and a_2 are thus both equal to $m^2/8s^3 = 3.083kT$.

In the treatment of Macdonald and Barlow, images were assumed to be induced in the metal and in the diffuse double layer charge. Implicit in this is the assumption that the latter behaves as a perfect conductor, since the formulae given for a_1 and a_2 in ref. 20 contain neither the screening length for the diffuse layer (calculated from the Gouy-Chapman theory) nor depolarization factors $(\varepsilon-1)/(\varepsilon+1)$ reflecting the reduction of the field by dielectric polarization.

In view of the treatment given by Bockris and Habib of simultaneous conductive and dielectric imaging, it is of interest to apply this method to the calculation of the corresponding imaging energy of the adsorbed dipoles. In order to do this, it is first necessary to construct a Fourier-Bessel integral representation of the potential due to a dipole of arbitrary

orientation.

In terms of the polar angles defined earlier, the potential due to a dipole of vector moment $\mathbf{m} = (m_1, 0, m_2)$ at the origin is

$$\mathbf{m}.\mathbf{r}/r^3 = (m_1 \sin\theta\cos\theta + m_2\cos\phi)/r^2 \qquad [44]$$

This choice of the components of $\mathbf{m}$ is equivalent to the definition of ϕ as the angle between the vectors $\mathbf{r}$ and $\mathbf{m}$ in the plane $z = 0$. The radial distance ρ from the origin in the plane $z = 0$ is related to z and θ by

$$\sin\theta = \rho/(\rho^2+z^2)^{1/2}$$

$$\cos\theta = z/(\rho^2+z^2)^{1/2}$$

Since the inverse distance in cylindrical polar coordinates has the integral representation [25]

$$\int_0^\infty e^{-k|z|}J_0(k\rho)dk = 1/(\rho^2+z^2)^{1/2} \qquad [45]$$

the factors $\sin\theta/r^2$ and $\cos\theta/r^2$ may be defined by the following integrals:

$$\sin\theta/r^2 = -(\partial/\partial\rho)(\rho^2+z^2)^{-1/2} = \int_0^\infty kJ_1(k\rho)e^{-k|z|}dk \qquad [46]$$

$$\cos\theta/r^2 = -(\partial/\partial z)(\rho^2+z^2)^{-1/2} = \int_0^\infty kJ_0(k\rho)\,\mathrm{sign}(z)e^{-k|z|}dk \qquad [47]$$

where $\mathrm{sign}(z) = 1$ if $z \geq 0$ and $\mathrm{sign}(z) = -1$ if $z < 0$. The potential defined in eqn. 52 therefore has the integral representation

$$\mathbf{m}.\mathbf{r}/r^3 = m_2\int_0^\infty k\,\mathrm{sign}(z)e^{-k|z|}J_0(k\rho)dk + m_1\cos\phi\int_0^\infty ke^{-k|z|}J_1(k\rho)dk \qquad [48]$$

The presence of the second term, with its factor of $\cos\phi$, is necessary to account for the deviation from the circular symmetry present in the Bockris-Habib calculation for single charges.

The consistency of eqn. 48 may be demonstrated by calculating the potential energy of a dipole $\mathbf{m} = (m_1, 0, m_2)$ at the origin, adjacent to a semi-infinite continuum of dielectric

constant ε, bounded by the plane $z = -s$. The potential is assumed to have the following forms:

$$z<-s:\ V_1 = m_2\int_0^\infty k e^{kz} f_1(k) J_0(k\rho)dk + m_1\cos\phi\int_0^\infty k e^{kz} g_1(k) J_1(k\rho)dk \quad [49]$$

$$z>-s:\ V_2 = m_2\int_0^\infty k\,\mathrm{sign}(z) e^{-k|z|} J_0(k\rho)dk + m_1\cos\phi\int_0^\infty k e^{-k|z|} J_1(k\rho)dk$$
$$+ m_2\int_0^\infty k e^{-kz} f_2(k) J_0(k\rho)dk + m_1\cos\phi\int_0^\infty k e^{-kz} g_2(k) J_1(k\rho)dk \quad [50]$$

Application of the boundary conditions

$$V_1 = V_2, \quad (\varepsilon\partial/\partial z)V_1 = (\partial/\partial z)V_2 \text{ at } z = -s \quad [51]$$

results in two parallel sets of simultaneous equations for the unknown functions f_1, f_2, g_1, and g_2, which have the solutions

$$f_1 = -(1-\beta) \qquad f_2 = \beta e^{-2ks}$$
$$g_1 = 1-\beta \qquad g_2 = -\beta e^{-2ks} \quad [52]$$

where

$$\beta = (\varepsilon-1)/(\varepsilon+1).$$

The potential energy of the dipole due to the induced polarization of the dielectric is $\mathbf{m}.\nabla\phi$ where

$$\phi = \beta m_2\int_0^\infty e^{-k(z+2s)} J_0(k\rho)dk - \beta m_1\cos\phi\int_0^\infty k e^{-k(z+2s)} J_1(k\rho)dk \quad [53]$$

and the gradient is to be taken in cylindrical polar coordinates. Putting $m_1 = m\sin\theta$, $m_2 = m\cos\theta$, one has

$$\partial\phi/\partial\rho = -\beta m\cos\theta\int_0^\infty k^2 e^{-k(z+2s)} J_1(k\rho)dk \quad [54]$$
$$-\beta m\sin\theta\cos\phi\int_0^\infty k^2[J_0(k\rho)-J_1(k\rho)/k\rho]e^{-k(2s+z)}dk$$
$$= -\beta m\cos\theta/(2s)^3 \text{ as } (\rho,\phi,z) \to (0,0,0)$$
$$\partial\phi/\partial z = -\beta m\cos\theta\int_0^\infty k^2 e^{-k(z+2s)} J_0(k\rho)dk \quad [55]$$
$$+ \beta m\sin\theta\cos\phi\int_0^\infty k^2 e^{-k(z+2s)} J_1(k\rho)dk$$
$$= -2\beta m\cos\theta/(2s)^3 \text{ as } (\rho,\phi,z) \to (0,0,0)$$

The image energy is

$$\mathbf{m}.\nabla\phi = -(\beta m^2/8s^3)[1+\cos^2\theta] \quad [56]$$

which approaches that given by eqn. 45 as $\varepsilon \to \infty$, as it should.

To apply these results to the double layer, it is required, as before, to find the secondary imaging contribution to the potential energy of the adsorbed dipoles. This is done using the approach employed by Bockris and Habib, but replacing the Fourier-Bessel integral for the potential due to the single charge with that due to a dipole of vector moment $\mathbf{m} = m(\sin\theta, 0, \cos\theta)$. The potential distribution is assumed to have the following forms:

for $-s<z<z_1$:

$$V_1 = m\cos\theta\int_0^\infty k\,\mathrm{sign}(z)e^{-k|z|}J_0(k\rho)dk + m\sin\theta\cos\phi\int_0^\infty k e^{-k|z|}J_1(k\rho)dk + \psi \qquad [57]$$

where

$$\psi = m\cos\phi\int_0^\infty k[f_1(k)e^{kz}+f_2(k)e^{-kz}]J_0(k\rho)dk + m\sin\theta\cos\phi\int_0^\infty k[g_1(k)e^{kz}+g_2(k)e^{-kz}]J_1(k\rho)dk \qquad [58]$$

and for $z_1<z<\infty$,

$$V_2 = m\cos\theta\int_0^\infty k f_3(k)e^{-kz}J_0(k\rho)dk + m\sin\theta\cos\phi\int_0^\infty k g_3(k)e^{-kz}J_1(k\rho)dk \qquad [59]$$

Applying the boundary conditions

$$V_1 = 0 \text{ at } z = -s \qquad [60a]$$

$$V_1 = V_2 \text{ at } z = z_1 \qquad [60b]$$

$$(\partial/\partial z)V_1 = (\varepsilon\partial/\partial z)V_2 \text{ at } z = z_1 \qquad [60c]$$

results in two parallel sets of simultaneous equations for the unknown functions f_1, f_2, g_1 and g_3, with solutions

$$f_1 = -\beta e^{-2kz_1}(1 + e^{-2ks})/[1 - \beta e^{-2k(z_1+s)}] \qquad [61a]$$

$$f_2 = [\beta e^{-2k(z_1+s)} + e^{-2ks}]/[1 - \beta e^{-2k(z_1+s)}] \qquad [61b]$$

$$g_1 = -\beta e^{-2kz_1}(1 - e^{-2ks})/[1 - \beta e^{-2k(z_1+s)}] \qquad [61c]$$

$$g_2 = [\beta e^{-2k(z_1+s)} - e^{-2ks}]/[1 - \beta e^{-2k(z_1+s)}] \qquad [61d]$$

As before, the secondary image potential $\psi^\dagger$ is given by

subtracting $\pm e^{-2ks}$ from the expressions for f_2 and g_2. The partial derivatives of $\Psi^\dagger$ at the point (0,0,0), with $z_1 = 2s = 3.0 \times 10^{-8}$ cm, are

$$\partial\Psi^\dagger/\partial\rho = (m/2)\sin\theta\int_o^\infty k^2[g_1(k) + g_2(k) + e^{-2sk}]dk$$

$$= -5.804 \times 10^{22} m\sin\theta/2 \qquad [62]$$

$$\partial\Psi^\dagger/\partial z = m\cos\theta\int_o^\infty k^2[f_1(k) - f_2(k) + e^{-2sk}]dk \qquad [63]$$

$$= -1.009 \times 10^{23}\ m\cos\theta$$

noting that the dimensions of each integral are cm^{-3}.

The corresponding interaction energy is again $\mathbf{m}.\nabla\Psi^\dagger$ which in this case is

$$\mathbf{m}.\nabla\Psi^\dagger = (m\sin\theta,\ 0,\ m\cos\theta).(\partial\Psi^\dagger/\partial\rho,\ 0,\ \partial\Psi^\dagger/\partial z)$$

$$= -m^2 \times 2.902 \times 10^{22} - m^2\cos^2\theta \times 7.188 \times 10^{22} \qquad [64]$$

The total image interaction energy experienced by the dipole is the sum of this quantity and that given by eqn. 45:

$$U_{image} = -m^2(1/8s^3 + 2.902 \times 10^{22}) - m^2\cos^2\theta(1/8s^3 + 7.188 \times 10^{22})$$

$$= -5.501kT - 9.070kT\cos^2\theta \qquad [65]$$

using the previous values of m,T and s.

In the previous discussion of ionic imaging, it was noted that, in addition to providing the contribution of secondary images to the energy of the central ion, the expression obtained for the potential V_1 could also be used to calculate the energy experienced by neighbouring species due to these images. In principle, the same remarks apply to the dipoles, but the above calculations assumed a constant orientation of the central dipole. If it were desired to work out the value of this contribution to the pairwise free energy of interaction, all possible values of the angular coordinates of both dipoles would

need to be considered; however, as has already been observed, the consideration of an isolated pair of dipoles does not seem to constitute an accurate approximation for the pairwise free energy of interaction for each member of a dipole lattice. An estimate of the effect could be made if it were assumed that $\cos\theta$ for the neighbouring dipole were given by the average normal component $\langle s \rangle$. This is equivalent to the mean field approximation, the consequences of which will be considered in later work.

It is of interest to calculate the difference in the electrical free energy per molecule which results from this sort of imaging. This is given by the equation

$$\text{free energy difference} = -kT\ln(z_w'/z_w) \qquad [66]$$

where z_w is given by eqn. 3 and the corresponding partition function z_w', including the image contribution, is given by

$$z_w' = \int_0^{\pi} \exp[(U_0/2kT+mE/kT)\cos\theta + (a_1+a_2\cos^2\theta)/kT]\sin\theta d\theta \times \exp(\alpha E^2/2kT+U_0/2kT) \qquad [67]$$

This energy difference is plotted as a function of E in Fig. 8, for a_1 and $a_2 = m^2/8s^3$, and for a_1 and a_2 given by eqn. 65, from which it can be seen that the interaction of the adsorbed dipole with its own image makes a significant contribution to the polarization free energy.

The polarization function appropriate to the dipole-image model is given by the logarithmic derivative of z_w' with respect to the field E:

$$\langle m \rangle/m = \frac{\int_{-1}^{1} y \exp[(U_0/2kT+mE/kT)y+(a_1+a_2y^2)/kT]dy}{\int_{-1}^{1} \exp[(U_0/2kT+mE/kT)y+(a_1+a_2y^2)/kT]dy} + \alpha E \qquad [68]$$

where the integrals have been simplified by means of the

Fig. 8: Effect of dipole images on polarization free energy with respect to free dipoles (cf. eqn. 66)

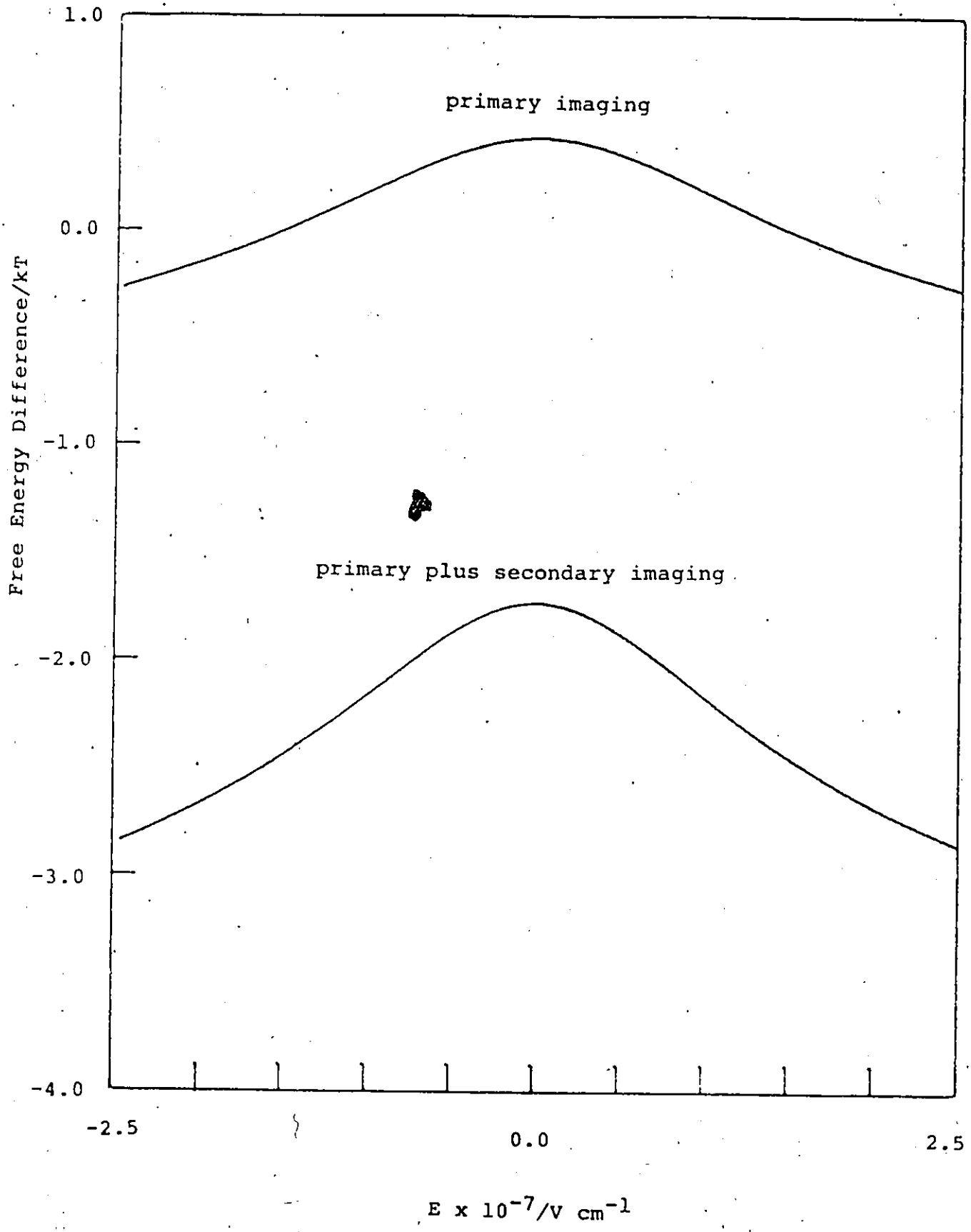

substitution $y = \cos\theta$.

As shown by Macdonald and Barlow [20], the behaviour of this expression as a function of E is qualitatively similar to that of the Langevin function, which would be obtained from this function with $a_1 = a_2 = 0$. The saturation limit is reached for lower values of mE/kT, however, which is to be expected from the presence of an extra positive term in the arguments of the exponentials in the numerator and denominator.

(iv) Redefinition of the Interaction Partition Functions

In order to calculate the adatom-dipole interaction partition function with the inclusion of the interaction energy between the dipole and its image, the term $mE\cos\theta$ in eqn. 50 must be replaced by **m.X** as defined earlier. The interaction energy is now a function of both angular coordinates, and proceeding as before one obtains

$$\zeta_{aw}' = \frac{\int_{-1}^{1} I_0(mX_x(1-y^2)^{1/2}/kT)\exp[(U_0/2kT+mX_z/kT)y+(a_1+a_2y^2)/kT]dy}{\int_{-1}^{1}\exp[(U_0/2kT+mE/kT)y+(a_1+a_2y^2)/kT]dy \times \exp[\alpha(X^2-E^2)/2kT]} \quad [69]$$

The Monte-Carlo simulation from which the function ζ_{ww} was derived did not include either the interaction energy of each dipole with its own image, or the interaction energy of each dipole with the images induced by its nearest neighbours. Hence, it is not strictly correct to combine this with the partition function z_w' appropriate for the dipole-image model. However, the similarities in the predicted polarization behaviour of the free-dipole model and the dipole-image model suggest that the interaction function ζ_{ww}' appropriate for the latter would

exhibit qualitatively the same E-dependence as ζ_{ww}. Of course, $\zeta_{ww'}$ could be determined in the same way as ζ_{ww} by carrying out a Monte-Carlo simulation as Schmickler did, and extracting the interaction part of the partition function by dividing by z_w' instead of z_w. Short of doing this, it is possible to examine the limiting value of the pairwise interaction energy corresponding to complete polarization of the dipole layer.

Considering one central dipole located at (0,0,0), one of its nearest neighbours at $(-r_0,0,0)$ and their respective images at the points (0,0,-2s) and $(-r_0,0,-2s)$, the required energy is that experienced by the central dipole due to interaction with its neighbour and its neighbour's image, plus the interaction energy between the neighbour and the image of the central dipole. (The interaction with its own image is assumed to be already taken into account by the definition of the electrical partition function.)

From eqn. 13, the interaction energy between the two dipoles themselves is m^2/r_0^3. The separation vector between the central dipole of moment $m_1 = (0,0,m)$ at (0,0,0) and the image of moment (0,0,m) at $(-r_0,0,-2s)$ is $\mathbf{r} = (0,0,2s)$, so that the interaction energy is

$$m^2/(r_0^2+4s^2)^{3/2} - 12m^2s^2/(r_0^2+4s^2)^{5/2}$$
$$= (m^2/r_0^3).b^3(b^2-2)/(1+b^2)^{3/2}$$

This will be the same as the interaction energy between the neighbour at $(-r_0,0,0)$ and the image of the central dipole at (0,0,-2s). When $b = 1$, this reduces to $(1/8)m^2/r_0^3$, so that the limiting value of the interaction energy between two adjacent

slightly different from the corresponding value m^2/r_0^3 for the single dipoles. Interestingly, the reduction of the interaction energy for two adjacent dipole-image pairs by including images, is much less than the corresponding energy difference for a pair of charged adatoms in the presence and the absence of the neighbouring image charges.

The assumption that $\zeta_{ww} \approx \zeta_{ww'}$ is equivalent to the neglect of the interaction energy between each dipole and the images induced by its neighbours. In the limit of complete polarization, where interactions of this type will be most important, it has been shown above that the value of this energy is $(1/4)m^2/r_0^3$, which for T = 293K is 0.778 kT. The maximum probable error in the use of this approximation is thus seen to be less than kT, and also less than the discrepancy noted earlier between m^2/r_0^3 and kT times the constant a in the empirical function representing ζ_{ww}. Therefore, in subsequent calculations the approximation $\zeta_{ww'} \approx \zeta_{ww}$ will be made.

The influence of a field-independent orientational potential energy, assumed to be given by $-U_0(1+\cos\theta)/2$ was seen earlier to by equivalent to that of a "natural" field of magnitude $U_0/2m$. This means that in the interaction partition functions ζ_{ww} and $\zeta_{ww'}$ the argument should include $U_0/2kT$ as well as mE/kT. Again, this will have the effect of shifting the minimum value of u_{ww} and $u_{ww'}$ from E = 0 to $E = -U_0/2m$, as well as having a corresponding effect on the polarization free energy.

6. Conclusions

The problem considered in the present chapter was that of defining and calculating pairwise interaction free energies for

adjacent adsorbed charges and dipoles arranged on the points of an hexagonal lattice. Knowledge of these energies is necessary for the construction of adsorption isotherms taking full account of dipolar discreteness, i.e. without relying on the adoption of a dielectric continuum approximation to describe the behaviour of adsorbed dipoles, as in existing treatments.

For point dipoles capable of assuming a continuous range of orientations with respect to the electrode surface, it is necessary to separate the interaction and polarization components of the free energy as a function of the applied interfacial field E. This may be effected by integration of <m> (as determined by Monte-Carlo simulation) with respect to E, followed by subtraction of the polarization free energy appropriate for non-interacting dipoles.

In order to calculate the interaction energy between adsorbed charges and dipoles, it is necessary to consider the total polarizing effect of the field E and the field generated by the adsorbed charge and images induced by it. The net effect due to the charge and its images is obtained by subtraction of the polarization free energy of the molecule in the field E.

The interaction- and self-image energies of adsorbed charges are calculated using a previously published result [15] for the potential distribution resulting from infinite dielectric-conductive imaging. Analogous results for adsorbed dipoles are determined by the use of Fourier-Bessel transforms, and the contribution of self-image interactions to the polarization free energy of these species are determined.

The next problem to be considered (in Chapter 5) is the use of the expressions of this chapter in the construction of adsorption isotherms, i.e. component (b) of the interaction problem, identified in the Introduction, with specific reference to a model faradaic electrodeposition process. As will be seen, this provides a convenient basis for the consideration of the nature of the errors implicit in such a lattice-gas approach to polar interactions at electrodes.

References

1. C.J.F. Boettcher
   "Theory of Electric Polarization", 2ed., Elsevier (1972), v.1
2. J.O'M. Bockris, M.A.V. Devanathan and K. Mueller
   Proc. Roy. Soc. Lond. **A274**: 55 (1963)
3. N.F. Mott and R.J. Watts-Tobin
   Electrochim. Acta **4**: 79 (1961)
4. W. Schmickler
   J. Electroanal. Chem. **157**: 1 (1983)
5. E. Blomgren and J.O'M. Bockris
   J. Phys. Chem. **63**: 1475 (1959)
6. J.W. Schultze and K.J. Vetter
   J. Electroanal. Chem. **44**: 63 (1973)
7. C.A. Barlow, jr. and J.R. Macdonald
   J. Chem. Phys. **40**: 1535 (1964)
8. C.A. Barlow, jr. and J.R. Macdonald
   J. Chem. Phys. **43**: 2575 (1965)
9. J.R. Macdonald and C.A. Barlow, jr.
   J. Electrochem. Soc. **113**: 978 (1968)
10. S. Levine, G.M. Bell and D. Calvert
    Can. J. Chem. **40**: 518 (1962)
11. V.S. Krylov, V.A. Kir'yanov and I.F. Fishtik
    Elektrokhimiya **16**: 340 (1980)
12. V.G. Levich, V.A. Kir'yanov and V.S. Krylov
    Doklady Akad. Nauk SSSR **155**: 662, (1962)
13. H.D. Hurwitz
    J. Chem. Phys. **48**: 1541 (1968)

14. S.L. Carnie and D.Y.C. Chan
J. Chem. Phys. 75: 3485 (1981)

15. J.O'M. Bockris and M.A. Habib
J. Res. Inst. Catal., Hokkaido Univ. 23: 47 (1975)

16. A.N. Frumkin
Z. Phys. Chem. 116: 466 (1925)

17. H. Wroblowa and Z. Kovac
Trans. Faraday Soc. 61: 1523 (1965)

18. S.K. Rangarajan
Chem. Soc. Specialist Periodical Reports on Electrochemistry
7: 203 (1980)

19. B.E. Conway and S. Marshall
Electrochim. Acta 28: 1003 (1983)

20. J.R. Macdonald and C.A. Barlow, jr.
J. Chem. Phys. 36: 3062 (1962)

21. W. Schmickler
J. Electroanal. Chem. 149: 15 (1983)

22. T.L. Hill
"An Introduction to Statistical Thermodynamics", Addison-Wesley, Reading, Mass. (1962)

23. K. Binder, in K. Binder (ed.)
"Monte-Carlo Methods in Statistical Physics", Springer Verlag (1979), p.1

24. D.F. Lawden
"A Course in Applied Mathematics", vol. 2, English Universities Press (1963)

25. W.R. Smythe
"Static and Dynamic Electricity", 3ed., McGraw-Hill (1968)

26. G.N. Watson
"A Treatise on the Theory of Bessel Functions", 2ed., Cambridge University Press (1966)

27. J.-P. Badiali, M.-L. Rosinberg and J. Goodisman
J. Electroanal. Chem. **150**: 25 (1983)

28. J.A. Schultz, W. Mclean, L. Pedersen and R.C. Jarnagin
Chem. Phys. Lett. **64**: 230 (1979)

29. J.R. Gonzales Maroto, D. Posadas and A.J. Arvia
J. Phys. Chem. **83**: 1733 (1979)

30. J.G. Kirkwood
Z. Phys. **33**: 57 (1932);
A. Mueller
Proc. Roy. Soc. Lond. **A154**: 624 (1936)

31. D. Nicholson and N.G. Parsonage
"Computer Simulation and the Statistical Mechanics of Adsorption", Academic Press, London (1982)

32. S.L. Marshall and B.E. Conway
J. Chem. Phys. **81**: 923 (1984)

33. B.E. Conway and S.L. Marshall
J. Electroanal. Chem. **178**: 185 (1984)

34. B.E. Conway and H.P. Dhar
Croat. Chim. Acta **45**: 173 (1973); see also
B.E. Conway, J.G. Mathieson and H.P. Dhar
J. Phys. Chem. **78**: 1226 (1974)

35. S. Trasatti
"Proceedings of the Symposium on the Chemistry and Physics of Electrocatalysis", The Electrochemical Society (1984),

p. 150.

36. J. Topping

Proc. Roy. Soc. Lond. **A114**: 67 (1927)

37. V.A. Kir'yanov

Elektrokhimiya **6**: 1173 (1970)

38. F.P. Buff and F.H. Stillinger, jr

J. Chem. Phys. **39**: 1911 (1963)

39. W.R. Fawcett

Isr. J. Chem. **18**: 3 (1979)

CHAPTER 5.

MOLECULAR POLARIZATION AND INTERACTION EFFECTS ON KINETICS OF SURFACE ELECTRODE PROCESSES

1. Introduction

The thermodynamic description of neutral molecule adsorption, as a replacement of adsorbed solvent molecules was first proposed by Butler [1], who derived an equation expressing the electrical free energy change for such processes in terms of the difference in dipole moments and polarizabilities, per unit volume, of adsorbate and solvent, and the interfacial electric field. A more detailed re-examination of this solvent replacement approach was undertaken by Bockris, Devanathan and Mueller (BDM) [2], in the context of a general microscopic theory of the double layer at electrodes. The BDM theory has been widely applied to the interpretation of adsorption data for a variety of substances [3,4], and further attempts at developing molecular theories of adsorption have been based on similar arguments [5].

In contrast, the consideration of solvent dipole replacement in the kinetics of electrode processes has received relatively little attention. The first instance in which a molecular polarization energy was included in the calculation of an electrochemical rate constant was in a study by Bockris and Potter [6] of the hydrogen evolution reaction at the nickel electrode. This calculation was rather crude in that it did not take account of the different possible polarization states of $H_2O(ads)$, as was done in later work on the structure of the double layer [7,8]. Subsequently, Gileadi and Stoner [9] derived

a similar equation which predicted the effect of solvent displacement on the kinetics of an electrosorption reaction. This employed the Watts-Tobin/BDM (two-state) isotherm to describe the behaviour of the water molecules [2,10], with the further assumption that the interfacial field is strong enough to achieve saturation polarization in the compact double layer.

Since the appearance of this paper, its results have been applied by Gileadi and co-workers to the interpretation of the kinetics of various organic reactions at the mercury electrode, such as the reduction of nitroalkanes [11], chloropyridines [12] and aldehydes [13], and the inhibition of iodide and bromide discharge at platinum by phenol [14]. In all of these cases, the influence of solvent replacement appears as a correction to the Tafel slope, the magnitude of which depends on the number of solvent molecules being displaced in the reaction. The most recent theoretical treatment of dipolar effects on the transition states of electrode reactions is that of Fawcett and Gardner [15]; however, this was directed towards consideration of reactions involving reactants and products in solution.

In the above applications of the results of Gileadi and Stoner [9], the linearity of Tafel slopes indicated that the assumption of the limiting value of the orientational polarization was justified. Also, in the treatment of Fawcett and Gardner, no account was taken of the interactions between the dipolar species in the interface.

It is the purpose of the present chapter to extend the results of these authors to include the potential-dependence of

the polarization and interaction free energies of the adsorbed species, according to well-defined statistical-mechanical approximations. The specific problem which will be considered is the kinetics of a simple electrosorption reaction involving the partial discharge of an anion at a metal surface, as manifested by the predicted potential-dependence of the coverage fraction and reaction pseudocapacitance.

An alternative approach to the thermodynamic analysis of adsorption at electrodes was developed by Frumkin, Damaskin and co-workers [16,17]. This theory, in contrast to those described above which emphasised molecular replacement, employs the classical electrostatic formula for the energy of a parallel-plate condenser in order to calculate the potential-dependence of electrode coverage and the associated capacitance; its applicability to systems removed from equilibrium seems doubtful. A comparison of the thermodynamic implications of the Frumkin-Damaskin and molecular-replacement theories has been given by Gileadi [18].

2. Molecular Models for the Interface and its Components

In order to establish an approximate treatment of the effects of molecular polarization and interactions on the kinetics of surface electrode processes, a primitive model for the interface is considered, as in the previous chapters. In this case, the surface layer, in which the reaction occurs, is an hexagonal array (with lattice parameter r_0) consisting of adsorbed dipoles and partially discharged anions. The potential profile from the electrode surface to the bulk of the solution is as given by Fig. 1 of Chapter 1. The implications of non-

primitive models of the double layer [19], with respect to the kinetics of electrode processes, have not yet been considered.

2.1 Solvent Molecules

The characteristics of various theories of interfacial solvent polarization and their comparison with experiment have been discussed earlier, and have been the subject of several recent reviews [20,21]. For the purpose of the present discussion, it is to be observed that the predictions of the single-molecule theories, e.g. those proposing two [2,10], three [22] or a continuous range [8] of dipole orientations with respect to the interfacial electric field, are qualitatively similar. Specifically, the polarization <m> (or average dipole moment per molecule) describes a sigmoidal curve as a function of field, tending to limiting values of $\pm m$ for large fields and being approximately linear for small fields. Similar remarks apply to models which propose that the adsorbed solvent molecules behave as clusters, insofar as these clusters may be considered to be composed of molecules with fractional components of their dipole moments in the field direction - see, for example, the elaboration by Parsons [23] of the Damaskin-Frumkin cluster model [24].

Discussion of the free-energy changes of surface electrode reactions involving polarized adsorbed species requires consideration of the chemical potential and hence the appropriate factor of the molecular partition function. This is related to the angular and electrostatic potential energy $u(\theta,E)$ by

$$z_w = \int_0^{\pi} \exp[-u(\theta,E)/kT].2\pi\sin\theta d\theta \qquad [1]$$

and, as discussed in Chapter 4, has the form

$$z_w = 4\pi\exp(\alpha E^2/2kT+U_0/2kT)\sinh(mE/kT+U_0/2kT)/(mE/kT+U_0/2kT) \quad [2]$$

for dipoles orienting under the influence of the interfacial field and an orientational potential energy varying with $\cos\theta$ between 0 and $-U_0$. The inclusion of the interaction energy between the dipole and the multiple images it induces in the metal and dielectric of the diffuse double layer, adds a contribution $a_1+a_2\cos^2\theta$ to $u(\theta,E)$, where $a_1 = -5.501kT$ and $a_2 = -9.070kT$ at $T = 293K$. The partition function is accordingly modified to

$$z_w' = 2\pi\exp(\alpha E^2/2kT+U_0/2kT)\int_{-1}^{1}\exp[(mE/kT+U_0/2kT)y+(a_1+a_2y^2)/kT]dy \quad [3]$$

Throughout the present chapter it is assumed that $U_0=0$.

2.2 Partially Charged Adatoms

The product of the electrode reaction being considered may be modelled as a sphere of radius s bearing total negative charge $-\gamma e_0$, where γ is between 0 and 1 (this chapter considers the behaviour predicted by simple isotherms for $\gamma \leq 0.15$). The electrical partition function of this species, including the energy of interaction it experiences with images induced in the metal and the diffuse double layer, is

$$z_a = \exp[(V - \Delta\phi_2)\gamma e_0/2kT - T\gamma e_0/kT] \quad [4]$$

where $\Delta\phi_2$ is the potential drop across the diffuse double layer, assumed to be negligible in the present chapter. The second term in the argument of this expression is the self-image energy, which has the value $-8.197kT$ at 293K.

2.3 Pairwise Interaction Free Energies and Partition Functions

The contribution of interactions to the free energies of

polar adsorbed species was considered in Chapter 4; it is convenient to summarize the results as follows:

(i) Interactions Between Water Molecules

The pairwise free energy of interaction of two adjacent water molecules as a function of the applied field is described by the empirical function (cf. Chapter 4, eqn. 9)

$$u_{ww} = -kT \ln(\zeta_{ww}) \qquad [5]$$

where

$$\zeta_{ww} = \exp[a-1/(c_1+c_2(mE/kT)^2+c_3(mE/kT)^4]$$

and the constants a, c_1, c_2, c_3 have the respective values a = 4.0905, c_1 = 0.3356, $c_2 = 3.7269\times10^{-3}$, $c_3 = -2.4977\times10^{-6}$, at 293 K.

(ii) Interactions Between Adatoms

The interaction energy between adjacent adatoms is the partial charge of one adatom times the potential due to the other and all the images which it induces in the metal and the diffuse double layer. The numerical value determined earlier is $u_{aa} = 177.4\gamma^2 kT$ at 293K, and the corresponding partition function factor is defined by

$$\zeta_{aa} = \exp(-u_{aa}/kT) \qquad [6]$$

(iii) Interactions Between Adatoms and Water Molecules

The pairwise free energy of interaction between a solvent dipole and a charge-image pair is,with no dipolar imaging

$$u_{aw} = -kT \ln(\zeta_{aw}) \qquad [7]$$

where

$$\zeta_{aw} = \frac{\int_{-1}^{1} I_0[mX_x(1-y^2)^{1/2}/kT]\exp(mX_z y/kT)dy}{2\ \sinh(mE/kT)/(mE/kT)}$$

$$x \exp[\alpha(X^2-E^2)/2kT] \qquad [8]$$

and the vector **X** has components given by

$$X_x = [b^3/(1+b^2)^{1/2}-1]\gamma e_0/r_0^2 - 1.833 \times 10^5\gamma \text{ statC cm}^{-2}$$

$$X_y = 0.$$

$$X_z = E + (\gamma e_0/r_0^2).b^2/(1+b^2)^{3/2} + 5.983 \times 10^4\gamma \text{ statC cm}^{-2}$$

where $b = r_0/2s$.

The numerical values correspond to the contribution to the field exerted by the secondary ionic images induced in the metal and the diffuse double layer. With the inclusion of the dipole image contribution, ζ_{aw} as defined by eqn. 8 is to be replaced by

$$\zeta_{aw}' = \frac{\int_{-1}^{1} I_0[mX_x(1-y^2)^{1/2}/kT]\exp[mX_z y/kT+(a_1+a_2y^2)/kT]dy}{\int_{-1}^{1}\exp[mEy/kT+(a_1+a_2y^2)kT]dy} \times \exp[\alpha(X^2-E^2)/2kT] \qquad [9]$$

The calculation of the chemical potentials of the species in the compact double layer requires the adoption of an additional assumption concerning the distribution of the possible pairs aa, aw, and ww. This, in turn, permits the construction of an isotherm which defines the coverage fraction θ as a function of the electrode-solution potential difference, V, including the field (i.e. potential) dependence of both the polarization and interaction components of the free energy of each species. In the calculations to be presented later, it will be of interest to be able to distinguish the qualitative effects resulting from the inclusion of each of these components. Therefore, a simpler approach is first adopted which, although it may be criticized for lack of generality, nevertheless provides some interesting perspectives on the problem. The earlier theoretical approaches

due to Gileadi and Stoner [9] and Fawcett and Gardner [15] will be shown to result from this treatment as special limiting cases.

3. Simplified Approach Without Considering Interactions

3.1 Quasi-Equilibrium Limit

In this section, the contribution of solvent displacement energy to the electrosorption reaction

$$A^-(aq) + H_2O(ads) = A(ads) + H_2O(aq) + e^-(metal) \qquad [10]$$

will be derived using a thermodynamic argument, assuming for simplicity a two-state model [10] for $H_2O(ads)$. The process may be described by two concurrent reactions, viz.

$$A^-(aq) + H_2O(ads)\uparrow = A(ads) + H_2O(aq) + e^-(metal) \qquad [11a]$$

$$A^-(aq) + H_2O(ads)\downarrow = A(ads) + H_2O(aq) + e^-(metal) \qquad [11b]$$

where the symbols $\uparrow$ and $\downarrow$ denote orientation with and against the field (which is normal to the surface) respectively.

The activity of $H_2O(ads)$ in each configuration may be expressed in terms of the respective fractions of $1-\theta$, $\phi\uparrow$ and $\phi\downarrow$, and the field energy of $\pm N_0 mE$ per mole, where N_0 is Avogadro's number. The chemical potential of the $H_2O(ads)$ in each configuration is therefore given by

$$\mu_w^{\uparrow} = \mu_w^{o} + RT \ln(\phi\uparrow) + RT \ln(1-\theta) - N_0 mE + U\uparrow \qquad [12a]$$

$$\mu_w^{\downarrow} = \mu_w^{o} + RT \ln(\phi\downarrow) + RT \ln(1-\theta) + N_0 mE + U\downarrow \qquad [12b]$$

where μ_w^o is the standard chemical potential of $H_2O(ads)$ in both states, and $U\uparrow$ and $U\downarrow$ are residual orientational energies. Assuming that the potential difference across the compact layer is approximately equal to the electrode-solution potential difference V, the field acting on the dipoles is $E = V/d$, d being the thickness of the layer. The condition for simultaneous

equilibrium of the above reactions is obtained by equating the sum of the chemical potentials of the reactants

$$\mu^{\circ}_{A^-} + RT \ln(a_{A^-}) + \mu^{\circ}_{w} + RT \ln[\phi\uparrow(1-\theta)] - N_0 mE + U\uparrow$$

$$\mu^{\circ}_{A^-} + RT \ln(a_{A^-}) + \mu^{\circ}_{w} + RT \ln[\phi\downarrow(1-\theta)] + N_0 mE + U\downarrow$$

to the sum of the chemical potentials of the products, which for both reactions is

$$\mu^{\circ}_{a} + RT \ln \theta + \mu^{\circ}_{H2O} + RT \ln(a_{H2O}) - FV$$

On rearranging the resulting equations, the equilibrium electrosorption isotherms for the above two concurrent processes are found to be

$$\theta/(1-\theta)\phi\uparrow = K\uparrow a_{A^-} \exp(FV/RT).\exp[-mV/dkT] \qquad [13a]$$

$$\theta/(1-\theta)\phi\downarrow = K\downarrow a_{A^-} \exp(FV/RT).\exp[+mV/dkT] \qquad [13b]$$

where the activity of $H_2O(aq)$ has been taken as unity and the differences in standard chemical potentials for the two reactions have been absorbed into the equilibrium constants $K\uparrow$ and $K\downarrow$.

Solution of the simultaneous eqns. 13 for $\phi\uparrow$ and $\phi\downarrow$ gives

$$\phi\uparrow = (K\uparrow/K\downarrow)/(p^2 + K\uparrow/K\downarrow) \qquad [14a]$$

$$\phi\downarrow = 1 - \phi\uparrow \qquad [14b]$$

where $p = \exp[mV/dkT]$. When the residual energies $U\uparrow$ and $U\downarrow$ of $H_2O(ads)$ are equal, $K\uparrow$ and $K\downarrow$, and it is readily verified that

$$\phi\uparrow - \phi\downarrow = \tanh[mV/dkT] \qquad [15]$$

which is equal to $\langle m \rangle/m$ for the two state model, as used by Mott and Watts-Tobin. This provides a check on the consistency of these results.

The adsorption pseudocapacitance for the reaction symbolised by eqn. 10 is proportional to the derivative of θ with respect to V: $C = qd\theta/dV$, where q is the charge density required for monolayer coverage. After some manipulations, one obtains

$$d\theta/dV = \theta(1-\theta)[F/RT + (m/dkT).(K_{\uparrow}/K_{\downarrow} - p^2)/(K_{\uparrow}/K_{\downarrow} + p^2)] \quad [16]$$

This result is interesting because it shows that the reaction may be represented formally by the behaviour of two parallel capacitors. The first of these is the adsorption pseudocapacitance, of the same form as derived by Conway and Gileadi [26] for a reaction of this type (without consideration of solvent replacement energy) which corresponds to a formal separation of charge. The second term in the bracket of eqn. 16 is more similar to a true capacitance, being connected with a charge separation by molecular polarization.

Alternatively, the effect of both polarization states may be included simultaneously by using the partition function z_w to introduce the chemical potential $-RT \ln z_w$. For the simple two-state model under consideration, the partition function may be written

$$z_w = z_w^{\circ}[\exp(-U_{\uparrow}/kT)\exp(mE/kT) + \exp(-U_{\downarrow}/kT)\exp(-mE/kT)] \quad [17]$$

where z_w° represents the partition function for the non-orientational degrees of freedom. The chemical potential balance for the overall reaction, eqn. 10, is now

$$\mu_{A^-}^{\circ} + RT\ln(a_{A^-}) + \mu_w^{\circ} - RT\ln(z_w) + RT\ln(1-\theta) = \mu_a^{\circ} + RT\ln\theta + \mu_{H2O}^{\circ} + RT\ln a_{H2O} - FV \quad [18]$$

which results in the isotherm

$$\theta/(1-\theta) = K(a_{A^-}/a_{H2O})\exp(FV/RT)/z_w \quad [19]$$

In this case, the pseudocapacitance is obtained by taking logs and differentiating implicitly,

$$d\theta/dV = \theta(1-\theta)[F/RT - (m/dkT)d\ln z_w/dE] \quad [20]$$
$$= \theta(1-\theta)[F/RT - \langle m\rangle/dkT]$$

where <m> is the average polarization per molecule. It is readily shown that, for the simple two-state model assumed,

$$d\ln(z_w)/dE = \frac{\exp(2mE/kT) - \exp[(U\uparrow - U\downarrow)/kT]}{\exp(2mE/kT) + \exp[(U\uparrow - U\downarrow)/kT]} . m/kT \qquad [21]$$

$$= \frac{\exp(2mE/kT) - K\uparrow/K\downarrow}{\exp(2mE/kT) + K\uparrow/K\downarrow} . m/kT \qquad [22]$$

using the notation of the earlier "parallel-reaction" approach (cf. eqns 11a and 11b), so that eqn. 20 is identical to eqn. 16.

Thus, it is seen that the use of the partition function to account for the different polarization states is quite equivalent to the consideration of concurrent reactions given earlier, but involves much less algebra. Indeed, it is evident that the earlier approach would become unmanageably complex if it were to be applied to a multi-state polarization model. Nevertheless, the parallel-reaction approach is more commonly used, as exemplified by two recent theoretical treatments [5,31] of adsorption processes in which adsorbed species are present in different orientations.

Pseudocapacitance curves calculated for reaction 10 from eqn. 20, using two-state [2], three-state [22] and continuous-orientation [7,8] models for $H_2O(ads)$, are shown in Fig. 1. The electrostatic partition function and polarization appropriate for the three-state model, in which the third orientation is perpendicular to the field and has residual energy U, are as follows:

$$z_w = \exp(-U\uparrow/kT)\exp(mE/kT) + \exp(-U\downarrow/kT)\exp(-mE/kT) + \exp(-U/kT) \qquad [23a]$$

Fig. 1: Reduced quasi-equilibrium pseudocapacitance $C/q = d\theta/dV$ from eqn. 20, for various polarization models of $H_2O(ads)$.

Curve 0: No solvent effect considered [26]; $z_w = 1$

Curve 1: Two-state model

Curve 2: Three-state model ($U = 0$)

Curve 3: Continuous-orientation model

$m = 1.8 \times 10^{-18}$ statC cm, $T = 298$ K, $c_{A^-} = 1.0$ mol/l.

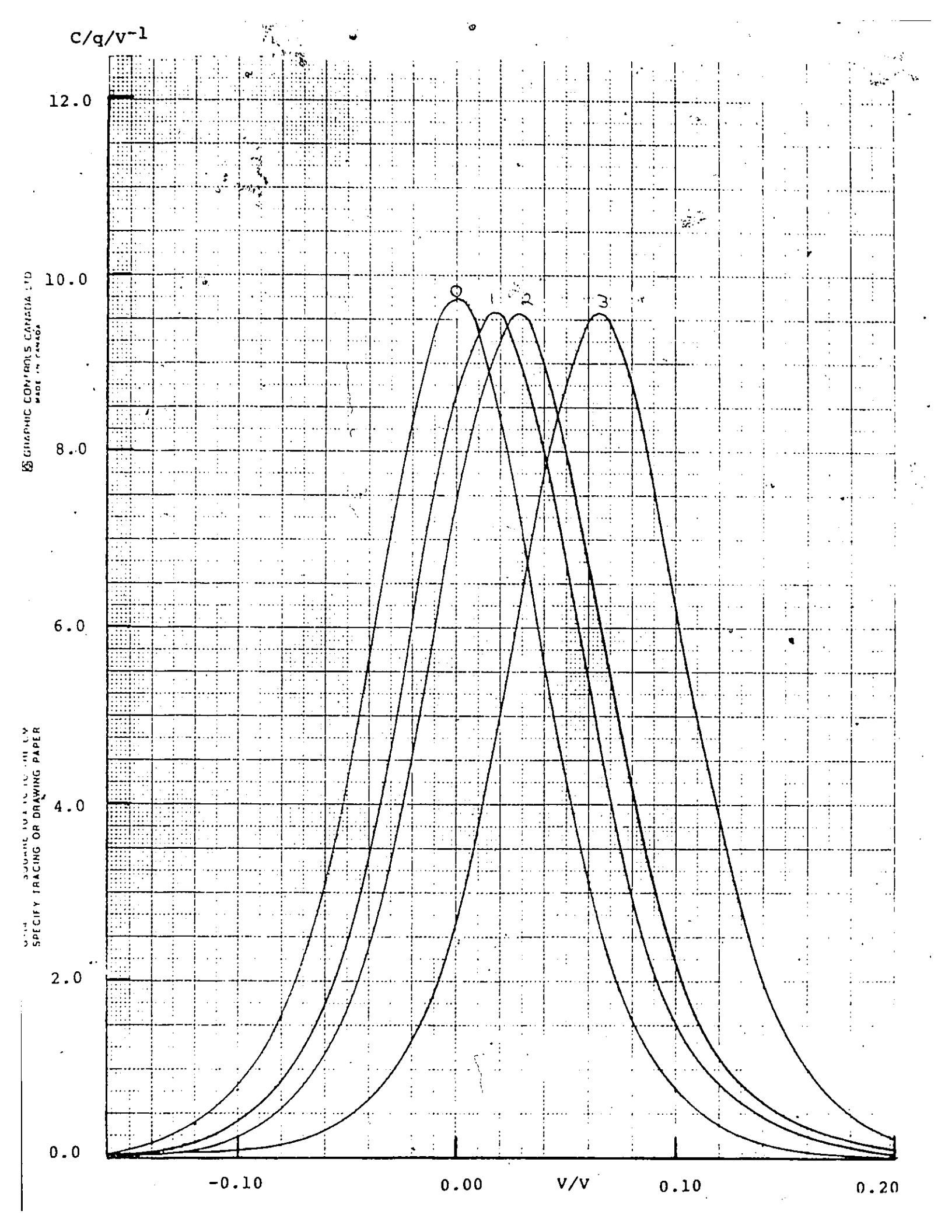
C/q/v-1
12.0
10.0
8.0
6.0
4.0
2.0
0.0
0
1
2
3
-0.10
0.00
V/V
0.10
0.20

$$\langle m \rangle = m.\frac{\exp(-U_{\uparrow}/kT)\exp(mE/kT) - \exp(-U_{\downarrow}/kT)\exp(-mE/kT)}{\exp(-U_{\uparrow}/kT)\exp(mE/kT) + \exp(-U_{\downarrow}/kT)\exp(-mE/kT) + \exp(-U/kT)} \quad [23b]$$

whilst, for the continuous-orientation model, z_w is given by eqn. 2 (with $U_0 = 0$) and $\langle m \rangle = mL(mE/kT)$ where $L(x) = \coth(x) - 1/x$ is the Langevin function. That the curves are symmetrical, with peak coverage of $\theta = 0.5$, follows from the fact that z_w is an even function of E for each of the polarization models considered. Comparison with the curve calculated for the reaction

$$A^-(aq) = A(ads) + e^-(metal) \quad [10a]$$

according to the isotherm of Conway and Gileadi [26] shows that the explicit inclusion of solvent replacement effects results in a shift of the peak potential in a positive direction; this shift is most pronounced for the continuous-orientation model and least for the two-state, but the peak heights are the same for the three curves. Interestingly, the quasi-equilibrium behaviour of eqn. 10 is much the same for each model considered.

3.2 General Kinetic Equations

(i) Activation Energies and Rate Constants

In this section the foregoing results are extended to cases where the reaction 10 departs appreciably from equilibrium.

According to the conventional formulation of electrode kinetics in terms of transition-state theory, the potential-dependent contribution to the free energy of activation may be expressed as a fraction of the total electrical free energy difference between reactants and products. The value of this fraction reflects the symmetry of the energy barrier plotted as a

function of the reaction coordinate. If the standard chemical potential of the transition state be represented as $\mu^{\ddagger}$, the difference in the standard chemical potential between reactants and transition state can be written as

$$\Delta\mu^{\ddagger}_{f} = \mu^{\ddagger} - \mu^{o}_{A-} - \mu^{o}_{w} + \beta[-F\eta - FV_r + RT\ln(z_w)] \quad [24]$$

for the forward reaction and

$$\Delta\mu^{\ddagger}_{b} = \mu^{\ddagger} - \mu^{o}_{a} - \mu^{o}_{H2O} - (1-\beta)[-F\eta - FV_r + RT\ln(z_w)] \quad [25]$$

for the reverse reaction, where V_r is the reversible potential and η is the overpotential, $V - V_r$. The respective rate constants are therefore

$$k_f' = (kT/h)\exp[-(\mu^{\ddagger} - \mu^{o}_{A-} - \mu^{o}_{w})/RT].\exp[\beta F(V_r + \eta)/RT](1/z_w)^{\beta} \quad [26a]$$

$$k_b' = (kT/h)\exp[-(\mu^{\ddagger} - \mu^{o}_{a} - \mu^{o}_{H2O})/RT].\exp[-(1-\beta)F(V_r + \eta)/RT] \times (z_w)^{1-\beta} \quad [26b]$$

The rate equation for θ may now be written

$$d\theta/dt = k_f a_{A-}(1-\theta)\exp[\beta F(\eta + V_r)/RT].(1/z_w)^{\beta} - k_b\theta a_{H2O}\exp[-(1-\beta)F(\eta + V_r)/RT].(z_w)^{1-\beta} \quad [27]$$

The rate constants in this expression contain the universal frequency factor kT/h, the non-electrostatic activation free energies, and the constants necessary to convert the bulk activities a_{A-} and a_{H2O} to surface activities adjacent to the electrode. In terms of the current density, $i/q = d\theta/dt$.

The consistency of eqn. 27 may be readily verified by putting $d\theta/dt = 0$, i.e. setting $V=V_r$. One then has

$$\theta/(1-\theta) = (a_{A-}/a_{H2O})(k_f/k_b)\exp(FV_r/RT).1/z_w \quad [28]$$

The constant pre-exponential factors in the definitions of k_f and k_b cancel out leaving

$$k_f/k_b = \exp[-(\mu^o_{A^-} + \mu^o_w - \mu^o_a - \mu^o_{H2O})/RT] \quad [29]$$

which is the non-electrochemical equilibrium constant defined in the previous section.

(ii) Tafel Slope

It is interesting to note that the result of dividing the electrochemical free energy change into fractions β and $1-\beta$ is that the average dipole moment $\langle m \rangle$ does not occur in the rate equation, as it did for the quasi-equilibrium case. This does occur, however, when the Tafel slope is calculated. To do this, consider the completely irreversible limit of eqn. 27, viz.

$$i/q = d\theta/dt = k_f a_{A^-}(1-\theta)\exp[\beta F(\eta + V_r)/RT].\exp(-\beta \ln z_w) \quad [30]$$

Upon taking logs and differentiating there results

$$(\partial/\partial\eta)\ln i = (\partial/\partial V)\ln i = \beta F/RT - (\beta\partial/\partial E)\ln(z_w).dE/dV \quad [31]$$

$$= \beta[F/RT - \langle m \rangle/dkT]$$

The Tafel slope is defined [27] as

$$b = 1/2.303[(\partial/\partial\eta)\ln i] \quad [32]$$

$$= 2.303(RT/\beta F)/[1 - (RT/\beta F).\beta\langle m \rangle/dkT]$$

$$= 2.303(RT/\beta F)/[1 - \langle m \rangle/e_0 d]$$

As $|E| \to \infty$ the expression for $\langle m \rangle \to \pm m$, so that the limiting values of the Tafel slope, corresponding to complete polarization of the solvent dipoles, are

$$b = 2.303(RT/\beta F)/[1 \pm m/e_0 d] \quad [33]$$

The quantity $m/e_0 d$ has the value 0.14, so that the denominator of this expression ranges between 0.86 and 1.14. The expression given by Gileadi and Stoner [9] for such a discharge reaction involving the displacement of n water molecules is

$$b = 2.303 \times 2RT/F/(1 + 0.14n) \quad [34]$$

which is seen to be a special case of eqn. 32, if $\beta = 0.5$ and $n = 1$.

(iii) Intrinsic and Corrected Symmetry Factors

In connexion with the above evaluation of the Tafel slope, it is interesting to compare the present discussion with that given by Fawcett and Gardner. According to these authors, the work done in transporting a dipolar species of (fixed) moment p_i to the reaction site, where the local field is E_r, is given by

$$II_i^r = -N_0 . \int_0^{E_r} p_i^r dE \qquad [35]$$

It is easily shown that this is a simple case of the procedure used above if the quantity p_i^r be identified with the statistical-mechanical average $\langle m \rangle$, defined in terms of the local field. In this case

$$II_i^r = -N_0 . \int_0^{E_r} \langle m \rangle dE \qquad [36]$$

$$= -RT \ln z_{i,el}$$

by definition; since the reaction is assumed to take place in the compact region of the double layer, $E_r = V/d$.

The interpretation of the significance of solvent polarization effects given by these authors was in terms of a potential-dependent deviation of the symmetry factor for the reaction from its intrinsic (i.e. potential-independent) value. Their "corrected" symmetry factor was derived in essentially the same way as eqn. 31, viz. by differentiation of the log of the rate constant with respect to field (and hence interfacial potential difference). This is again consistent with the results of the present chapter, since the above expression for the potential-dependent Tafel slope can obviously be rewritten in

terms of a corrected symmetry factor given by

$$\beta_c = \beta[1 - \langle m \rangle / e_0 d] \qquad [37]$$

where β represents the intrinsic symmetry factor. In an extreme case, it appears from eqn. 38 that one could have a symmetry factor varying between 0 and 1 (i.e. a so-called "barrierless" discharge [28]) but it is unlikely that the condition $m \ll e_0 d$ would be satisfied for real molecules.

In Fig. 2, the calculated transient response of 10 under potential-sweep conditions is compared with that of 10a. There are slight differences in the peak heights which are not present for the reversible curves (Fig. 1) but it is interesting to note that the separation between the anodic and cathodic peak potentials is the same for each curve, including the solvent-displacement effect. The most important characteristic of these irreversible curves is a difference of about 10% in the heights of the anodic and cathodic pseudocapacitance peaks, which disappears for values of s/k less than 1. This effect is observed in calculated responses of 10a using a symmetry factor unequal to 0.5 [29], which lends support to the interpretation of solvent polarization effects as causing a potential-dependent asymmetry of the energy barrier for the discharge process.

In this section it has been shown how the inclusion of the polarization term in the chemical potential balance affects the predicted kinetic behaviour of a simple electrode reaction. The above results are now extended to include potential-dependent free energies of interaction between the species in the surface layer.

Fig. 2: Reduced non-equilibrium pseudocapacitance curves from eqn. 27, plotted as $(d\theta/dt)/(dV/dt)$ with $k_f = k_r = 1$, $(dV/dt) = 1$ V/s. Other parameters as for Fig. 1.

Curve 1: No solvent effect considered (cf. ref. 26)

Curve 2: Continuous orientation model

Curve 3: Three-state model (U = 0)

Curve 4: Two-state model

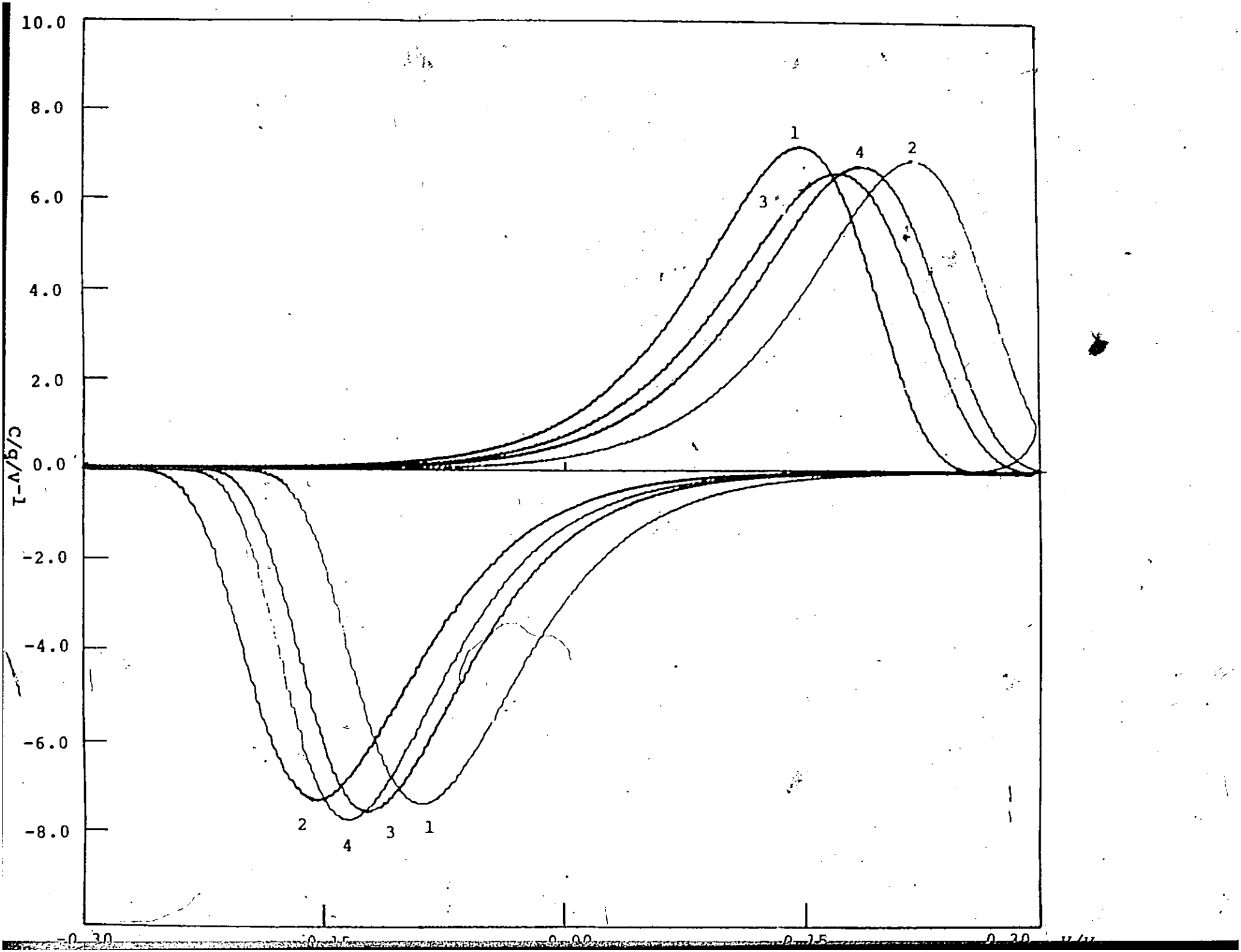
10.0
8.0
6.0
4.0
2.0
0.0
-2.0
-4.0
-6.0
-8.0
C/q/V-1
1
2
3
4
2
4
3
1
-0.30
0.00
0.30
V/V

4. Bragg-Williams Approximation

The starting point for the derivation of statistical-mechanical expressions for the chemical potential of each adsorbed species, and hence the isotherm, is the partition function for the surface layer, which consists of N_a adatoms and N_w co-adsorbed water molecules. (N_w is dimensionless in this section, in contrast to the number density N_w used earlier.)

According to the Bragg-Williams approximation, the occupants of the lattice are distributed randomly, despite the existence of interactions; this assumption is adopted first, to facilitate the interpretation of the results of the next section, in which deviations from randomness will be taken into account approximately. The partition function can be written [25]

$$Z = [z_a^o z_a \exp(-cu_{aa}/2kT)]^{N_a}[z_w^o z_w . \exp(-cu_{ww}/2kT)]^{N_w}\exp[\langle N_{aw}\rangle u/2kT] \times (N_a+N_w)!/N_a!N_w! \qquad [38]$$

where c is the coordination number for the lattice (which is 6 in this case), z_a^o, z_a and z_w^o, z_w are field-independent and electrical partition functions, respectively, and $\langle N_{aw}\rangle$ is the average number of adjacent "aw" pairs, given by

$$\langle N_{aw}\rangle = cN_aN_w/(N_a+N_w)$$

The quantity u is called the interchange energy, defined by

$$u = u_{ww} + u_{aa} - 2u_{aw}$$

and the factors of 1/2 are required to prevent counting of pairwise interactions twice. Using eqns. 5,6 and 7, the partition function can be expressed as

$$Z = (z_a^o z_a \zeta_{aa}^3)^{N_a}(z_w^o z_w \zeta_{ww}^3)(\zeta_{aw}^2/\zeta_{aa}\zeta_{ww})^{3\langle N_{aw}\rangle}(N_a+N_w)!/N_a!N_w! \qquad [39]$$

whence, on use of Stirling's approximation for the factorials,

$$\ln Z = N_a \ln(z_a^o z_a \zeta_{aa}^3) + N_w \ln(z_w^o z_w \zeta_{ww}^3) + (N_a+N_w)\ln(N_a+N_w) - N_a - N_w$$

$$-N_a \ln N_a + N_a - N_w \ln N_w + N_w + \ln[(\zeta_{aw}^2/\zeta_{aa}\zeta_{ww}).3N_aN_w/(N_a+N_w)] \quad [40]$$

The chemical potential of the adatoms is given by

$$-\mu_a/kT = \partial \ln Z/\partial N_a = \ln(z_a^o z_a \zeta_{aa}^3) + \ln(N_a+N_w) - \ln N_a + 3\ln(\zeta_{aw}^2/\zeta_{aa}\zeta_{ww}).N_w^2/(N_a+N_w)^2 \quad [41]$$

so that

$$\mu_a = -kT\ln z_a^o - kT\ln(z_a\zeta_{aa}^3) + kT\ln\theta - 3kT(1-\theta)^2\ln(\zeta_{aw}^2/\zeta_{aa}\zeta_{ww}) \quad [42]$$

where the coverage fraction $\theta = N_a/(N_a+N_w)$ has been introduced. Proceeding analogously, the chemical potential for the adsorbed water molecules is

$$\mu_w = -kT\ln z_w^o - kT\ln(z_w\zeta_{ww}^3) + kT\ln(1-\theta) - 3kT\theta^2\ln(\zeta_{aw}^2/\zeta_{ww}\zeta_{aa}) \quad [43]$$

If the product of the surface electrode reaction is an adatom bearing a partial charge $-\gamma e_0$, then the equation for the reaction 10 should be rewritten

$$A^-(aq) + H_2O(ads) = A^-(ads) + H_2O(aq) + (1-\gamma)e^- \quad [44]$$

to satisfy conservation of charge. The isotherm for this process is obtained, as before, by equating the sum of the chemical potentials of the reactants to that of the products. On doing this and collecting terms, there results, in molar units,

$$(\mu_{A^-}^o - RT\ln z_w^o - \mu_{H2O}^o + RT\ln z_a^o) + RT\ln(a_{A^-}/a_{H2O}) + RT\ln(z_a\zeta_{aa}^3/z_w\zeta_{ww}^3) + (1-\gamma)FV + 3RT\ln(\zeta_{aw}^2/\zeta_{ww}\zeta_{aa})[(1-\theta)^2-\theta^2] = \ln[\theta/(1-\theta)] \quad [45]$$

and on dividing by RT and taking exponentials,

$$\theta/(1-\theta) = K(a_{A^-}/a_{H2O})\exp[(1-\gamma)FV/RT - g\theta].z_a\zeta_{aw}^6/z_w\zeta_{ww}^6 \quad [46]$$

where

$$K = \exp[-(-\ln z_a^o - \mu_{H2O}^o/RT + \ln z_w^o - \mu_{A^-}^o/RT)]$$

$$g = 6\ln(\zeta_{aw}^2/\zeta_{aa}\zeta_{ww})$$

This isotherm is formally similar to the Frumkin isotherm [32]

$$\theta/(1-\theta) = K' \exp(FV/RT - g'\theta) \qquad [47]$$

which has been widely used in the interpretation of electrochemical adsorption experiments. In most applications, both K' and g' are assumed to be constant with potential; as will be seen, the potential dependence of the corresponding quantities in eqn. 46 results in predicted kinetic behaviour which is quite different from that usually attributed to eqn. 47.

In order to calculate the quasi-equilibrium pseudocapacitance for this isotherm, it is convenient to take logs first, and then differentiate implicitly with respect to V:

$$[1/\theta + 1/(1-\theta)]d\theta/dV = \theta(1-\theta)F/RT - gd\theta/dV - \theta dg/dV$$
$$+ 6(d\ln\zeta_{aw}/dV - d\ln\zeta_{ww}/dV) + d\ln z_a/dV - d\ln z_w/dV \qquad [48]$$

where

$$dg/dV = 12d\ln\zeta_{aw}/dV - 6d\ln\zeta_{ww}/dV$$

recalling that ζ_{aa} is independent of V. Collecting terms and solving for $d\theta/dV$,

$$d\theta/dV = [F(1-\gamma)/RT - \theta dg/dV + 6(d\ln\zeta_{aw}/dV - d\ln\zeta_{ww}/dV)$$
$$+ d\ln z_a/dV - d\ln z_w/dV].\theta(1-\theta)/[1 + g\theta(1-\theta)] \qquad [49]$$

This expression can be further simplified by substituting the above expression for dg/dV, using the identity $d/dV = (1/d)d/dE$ and recalling the earlier definitions of $\langle m \rangle$ and z_a, viz.

$$\langle m \rangle = kT\ d\ln z_w/dE,\ d\ln z_a/dV = e_0/2kT \qquad [50]$$

The final expression for the pseudocapacitance is therefore

$$d\theta/dV = [F(1-\gamma/2)/RT - \langle m \rangle/dkT + (6/d)(1-2\theta)d\ln\zeta_{aw}/dE - (6/d)d\ln\zeta_{ww}/dE]$$
$$x\ \theta(1-\theta)/[1+g\theta(1-\theta)] \qquad [51]$$

This function is plotted as a function of V in Figs. 3 and 4, for various values of γ, and for both possible definitions of z_w and ζ_{ww}, viz. with and without the inclusion of the dipolar image interaction. (Following ref. 33, the quantity in fact plotted is $C/(1-\gamma)^2 q$, to account for the decrease in C which would result from a value of γ less than 1 in eqn. 44.) The most interesting feature of these curves is that there is an appreciable deviation from ideality even when $\gamma = 0$; this is because in this case, the adatoms continue to influence the interactions between the water molecules simply by occupying sites on the lattice. This is in obvious contrast to behaviour predicted by existing theories of interaction between adsorbed charge-image pairs, for example the "$\theta^{3/2}$" isotherm [33,34]:

$$\theta/(1-\theta) = Kc_A \exp[(1-\gamma)FV/RT - g'\theta^{3/2}] \qquad [52]$$

The g'-parameter in this equation is defined by

$$g' = (1-\gamma)^2 e_0^2 4s^2/\varepsilon r_0^3 \qquad [53]$$

assuming an effective (constant) dielectric constant ε for the co-adsorbed water molecules, and obviously vanishes when the charge on the adatoms becomes zero, giving an "ideal" Langmuir curve of the type first calculated by Conway and Gileadi [26]. This becomes unreasonable as θ approaches unity, since implicitly the water molecules exert a constant influence on the interaction energy even though there are decreasing numbers of them on the surface. However, even if a potential dependence of ε were to be incorporated into the definition of g', curves calculated for this isotherm would still assume the "ideal" limit for $\gamma = 0$. Thus, in addition to being of doubtful applicability to the

Fig. 3: Reduced quasi-equilibrium pseudocapacitance $C/(1-\gamma)^2 q$ calculated according to the Bragg-Williams approximation, eqn. 49, with inclusion of dipolar image energy.

Curve 1: $\gamma = 0.15$

Curve 2: $\gamma = 0.10$

Curve 3: $\gamma = 0.05$

Curve 4: $\gamma = 0.00$

$m = 1.835 \times 10^{-18}$ statC cm, $T = 293$ K, $c_{A^-} = 1$ mol/l

$K_{eq} = 100$.

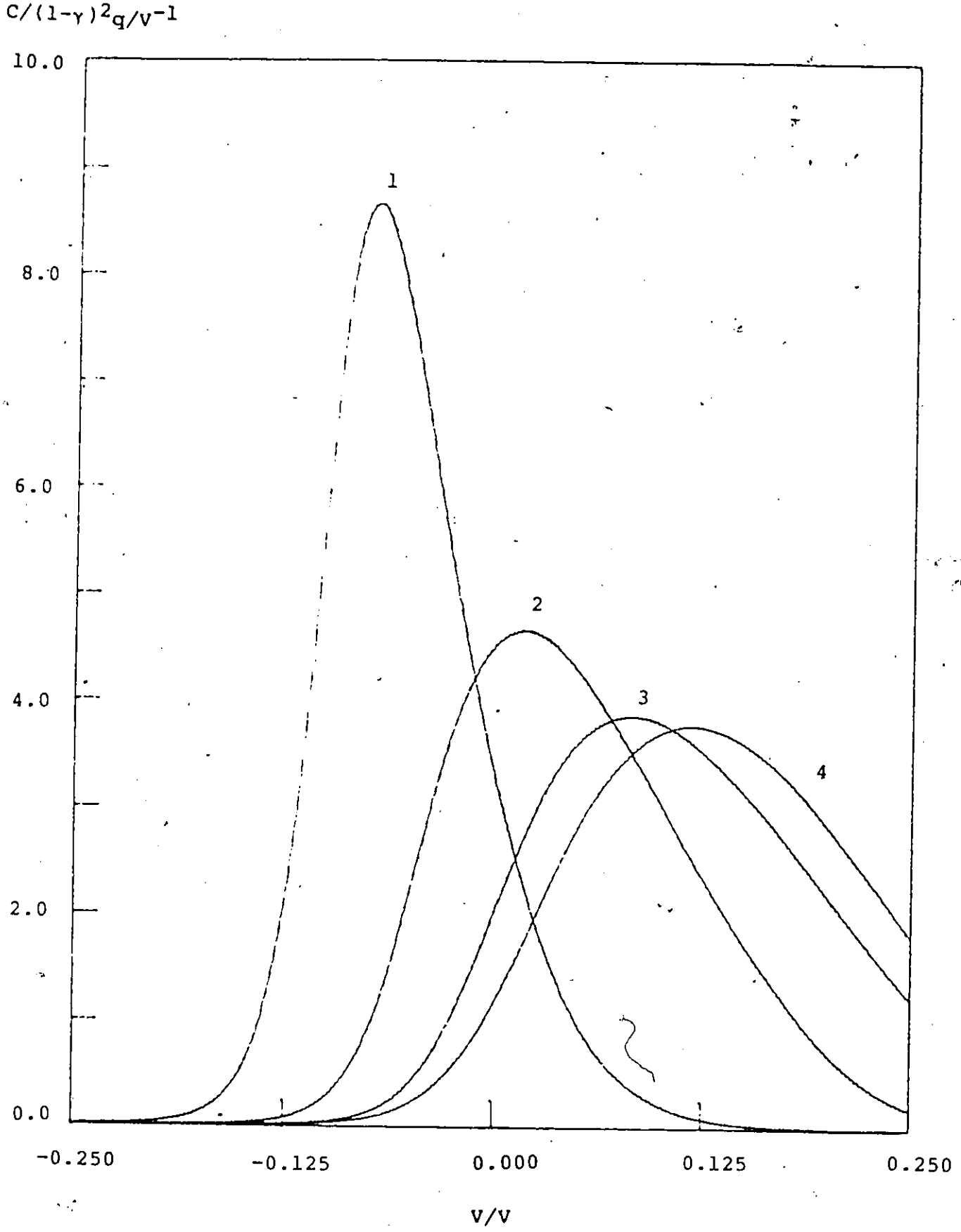
C/(1-γ)²q/v-1
10.0
8.0
6.0
4.0
2.0
0.0
1
2
3
4
-0.250
-0.125
0.000
0.125
0.250
V/V

Fig. 4: Reduced quasi-equilibrium pseudocapacitance from eqn. 49, without inclusion of dipolar image energy. Values of γ for each curve and other parameters as in Fig. 3.

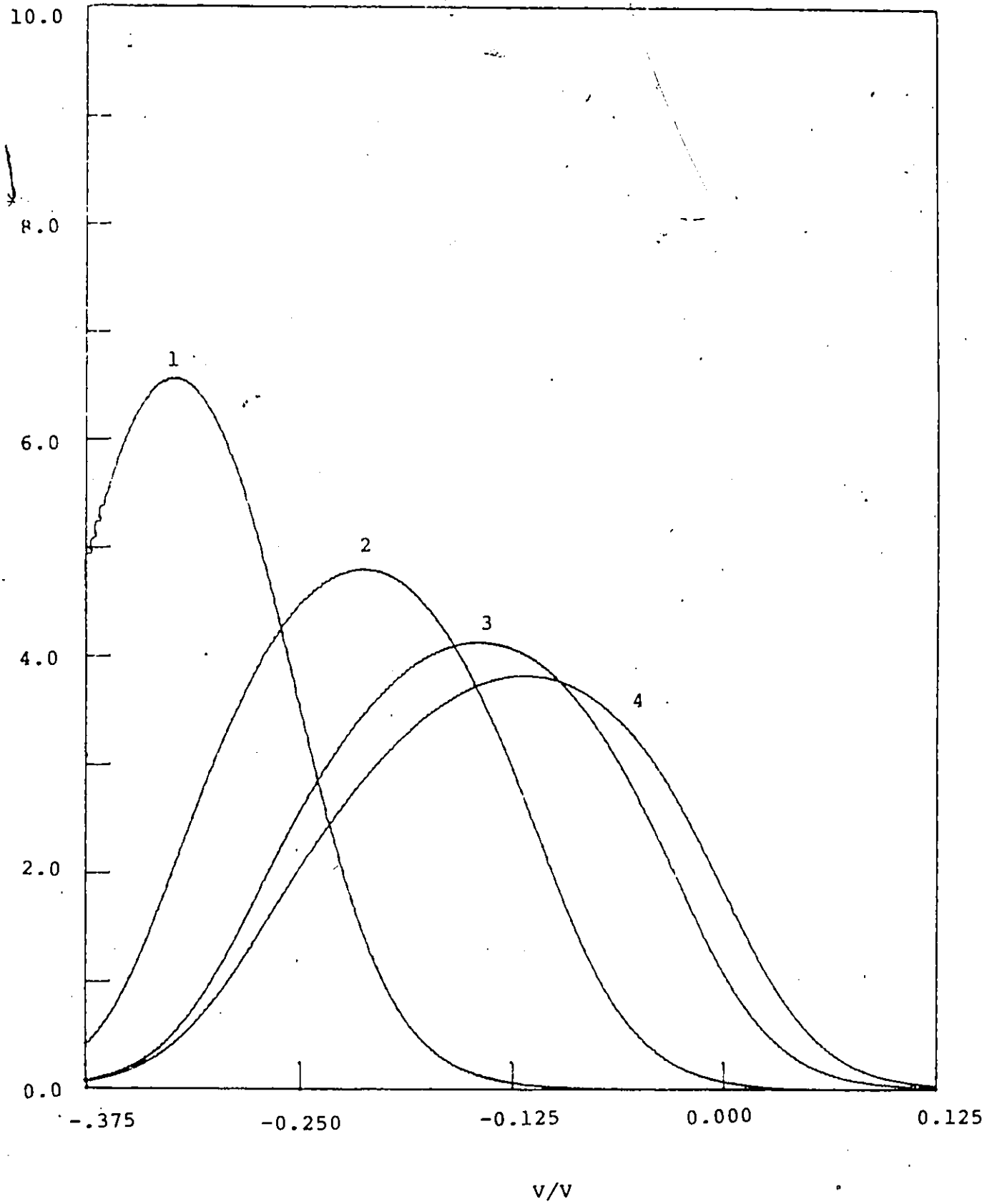

description of interactions between such surface species in the first place, the dielectric continuum approximation embodied in eqn. 53 neglects the polarization and interaction contribution of the water molecules to the chemical potential balance defining the isotherm.

Surprisingly, however, the asymmetric shape of the curves for $\gamma > 0$ is not unlike that in pseudocapacitance curves calculated from eqn. 52. On the other hand, for increasing γ, the curves of Figs. 3 and 4 become taller, whilst the opposite effect is predicted from eqn. 52. From the definition of g in the Bragg-Williams isotherm, this is probably due to the increasingly negative interaction energy between the charge-image species and the adsorbed water molecules, which can be thought of as a surface "solvation energy". This is another component of the problem which cannot be conveniently dealt with using a dielectric continuum approximation of the type used in eqn. 53.

As seen by comparing Figs. 3 and 4, the effect of including the dipole-image interaction energy is the prediction of considerably "sharper" pseudocapacitance peaks. This can be rationalized by considering the variation of g with potential, which is shown, with and without consideration of dipolar imaging, in Fig. 5. It is seen that when dipolar imaging is taken into account, g can become negative; that pseudocapacitance curves predicted from isotherms in the form of eqn. 47 become sharper for negative g has already been demonstrated [30]. This is in turn explicable in terms of the differences between the behaviour of ζ_{aw} (without imaging) and ζ_{aw}' (with imaging), as a function of E; it will be recalled that the differences in the

Fig. 5: Variation of g with potential, for Bragg-Williams isotherm (eqn. 46).

Curve 1: $\gamma = 0.00$, dipolar imaging not included

Curve 2: $\gamma = 0.15$, dipolar imaging not included

Curve 3: $\gamma = 0.15$, dipolar imaging included

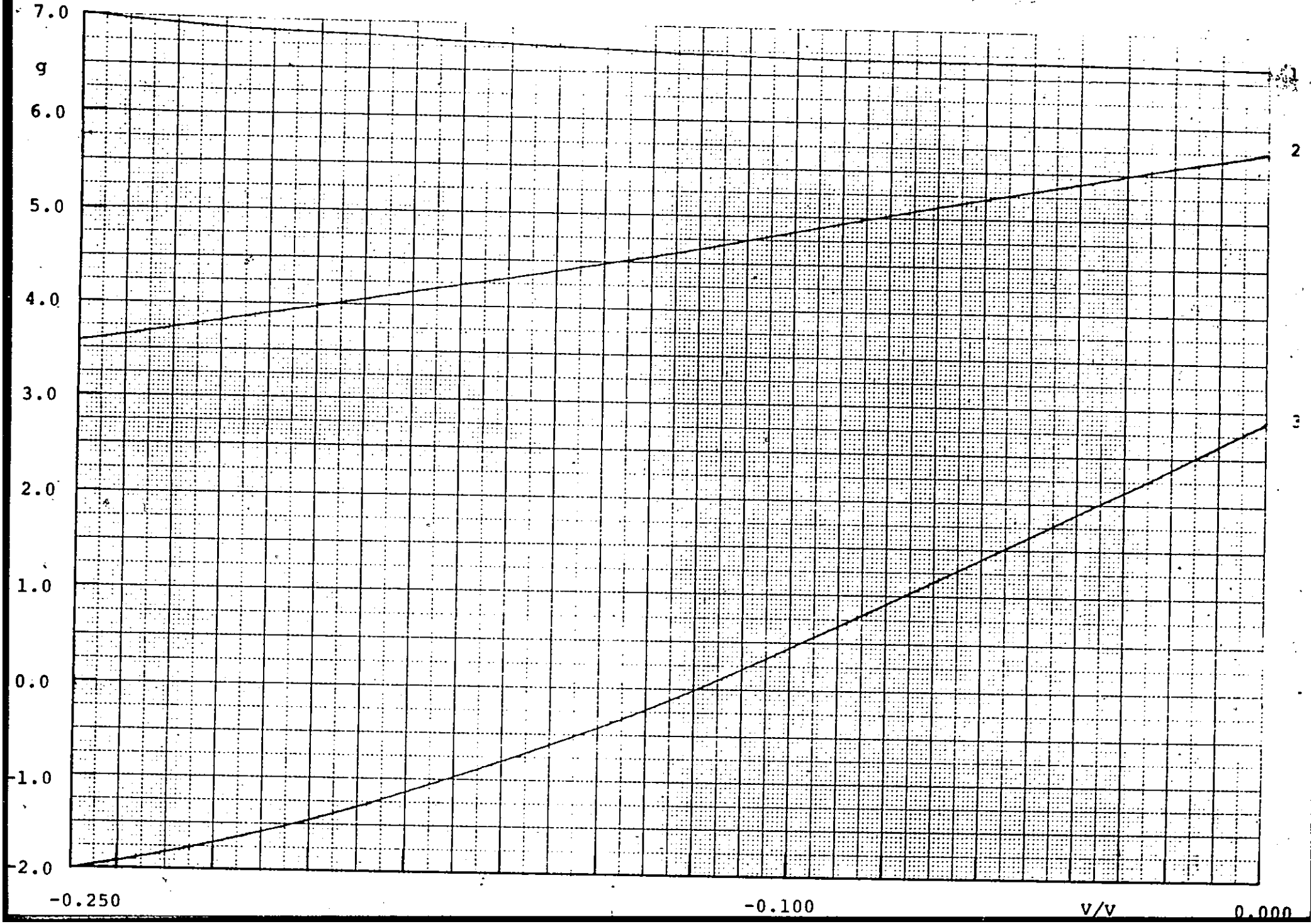
7.0
g
6.0
5.0
4.0
3.0
2.0
1.0
0.0
-1.0
-2.0
-0.250
-0.100
V/V
0.000
1
2
3

corresponding free energies are pronounced. Such differences will be made even more pronounced by the definition of g, since the logarithm of ζ_{aw} is multiplied by 12.

5. Quasi-Chemical Approximation

According to the quasi-chemical approximation, pairs of nearest-neighbour sites are treated independently, and to compensate for the resulting over-counting of configurations, the configurational degeneracy of the lattice is normalized to $(N_a+N_w)!/N_a!N_w!$ by the insertion of a multiplicative factor in the partition function for the lattice. By a rather involved combinatorial argument (details of which are presented by Guggenheim [35] and Hill [25]), an expression is produced for the probable number of adjacent "aw" pairs in terms of the interchange energy, and this in turn results in the following expressions for the chemical potentials of species a and w, in molar units:

$$\mu_a = -RT\ln(z_a^o z_a \zeta_{aa}^3) + 3RT\ln[(\delta-1+2\theta)/(\delta+1)\theta] + RT\ln\theta \quad [54]$$

$$\mu_w = -RT\ln(z_w^o z_w \zeta_{ww}^3) + 3RT\ln[(\delta+1-2\theta)/(\delta+1)(1-\theta)] + RT\ln(1-\theta) \quad [55]$$

where

$$\delta^2 = 1-4\theta(1-\theta)(1 - \zeta_{aa}\zeta_{ww}/\zeta_{aw}^2) = 1 + 4\theta(1-\theta)(G-1)$$

and, as before, the interaction energies have been replaced by the logarithms of the corresponding partition functions multiplied by -kT.

By equating the sum of the chemical potentials of the reactants to that of the products, the isotherm is obtained:

$$(\mu_{A^-}^o - RT\ln z_w^o - \mu_{H2O}^o + RT\ln z_a^o) + RT\ln(a_{A^-}/a_{H2O}) + (1-\gamma)FV$$

$$+ RT\ln(z_a\zeta_{aa}^3/z_w\zeta_{ww}^3)$$

$$= 3RT\ln(\delta-1+2\theta) - 3RT\ln(\delta+1) - 3RT\ln\theta + RT\ln\theta$$

$$- 3RT\ln(\delta+1-2\theta) + 3RT\ln(\delta+1) + 3RT\ln(1-\theta) - RT\ln(1-\theta) \quad [56]$$

or

$$K(a_{A^-}/a_{H2O})\exp[(1-\gamma)FV/RT]z_a\zeta_{aa}^3/z_w\zeta_{ww}^3$$

$$= [(1-\theta)/\theta]^2[(\delta-1+2\theta)/(\delta+1-2\theta)]^3 \quad [57]$$

To derive the quasi-equilibrium pseudocapacitance, this expression is differentiated logarithmically:

$$[-2/\theta(1-\theta)]d\theta/dV + [3/(\delta-1+2\theta)](d\delta/dV + 2d\theta/dV)$$

$$- [3/(\delta+1-2\theta)](d\delta/dV - 2d\theta/dV) = d\ln K'/dV \quad [58]$$

where K' refers to all the terms on the right hand side of eqn. 57, and

$$d\delta/dV = [2\theta(1-\theta)/\delta]dG/dV + [2(1-2\theta)(G-1)/\delta]d\theta/dV \quad [59]$$

Collecting terms and solving for $d\theta/dV$ provides, after lengthy algebra,

$$d\theta/dV = \frac{\delta(\delta+1-2\theta)(\delta-1+2\theta)d\ln K'/dV - 12\theta(1-\theta)(1-2\theta)dG/dV}{6\theta(1-\theta)[(1-2\theta)^2(G-1)+\delta^2] - (\delta+1-2\theta)(\delta-1+2\theta)}.\theta(1-\theta)/2 \quad [60]$$

Since $G = \zeta_{aa}\zeta_{ww}/\zeta_{aw}^2$,

$$dG/dV = (G/d)[d\ln\zeta_{ww}/dE - 2d\ln\zeta_{aw}/dE] \quad [61]$$

and from eqn. 57,

$$d\ln K'/dV = (1-\gamma)F/RT + F/2RT - d\ln z_w/dV - 3d\ln\zeta_{ww}/dV \quad [62]$$

$$= (1-\gamma/2)F/RT - \langle m\rangle/dkT$$

from the earlier discussion.

Plots of $(d\theta/dV)/(1-\gamma)$ are shown in Figs. 6 and 7. For both the free-dipole model and the dipole-image model of H_2O(ads), the most striking feature of these curves is the emergence of a second peak, even for $\gamma = 0$; in the interpretation of

Fig. 6: Reduced quasi-equilibrium pseudocapacitance, according to the quasi-chemical isotherm, eqn. 60, without inclusion of dipolar imaging energy. $K_{eq} = 0.01$, $c_{A^-} = 1$ mol/l.

Curve 1: $\gamma = 0.00$

Curve 2: $\gamma = 0.05$

Curve 3: $\gamma = 0.10$

Curve 4: $\gamma = 0.15$

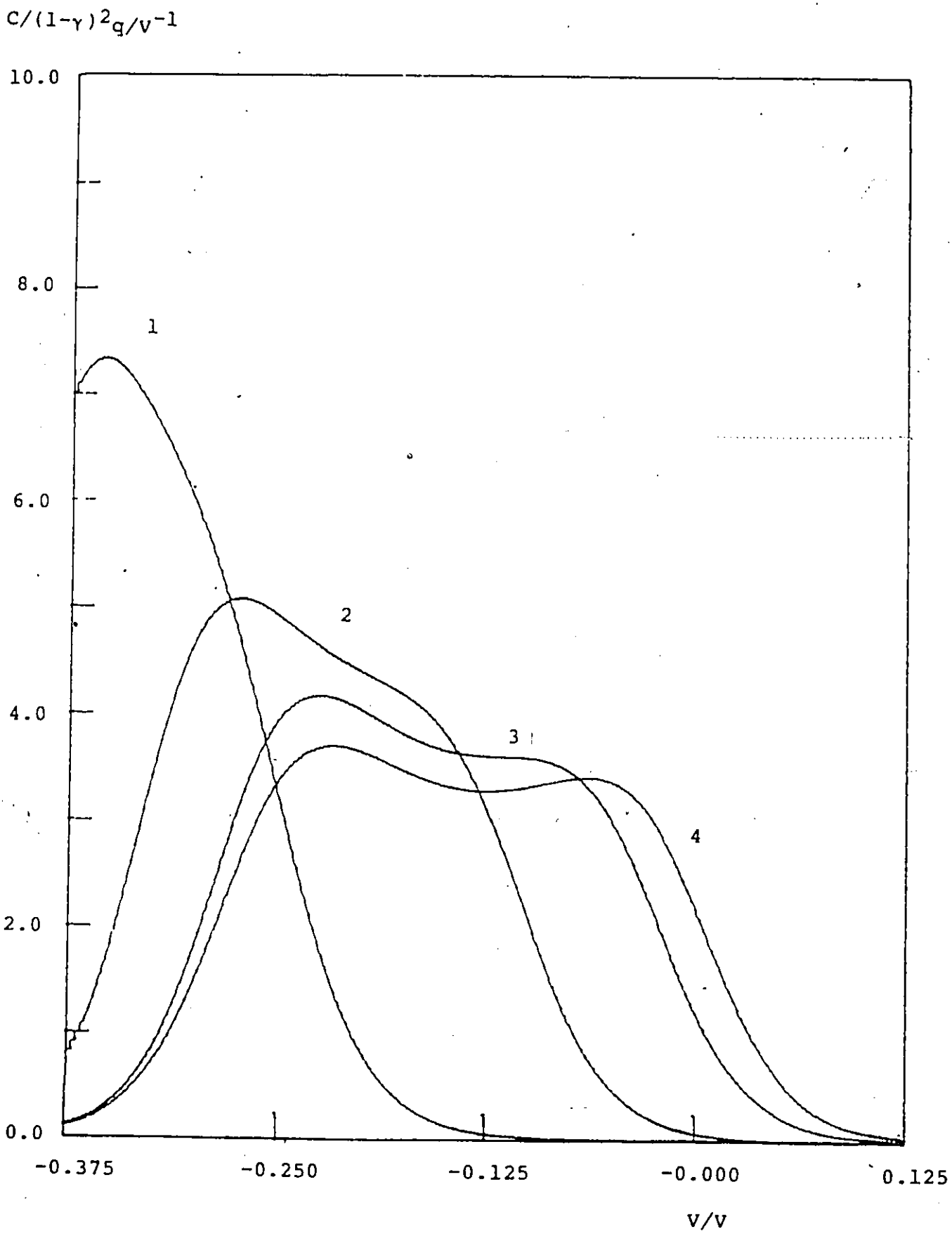
C/(1-γ)²q/v-1
10.0
8.0
6.0
4.0
2.0
0.0
1
2
3
4
-0.375
-0.250
-0.125
-0.000
0.125
V/V

Fig. 7: Reduced quasi-equilibrium pseudocapacitance, according to the quasi-chemical isotherm, eqn. 60, with inclusion of dipolar imaging energy. Values of γ for each curve and other parameters as for Fig. 6.

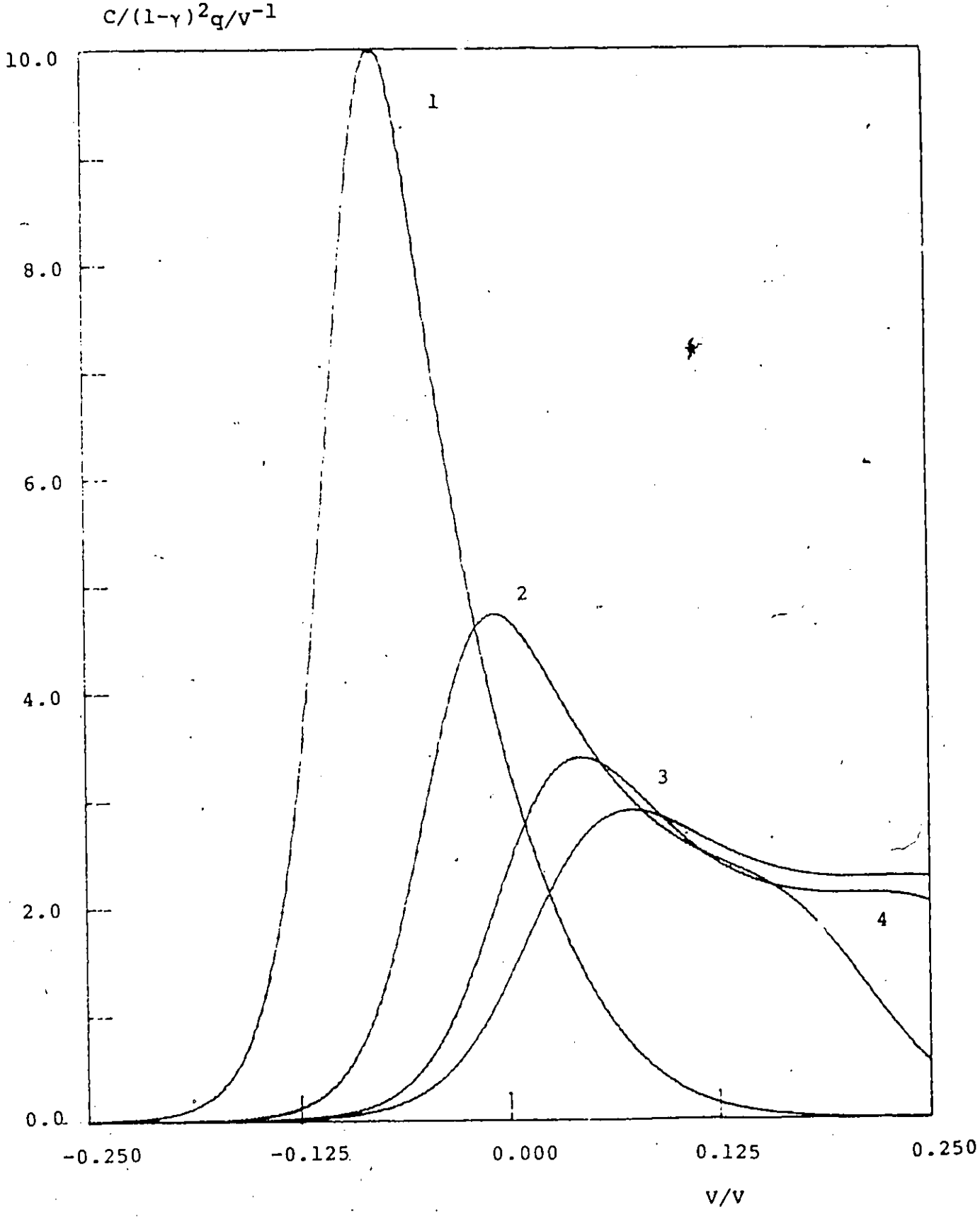

experimental pseudocapacitance curves, this sort of result is usually taken to be evidence of two concurrent electrode processes. Despite the presence of this extra peak, however, the asymmetry present in these curves to some extent parallels that in those calculated for the Bragg-Williams isotherm, in that both sets of curves are steeper on the increasing side of the first peak. It seems from comparing them that there is a "detail" in the quasichemical results, of which only vestiges remain in the Bragg-Williams curves.

From the nature of the assumptions made in the two treatments, the appearance of two peaks probably results from an energetic preference for the displacement of one H_2O(ads) over another (e.g. in an "aw" pair as opposed to a "ww" pair or vice versa, depending on the potential), which would be "blunted" by the assumption of random-mixing imposed by the Bragg-Williams treatment.

Unfortunately, the limitations of the present treatment allow the prediction of only which of the various possible pairs of sites will be the most favourable for a given V. Ideally, one wants to be able to extract from the isotherm a picture of what molecular environment (considering all nearest neighbours of a given site) is most favourable. This, however, would require an exact treatment of the two-dimensional lattice gas which, apart from the (rather uninteresting!) case of $\theta = 1/2$, remains a major unsolved problem of theoretical physics. It would be interesting to investigate the implications of certain elaborations of the quasichemical approximation worked out by Guggenheim, viz. that based on systems of triangles (which for the hexagonal lattice

under consideration, seems a more "natural" subunit), and the treatment including explicit consideration of next-nearest neighbours. The interaction partition functions would have to be redefined, but the algebraic manipulations associated with the configurational component of the problem may become unmanageably complex.

The prediction of two peaks in the pseudocapacitance curve for a single electrode process immediately suggests a possible relevance of the present results to an experimental problem of current interest, viz. the observation of discrete stages in the formation of electrodeposited monolayers [36]. The question of interest in this connexion is whether the onset of the second peak occurs for any characteristic value of the coverage.

The coverage-potential curves corresponding to Fig. 7 are shown in Fig. 8. The minima between the peaks in the C-V curves are seen not to correspond to very pronounced changes in the θ-V curves, e.g. plateaux, which would be more obviously indicative of a process occurring in discrete stages. More importantly, the values of θ corresponding to the onset of the second peak depend quite strongly on the value assumed for γ, which tends to rule out the direct applicability of the present isotherm to this particular aspect of such systems. A more likely explanation for this phenomenon is the successive formation of interpenetrating superlattices, to each of which, perhaps, some of the considerations of the present chapter might apply.

6. Isotherms For Single Adsorbed Charges

This section examines the application of the above isotherms

Fig. 8: Coverage θ corresponding to the pseudocapacitance curves of Fig. 7.

Curve 1: $\gamma = 0.00$

Curve 2: $\gamma = 0.05$

Curve 3: $\gamma = 0.10$

Curve 4: $\gamma = 0.15$

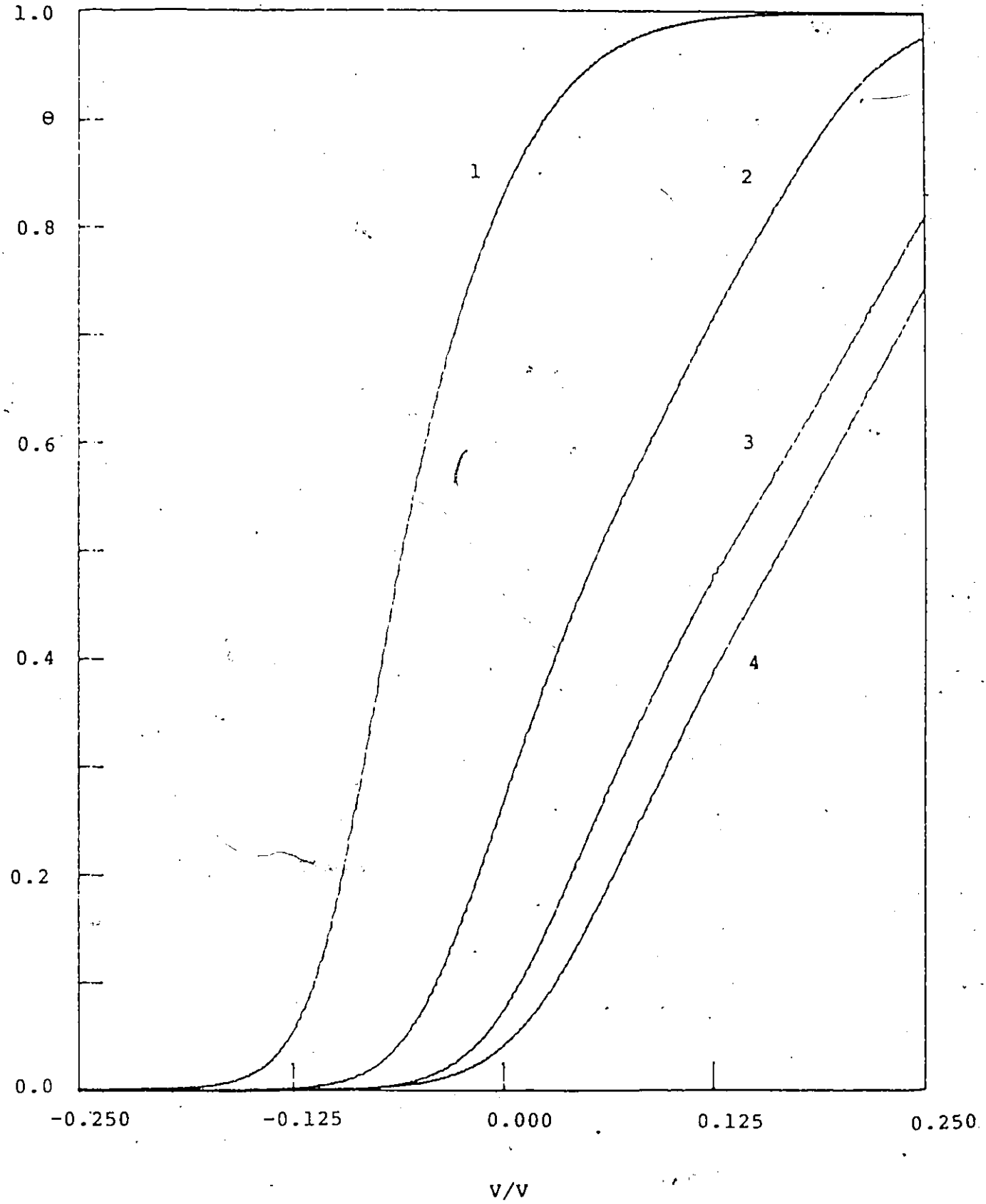
1.0
θ
0.8
0.6
0.4
0.2
0.0
1
2
3
4
-0.250
-0.125
0.000
0.125
0.250
V/V

to the hypothetical case of an electrode reaction depositing a monolayer of partial charges on the surface, without consideration of the images induced by them. Admittedly, this is a quite unrealistic physical model, but the calculation will serve to demonstrate the importance of the ionic image energy contribution in more realistic treatments. Consideration of the configurational aspect of this problem is also of interest in the light of a recent paper [34], in which it was shown that the isotherm of the Blomgren-Bockris type [37], appropriate for this particular physical model, proposing an interaction energy proportional to $\theta^{1/2}$, gives rise to some quite unrealistic behaviour when the corresponding pseudocapacitance is calculated. Specifically, the isotherm becomes singular as θ approaches 0, and the corresponding reaction pseudocapacitance becomes negative.

The steps required to derive the isotherm in the Bragg-Williams approximation are precisely as described previously, but the partition functions for the adsorbed species and their pairwise interactions have to be modified in the following ways:

(i) For a single charge $-\gamma e_0$ adjacent to a lattice point the effective field **X** is simply the vector sum of the electrode's field **E** = (0,0,E) and $(-\gamma e_0/r_0^2,0,0)$, so that

$$X^2 = E^2 + (\gamma e_0/r_0^2)^2 \qquad [63]$$

and, using the free-dipole model for H_2O(ads), there results

$$\zeta_{aw} = \frac{\int_0^{\pi} I_0(m\gamma e_0 \sin\theta/r_0^2 kT)\exp(m\mathrm{E}\cos\theta/kT)\sin\theta d\theta}{\int_0^{\pi}\exp(m\mathrm{E}\cos\theta/kT)\sin\theta d\theta} \times \exp[\alpha(X^2-E^2)/2kT] \qquad [64]$$

(ii) The interaction energy for the adatoms is simply that between two like charges of $-\gamma e_0$ separated by a distance r_0. Therefore

$$\zeta_{aa} = \exp[-(\gamma e_0)^2/r_0 kT] \qquad [65]$$

(iii) The previous definition of the electrical partition function for a single adatom included the interaction energy with its own image. According to this particular model, however, only the energy of the adatom in the field **E** is included, so that

$$z_a = \exp(-\gamma e_0 V/2kT) \qquad [66]$$

Pseudocapacitance curves calculated from the Bragg-Williams isotherm incorporating these functions are shown in Fig. 9. In contrast to those of Fig. 3, the g parameter does not change appreciably with V, and is shown next to the appropriate γ's. As pointed out previously, the argument of the exponential in eqn. 65 is $191\gamma^2$. From eqn. 46, it is seen that as γ increases, the value of g will rapidly become dominated by that of ζ_{aa}, which corresponds physically to a prohibitively large, positive, replacement energy for an adsorbed water molecule next to a charged adatom. The variation of the g with the assumed charge carried by the adatoms is thus similar to that expected from the existing theories [34,35], and the shape of the C-V curves calculated according to this model is qualitatively consistent with previously reported work involving the application of the Frumkin-type isotherm to the process 44.

While the pseudocapacitance curves calculated according to this model are not very convincing representations of experimental results, they are nevertheless well-defined functions of potential which show none of the "catastrophic"

Fig. 9: Reduced quasi-equilibrium pseudocapacitance, according to the Bragg-Williams isotherm for adsorbed charges and dipoles without images.

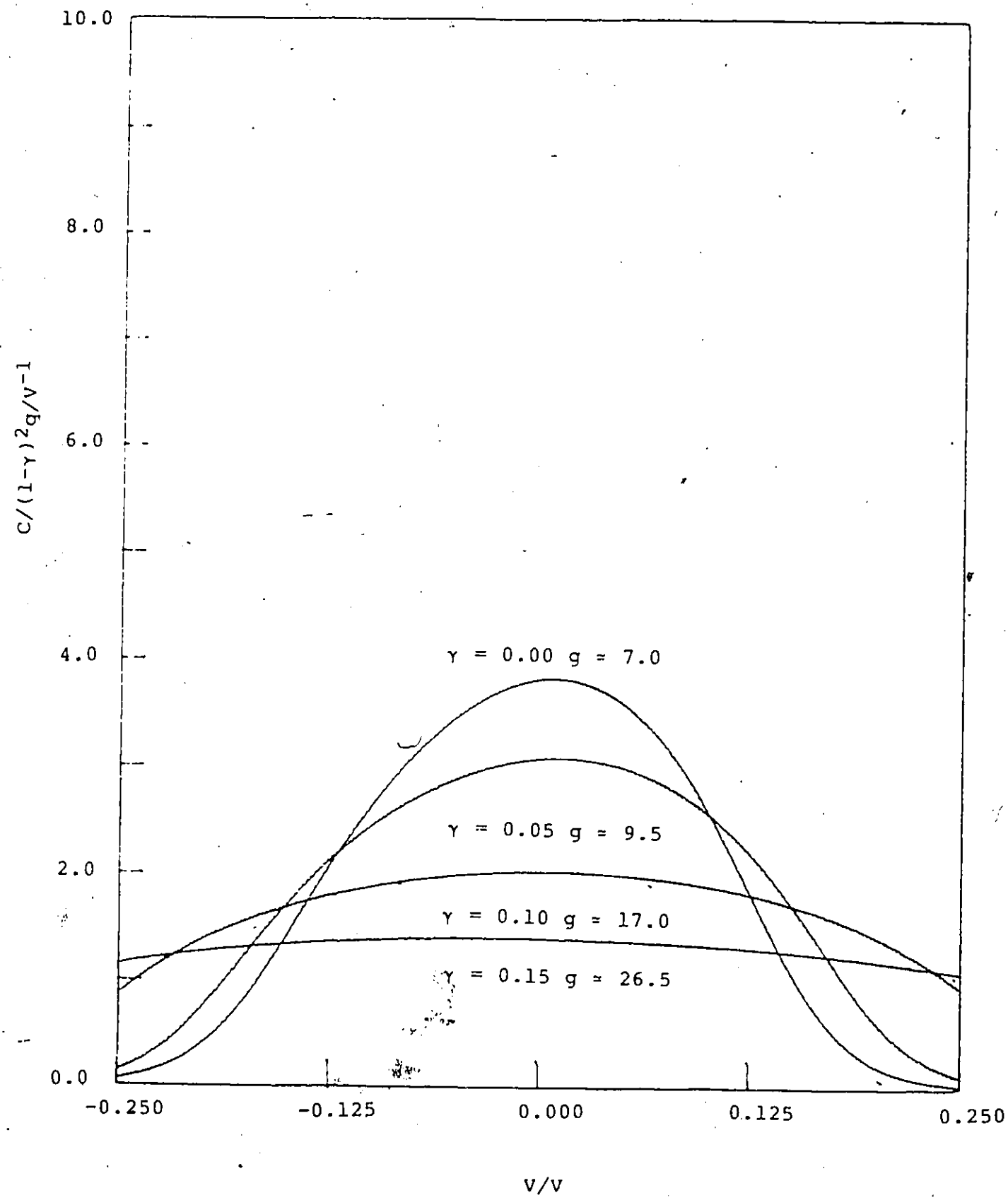

behaviour associated with the "$\theta^{1/2}$" isotherm appropriate for single charges, to which attention was drawn in ref. 34. There, the free energy of interaction between the surface charges was represented as proportional to $\theta^{1/2}$, again using a dielectric continuum approximation to describe the H_2O(ads), so that the chemical potential, which is required for the construction of the isotherm and pseudocapacitance expressions, is in turn proportional to $\theta^{-1/2}$ and is hence singular as θ tends to 0. It is apparent from the present section that this behaviour results from the use of the $\theta^{1/2}$ function to represent the free energy, since if the physical model is treated as described in this section, results are obtained which are at least consistent with the much less favourable interaction energy expected between simple charges than between charge-image pairs. On the other hand, in the developments of the $\theta^{1/2}$ type isotherms [37], the precise thermodynamic significance of the "interaction energy" is unclear, viz. whether or not it is a free energy (and hence in need of differentiation to produce the chemical potential) or is already a chemical potential. In the approach described in the present chapter, however, the relevant chemical potentials are quite unambiguously related, in the usual manner, to the partition function for the entire surface layer.

7. Limitations and Extensions

(i) Approximations to the Free Energy of Mixing

In the light of the above approximate treatments of interactions, it is natural to inquire to what extent they would differ from the (hypothetical) exact treatment, in the prediction

of the total free energy of mixing characterizing the formation of the surface phase considered here. There are two components to the approximations employed here: the first is the reliability of the lattice statistics, and the second is the accuracy of the interaction free energies and corresponding partition functions. These components are, however, closely related.

In the Quasi-Chemical Approximation, the underlying assumption is that the pairs can be considered as independent for the purposes of enumerating the total number of possible surface configurations. Furthermore, the discussion of the calculation of interaction free energies, given in Chapter 4, implies the assumption that the pairs can be considered to be energetically independent.

The accuracy of the present approach can thus be assessed in two ways:

(a) With respect to an exact treatment of the respective lattice-gas approximations, in which all dipole-dipole and adatom-dipole interactions are calculated exactly;

(b) With respect to an exact treatment of the lattice-gas problem itself, which would include all the polar interactions implied in (a).

From Chapter 4, it is evident that the pairwise free energies of interaction would be over-estimated by the functions ζ, except for the adatom-adatom interaction energy, which implies only one mutual configuration of charges. For example, the function ζ_{ww} was derived from a Monte-Carlo simulation of polarization behaviour in the absence of other adsorbed species. Thus, the use of this function to describe dipole-dipole

interactions for a finite value of θ will result in an over-estimation of the effect of neighbouring solvent dipoles on each other. Similar observations apply to the function ζ_{aw}, which was calculated without consideration of the effects of other neighbouring ions or dipoles. Thus, supposing that it were possible to derive "exact" expressions for the ζ-functions (which would evidently be dependent on coverage), the calculations presented above would tend to over-estimate the free energy of mixing, with respect to the corresponding calculations using the hypothetical "exact" ζ-functions.

It is rather more difficult to speculate on the comparison between a treatment of the type (b) and the isotherms derived in the present chapter, principally because the exact two-dimensional lattice-statistics problem has not been solved analytically. Thus, in order to provide an authoritative estimate of the accuracy of these results, one would need to conduct a computer simulation in which the energy of the surface layer, for each value of θ, would be averaged over all possible arrangements of the ions and dipoles on the surface, as well as their mutual orientations.

(ii) Non-Nearest-Neighbour Interactions

A question of fundamental importance and interest is that of the relative importance of nearest-neighbour- and non-nearest-neighbour interaction energies in determining the predicted pseudocapacitance behaviour of reaction 10.

In order to extend the treatment given in this chapter to allow for the inclusion of long-range coulombic effects using the

mean-field approximation, the average reduced dipole moment $\langle s \rangle = \langle m \rangle / m$ in the surface layer would have to be determined, in addition to θ, since this is required to calculate the components of the effective field and potential due to the dipoles. This in turn would require the solution of a second statistical-mechanical equation defining the polarization of the layer in terms of the effective field. The polarization for the adsorbed dipoles would still be defined as the partial derivative of $\ln z_w$ with respect to field, but with the added condition that θ = constant; the field-dependence of the interaction partition functions would evidently have to be taken into account.

(iii) Calculation of Double-Layer Effects

The other major assumption made throughout this chapter is that the diffuse-layer potential drop may be neglected. The treatment of the more general case where this is not necessarily so would require the calculation of the surface charge density q_M as a function of V, which would require, in addition to the statistical-mechanical relations satisfied by the ions and dipoles, an electrical boundary condition relating q_M to the charge densities associated with θ and $\langle s \rangle$. This problem is considered in Chapter 6, in connexion with the construction of ionic adsorption isotherms.

The calculation of the surface charge and corresponding differential capacity in the presence of a surface electrode reaction is a problem which has not been considered in the literature. Indeed, in discussions of the kinetics of such electrode processes, the double layer capacitance is usually assumed to behave as if it were in parallel with the reaction

pseudocapacitance. This seems quite reasonable if only diffuse-layer effects are considered; in the present chapter, however, the fact that the product of the surface reaction bears a charge means that the progress of the reaction will involve a unidirectional change in the potential distribution of the double layer. As before, the calculation of the capacitance according to the primitive model requires the calculation of the inner-layer potential drop as a function of V and, as discussed in Chapter 3, it is necessary to include in the expression for C_1 the effect of the change in inner-layer composition. But considering the dependence of θ on both components of the interfacial potential drop (as expressed by, e.g., the Frumkin correction [27]) it is evident that the capacitance and pseudocapacitance will not be neatly separable, as generally assumed.

8. Conclusions

This chapter has considered the implications of including free energies of polarization and interaction on the predicted kinetic behaviour for a one-electron electrodeposition reaction, involving the displacement of polarized adsorbed solvent molecules.

The inclusion of the polarization free energy contribution to the activation free energy, via the electrical partition function appropriate for the model of orientational polarization, results in a potential-dependence of the symmetry factor for the reaction.

Pairwise interactions may be treated with the aid of two approximations of lattice-gas theory, viz. the Bragg-Williams and

Quasi-Chemical Approximations, the free energies of interaction between the various possible nearest-neighbour pairs being given by the expressions derived in Chapter 4.

The Bragg-Williams Approximation results in an isotherm which is formally similar to the Frumkin Isotherm [32]. The significance of the g-parameter, defining the strength of interactions, is, however, fundamentally different from that attributed to it in existing treatments, in two important respects:

(i) It is dependent on the interfacial field, i.e. electrode-solution potential difference;

(ii) Rather than referring solely to the strengths of interaction between adsorbed species, it is also dependent on the strengths of interactions between pairs of solvent molecules, and between adatoms and solvent molecules.

In other words, the g-parameter is a measure of the "solvation energy" characterizing the surface phase, an effect which is not considered by existing treatments of interactions between adsorbed, partially discharged atoms, all of which assume that co-adsorbed solvent molecules may be treated as a dielectric continuum.

The approach described also avoids the prediction of the physically unreasonable pseudocapacitance behaviour [34] associated with treatments estimating surface interaction energies in terms of $\theta^{1/2}$ [37].

Application of the Quasi-Chemical Approximation results in predicted pseudocapacitance behaviour which is usually considered as evidence for the occurrence of two concurrent reactions.

References

1. J.A.V. Butler

Proc. Roy. Soc. Lond. **A122**: 399 (1929);

A135: 348 (1932). See also

J.A.V. Butler and C. Ockrent

J. Phys. Chem. **34**: 2286 (1934)

2. J.O'M. Bockris, M.A.V. Devanathan and K. Mueller

Proc. Roy. Soc. Lond. **A274**: 55 (1963)

3. J.O'M. Bockris, E.Gileadi and K. Mueller

Electrochim. Acta **12**: 1301 (1967)

4. B.E. Conway and H.P. Dhar

Croat. Chim. Acta **45**: 109 (1973);

B.E. Conway, H.P. Dhar and S. Gottesfeld

J. Colloid and Interface Sci. **43**: 303 (1973)

5. R. Guidelli

J. Electroanal. Chem. **123**: 59 (1981)

6. J.O'M. Bockris and E.C. Potter

J. Chem. Phys. **20**: 614 (1952)

7. J.R. Macdonald

J. Chem. Phys. **22**: 1857 (1954)

8. J.R. Macdonald and C.A. Barlow, Jr.

J. Chem. Phys. **36**: 3062 (1962)

9. E. Gileadi and G.E. Stoner

J. Electrochem. Soc. **118**: 1316 (1971)

10. N.F. Mott and R.J. Watts-Tobin

Electrochim. Acta **4**: 79 (1961)

11. S. Kashti, E. Kirowa-Eisner and E. Gileadi

Israel J. Chem. **12**: 1003 (1974)

12. S. Kashti and E. Kirowa-Eisner
J. Electroanal. Chem. **103**: 119 (1979)

13. E. Kirowa-Eisner and E. Gileadi
J. Electroanal. Chem. **38**: 191 (1972), **42**: 111 (1973)

14. I. Rubinstein
J. Phys. Chem. **85**: 1899 (1981)

15. W.R. Fawcett and C.L. Gardner
J. Electroanal. Chem. **82**: 303 (1977)

16. A.N. Frumkin
Z. Physik **35**: 792 (1926)

17. A.N. Frumkin and B.B. Damaskin, in J.O'M. Bockris and B.E. Conway (eds.)
"Modern Aspects of Electrochemistry", vol. 2, Butterworths, London (1964), chapter 3

18. E. Gileadi
J. Electroanal. Chem. **30**: 123 (1971)

19. D. Henderson
Prog. Surf. Sci. **13**: 197 (1983)

20. W.R. Fawcett
Israel J. Chem. **18**: 3 (1979)

21. B.E. Conway and S. Marshall
Aust. J. Chem. **36**: 2145 (1983)

22. W.R. Fawcett
J. Phys. Chem. **82**: 1385 (1978)

23. R. Parsons
J. Electroanal. Chem. **59**: 229 (1975)

24. B.B. Damaskin and A.N. Frumkin

Electrochim. Acta **19**: 173 (1974)

25. T.L. Hill
"An Introduction to Statistical Thermodynamics", Addison-Wesley, Reading, Mass. (1962)

26. B.E. Conway and E. Gileadi
Trans. Faraday Soc. **58**: 2493 (1962); see also
B.E. Conway and E. Gileadi
Can. J. Chem. **42**: 90 (1964)

27. J.O'M. Bockris and A.K.N. Reddy
"Modern Electrochemistry", vol. 2, Plenum, N.Y. (1972), chapter 8

28. L.I. Krishtalik
Electrochim. Acta **13**: 1045 (1968)

29. H. Angerstein-Kozlowska and B.E. Conway
J. Electroanal. Chem. **95**: 1 (1979)

30. J.G. Klinger
Ph.D. Thesis, University of Ottawa (1977)

31. M. Karolczak
Electrochim. Acta **30**: 325 (1985)

32. A.N. Frumkin
Z. Phys. Chem. **116**: 466 (1925)

33. B.E. Conway and H.A. Kozlowska
J. Electroanal. Chem. **113**: 63 (1980)

34. B.E. Conway and S. Marshall
Electrochim. Acta **28**: 1003 (1983)

35. E.A. Guggenheim
"Mixtures", Oxford University Press (1952)

36. B.E. Conway and H.A. Kozlowska
Acc. Chem. Res. 14: 49 (1981)
37. E. Blomgren and J.O'M. Bockris
J. Phys. Chem. 63: 1475 (1959)

CHAPTER 6

CONSTRUCTION OF IONIC ADSORPTION ISOTHERMS AND CAPACITANCE EXPRESSIONS

The previous two chapters have discussed in turn the calculation of electrostatic free energies of interaction between adsorbed species, and the construction of isotherms for simple faradaic adsorption reactions, or, alternatively, the electrostatic and configurational components of the polar interaction problem identified in Chapter 4. The treatment of ionic adsorption requires consideration of a third component, viz. the relationship between the adsorbed free-charge density q_{ion}, the bound-charge density q_{dip}, and the electrode's surface charge density q_M, as a function of the electrical boundary conditions imposed on the interface. Thus, the statistical-mechanical equations defining the equality of chemical potentials of each component between the adsorbed and bulk phases must be combined with the conditions of electroneutrality and potential continuity.

It is the purpose of the present chapter to use these statistical-mechanical and electrostatic conditions to determine the ionic coverage and capacitance resulting from substitutional adsorption by anions at electrodes, according to the primitive model of the double layer. The relationship between the relevant charge densities is considered first; following this, the various approaches to the determination of ionic adsorption micropotentials are briefly reviewed, and extensions of these calculations to include effects of discreteness of adsorbed

dipoles are described. The resulting ionic and dipolar contributions to the micropotential and its derivative are then used to construct ionic adsorption isotherms, with long-range interactions treated according to the Mean Field Approximation.

1. Relation Between Charge Densities

In Chapter 2 the implications of representing E_1 as $4\pi(q_M - q_{dip})$ were considered, and in particular, the problem of determining q_M and q_{dip} self-consistently as a function of V. In the presence of an adsorbed free-charge density, q_{ion}, in the compact double layer, the representation of the field E_1 must be modified thus:

$$E_1 = 4\pi(q_M + q_{ion} - q_{dip}) \qquad [1]$$

Since the existing treatments of ionic adsorption have always assumed the adsorbed solvent molecules to function as a dielectric continuum with constant permittivity, they implicitly ignore the relationship between the charge densities in eqn. 1. With the assumption that there are no adsorbed charges, the use of a constant inner-layer permittivity leads to physically impossible values of the polarization, as shown in Chapter 2. In contrast, when ionic adsorption is assumed to occur, it is quite possible for the adsorbed charge density to exceed the electrode surface charge density, provided that the discrepancy be balanced by an appropriate diffuse-layer charge density. Thus, the "paradoxical" behaviour associated with the use of a constant inner-layer dielectric constant is concealed. For a given adsorption isotherm, it would be quite possible to calculate the adsorbed charge density q_{ion} as a function of q_M, by simply

applying the condition of electroneutrality to the interface, assuming the diffuse layer to be described by, e.g., the Gouy-Chapman theory. Problems would arise, however, if it were attempted to calculate q_M and q_{ion} as a function of V, since the potential differences across the compact and diffuse regions of the double layer would be inconsistent even in the limit of negligible ionic adsorption, where such paradoxical behaviour would no longer be masked. In interpreting adsorption data, however, it is more usual to treat q_M as the independent variable.

Therefore, before treating the interaction component of the ionic adsorption phenomenon, it is of interest to consider first the behaviour predicted by an isotherm for a simple substitutional adsorption reaction

$$A^-(aq) + H_2O(ads) = A^-(ads) + H_2O(aq) \qquad [2]$$

where the electrical free energies of the adsorbed species are defined in terms of a field given by eqn. 1, thus neglecting for the moment the interaction energies between all the species, corresponding to the micropotential and its derivative. The calculation of these quantities will be considered subsequently.

The adsorbed monolayer is assumed to be a lattice, as in the previous chapter, with a fraction θ of sites occupied by anions of charge $-e_0$, and the remaining fraction $1-\theta$ occupied by dipoles of average moment $\langle m \rangle = m\langle s \rangle$ and polarizability α. If the lattice sites have a number density N_w per unit volume and d is the layer thickness, then the adsorbed charge components can be defined as $q_{ion} = -N_w e_0 d.\theta$ and $q_{dip} = N_w \langle m \rangle .(1-\theta)$. $\langle m \rangle$ is defined as before in terms of the logarithmic derivative of the electrostatic

partition function $z_w(E_1)$. The coverage fraction θ is then determined by equating the sum of the electrochemical potentials of the reactants and products of reaction 2; this results in the isotherm

$$\theta/(1-\theta) = K_{eq}.(a_{A^-}/a_{H2O}).z_a(E_1)/z_w(E_1) \equiv K(E_1) \qquad [3]$$

where the electrical partition functions z_a and z_w for the adsorbed ions and dipoles are respectively (see Chapter 4, Section 4)

$$z_a(E_1) = \exp(E_1 d.e_0/2kT)$$

$$z_w(E_1) = 4\pi\exp(\alpha E_1^2/2kT)\sinh(mE_1/kT)/(mE_1/kT) \qquad [4]$$

assuming a free-dipole model for H_2O(ads).

Charge balance across the interface requires that q_M be equal and opposite to the total free charge residing in the compact and diffuse regions of the double layer. Representing the diffuse layer charge in terms of $\Delta\phi_2 = V - \Delta\phi_1$ (in the notation of Chapter 2) and using the Gouy-Chapman theory, one obtains

$$q_M = -(-N_w e_0 d\theta) + 2A\sinh(e_0\Delta\phi_2/2kT); \quad A = (\varepsilon kTN_0/2\pi)^{1/2}$$

or

$$q_M + q_{ion} = 2A\sinh(e_0\Delta\phi_2/2kT). \qquad [5]$$

where N_0 is the number of ions per unit volume, and ε is the dielectric constant of the diffuse layer.

The definition of E_1 in eqn. 1 can be rearranged to give

$$q_M + q_{ion} = E_1/4\pi + q_{dip}$$

$$= E_1/4\pi + (1-\theta)N_w kT.\partial\ln z_w(E_1)/\partial E_1 \qquad [6]$$

so that E_1 may be determined, for a given value of θ, by solving the equation

$$E_1/4\pi + (1-\theta).N_w kT\partial\ln z_w(E_1)/\partial E_1 = 2A\sinh[(V-E_1 d)e_0/2kT] \qquad [7]$$

In Chapter 2, the capacity of the inner layer was expressed in terms of the derivative dq_{dip}/dq_M. With E_1 defined as in eqn. 1, however, one has

$$1/C_1 = d(E_1 d)/q_M = 4\pi d(1 + dq_{ion}/dq_M - dq_{dip}/dq_M) \qquad [8]$$

so that the determination of C_1 in the presence of ionic adsorption requires two equations for the derivatives dq_{ion}/dq_M and dq_{dip}/dq_M. Since

$$q_{dip} = (1-\theta).N_w kT \partial \ln z_w(E_1)/\partial E_1 \qquad [9]$$

differentiation with respect to q_M provides

$$dq_{dip}/dq_M = (1-\theta)N_w kT \partial^2 \ln z_w(E_1)/\partial E_1^2 .4\pi(1+dq_{ion}/dq_M - dq_{dip}/dq_M) + (kT/e_0 d)\partial \ln z_w(E_1)/\partial E_1 . dq_{ion}/dq_M \qquad [10]$$

where $q_{ion} = -N_w e_0 d.\theta$ has been used in the second term; alternatively, eqn. 10 may be written:

$$dq_{dip}/dq_M = 4\pi h_1(1 + dq_{ion}/dq_M - dq_{dip}/dq_M) + h_2 dq_{ion}/dq_M \qquad [11]$$

where, applying the definitions of z_w and z_a given by eqns. 4,

$$h_1 = (1-\theta)N_w[\alpha + (m^2/kT).L'(mE_1/kT)]$$

$$h_2 = (1/e_0 d).[\alpha E_1 + mL(mE_1/kT)]$$

$$L(x) = \coth x - 1/x$$

$$L'(x) = 1/x^2 - \operatorname{cosech}^2 x$$

The other required equation is obtained by differentiation of the isotherm:

$$dq_{ion}/dq_M = -4\pi h_3(1 + dq_{ion}/dq_M - dq_{dip}/dq_M) \qquad [12]$$

where

$$h_3 = N_w e_0 d.\theta(1-\theta)d\ln K(E_1)/dE_1$$

$$= (N_w e_0 d/kT).\theta(1-\theta)[e_0 d/2 - \alpha E_1 - mL(mE_1/kT)]$$

Simultaneous solution of eqns. 11 and 12 results in

$$dq_{ion}/dq_M = -4\pi h_3/[1 + 4\pi(h_1+h_3-h_2 h_3)]$$

$$dq_{dip}/dq_M = 4\pi(h_1-h_2 h_3)/[1 + 4\pi(h_1+h_3-h_2 h_3)] \qquad [13]$$

An interesting consequence of eqn. 5 is that $\Delta\phi_2$ and hence its derivative $d\Delta\phi_2/dq_M \equiv 1/C_2$, is dependent on q_{ion}. For, from eqn. 5,

$$1 + dq_{ion}/dq_M = (e_0A/kT)\cosh(e_0\Delta\phi_2/2kT).d\Delta\phi_2/dq_M \quad [14]$$

so that

$$C_2 = dq_M/d\Delta\phi_2 = (e_0A/kT)\cosh(e_0\Delta\phi_2/2kT)/[1 + dq_{ion}/dq_M]$$
$$= (e_0A/kT)\cosh(e_0\Delta\phi_2/2kT)/dq_{dip}/dq_M \quad [15]$$

using eqn. 13. From this equation it is evident that C_2 could, at least in principle, assume negative values, a situation at first suggestive of the "paradoxical" behaviour discussed in Chapter 2. In this case, however, one can see physically how such a negative capacity could arise. If q_M were large and positive, the value of E_1 would be such that adsorption of the anions would be energetically favourable. With increasing values of positive V, charge would tend to accumulate in the compact double layer at the expense of the diffuse layer. Alternatively, this could be considered as a decrease of $\Delta\phi_2$ with increasing V. Under conditions when this would be possible, however, the values of C_2 would be several orders of magnitude greater than those of C_1, so that the resultant capacity of the interface would be almost entirely determined by C_1 rather than C_2.

In order to determine E_1, it is first necessary to substitute the value of θ from eqn. 3 into eqn. 7. Since (cf. eqn. 3)

$$\theta = K(E_1)/[K(E_1) + 1]$$

the equation to be solved for E_1 becomes

$$E_1/4\pi + N_wkT[K(E_1) + 1]^{-1}\partial\ln z_w(E_1)/\partial E_1 = 2A\sinh[(V-E_1d)e_0/2kT]$$

[16]

or from eqn. 4 for z_w,

$$E_1/4\pi + N_w[mL(mE_1/kT) + \alpha E_1]/[1 + K(E_1)] = 2A\sinh[(V-E_1d)/e_0/2kT] \quad [17]$$

In Fig. 1, the total capacity $C \equiv C_1C_2/(C_1+C_2)$ is shown as a function of V for various values of the intrinsic equilibrium constant K_{eq}, which contains the field-independent parameters describing the adsorption free energy (i.e. the standard chemical potentials of each species). Predictably, the onset of adsorption is delayed by a very small value of K_{eq}, but when the electrical partition function $z_a(E_1)$ dominates the value of the field-dependent equilibrium constant $K(E_1)$, the capacity increases markedly. This rapidity is, of course, the result of the (entirely unrealistic) neglect of the long-range coulombic interaction energies, but it is nevertheless interesting to note that even very small values of Θ can profoundly affect the capacity of the interface; a given charge density on the electrode surface can be much more "efficiently" balanced by the accumulation of ions than by polarization of adsorbed dipoles. For instance, the very large capacity of 92×10^{-6} F cm^{-2} in curve 1 at V = -100 mV corresponds to a coverage of about 0.022.

The effect of the supporting electrolyte concentration on the capacitance is shown in Fig. 2, which has some qualitative resemblance to experimental behaviour in the limit of increasing ionic strength, in that the "fine structure", associated with the predominance of the diffuse layer capacity component at low concentrations, disappears.

The inclusion of a field-independent orientational energy

Fig. 1: Differential capacitance as a funtion of potential, with ionic specific adsorption, for various values of K_{eq}. m = 1.835 x 10^{-18} statC cm, d = 3.0 x 10^{-8} cm, N_w = 3.342 x 10^{22} cm^{-3}, c_{A^-} = 0.01 mol/l, T = 293 K, supporting electrolyte concentration = 0.1 mol/l.

Curve 1: K_{eq} = 100

Curve 2: K_{eq} = 10

Curve 3: K_{eq} = 1

Curve 4: K_{eq} = 0.1

Curve 5: K_{eq} = 0.01

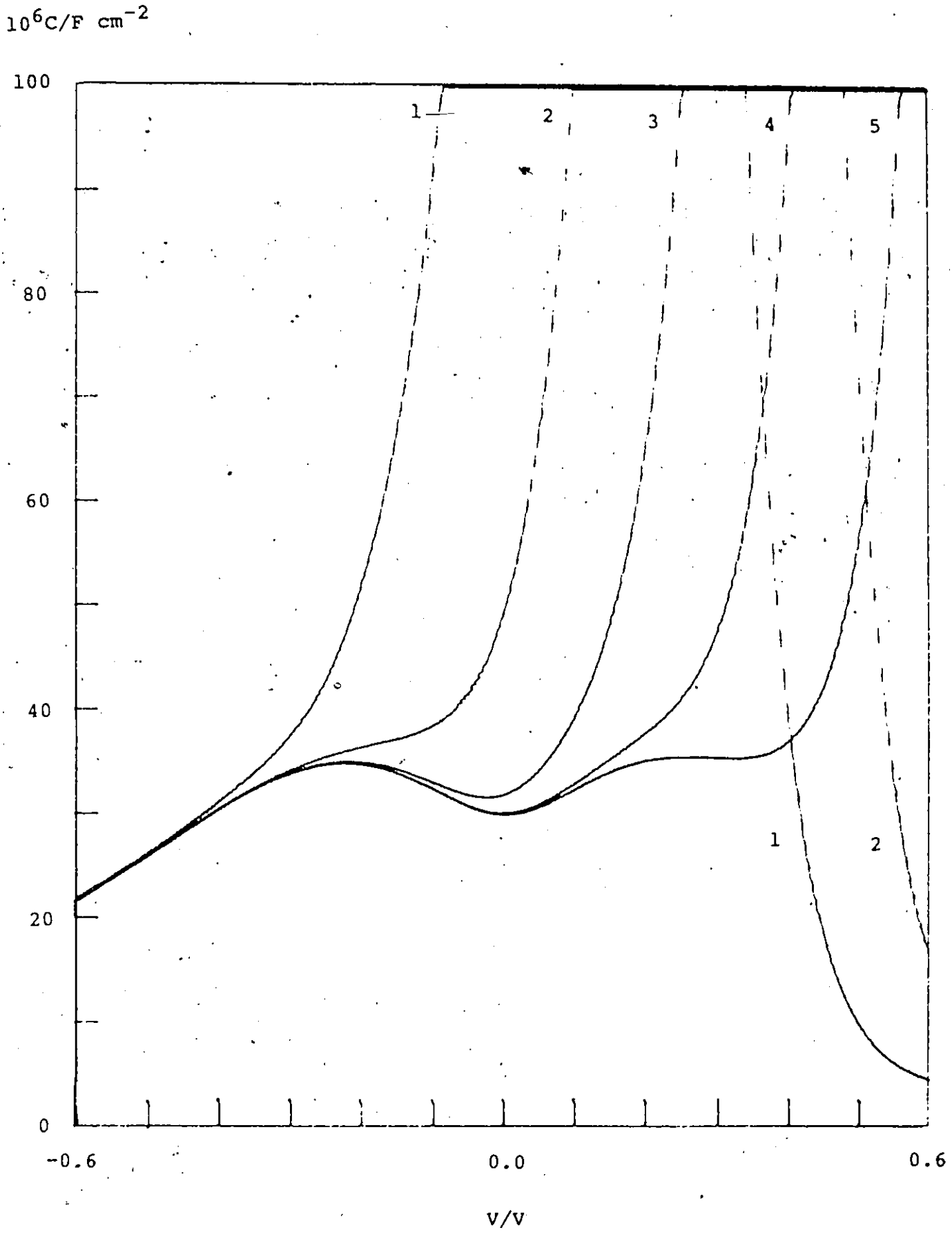
10^6C/F cm^{-2}
100
80
60
40
20
0
1
2
3
4
5
1
2
-0.6
0.0
0.6
V/V

Fig. 2: Differential capacitance as a function of potential, with ionic specific adsorption. Effect of supporting electrolyte concentration c_I; c_{A^-} = 0.0001 mol/l, K_{eq} = 100.

Curve 1: c_I = 1.0 mol/l

Curve 2: c_I = 0.1 mol/l

Curve 3: c_I = 0.01 mol/l

Curve 4: c_I = 0.001 mol/l

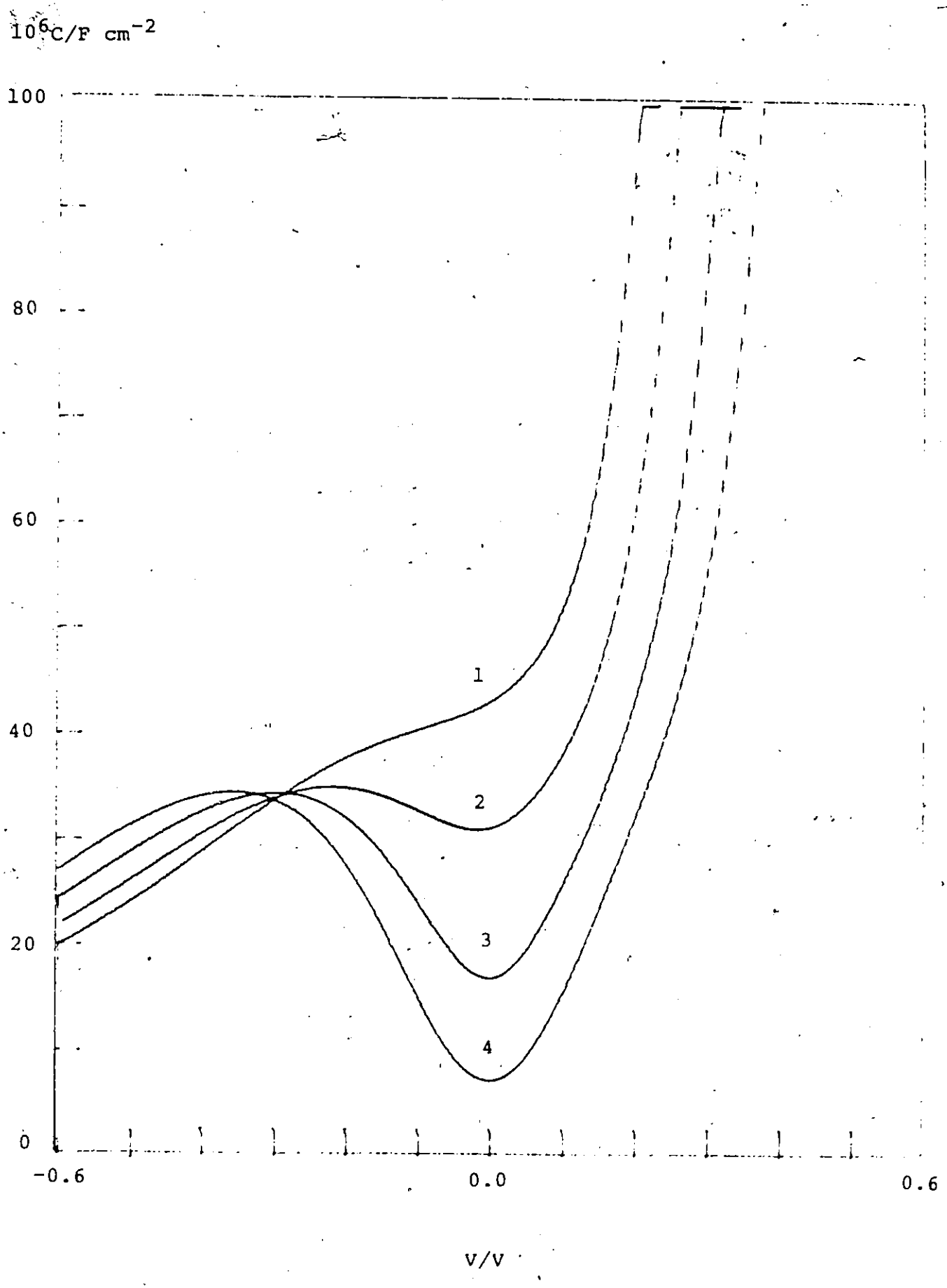
10^6C/F cm^{-2}
100
80
60
40
20
0
1
2
3
4
-0.6
0.0
0.6
V/V

Fig. 3: Differential capacitance as a function of potential, with specific ionic adsorption, for different values of U_0/kT. $K_{eq} = 1$, $c_{A^-} = 0.01$ mol/l, $c_I = 0.1$ mol/l

Curve 1: $U_0/kT = 2$

Curve 2: $U_0/kT = 0$

Curve 3: $U_0/kT = -2$

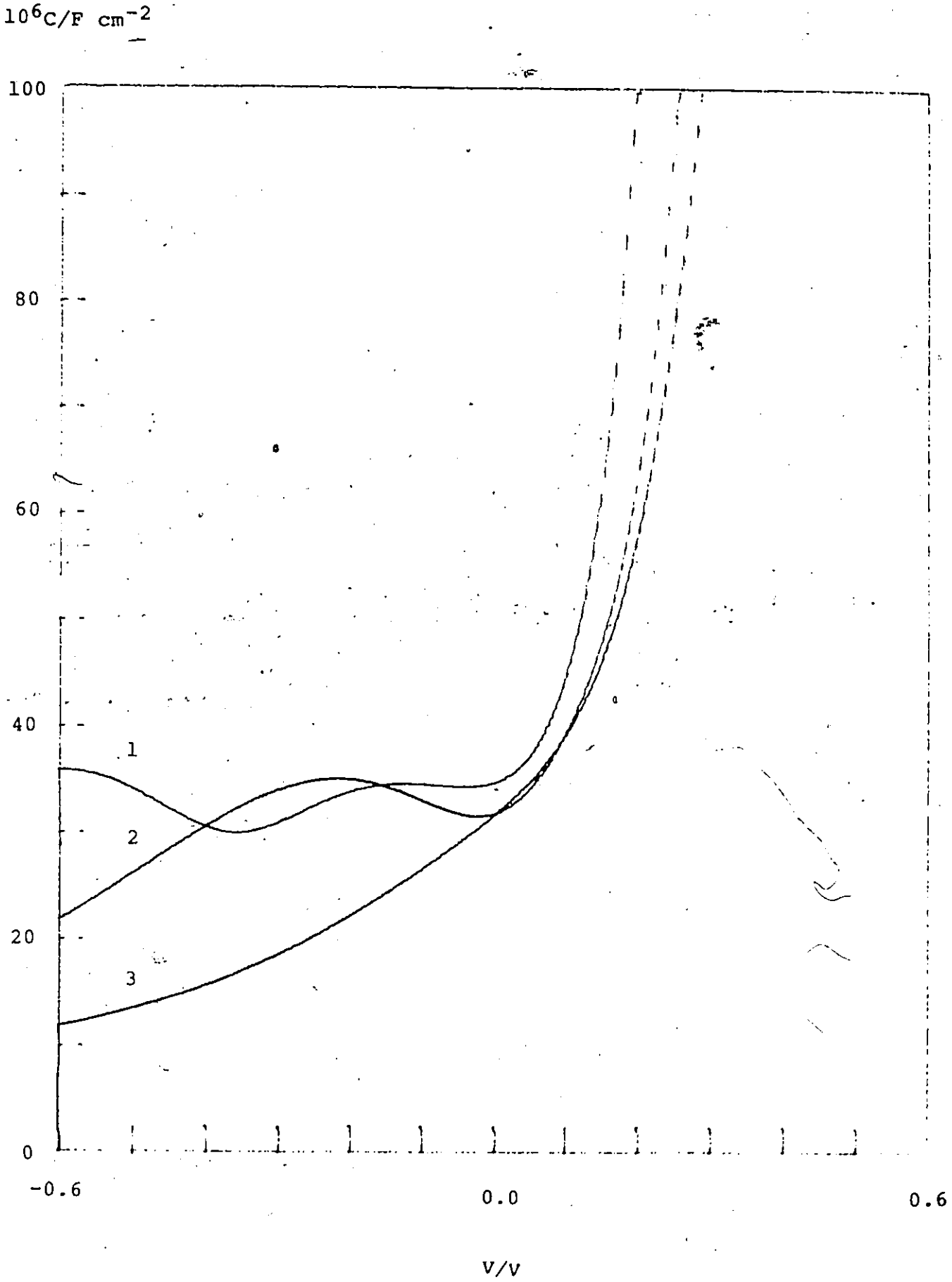
10^6C/F cm^{-2}
100
80
60
40
20
0
1
2
3
-0.6
0.0
0.6
V/V

difference U_0 of the adsorbed dipoles is shown in Fig. 3; this is equivalent to the replacement of mE_1/kT in the orientational polarization and partition function for the dipoles by $mE_1/kT + U_0/2kT$. This is somewhat similar to the to the results of Fig. 1, in that the curves are diplaced to the right for larger values of U_0, but in this case the ionic concentration is such that the capacitance minimum is absent. There is also a similarity with the results presented in Chapter 2, calculated with the assumption that ionic adsorption is absent; the onset of adsorption is marked by a rapid increase in C as a function of V. The superposition of the dipole-capacity curve and the increase due to the ionic adsorption is seen to give rise to a capacitance "hump", of a type similar to those observed for the adsorption of Cl^- ions at mercury [1]. There has been considerable debate in the literature as to whether such features result from (a) orientational polarization of co-adsorbed solvent molecules [2-4] or (b) ionic adsorption [5-7]. It is not possible to answer this question authoritatively, on the basis of the existing primitive-model theoretical treatments of the double layer. Those of opinion (a) assume that adsorption of ions is negligible, whilst those of opinion (b) construct ionic adsorption isotherms based on the assumption of a dielectric continuum model for the solvent in the adsorbed monolayer. Obviously, the crudity of the model that has been considered in the present section does not permit preference for either position, but the results nevertheless indicate that the inclusion of both ions and dipoles predicts behaviour which, qualitatively at least, is not inconsistent with

experimental results.

2. Review of Existing Theoretical Treatments

Since the original suggestion by Frumkin [8] that the discreteness of adsorbed charges could be important in determining the electrostatic contribution to their adsorption energy, much attention has been devoted to the calculation of such discreteness-of-charge effects. Inspection of the literature reveals an interesting collection of advanced mathematical techniques which have been brought to bear on the problem. The differences between the physical models to which the treatments are assumed to apply are, however, relatively few in number, and permit existing work to be classified in the following broad categories:

(i) ions imaged conductively in the metal surface;

(ii) ions imaged conductively in the metal surface and diffuse layer;

(iii) ions imaged conductively in the metal surface and dielectrically in the diffuse layer;

(iv) anisotropy of dielectric constant assumed for the compact layer.

All the existing theories involve the assumption that the solvent present in the adsorbed layer may be treated as a dielectric continuum (i.e. that discreteness of dipolar charge density may be neglected), and nearly all assume that the metal is a perfect conductor (however, as discussed below, some attempts have been made to consider deviations from this idealized situation). In addition, the use of a primitive model implies, of course, a neglect of interactions between the

adsorbed ions and dipoles and species located in the diffuse layer.

The most recent statistical-mechanical approaches to the theory of electrified interfaces [9] abandon all continuum approximations; micropotential calculations of the type to be described presently are thus fundamentally inapplicable. One of the aims of the present chapter is to examine the consequences of dipolar discreteness, within the framework of the primitive model, with particular reference to the problem of ionic adsorption.

Before considering each of the categories (i)-(iv) in turn, it is appropriate to state some mathematical results which, in addition to being of fundamental importance, permit the identification of important similarities between a number of apparently distinct treatments.

2.1 The Potential Problem

The most conspicuous respect in which the study of interfacial phenomena is complicated, with respect to their isotropic counterparts, is the replacement of spherical symmetry by cylindrical symmetry. It is thus required to determine a potential distribution V in terms of a cylindrical polar coordinate system (ρ,ϕ,z) (see Chapter 4, Fig. 6). In the case of Laplace's equation, on which most theories of the micropotential are based,

$$\nabla^2 V \equiv \partial^2 V/\partial\rho^2 + (1/\rho)\partial V/\rho + \partial^2 V/\partial\phi^2 + \partial^2 V/\partial z^2 = 0 \qquad [18]$$

a solution is sought in the form

$$V = R(\rho)\Phi(\phi)Z(z)$$

Then, by an argument which is discussed in most textbooks on higher mathematics (see, for example, ref. 10), the solution which is bounded at the origin is

$$V \propto J_n(k\rho).e^{\pm in\phi}.e^{\pm kz} \qquad [19]$$

where n and k are constants, and J_n is the Bessel function of the first kind of order n. In the special case of axial symmetry, which most often obtains in situations of electrochemical interest, n = 0, and

$$V \propto J_0(k\rho).e^{\pm kz} \qquad [20]$$

The solution will be a linear combination of terms of this type, in which the coefficients are determined by applying the boundary conditions, such as continuity of potential and dielectric displacement. From the nature of Bessel functions, it follows that k should be treated as freely variable, implying an integration over k rather than a summation; the simplest potential which can be thus represented is that due to a point charge e_0 at the origin:

$$V = e_0/(\rho^2+z^2)^{1/2} = e_0\int_0^\infty J_0(k\rho)e^{-k|z|}dk \qquad [21]$$

using an integration formula originally due to Lipschitz [11]; the solution containing $e^{+k|z|}$ has been discarded in view of the requirement that V be finite as $z,\rho \to \infty$. In the case of a more general potential, assumed to be of the form

$$\int_0^\infty [f_1(k)e^{kz}+f_2(k)e^{-kz}]J_0(k\rho)dk \qquad [22]$$

the result which permits the determination of the functions $f_1(k)$ and $f_2(k)$ is the Fourier-Bessel Inversion Theorem, due to Hankel [11], which states that, subject to suitable restrictions on the form of F(x),

$$\text{if } G(x) = \int_0^\infty kF(k)J_n(kx)dk, \text{ then } F(x) = \int_0^\infty kG(k)J_n(kx)dk \qquad [23]$$

A consequence of this is that if

$$\int_0^\infty kF(k)J_0(kx)dk = 0 \qquad [24]$$

for all $x \geq 0$, then $F(k)=0$ for all k. The justification of this result is to be found in several monographs on the theory of Bessel functions (e.g. refs. 11 and 12).

The form of the coefficient functions $f_1(k)$ and $f_2(k)$ is determined entirely by the boundary conditions. Many of the micropotential calculations consider the problem of determining the potential distribution due to charges simultaneously imaged in two parallel planes. In these cases, f_1 and f_2 are geometric series of exponential terms which, when multiplied by $J_0(k\rho)$ and integrated termwise, give infinite series of coulombic potentials in the form of eqn. 21. The two integrals in eqn. 22 are thus merely closed-form representations of infinite series of image charge potentials, which could be constructed from purely geometric considerations. The utility of the Fourier-Bessel integral approach is that it can be readily applied to more complicated imaging situations, which are less easily treated by geometric arguments, simply by using a solution of Laplace's (or Poisson's) equation consistent with the symmetry (or asymmetry) inherent in the charge configurations.

The remaining micropotential theories require the solution of the linearized Poisson-Boltzmann or Fermi-Thomas equations, which are of the form

$$\nabla^2 V - \lambda^2 V = 0 \qquad [25]$$

where λ is a constant with dimensions of reciprocal length. In this case, with axial symmetry assumed, the solution is sought in

the form

$$\int_0^\infty f(k)J_0(k\rho)\exp[-z(k^2+\lambda^2)^{1/2}]dk \qquad [26]$$

and the procedure used to determine f(k) from the boundary conditions is the same. Solutions of this equation are readily shown to be Fourier-Bessel integral representations of screened coulomb potentials, of which the simplest example is (cf. ref. 12, p.243)

$$\int_0^\infty dk\ kJ_0(k\rho)\exp[-z\sqrt{(k^2+\lambda^2)}]/\sqrt{(k^2+\lambda^2)} = \exp[-\sqrt{(z^2+\rho^2)}]/\sqrt{(\rho^2+z^2)} \qquad [27]$$

2.2 Micropotential Calculations

(i) Ions Imaged Conductively in the Metal Surface

A first approximation to the electrostatic effect of image charges induced in a perfect conductor by ions adsorbed on its surface was given by Mott and Watts-Tobin [13], who treated both adsorbed and induced charges as continuous charged layers; the reference ion was assumed to be equivalent to a circular disc with a radius inversely proportional to the square root of the number of ions adsorbed per unit area.

The actual discreteness of the image charges was considered by Bockris, Devanathan and Mueller, [1] who approximated the potential experienced by an ion, located at a distance r_a from a second charge-image pair, by the first two terms of the binomial expansion of the distance between the ion and the neighbour's image. The distance r_a was then related to the number density of adsorbed ions n_a by $\pi r_a^2 = 1/n_a$; when substituted into the appropriate potential, this gave an interaction energy U_{rep} linear in $n_a^{3/2}$ and $n_a^{5/2}$. The coverage (i.e. n_a) was then obtained by writing $n_a \propto \exp(-U_{rep}/kT)$ and solving the resulting

non-linear equation. The most obvious defects in this argument are (a) the neglect of the unoccupied fraction of the surface in the construction of the isotherm; and (b) that the ion-image potentials due to all of the ions are not included in the expression for U_{rep}.

Both these points were dealt with in a more detailed investigation by Wroblowa and Kovac [7], who performed the summation due to all ions by dividing the hexagonal planar lattice into concentric rings of charge, each containing a multiple of 6 ions. The lattice parameter was again assumed to be proportional to $n_a^{-1/2}$, but in working out the coulombic potential at the ion due to each ring of ion-image pairs, the charge distribution is considered to consist of two annular elements of uniform charge density.

The most thorough treatment of the single-image model for adsorbed ions was given by Barlow and Macdonald [14]. Here, the exact coulombic potential due to all ion-image pairs was used, and the approximation of uniform concentric rings of charge was replaced by summation over all coordinates of an hexagonal lattice. The potential problem in this case was quite simple; the major difficulty faced by the authors was that of evaluating these lattice sums, which converge very slowly. An analytical transformation developed by van der Hoff and Benson [15] and Mackenzie [16] was applied, resulting in a closed-form expression and a very rapidly converging series involving the modified Bessel function K_0. This involves the following steps:

(a) the coulombic potential terms due to the charges and images

are represented as integrals by using the Gamma function:

$$\Gamma(1/2)x^{-1/2} = \int_0^\infty t^{-1/2}e^{-xt}dt \qquad [28]$$

(b) the order of summation and integration is interchanged, and the sum of exponential terms is transformed with the result

$$\sum_{-\infty}^{\infty}\exp[-(k+a)^2t] = (\pi/t)^{1/2}\sum_{-\infty}^{\infty}\cos(2\pi as)\exp(-s^2\pi^2/t^2) \qquad [29]$$

(c) the integrals are then reduced to Bessel functions using the representation

$$\int_0^\infty t^{-n}\exp[-k^2t-s^2\pi^2/t]dt = 2(\pi|s|/k)^nK_n(2\pi k|s|) \qquad (n=0) \quad [30]$$

(d) the dominant term is that for which s=0, which has to be obtained by a limiting procedure. The summation with respect to the second lattice index requires treatment of a second slowly converging series of logarithmic terms, which can be summed using the infinite product representations of hyperbolic functions.

A similar expression for this lattice sum is derived in the appendix, but the result is simpler and the derivation is more direct, using the Poisson Summation Formula. The method obtains the Bessel functions immediately from the formula

$$\int_0^\infty dx\ \cos(tx)/(x^2+a^2)^{1/2} = K_0(at) \qquad [31]$$

and the logarithmic terms correspond to the case t=0, which is the difference of two divergent integrals

$$\int_0^\infty dx[1/(a_1^2+x^2)^{1/2} - 1/(a_2^2+x^2)^{1/2}] = \ln(a_2/a_1) \qquad [32]$$

The work of Barlow and Macdonald is thus the most realistic in its treatment of interactions for the single-image model for ionic adsorption. These authors have also considered the related problem of the change in work function resulting from the adsorption of polarizable ions [17]. The effect of induced dipoles was included here in a self-consistent way; cf. the discussion in Chapter 2 on the representation of interfacial

fields.

(ii) Ions Imaged Conductively in the Metal and Diffuse Layer

The earliest attempt at calculating the discreteness-of-charge effect was that of Ershler [18], who considered multiple reflections of adsorbed anions on the metal surface and the outer Helmholtz plane (o.H.p). The concentration of the electrolyte was assumed to be sufficiently high that the diffuse-layer charge could be considered as localised on the o.H.p.. A similar assumption was made in the work of Levine, Bell and Calvert [19], but within the adsorption plane, each ion was represented (following Grahame [63]) as a "cut-off disc" of radius r_0 determined by the condition $\pi r_0^2 \sigma = e_0$, where σ is the average adsorbed charge density (in the inner Helmholtz plane (i.H.p.)) and e_0 is the charge of each ion. The energy of interaction was found by increasing e_0 to its final value using a Guntelberg charging process. The configurational part of the isotherm, expressed by the relationship between r_0 and σ, is evidently the same as that in the single-image approaches by Bockris and co-workers [1,5-7] considered in section (i). The image potential obtaining at the site of a single ion is given by the expression

$$\phi = (2\pi\sigma/\varepsilon_1)[r_0 + 2\sum_1^\infty (-1)^n[(r_0^2+n^2d^2)^{1/2}-nd]] \qquad [33]$$

where ε_1 is the dielectric constant of the inner layer and d is its thickness. The summation of the series was effected using the Poisson Summation Formula.

The assumption of a continuous layer of adsorbed charges was abandoned by Barlow and Macdonald [20] who expressed the total coulombic potential resulting from simultaneous conductive

imaging as a triply-infinite series of point-charge potentials. As in their previous treatment of the single-imaging situation, an analytical transformation is used to accelerate the convergence, based on a method developed by Ewald [21] for the calculation of Madelung constants of ionic crystals. The analysis required to establish this transformation is interesting but exceedingly involved, and space does not permit a detailed discussion here; interestingly, however, a result rather similar to the Poisson Summation Formula does appear in one of the steps (see Appendix II of ref. 20).

As pointed out by Levine et al. [22], the disadvantage with the lattice approach which forms the basis of the work of Barlow and Macdonald, is that, in addition to the assumption that the diffuse layer may be treated as a perfect conductor, their work assumes that the ion distribution in the i.H.p. is temperature-independent. This is true inasmuch as thermal motion effects within the ionic lattice are neglected, but the micropotential calculations could nevertheless be used to set up expressions for the chemical potential of adsorbed ions; the equilibrium condition applied to the adsorption process would result in a coverage which would depend on the magnitude of the total coulombic interaction energy with repect to the mean thermal energy, and would thus be temperature-dependent. The use of the micropotential calculations in the construction of ionic adsorption isotherms was not considered by Barlow and Macdonald but in subsequent work [23] they did, however, consider the conditions under which such an adsorbed ionic lattice would be thermally stable. The point which Levine et al. were referring to

was that the extent to which images could be induced in the diffuse layer, was assumed to be temperature-independent. The effect of thermal disordering is implied by the use of a linearized Poisson-Boltzmann equation to describe the potential distribution in the diffuse double layer; in such a case, the ions would thus be assumed to induce images in an imperfectly-conducting diffuse layer.

The solution of the linearized Poisson-Boltzmann equation in cylindrical polar coordinates was carried out by Stillinger [24] as part of an investigation of the work involved in compression of a spherical ionic atmosphere into a hemisphere. This paper derives a number of interesting formulae, and gives an illuminating heuristic argument showing how the Bessel functions arise naturally in problems of this type, from physical considerations.

The refinement of a discontinuity of the dielectric constant between the compact and diffuse regions of the double layer was introduced into such calculations by Buff and Stillinger [25], and again the potential distribution was determined using Fourier-Bessel integrals. However, rather than assuming a lattice model for the purposes of calculating the interaction energy required by the isotherm, the authors applied cluster integral expansions in terms of two-dimensional pairwise correlation functions. As Barlow and Macdonald pointed out [14], this approach is appropriate for a system exhibiting a low degree of long-range order, and higher-order correlations should be taken into account. The use of cluster integral expansions was

continued by Hurwitz [26], who approximated the Fourier-Bessel integrals for the potential by the first two terms in their expansions. Expressions for the excess free energy of adsorption were given in terms of the pairwise distribution functions for the adsorbed layer, these in turn being expressed as power series in the density of adsorbed ions. This is an alternative to the Debye-Hueckel approach used by Levine and coworkers [22], and comparisons with the cut-off disc and ionic lattice approaches were given, with respect to the calculation of the excess free energy of adsorption. A fundamental objection which can be raised to this type of treatment is that the cluster-integral or virial expansion is known [27] to be divergent for densities approaching those of condensed phases; this should be true a fortiori for systems with long-range interactions such as the coulombic potential. Nevertheless, this work is of interest in that it anticipates, to some extent, the more recent approaches to double-layer structure based on integral equations of the theory of dense fluids.

A Fourier-Bessel integral analysis of adsorbed ionic imaging in an imperfectly conducting diffuse layer was also undertaken by Kir'yanov [28]. The potential distribution in both phases was assumed to be given by a Poisson equation, viz.

$$\nabla^2\psi_1 = -(4\pi/\varepsilon_1)e_0\delta(z)\delta_{n,m}\delta(x-x_{m,n})\delta(y-y_{m,n}) \qquad [34]$$

in the compact double layer, where the ions are located in the plane at points $(x_{m,n}, y_{m,n})$ and δ represents the Dirac delta function, and

$$\nabla^2\psi_2 = \kappa^2\psi_2 \qquad [35]$$

for the diffuse layer, where κ represents the Debye reciprocal

length. The Bessel functions in the potential distribution are derived by application of the identity

$$\delta(x)\delta(y) = \delta(\rho)/2\pi\rho = (1/2\pi)\int_0^\infty J_0(k\rho)kdk,\ \rho = (x^2+y^2)^{1/2} \quad [36]$$

The lattice sum over all possible values of the coordinates m,n is approximated by an integration:

$$\sum_{m,n} J_0(k\rho_{m,n}) = 2\pi\theta\Gamma^\infty \int_{r0}^\infty J_0(kx)xdx \quad [37]$$

where Γ_∞ is the limiting value of the adsorbed ion density. In other work of a similar nature originating from the Soviet school [29], the resulting Fourier-Bessel integrals are transformed into infinite series of K_0 Bessel functions, by means of formulae such as

$$\int_0^\infty dk\ J_0(k\rho)\sinh(kz)/\cosh(ka) = 2\sum_1^\infty K_0[(2n+1)\pi\rho/2a] \times \sin[(2n+1)\pi z/2a]/a\sin[(2n+1)\pi/2] \quad [38]$$

of which the derivation is to be found in ref. 12, p.146. This expression is much more computationally useful for large values of ρ than the integral itself, and the summation wih respect to the lattice coordinates can be carried out explicitly, with the lattice parameter of the assumed hexagonal lattice being given in terms of the coverage by $(\Gamma_\infty\sqrt{3}/2)^{1/2}$. This potential problem has arisen in the course of consideration of a number of interfacial phenomena, notably competitive ion adsorption [30], effects of ionic adsorption on the kinetics of electrode reactions [31,32], formation of ion pairs at a metal surface [33], double layer effects on faradaic impedance of an electron-transfer reaction [34], and adsorption isotherms for surface-active compounds with permanent dipole moments [29,35].

(iii) Ions Imaged Conductively in the Metal and Dielectrically in the Diffuse Layer

The treatment of the diffuse double layer as a semi-infinite dielectric continuum, rather than as a perfect or imperfect conductor is considerably less popular than the models considered in the previous two categories. It is, however, worthy of consideration, not only in view of the well-known inconsistencies of the Poisson-Boltzmann equation (see, e.g. ref. 5 vol. 1), but as a limiting case which might be approached in the limit of very low electrolyte concentrations, near the potential of zero charge.

The most comprehensive analysis of this model was again given by Macdonald and Barlow [36], who constructed an image series of point charges of alternating signs and magnitude β^n, where β is the depolarization factor $(\varepsilon_2-\varepsilon_1)/(\varepsilon_2+\varepsilon_1)$, $\varepsilon_2,\varepsilon_1$ are the respective dielectric constants of the compact and diffuse regions, and n describes the order of each electrostatic reflection. The induced potential and field in the compact double layer were conveniently expressed in terms of the corresponding quantities for the single-imaging model treated by the same authors in ref. 14.

The conductive-dielectric imaging model was first considered by Buff and Stillinger [25] and subsequently by Bockris and Habib [37] in terms of Fourier-Bessel integrals. In order to deduce the potential due to all charges induced in the metal and the dielectric continuum, the potential was assumed to be of the form

$$V_1 = (e_0/\varepsilon_1)\int_0^\infty [e^{-k|z|}+f_1(k)e^{kz}+f_2(k)e^{-kz}]J_0(k_\rho)dk \qquad [39]$$

in the compact double layer $(-s\leq z\leq z_1)$ of dielectric constant ε_1,

and for the diffuse layer ($z_1 \leq z < \infty$) of dielectric constant ε_2,

$$V_2 = (e_0/\varepsilon_2)\int_0^\infty f_3(k)e^{-kz}J_0(k\rho)dk \qquad [40]$$

The second and third terms in the definition of V_1 are clearly the total contributions of image charges to the potential in the compact double layer, and the potential V_2 is that due to the charge located at z=0, but screened by the polarization-induced at the dielectric boundary. The expressions for $f_1(k)$ and $f_2(k)$, which satisfy the boundary conditions

$$V_1 = 0 \qquad (z = -s)$$

$$V_1 = V_2 \qquad (z = z_1)$$

$$\varepsilon_1 \partial V_1/\partial z = \varepsilon_2 \partial V_2/\partial z \qquad (z = z_1) \qquad [41]$$

were determined to be

$$f_1(k) = -\beta_1 e^{-2kz_1}(1-e^{-2ks})/[1-\beta_1 e^{-2k(s+z_1)}]$$

$$f_2(k) = [-e^{-2ks}+\beta_1 e^{-2k(s+z_1)}]/[1-\beta_1 e^{-2k(s+z_1)}] \qquad [42]$$

$$\beta_1 = (\varepsilon_2-\varepsilon_1)/(\varepsilon_2+\varepsilon_1)$$

This result was then used to work out the energy experienced by each charge due to interaction with the images induced by it. The second part of the paper is devoted to the construction of an isotherm for ionic adsorption, in essentially the same manner as previously [5-7], viz. considering the energy of interaction U_{rep} between the central ion and the concentric rings of charge-image pairs:

$$U_{rep} = (3\pi^{1/2}e_0^2\theta^{1/2}/(\varepsilon_1 r_i))\sum_1^\infty[1-(1+\pi\theta/4n^2)^{-1/2}] \qquad [43]$$

where r_i is the ionic radius. The inclusion of only primary image energies in this equation seems at first inconsistent with the previous analysis of infinite imaging; the arguments presented by Bockris and Habib in justification of this will be considered in

the next section.

(iv) Anisotropy of Inner-Layer Dielectric Constant

The first thorough investigation of the implications of a variable dielectric constant $\varepsilon_1(z)$ in the compact double layer was carried out by Buff et al. [38,39], the specific problem considered being the contribution of such anisotropy to the image energy of charges at diffuse interfaces. The potential at the point $\mathbf{R}$ due to a charge located at $\mathbf{R}'$ is given by the Poisson equation, which in the case of variable ε assumes the form

$$\nabla.(\varepsilon\mathbf{E}) = \varepsilon\nabla.\mathbf{E} + \mathbf{E}.\nabla\varepsilon = -4\pi\delta(\mathbf{R}-\mathbf{R}'); \quad \mathbf{E} = -\nabla\phi \qquad [44]$$

In order to solve this equation for ϕ, one again uses a Fourier-Bessel integral representation; in this case, however, the problem reduces to a differential equation for the coefficient functions, rather than a pair of simple algebraic equations as in the calculations considering ε to be constant.

Subsequent considerations of discreteness-of-charge effects by Levine et al. also assumed a dielectrically non-uniform compact layer. In ref. 40, the compact layer was divided into two regions of different dielectric constants, each lower than that in the diffuse layer. In addition to the screening effect if the diffuse layer charge density, the thermal motion of the other adsorbed ions is taken into account by using a two-dimensional Boltzmann distribution law in the vicinity of a given ion. The potential distribution in the two-dimensional ionic cloud surrounding the ion in the i.H.p. was shown to satisfy an integral equation. This work was extended [41] to consider the more general case where the dielectric constant is assumed to vary continuously with normal distance z; an empirical function

originally suggested by Buff et al. [38] was chosen:

$$\epsilon_1(z) = \epsilon_0 \cosh^2 s_1(z-s) \text{ for } -s<z<0$$
$$= \epsilon \cos^2 s_2(z_1-z) \text{ for } 0<z<z_1 \quad [45]$$

The electrode surface is, as before, the plane z = -s, with the ions located at z = 0. The constants s_1 and s_2 were selected so as to ensure the continuity of ϵ_1 and its normal derivative at z = 0; ϵ_1 varies sigmoidally from its minimum value ϵ_0 at the electrode surface to the bulk value ϵ at the o.H.p.. A comparison was made between the discreteness-of-charge potentials calculated with a continuous variation of dielectric constant and using the earlier assumption of a discontinuity within the compact layer [40], and it was concluded that the two models predict similar values.

The dielectric-conductive imaging calculation discussed in category (iii) was used by Bockris and Habib [37] as part of an investigation of dielectric anisotropy effects in the compact double layer. In contrast to the treatments mentioned above, which attempted an analytical solution of the Laplace or Poisson equations with an assumed continuous variation of ϵ as a function of z, the field in the diffuse layer was described by a generalization of the Poisson-Boltzmann equation with variable ϵ, with ϵ in turn defined in terms of field using an empirical equation due to Grahame [42]. This equation was transformed into a Volterra integral equation and solved parametrically, thus providing the electric field and dielectric constant as a function of distance, the latter being represented by an empirical polynomial.

In order to calculate the imaging energy of an adsorbed ion, the inner region was assumed first to be composed of layers of different dielectric constants, and finite thickness. Conditions of continuity of potential and dielectric displacement were applied across each dielectric boundary; the imaging energy was thus calculated for an ion in the presence of the perfectly conducting metal surface and two, three, four and five dielectric slabs. The consideration of imaging in a region with continuous variation of dielectric constant was effected by considering the solution obtained for finite numbers of dielectric slabs in the limit of an infinite number of slabs of infinitesimal thickness, combined with the empirical representation of ε determined first. It was concluded that (a) the diffuse dielectric boundary gives an imaging energy about 40 times less than the corresponding energy for a sharp dielectric boundary, and (b) the imaging energy for a diffuse dielectric boundary is only 1% more than that considering only primary imaging in the metal. This calculation thus provided the justification for the inclusion of only primary images in the construction of the adsorption isotherm.

(v) Comparison

It is evident that, even within the limits of primitive double-layer models, there exists a considerable diversity of treatments of the imaging energy experienced by adsorbed ions. The natural question of whether the diffuse double layer is more realistically treated as a dielectric or as an imperfect conductor is difficult to answer, principally because of the lack of coincidence between the conditions under which the equations

admit analytical solutions, and those under which they provide a physically realistic description of the system. (Of course, this question remains in spite of the fact that, as shown in Chapter 4, the effects of diffuse layer ions on the potential distribution in the compact layer is small, provided the dielectric constant of the diffuse layer is assumed to be sufficiently large.) Thus, the linearization of the Poisson-Boltzmann equation is valid only in the limit of small values of the diffuse-layer potential drop, which restricts the values of not only the potential applied to the electrode (with respect to the p.z.c), but also the extent of adsorption, since the adsorbed charge as well as that residing on the electrode must be balanced by that in the diffuse layer. Under the other conditions where the diffuse layer potential drop would be small, viz. high concentration of supporting electrolyte, the neglect of ionic interactions renders the Poisson-Boltzmann equation unrealistic from a statistical-mechanical point of view. Furthermore, as pointed out by several authors [5,43], the solution of the unlinearized equation (which is apparently impossible in cylindrical coordinates), would not provide a fundamentally more realistic description, because of the implied non-linear charge-potential relationship. Under conditions where the dielectric model of the double layer is to be preferred, viz. those of low electrolyte concentrations, the diffuse-layer potential drop is more likely to be significant, without the additional restriction to potentials close to the p.z.c..

It is much easier to criticize the use of dielectric

constants as being fundamentally inconsistent with a molecular picture of the double layer, than it is to provide a reasonable alternative. Assuming, for the present purpose of assessing the existing theoretical approaches, that use of dielectric constants is justified, it is pertinent to consider the physical basis of the functions proposed to describe the variation of ε with distance. The major objection which can be raised to the assumption that the anisotropy is independent of the local electric field as a function of distance z from the metal surface is that this implies that purely "chemical" forces are responsible, which is unlikely if the dielectrically non-uniform region is proposed to extend over several molecular thicknesses. Thus, the need for introducing the variation of ε in a self-consistent way is indicated.

The work of Bockris and Habib [37] addressed this point to a certain exent, but in calculating the variation of dielectric constant with distance they assumed an ionic concentration of 0.1 mol/l, which is high enough to suggest that a conductive-imaging treatment would be more appropriate to describe the behaviour of the diffuse layer. In other words, it seems rather inconsistent to consider the effect of the diffuse-layer ions on the dielectric constant but not on the imaging energy of the adsorbed ions. Further, the effect of the adsorbed ions on the potential distribution in the diffuse layer was not considered. The need for a treatment of interfacial polarization which includes calculation of both free and bound charge densities, in an electrostatically and statistical-mechanically consistent manner, was noted even in the early treatments of dielectric anisotropy

by Buff et al., but this been achieved only recently [9].

The deviations of the metal from behaviour as a perfect conductor have received relatively little attention in the electrochemical context. It was shown by Newns [44] that the use of a linearized Fermi-Thomas equation to describe polarization of a metal surface by an adjacent point charge, results in considerable deviations from the classical image interaction energy. The linearized Fermi-Thomas equation also formed the basis of several adsorption calculations by authors of the Soviet school [45,46], and subsequently, the use of more realistic dielectric response functions to describe such non-classical effects was considered by Kornyshev [47] and Kohn and Lang [48]. In all these contributions, however, the space-charge layer at the metal surface is considered to be bounded by a plane. The consequences of diffuseness of electron charge distribution close to the metal surface have been considered recently, by Badiali et al. [49] and by Schmickler [50] with regard to capacitance behaviour, in the absence of ionic adsorption.

3. Treatment of Interactions using the Mean Field Approximation

The long-range nature of the coulombic forces (and in particular of those arising from ions bearing complete electronic charges) renders a nearest-neighbour pairwise interaction approach to the interaction problem, such as that developed in Chapter 4, entirely inadequate. On the other hand, extension of the Guggenheim quasichemical isotherm to include explicitly non-nearest-neighbour interactions results in expressions of unmanageable complexity. The compromise indicated is thus to

consider explicitly the free energy of nearest neighbour pairwise interactions, and to treat the non-nearest-neighbour interactions using the Mean Field Approximation (MFA), which is tantamount to the assumption that the non-nearest neighbours of a given species are distributed randomly in spite of interactions. This is the approach used by Schmickler [51] in his recent Monte-Carlo simulation study of dipole-dipole interactions in a plane lattice of point dipoles polarized by an external field.

The ionic adsorption problem requires the calculation of the micropotential and the associated field, viz. the field and potential at a given site of an hexagonal lattice occupied by ions and dipoles, which are imaged conductively in the metal and dielectrically in the diffuse layer, is the subject of this section, and the Appendix, in which the mathematical details are presented. These fields and potentials will in turn be used to define an effective field and potential, with components proportional to the coverage fraction θ (due to ions) and the dimensionless average normal dipole moment $\langle s \rangle$ (due to the dipoles), in terms of which the electrical partition functions of the adsorbed species will be defined. As discussed below in Section 3.6, such an explicit inclusion of the dipole component of the effective potential avoids the need to attentuate the ionic field and potential by the factor $1/\varepsilon_1$, in order to express the screening effect due to the dipoles.

Before proceeding to the details of these field and potential calculations, it is appropriate to consider the relationship between the MFA, which gives rise to interaction energies proportional to θ (i.e. isotherms of the Frumkin type

[52]) and other approaches [5-7] which propose interaction energies given as polynomials in $\theta^{1/2}$.

The nature of the approximation inherent in the "$\theta^{1/2}$" treatments is expressed neatly in an interesting derivation of the relation $\langle r \rangle \propto \theta^{-1/2}$, presented by Barlow and Macdonald [53] in the course of a comprehensive review of micropotential calculations. The probability density P(r), such that the probability that the nearest neighbour to a given particle is located between r and r+dr is P(r)dr, is shown to satisfy the differential equation

$$(d/dr)\int_0^r P(x)dx = 2\pi rn[1 - \int_0^r P(x)dx] \qquad [46]$$

in which n is the average number of particles per unit area. On integration, there results

$$\int_0^r P(x)dx = 1 - \exp(-\pi r^2 n)$$

$$P(r) = 2\pi r.\exp(-\pi r^2 n) \qquad [47]$$

so that the mean distance $\langle r \rangle$ is given by

$$\langle r \rangle = \int_0^\infty rP(r)dr = 2\pi n\int_0^\infty r^2\exp(-\pi r^2 n)dr = 1/2n^{1/2} \qquad [48]$$

which is clearly equivalent to the identification $\langle r \rangle \propto 1/\theta^{1/2}$, used in in the construction of isotherms. From eqn. 46, it is clear that the assumption of random distribution (and hence the absence of interactions) is necessary to obtain the probability $n.2\pi rdr$ that the nearest neighbour is located in the annular element between r and r+dr. The question now arises: "Why does the assumption of randomness give rise to interaction energies depending on θ in some approaches, but on $\theta^{1/2}$ in others?"

In addressing this question it is to be observed first that the ionic adsorption isotherms employing $\theta^{-1/2}$ as a measure of

<r> arise from the approximation of an exact charge-image potential, such as that in eqn. 43, by the leading terms in its binomial expansion. The numerical validity of such an approximation has been considered by Levine (quoted by Bockris and Habib in ref. 37); for present purposes, however, it is desirable to examine the summation of the exact potential in order to determine whether or not this dependence on θ is merely an artefact of the approximation. This requires the summation of the slowly-convergent series

$$\sum_1^\infty [1 - (1+a^2/n^2)^{-1/2}] = \sum_1^\infty [1 - n/(a^2+n^2)^{1/2}] \qquad [49]$$

where $a^2 = \pi\theta/4$, which may be effected by the Laplace Transform Technique [59].

The summand in eqn. 49 can be identified as the Laplace Transform of the function $aJ_1(at)$, defined by

$$\int_0^\infty e^{-nt}.aJ_1(at)dt = 1 - n/(n^2+a^2)^{1/2} \qquad [50]$$

Therefore

$$\begin{aligned}\sum_1^\infty [1 - n/(n^2+a^2)^{1/2}] &= \sum_1^\infty \int_0^\infty e^{-nt} aJ_1(at)dt \\ &= \int_0^\infty \sum_1^\infty e^{-nt} aJ_1(at)dt \\ &= \int_0^\infty dt\ aJ_1(at)/(e^t-1) \qquad [51]\end{aligned}$$

The summation of the series is thus reduced to the evaluation of the integral 51. A variety of numerical techniques may be employed, but the most appropriate of these is based on the observation that, because the function $J_1(at)$ is expansible in odd powers of its argument, the integral can be expressed as an infinite series of Riemann zeta functions of even argument, for which closed-form representations are available in terms of the Bernoulli numbers. With [12]

$$J_1(at) = \sum_0^\infty (-1)^k (at/2)^{2k+1}/k!^2(k+1) \qquad [52]$$

one has

$$a\int_0^\infty dt J_1(at)/(e^t-1) = a\sum_0^\infty [(-1)^k(a/2)^{2k+1}/k!^2(k+1)]\int_0^\infty dt\, t^{2k+1}/(e^t-1)$$
$$= a\sum_0^\infty [(-1)^k(a/2)^{2k+1}/k!^2(k+1)].(2k+1)!\zeta(2k+2)$$
$$= \sum_0^\infty [(-1)^k(a/2)^{2k+2}/(k+1)!^2].2^{2k+1}\pi^{2k+2}B_{k+1} \qquad [53]$$

where the Bernoulli numbers B_k are defined by the expansion

$$x/(e^x-1) = 1 - x/2 + B_1x^2/2! - B_2x^4/4! + B_3x^6/3! -\ldots \quad |x|<2\pi \qquad [54]$$

The use of the expansion 53 to calculate the integral is equivalent to the method used in the construction of the isotherm of Wroblowa and Kovac, but with the inclusion of all terms in the expansion of the square root instead of just the first two.

The integral 51 is shown as a function of Θ in Fig. 4, along with the first few polynomial approximants

$$p_n = \sum_1^n c_k a^{2k} \qquad [55]$$

where

$$c_1 = \pi^2/12$$
$$c_2 = -\pi^4/240$$
$$c_3 = \pi^6/3024$$
$$c_4 = -\pi^8/34560$$
$$c_5 = \pi^{10}/1900800$$

This figure gives the ranges of Θ for which each approximation is accurate. Thus p_1 may be used below $\Theta = 0.1$, p_2 below 0.23, p_3,p_4 below 0.4 and p_5 below 0.55. The calculations of Wroblowa and Kovac [7] were based on a two-term approximation to the sum (i.e. p_2); inasmuch as experimentally observed ionic coverages are less than about 0.2, this seems reasonable, but if the complete sum were to be used in calculating the interaction energy (i.e. in

Fig. 4: Evaluation of

$$\sum_1^\infty [1 - n/(n^2+a^2)^{1/2}] = \int_0^\infty dt\, J_1(at)/(e^t-1),\ a^2 = \pi\theta/4$$

compared with various polynomial approximants.

Curve 0: complete sum

Curve 1: p_1

Curve 2: p_2

Curve 3: p_3

Curve 4: p_4

Curve 5: p_5

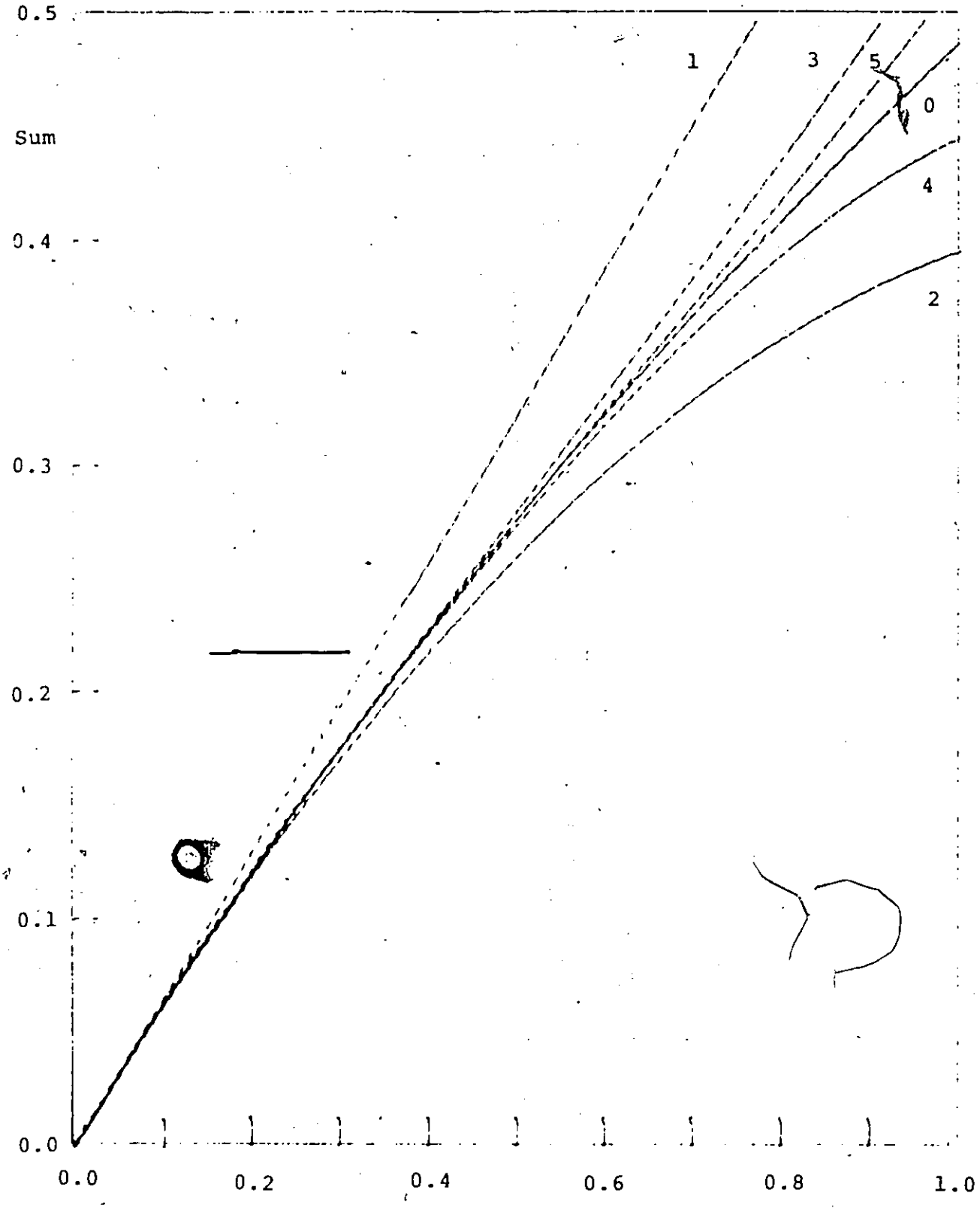
0.5
Sum
0.4
0.3
0.2
0.1
0.0
0.0
0.2
0.4
0.6
0.8
1.0
θ
1
3
5
0
4
2

the argument of the exponential term of the adsorption isotherm), different values of θ might be predicted.

In the isotherm eqn. 43, the energy is given by the product of the sum and a term proportional to $\theta^{1/2}$. Interestingly, the sum exhibits a linear log-log plot in the range $0.02 \leq \theta \leq 0.6$, with a slope of approximately 0.95; thus, the total interaction energy for such intermediate values of θ is approximately proportional to $\theta^{3/2}$, in contradistinction to Frumkin-type treatments giving rise to interaction energies proportional to θ^2 (and hence chemical potentials linear in θ) The inconsistency appears to arise from the way in which the interactions are counted for a given value of θ. Thus, having assumed a random distribution of particles in order to obtain the relationship $\langle r \rangle \propto \theta^{-1/2}$, the isotherms of the "$\theta^{1/2}$" type then assume a regular arrangement (viz., adsorbed ions in concentric rings) for the purposes of calculating the total interaction energy experienced by each adsorbed ion.

In other words, one has the paradoxical situation in which an assumption of random distribution is combined with the opposite assumption of long-range periodicity in the location of the ions. Of course, the very existence of interactions is ipso facto inconsistent with random distribution, but with the MFA, it is not necessary to assume a long-range periodicity in the positions of the ions, even though a lattice model is being adopted. Accordingly, the total potential due to ions is expressed as the fraction θ of the corresponding potential for $\theta = 1$. Explicit inclusion of the field and potential contributions due to adsorbed dipoles is far more readily achieved with MFA;

these are simply $1-\theta$ times the field and potential for $\theta = 0$.

Summarizing, it can be stated that the two approaches are equally unrealistic in assuming a random distribution of adsorbed species in spite of interactions, which (as will be seen presently) are very large. However, the MFA is to be preferred, since its use does not require the additional assumption of a long-range periodicity in the ionic positions in order to sum the long-range Coulombic interactions over the surface.

3.1 Potential due to Adsorbed Ions

Considering an ion adsorbed on a site of an hexagonal lattice with parameter r_0 (cf. Fig. 6 of Chapter 4, facing page 94), it is required to find the potential obtaining at a neighbouring lattice site as a function of the vertical coordinate z. The compact double layer is bounded by the planes $z = -s$ and $z = z_1$, and the centres of the spherical anions are assumed to be located in the plane $z = 0$. The potential consists of an infinite superposition of image charge potentials, which can be regarded as discrete if the diffuse double layer is approximated by a dielectric or a perfect conductor, but which are line distributions if ionic screening effects are considered. The identities required to obtain the image series from the coefficient functions in the Fourier-Bessel integrals are summarized in Table 1; they may readily obtained from tables, or by appropriately differentiating eqn. 21 with respect to z. At a point with cylindrical coordinates (ρ,z), the potential due to a single ion at the origin is, using eqns. 42,

$$-e_0([\rho^2+z^2]^{-1/2} - [\rho^2+(z+2s)^2]^{-1/2})$$

$$+ \int_0^\infty [f_1(k)e^{kz} + f_2(k)e^{-kz} + e^{-2ks-kz}]J_0(k\rho)dk) \qquad [56]$$

where the term

$$-\int_0^\infty e^{-2ks-kz}J_0(k\rho)dk = -[\rho^2+(z+2s)^2]^{-1/2}$$

corresponding to the primary image at z=-2s has been subtracted from $f_2(k)$. Assuming that β is independent of k, expansion and termwise integration provides

$$\int_0^\infty [f_1(k)e^{kz} + f_2(k)e^{-kz} + e^{-2ks-kz}]J_0(k\rho)dk$$
$$= \sum_1^\infty \beta^j([\rho^2+(2jd+z)^2]^{-1/2} + [\rho^2+(2jd-z)^2]^{-1/2}$$
$$- [\rho^2+(2jd+2s+z)^2]^{-1/2} - [\rho^2+(2jd-2s-z)^2]^{-1/2}) \qquad [57]$$

In order to sum the potential contributions for the whole lattice, each square root term is written in the form

$$[\rho^2+z'^2]^{1/2} = [r_0^2(k^2-km+m^2)+z'^2]^{1/2}$$
$$= r_0[(m-k/2)^2+3k^2/4+(z'/r_0)^2]^{1/2} \qquad [58]$$

where

$$z' = 2jd+s\pm s\pm z$$

and summed over all values of m and k except k=m=0 (i.e. excluding the contribution of the ion at the origin), so that the potential at the origin of such a lattice of adsorbed ions is

$$b_3 = (-e_0/r_0).[2\sum_1^\infty\sum_{-\infty}^\infty([(m-k/2)^2+a_-^2]^{-1/2}-[(m-k/2)^2+a_+^2]^{-1/2})$$
$$+ 2\sum_1^\infty([m^2+z^2/r_0^2]^{-1/2} - [m^2+(z+2s)^2/r_0^2]^{-1/2})]$$
$$+ (-e_0/r_0).\sum_1^\infty\beta^j[2\sum_1^\infty\sum_{-\infty}^\infty([(m-k/2)^2+p_+^2]^{-1/2}-[(m-k/2)^2+q_+^2]^{-1/2}$$
$$+ [(m-k/2)^2+p_-^2]^{-1/2}-[(m-k/2)^2+q_-^2]^{-1/2})$$
$$+ 2\sum_1^\infty([m^2+(2jd+z)^2/r_0^2]^{-1/2} - [m^2+(2jd+2s+z)^2/r_0^2]^{-1/2}$$
$$[m^2+(2jd-z)^2/r_0^2]^{-1/2} - [m^2+(2jd-2s-z)^2/r_0^2]^{-1/2})] \qquad [59]$$

where the dimensionless quantities $a_\pm$, $p_\pm$ and $q_\pm$ are defined by

$$a_\pm^2 = 3k^2/4 + (z+s\pm s)^2/r_0^2$$
$$p_\pm^2 = 3k^2/4 + (2jd\pm z)^2/r_0^2$$
$$q_\pm^2 = 3k^2/4 + (2jd\pm 2s\pm z)^2/r_0^2$$

TABLE 1

Fourier-Bessel Integrals arising in Image-Potential Expansions

$$\int_0^\infty J_0(k\rho)e^{-kz}dk = 1/[\rho^2+z^2]^{1/2}$$

$$\int_0^\infty kJ_0(k\rho)e^{-kz}dk = -(\partial/\partial z)\int_0^\infty J_0(k\rho)e^{-kz}dk = z/[\rho^2+z^2]^{3/2}$$

$$\int_0^\infty k^2J_0(k\rho)e^{-kz}dk = (\partial^2/\partial z^2)\int_0^\infty J_0(k\rho)e^{-kz}dk$$

$$= 3z^2/[\rho^2+z^2]^{5/2} - 1/[\rho^2+z^2]^{3/2}$$

3.2 Field due to Adsorbed Charges

The potential given by eqn. 59 has field components in ρ and z directions. By symmetry, the radial components cancel when summed over the entire lattice, so that the quantity of importance is the normal component. By differentiation of eqn. 59 with respect to z,

$$b_1 = (-e_0/r_0^2).[2\sum_1^\infty\sum_{-\infty}^{\infty}([(m-k/2)^2+a_-^2]^{-3/2}.z/r_0 - [(m-k/2)^2+a_+^2]^{-3/2}.(z+2s)/r_0)$$
$$+ 2\sum_1^\infty([m^2+z^2/r_0^2]^{-3/2}.z/r_0 - [m^2+(z+2s)^2/r_0^2]^{-3/2}.(z+2s)/r_0)]$$
$$+(-e_0/r_0^2).\sum_1^\infty\beta^j[2\sum_1^\infty\sum_{-\infty}^{\infty}([(m-k/2)^2+p_+^2]^{-3/2}.(2jd+z)/r_0$$
$$-[(m-k/2)^2+q_+^2]^{-3/2}.(2jd+2s+z)/r_0+[(m-k/2)^2+p_-^2]^{-3/2}.(2jd-z)/r_0$$
$$-[(m-k/2)^2+q_-^2]^{-3/2}.(2jd-2s-z)/r_0)$$
$$+ 2\sum_1^\infty([m^2+(2jd+z)^2/r_0^2]^{-3/2}.(2jd+z)/r_0$$
$$- [m^2+(2jd+2s+z)^2/r_0^2]^{-3/2}.(2jd+2s+z)/r_0$$
$$+ [m^2+(2jd-z)^2/r_0^2]^{-3/2}.(2jd-z)/r_0$$
$$- [m^2+(2jd-2s-z)^2/r_0^2]^{-3/2}.(2jd-2s-z)/r_0)] \qquad [60]$$

3.3 Potential due to Adsorbed Dipoles

The potential at the point (0,0,z) due to a dipole of vector moment **m** is $\mathbf{m}.\mathbf{r}/r^3$, where **r** is the displacement vector from the position of the dipole to the field point. For a single dipole inclined at an angle θ with respect to the normal direction and located at a point $(\rho,0,0)$,

$$\mathbf{r} = (0,0,z) - (\rho,0,0) = (-\rho,0,z)$$

$$\mathbf{m} = m(\sin\theta,0,\cos\theta)$$

so that

$$\mathbf{m}.\mathbf{r}/r^3 = (-m\rho\sin\theta+mz\cos\theta)/(\rho^2+z^2)^{3/2} \qquad [61]$$

For the primary image dipole located at the point $(\rho,0,-2s)$

$$\mathbf{m} = m(-\sin\theta,0,\cos\theta)$$

$$\mathbf{r} = (-\rho, 0, z+2s)$$

$$\mathbf{m}.\mathbf{r}/r^3 = [-m\rho\sin\theta+(z+2s)\cos\theta]/[\rho^2+(z+2s)^2]^{3/2} \qquad [62]$$

When the orientations of all the dipoles are averaged over the surface, $\langle\sin\theta\rangle=0$ and $\langle\cos\theta\rangle=\langle s\rangle$, so that the potential due to all such dipole-primary image pairs is

$$(m\langle s\rangle/r_0^2).[2\sum_1^\infty\sum_{-\infty}^{\infty}([(m-k/2)^2+a_-^2]^{-3/2}.z/r_0 + [(m-k/2)^2+a_+^2]^{-3/2}.(z+2s)/r_0) + 2\sum_1^\infty([m^2+z^2/r_0^2]^{-3/2}.z/r_0+[m^2+(z+2s)^2/r_0^2]^{-3/2}.(z+2s)/r_0)] \qquad [63]$$

According to the analysis presented in Chapter 4, the total potential induced by such a dipole is

$$m\cos\theta\int_o^\infty[F_1(k)e^{kz}+F_2(k)e^{-kz}]kJ_0(k\rho)dk + m\sin\theta\cos\phi\int_o^\infty[G_1(k)e^{kz}+G_2(k)e^{-kz}]kJ_1(k\rho)dk \qquad [64]$$

where

$$F_1(k) = -\beta e^{-2kz_1}(1+e^{-2ks})/[1-\beta e^{-2k(s+z_1)}]$$

$$F_2(k) = (e^{-2ks}+\beta e^{-2k(s+z_1)})/[1-\beta e^{-2k(s+z_1)}]$$

$$G_1(k) = -\beta e^{-2kz_1}(1-e^{-2ks})/[1-\beta e^{-2k(s+z_1)}]$$

$$G_2(k) = (e^{-2ks}+\beta e^{-2k(s+z_1)})/[1-\beta e^{-2k(s+z_1)}]$$

If the sine and cosine of the angle θ be again identified with their average values for the layer, the integral involving $J_1(k\rho)$ disappears. After subtraction of the term e^{-2ks} from $F_2(k)$ (the primary image contribution) the series of secondary image potentials is

$$\int_o^\infty[F_1(k)e^{kz}+F_2(k)e^{-kz}-e^{-kz-2ks}]kJ_0(k\rho)dk = \sum_1^\infty\beta^j([\rho^2+(2jd+z)^2]^{-3/2}.(2jd+z)-[\rho^2+(2jd-z)^2]^{-3/2}.(2jd-z) +[\rho^2+(2jd+2s+z)^2]^{-3/2}-[\rho^2+(2jd-2s-z)^2]^{-3/2}.(2jd-2s-z)) \qquad [65]$$

so that the total potential due to the dipoles and all induced

dipoles is, in the limit of complete polarization (<s>=1)

$$b_4=(m/r_0^2).[2\sum_1^\infty\sum_{-\infty}^\infty([(m-k/2)^2+a_-^2]^{-3/2}.z/r_0 + [(m-k/2)^2+a_+^2]^{-3/2}.(z+2s)/r_0) + 2\sum_1^\infty([m^2+z^2/r_0^2]^{-3/2}.z/r_0 + [m^2+(z+2s)^2/r_0^2]^{-3/2}.(z+2s)/r_0)] + (m/r_0^2).\sum_1^\infty\beta^j[2\sum_1^\infty\sum_{-\infty}^\infty([(m-k/2)^2+p_+^2]^{-3/2}.(2jd+z)/r_0 - [(m-k/2)^2+q_+^2]^{-3/2}.(2jd+2s+z)/r_0+[(m-k/2)^2+p_-^2]^{-3/2}.(2jd-z)/r_0 -[(m-k/2)^2+q_-^2]^{-3/2}.(2jd-2s-z)/r_0) + 2\sum_1^\infty([m^2+(2jd+z)^2/r_0^2.(2jd+z)/r_0 + [m^2+(2jd+2s+z)^2/r_0^2]^{-3/2}.(2jd+2s+z)/r_0 + [m^2+(2jd-z)^2/r_0^2]^{-3/2}.(2jd-z)/r_0 + [m^2+(2jd-2s-z)^2/r_0^2]^{-3/2}.(2jd-2s-z)/r_0)] \quad [66]$$

3.4 Field due to Adsorbed Dipoles

The consideration of the field due to the dipoles in the compact double layer is complicated by the fact that, even in the limit of complete polarization, the radial component of the field will be non-vanishing except in the special case when z=0 (the situation assumed in existing treatments of interactions involving dipoles). The expression for the field at (0,0,z) due to a dipole m located at $(\rho,0,0)$ is $3(\mathbf{m}.\mathbf{r})\mathbf{r}/r^5 - \mathbf{m}/r^3$, where for the dipoles

$$\mathbf{r} = (-\rho,0,z),\ r=(\rho^2+z^2)^{1/2}$$

$$\mathbf{m} = m(\sin\theta,0,\cos\theta)$$

$$3(\mathbf{m}.\mathbf{r})\mathbf{r}/r^5-\mathbf{m}/r^3 = (3/r^5)[m(z\cos\theta-\rho\sin\theta)(-\rho),0,m(z\cos\theta-\rho\sin\theta)z] - (1/r^3)(m\sin\theta,0,m\cos\theta) \quad [67]$$

and for the primary images

$$\mathbf{r} = (-\rho,0,z+2s),\ r=[\rho^2+(z+2s)^2]^{1/2}$$

$$\mathbf{m} = m(-\sin\theta,0,\cos\theta)$$

$$3(\mathbf{m}.\mathbf{r})\mathbf{r}/r^5-\mathbf{m}/r^3$$

$$= (3/r^5)[(m_\rho \sin\theta + m(z+2s)\cos\theta)(-\rho), 0, (m_\theta \sin\theta + m(z+2s)\cos\theta)(z+2s)]$$
$$- m(-\sin\theta, 0, \cos\theta)/r^3 \qquad [68]$$

On summation over the lattice, $\langle\sin\theta\rangle=0$, $\langle\cos\theta\rangle=\langle s\rangle$, and the radial component can again be neglected by symmetry. Therefore the total field at the origin due to all the dipole-primary image pairs is

$$(m\langle s\rangle/r_0^3).[2\sum_1^\infty\sum_{-\infty}^\infty([(m-k/2)^2+a_+^2]^{-5/2}.3(z+2s)^2/r_0^2 - [(m-k/2)^2+a_+^2]^{-3/2} + [(m-k/2)^2+a_-^2]^{-5/2}.3z^2/r_0^2 - [(m-k/2)^2+a_-^2]^{-3/2}) + 2\sum_1^\infty([m^2+z^2/r_0^2]^{-5/2}.3z^2/r_0^2 - [m^2+z^2/r_0^2]^{-3/2} + [m^2+(z+2s)^2/r_0^2]^{-5/2}.3(z+2s)^2/r_0^2 - [m^2+(z+2s)^2/r_0^2]^{-3/2})] \qquad [69]$$

The secondary image dipole field is obtained by differentiating the corresponding potential with respect to z:

$$-(\partial/\partial z)\int_o^\infty[F_1(k)e^{kz}+F_2(k)e^{-kz}-e^{-kz-2ks}]kJ_0(k\rho)dk$$
$$= \int_o^\infty[F_2(k)e^{-kz}-F_1(k)e^{kz}-e^{-kz-2ks}]k^2J_0(k\rho)dk$$
$$= \sum_1^\infty\beta j([\rho^2+(2jd+z)^2]^{-5/2}.3(2jd+z)^2 - [\rho^2+(z+2s)^2]^{-3/2} + [\rho^2+(2jd-z)^2]^{-5/2}.3(2jd-z)^2 - [\rho^2+(2jd-z)^2]^{-3/2} + [\rho^2+(2jd+2s+z)^2]^{-5/2}.3(2jd+2s+z)^2 - [\rho^2+(2jd+2s+z)^2]^{-3/2} + [\rho^2+(2jd-2s-z)^2]^{-5/2}.3(2jd-2s-z)^2 - [\rho^2+(2jd-2s-z)^2]^{-3/2}) \qquad [70]$$

Therefore, the total field at the origin of a lattice of dipoles, in the limit of complete polarization ($\langle s\rangle=1$) is

$$b_2 = (m/r_0^3).[2\sum_1^\infty\sum_{-\infty}^\infty([(m-k/2)^2+a_+^2]^{-5/2}.3(2jd+z)^2/r_0^2 - [(m-k/2)^2+a_+^2]^{-3/2} + [(m-k/2)^2+a_-^2]^{-5/2}.3(2jd-z)^2/r_0^2 - [(m-k/2)^2+a_-^2]^{-3/2}) + 2\sum_1^\infty([m^2+(z+2s)^2/r_0^2]^{-5/2}.3(z+2s)^2/r_0^2 - [m^2+(z+2s)^2/r_0^2]^{-3/2} + [m^2+z^2/r_0^2]^{-5/2}.3z^2/r_0^2 - [m^2+z^2/r_0^2]^{-3/2})]$$

$$+ (m/r_0^3).\sum_1^\infty \beta^j [2\sum_1^\infty \sum_{-\infty}^{\infty} ([(m-k/2)^2+p_+^2]^{-5/2}.3(2jd+z)^2/r_0^2$$
$$- [(m-k/2)^2+p_+^2]^{-3/2} + [(m-k/2)^2+p_-^2]^{-5/2}.3(2jd-z)^2/r_0^2$$
$$- [(m-k/2)^2+p_-^2]^{-3/2} + [(m-k/2)^2+q_+^2]^{-5/2}.3(2jd+2s+z)^2/r_0^2$$
$$- [(m-k/2)^2+q_+^2]^{-3/2}+[(m-k/2)^2+q_-^2]^{-5/2}.3(2jd-2s-z)^2/r_0^2$$
$$- [(m-k/2)^2+q_-^2]^{-3/2})$$
$$+ 2\sum_1^\infty([m^2+(2jd+z)^2/r_0^2]^{-5/2}.3(2jd+z)^2/r_0^2-[m^2+(2jd+z)^2/r_0^2]^{-3/2}$$
$$+[m^2+(2jd+2s+z)^2/r_0^2]^{-5/2}.3(2jd+2s+z)^2/r_0^2-[m^2+(2jd+2s+z)^2/r_0^2]^{-3/2}$$
$$+ [m^2+(2jd-z)^2/r_0^2]^{-5/2}.3(2jd-z)^2/r_0^2 - [m^2+(2jd-z)^2/r_0^2]^{-3/2} +$$
$$[m^2+(2jd-2s-z)^2/r_0^2]^{-5/2}.3(2jd-2s-z)^2/r_0^2-[m^2+(2jd-2s-z)^2/r_0^2]^{-3/2})] \quad [71]$$

3.5 Calculations

The evaluation of the multiply-infinite imaging series in the expressions for the mean field and potential constants b_1, b_2, b_3 and b_4 is a difficult problem, which has to be carried out using several analytical transformations - the mathematical details are presented in the Appendix. As noted in Section 2, the evaluation of the lattice sums for infinite dielectric-conductive imaging of ions was first carried out by Macdonald and Barlow [36]; the present treatment evidently overlaps to a certain extent with their results. The reasons for repeating the calculations here are as follows:

(a) The calculations of Macdonald and Barlow were carried out primarily with a view to elucidating the discreteness-of-charge effect, whilst the result of most relevance to the present discussion is the effective coordination number; it is rather inconvenient to extract this from the results presented in ref. 36. Also, the parameter β was defined assuming the dielectric constant of the double layer to be greater than one, whereas here

it is taken to be one; the values of β used by Macdonald and Barlow do not correspond to this case.

(b) The most important objective of the present micropotential and microfield calculations is the determination of the components due to the dipoles, which have been neglected in previous theoretical treatments based on the dielectric continuum approximation. Indeed, the only result of this kind which has been widely used in the electrochemical context is the well-known calculation by Topping [56] of the effective field coordination number for a plane lattice of dipoles, neglecting all imaging effects, and assuming the field point to be coplanar with the lattice. The transformation method described in the Appendix is more readily applied to the calculation of the lattice sums for the dipoles than that employed by Macdonald and Barlow.

(c) The lattice sums appearing in the expressions for the dipole potential are obviously the same as those in the expressions for the ionic field. However, in the former case, the image series are added, whilst in the latter, they are subtracted. Thus, it is not possible to extract the dipole potential from the calculation of the ionic field presented in ref. 36.

(d) In ref. 36, the dielectric image series was expressed in terms of the series arising in the single-imaging calculation of ref. 14. As shown in the Appendix, the summation with respect to the third variable j (the order of the electrostatic reflections) may be partially effected by transformation to an improper integral using the Laplace Transformation Technique, leaving a series which converges very rapidly (usually after about three

terms). This is more computationally efficient than directly summing the single-image potentials, as done in ref. 36.

In addition to providing the values of the constants b_1, b_2, b_3, and b_4, the results about to be described provide interesting information on the relative importance of the primary- and secondary-image contributions to the field and potential, as well as on the qualitative differences between the image field- and potential-profiles due to the dipoles and ions.

3.5.1 Potential due to Ions

The quantity b_3, given by eqn. 59, is shown as a function of the reduced normal distance z/d in Fig. 5a, for various values of r_0/d. It is plotted as $b_3/(-e_0/r_0)$, i.e. as an effective coordination number. Thus, at the point z=0 on curve 1 of Fig. 5a, the potential obtaining is equal to 10.98266 times the potential due to a neighbouring ion at distance r_0. These potential profiles bear qualitative resemblance to those presented by Macdonald and Barlow [36].

The importance of the secondary image contribution is expressed by the ratio of the secondary image potential Φ_2 to the total potential $\Phi_1+\Phi_2$. This quantity is shown in Fig. 5b, for the same values of r_0/d used in Fig. 5a. It is seen that the secondary images become increasingly important as the ions become farther apart, which is essentially what would be expected.

3.5.2 Field due to Ions

The field b_1, corresponding to the potential b_3, is plotted as $b_1/(-e_0/r_0^2)$ in Fig. 6a, once again for various values of r_0/d. Predictably, for increasingly large ionic separation r_0, the variation of the field with normal distance becomes less and

Fig. 5a: Potential at origin site of an hexagonal latticeof adsorbed ions, with dielectric-conductive imaging.

Curve 1: r_0/d = 0.5

2: 0.6

3: 0.7

4: 0.8

5: 0.9

6: 1.0

7: 1.1

8: 1.2

9: 1.3

10: 1.4

11: 1.5

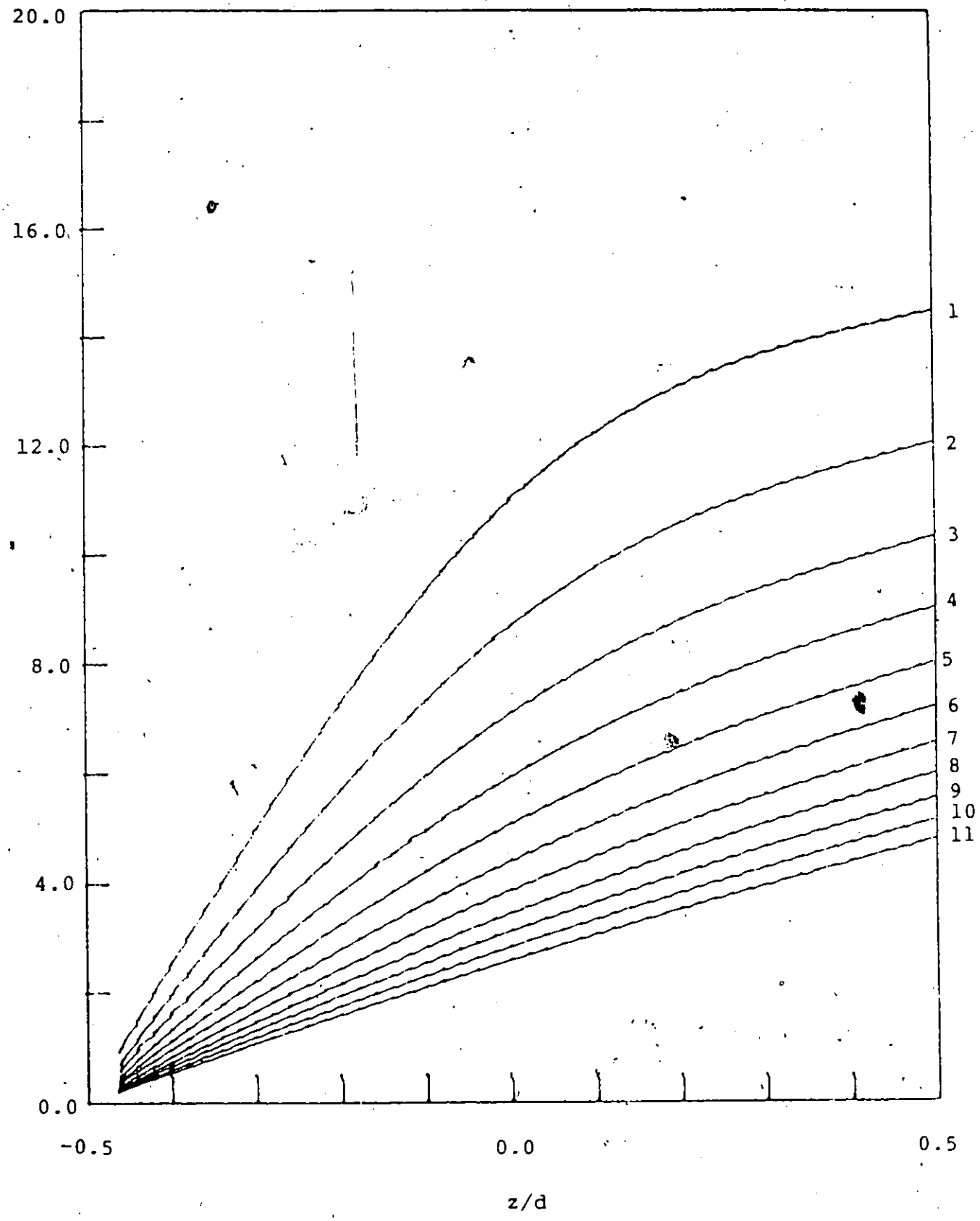
$b_3/(-e_0/r_0)$
20.0
16.0
12.0
8.0
4.0
0.0
-0.5
0.0
0.5
z/d
1
2
3
4
5
6
7
8
9
10
11

Fig. 5b: **Ratio of secondary ionic image potential contribution to total potential due to ions. Curve numbers and values of r_0/d as for Fig. 5a.**

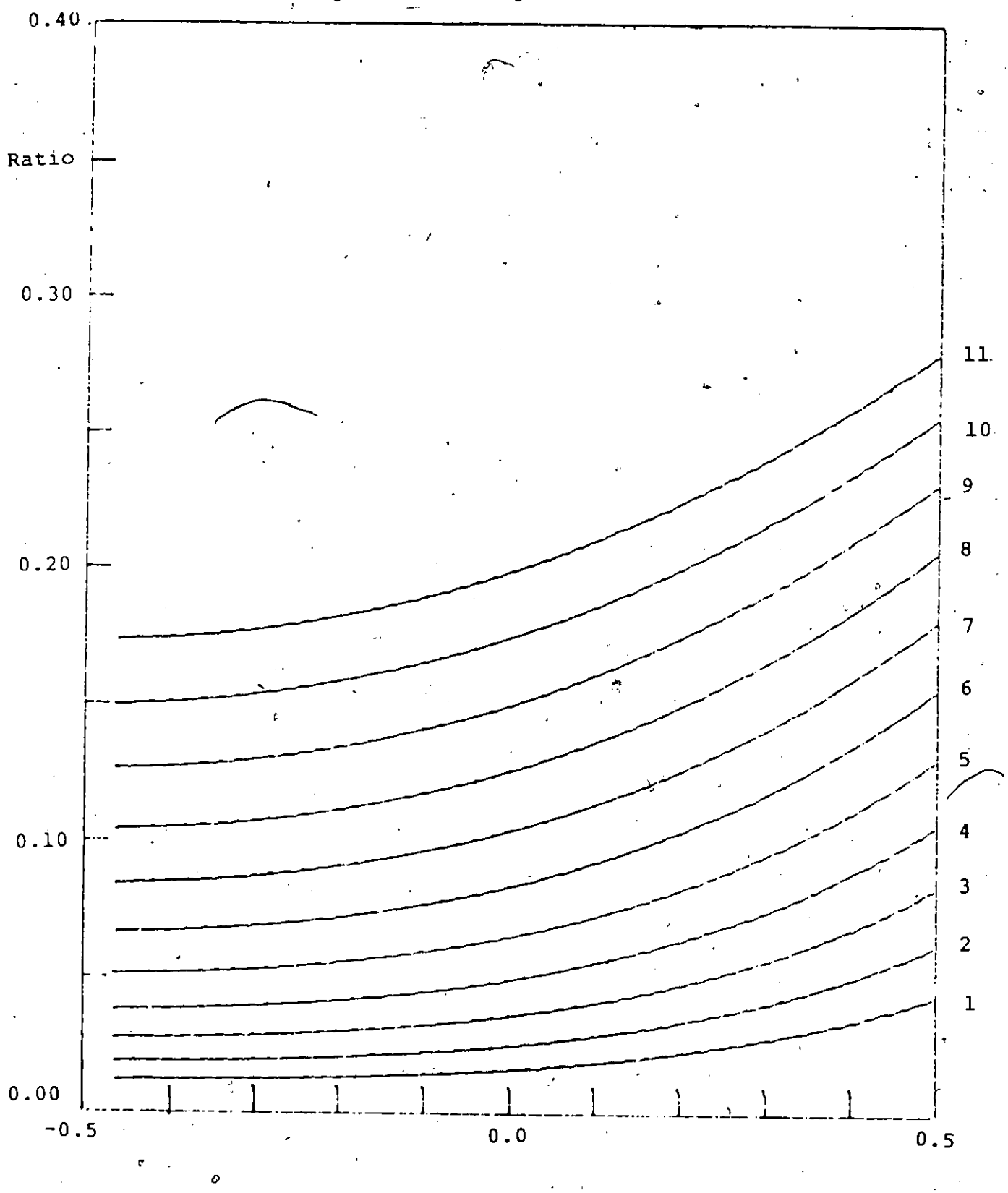

Fig. 6a: Field at origin site of an adsorbed hexagonal lattice of ions with dielectric-conductive imaging.

Curve 1: $r_0/d = 0.5$

2: 0.6

3: 0.7

4: 0.8

5: 0.9

6: 1.0

7: 1.1

8: 1.2

9: 1.3

10: 1.4

11: 1.5

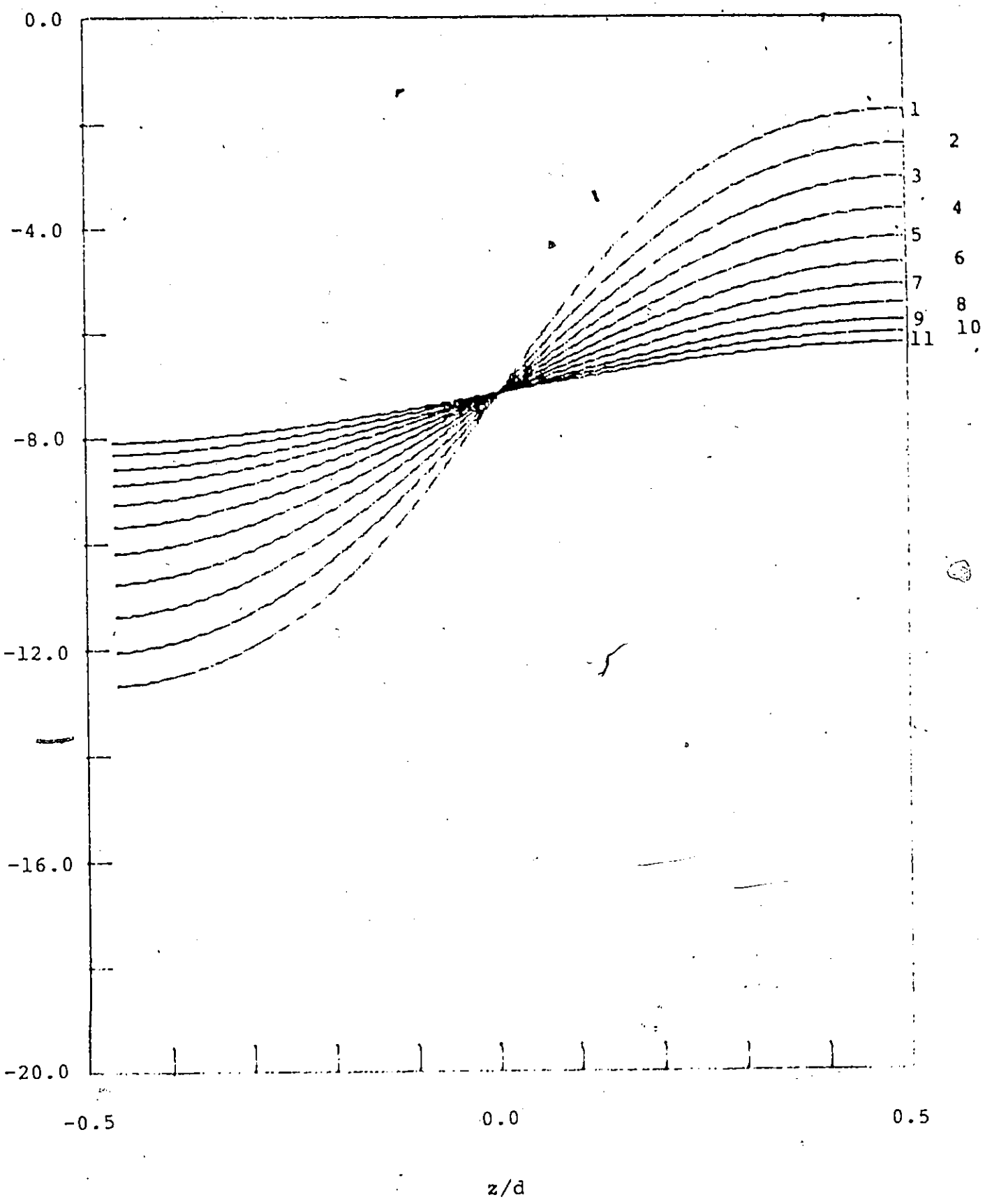
$b_1/(-e_0/r_0^2)$
0.0
-4.0
-8.0
-12.0
-16.0
-20.0
-0.5
0.0
0.5
z/d
1
2
3
4
5
6
7
8
9
10
11

Fig. 6b: Ratio of secondary ionic image field contribution to total field due to ions. Curve numbers and values of r_0/d as for Fig. 6a.

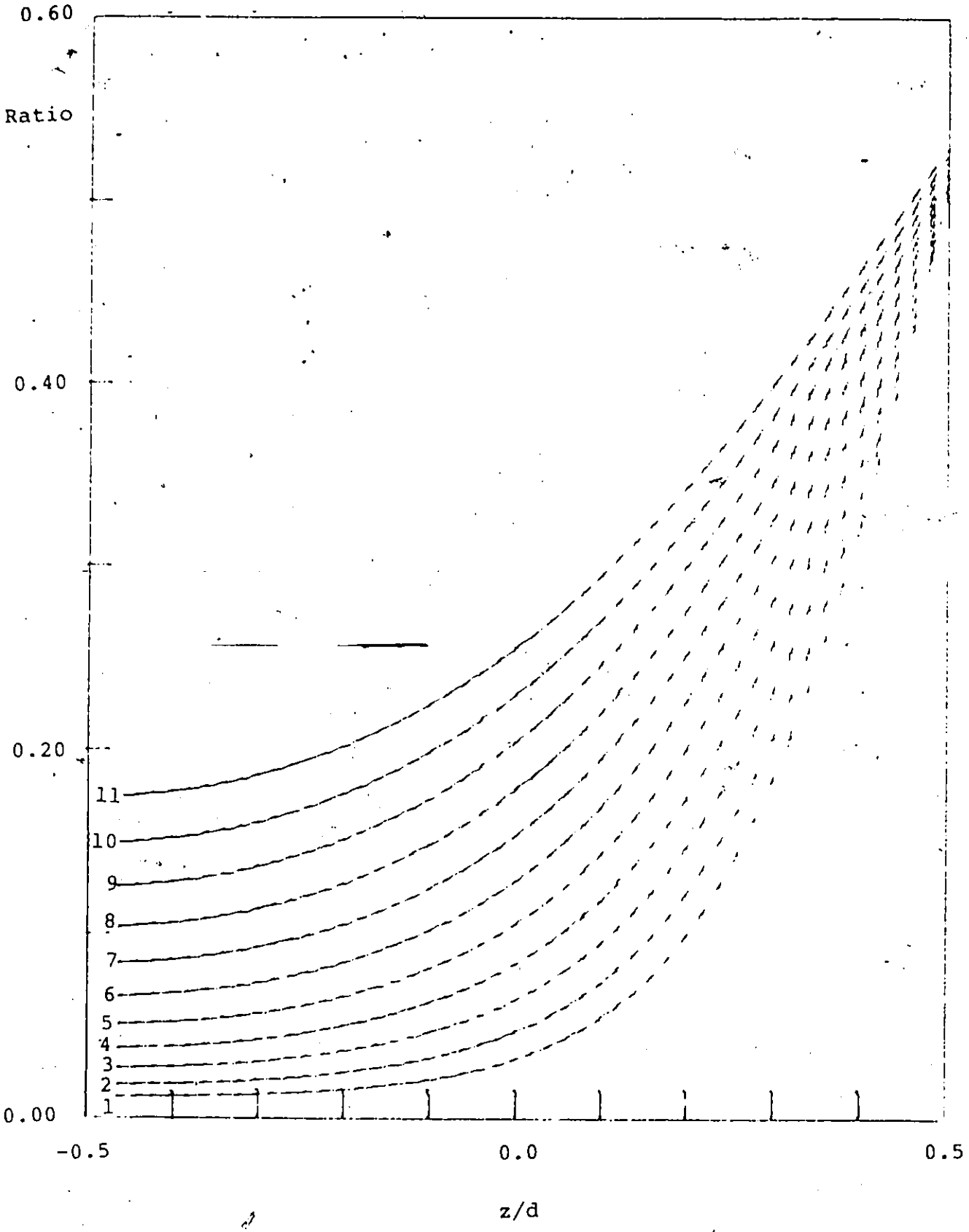

less pronounced. For sufficiently large r_0, one evidently obtains an almost constant field, so that the corresponding potential will be almost linear; this trend may be seen by comparing the curves of Fig. 5a for increasing r_0/d.

The fractions of the total field due to the secondary images, plotted in Fig. 6b, are smaller than the corresponding quantities for the potential, but depend more strongly on z/d. The higher-order dependence of the field on reciprocal distance causes the ratio to be smaller, and to be more strongly dependent on z/d.

3.5.3 Potential due to Dipoles

Fig. 7a shows the reduced dipole potential $b_4/(m/r_0^2)$ as a function of z/d, for a completely polarized lattice, with no ions. As in the variation of b_3 with z/d, the curves tend towards linearity with increasing r_0/d, but this limit is reached more rapidly; for $r_0/d > 1$, the curves are nearly indistinguishable.

Fig. 7b shows the z-dependence of the secondary image dipole potential ratio $\Psi_2/(\Psi_1+\Psi_2)$ (where Ψ_1 and Ψ_2 are the respective potentials due to dipoles and primary images, and secondary dipolar images). This bears an interesting contrast to that of the corresponding ionic field ratio (Fig. 6b). The dependence of the dipole-potential and ion-field on inverse distance is very similar; as already noted, the only difference is that the component series are added for the dipoles and subtracted for the ions. In the field due to the ions, the subtraction of the series for the ions and primary images (the most important part) permits the secondary image terms to assume a larger relative importance,

for values of z approaching the outer limit of the compact double layer.

3.5.4 Field due to Dipoles

The tendency of the curves in Fig. 7a towards linearity for increasing r_0 is more strikingly illustrated by the variation of the dipole field $b_2/(m/r_0^3)$ with z/d, which is shown in Fig. 8a. The inflexion shown by the potential results in a peak in its derivative, which becomes less pronounced as r_0/d increases.

The variation of the secondary dipole field ratio with z/d, shown in Fig. 8b, is predictably the most pronounced, in view of the dependence of the dipole field on the cube of the inverse distance.

3.5.5 Field due to Dipole Lattice Without Imaging

A useful byproduct of the present micropotential and microfield calculation is a generalization of Topping's lattice sum [56], to the more general situation in which the field point is not coplanar with the dipole array. It follows from eqn. 71 that this lattice sum is

$$S_T^h(z) = 2\sum_1^\infty\sum_{-\infty}^\infty([(m-k/2)^2+a_-^2]^{-5/2}.3z^2/r_0^2 - [(m-k/2)^2+a_-^2]^{-3/2} + 2\sum_1^\infty([m^2+z^2/r_0^2]^{-5/2}.3z^2/r_0^2 - [m^2+a_-^2]^{-3/2}) \quad [72]$$

which, when z=0, reduces to Topping's sum

$$S_T^h(0) = -2\sum_1^\infty\sum_{-\infty}^\infty[m^2-km+k^2]^{-3/2} - 2\sum_1^\infty m^{-3} \quad [73]$$

$S_T^h(z)$ is shown as a function of z in Fig. 9, for various values of r_0. The curves are, of course, symmetrical, since in this case the dipole layer is not in an anisotropic environment; more importantly, they all pass through the minimum -11.03419 when z=0, which is in satisfactory agreement with the values of $|S_T^h|$ = 11.0341754 and $11.034170<|S_T^h|<11.034184$ obtained respectively by

Fig. 7a: Potential at the origin site of an hexagonal lattice of adsorbed dipoles with dielectric-conductive imaging.

Curve 1: $r_0/d = 0.5$

2: 0.6

3: 0.7

4: 0.8

5: 0.9

6: 1.0

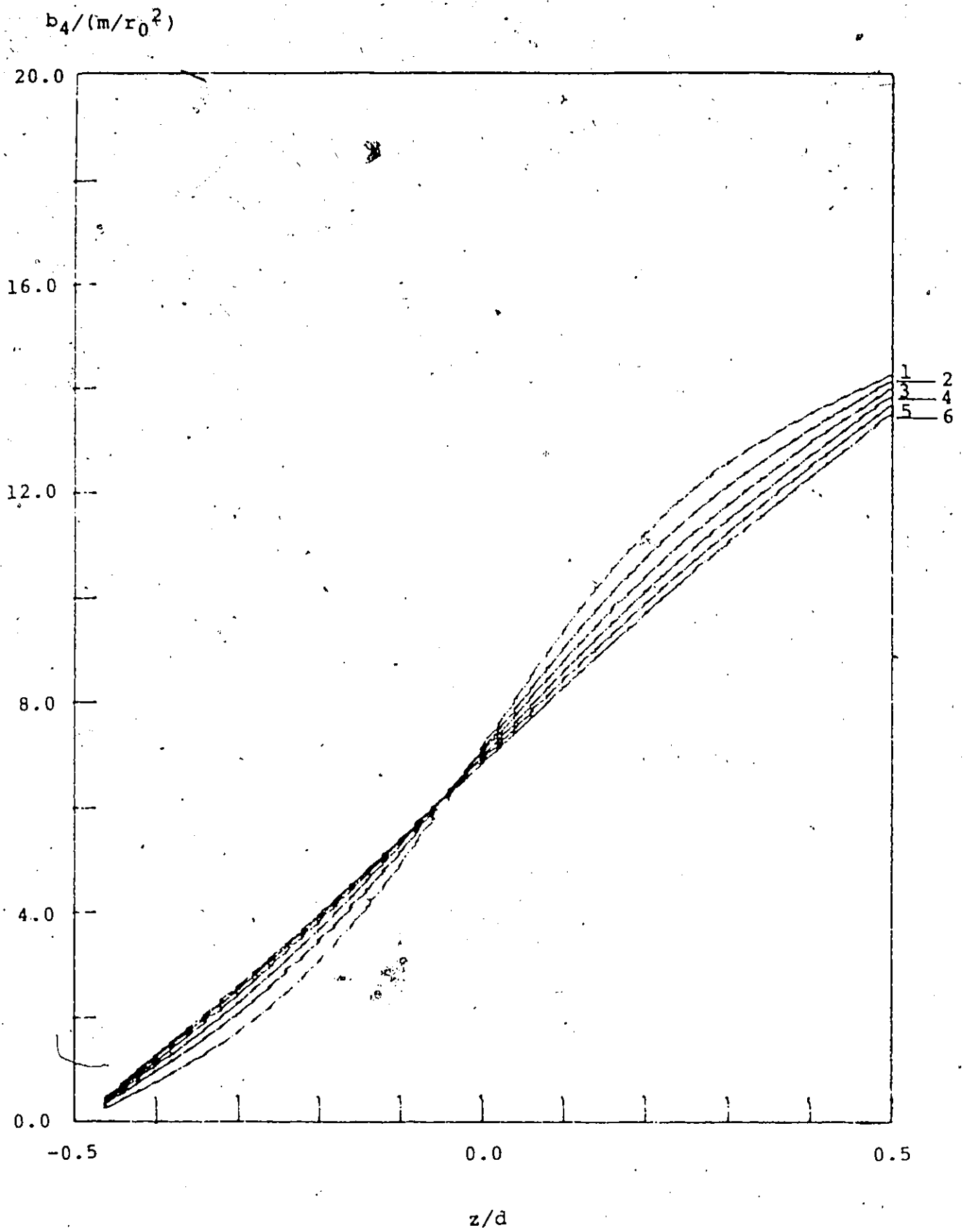
$b_4/(m/r_0^2)$
20.0
16.0
12.0
8.0
4.0
0.0
-0.5
0.0
0.5
z/d
1
2
3
4
5
6

Fig. 7b: Ratio of dipolar secondary image potential contribution to total potential due to dipoles. Curve numbers and values of r_0/d as for Fig. 7a.

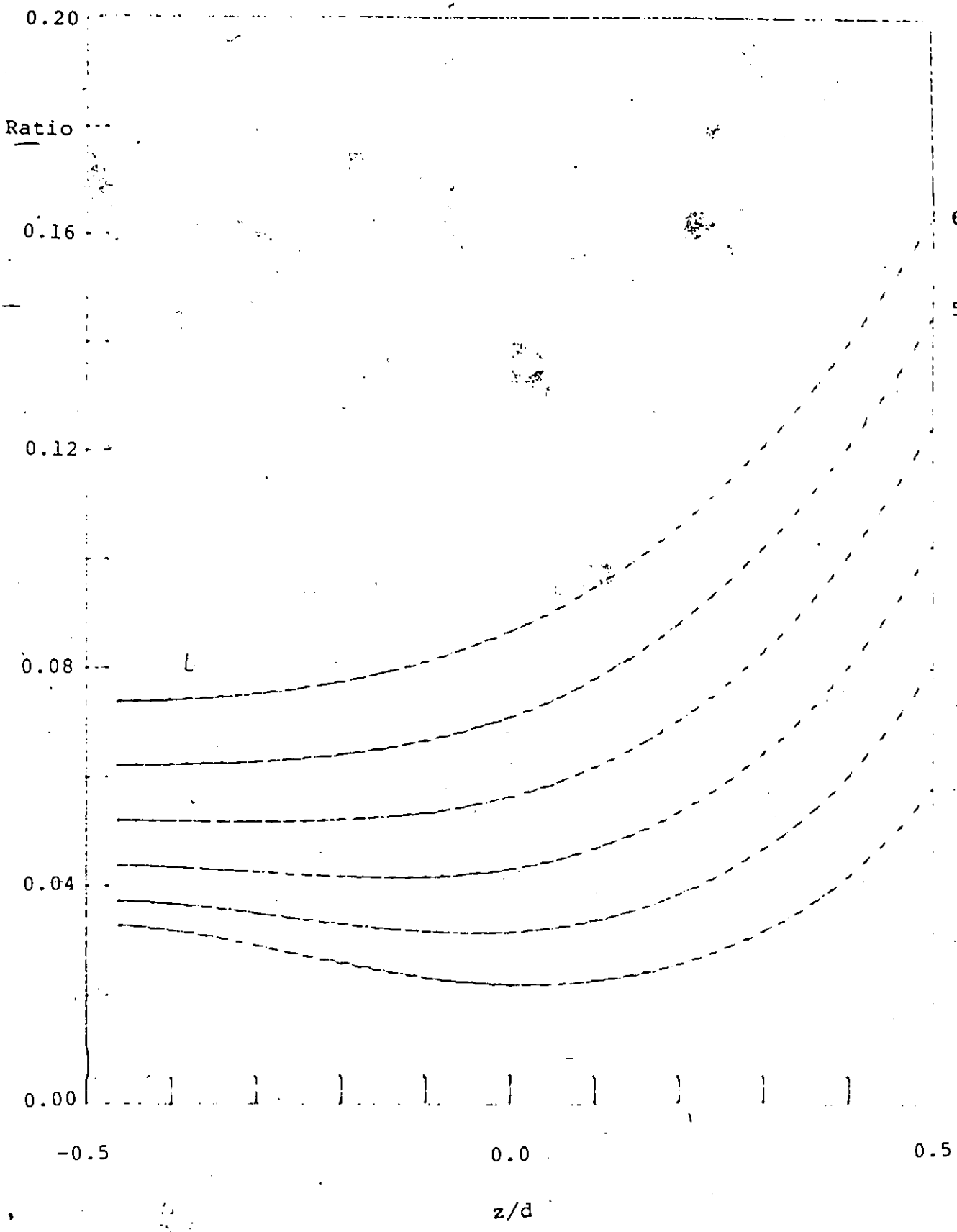

Fig. 8a: Field at origin site of an hexagonal lattice of adsorbed dipoles with dielectric-conductive imaging.

Curve 1: $r_0/d = 0.5$

2: 0.6

3: 0.7

4: 0.8

5: 0.9

6: 1.0

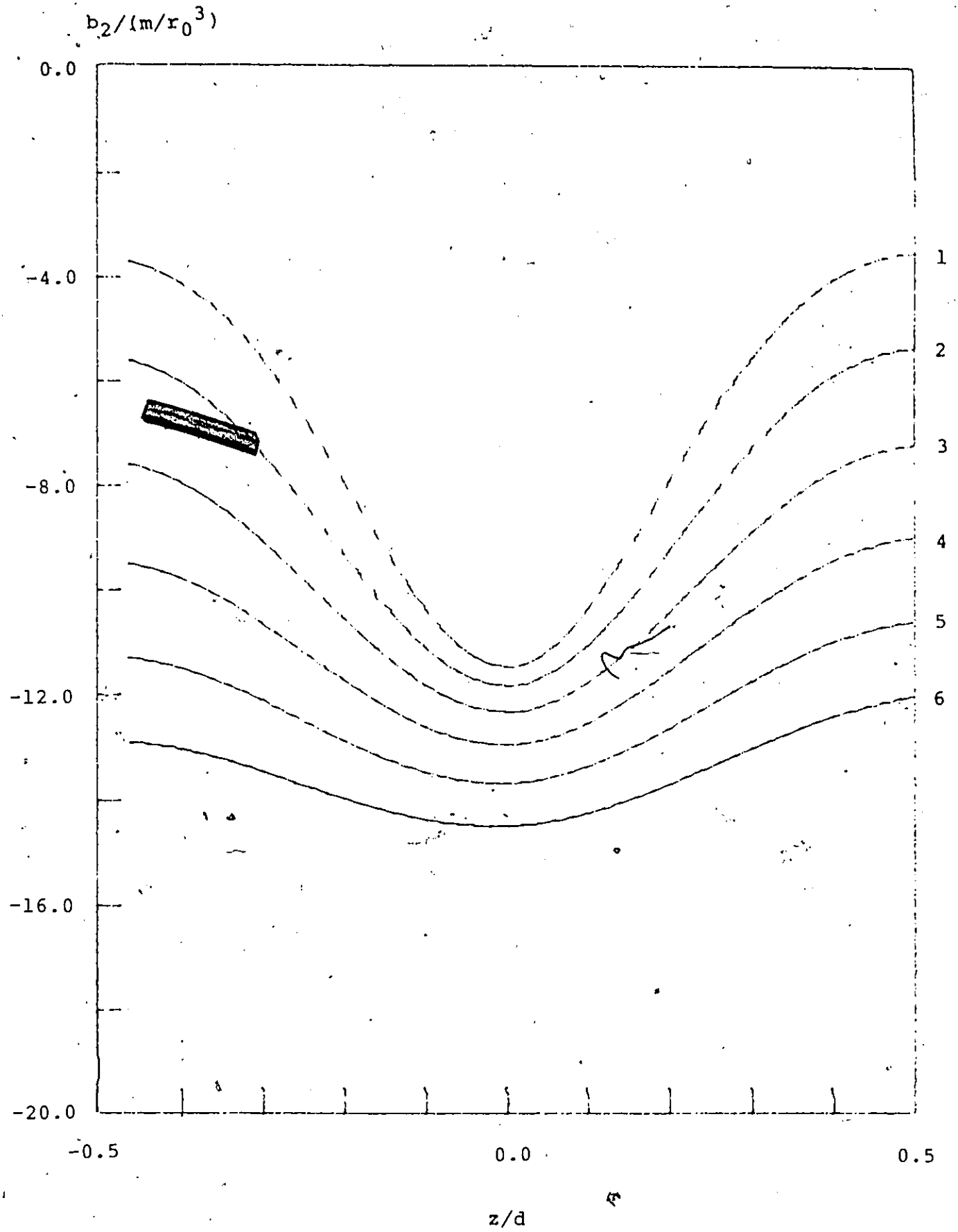
$b_2/(m/r_0^3)$
0.0
-4.0
-8.0
-12.0
-16.0
-20.0
-0.5
0.0
0.5
z/d
1
2
3
4
5
6

Fig. 8b: Ratio of secondary dipolar image field contribution to total potential due to dipoles. Curve numbers and values of r_0/d as for Fig. 8a.

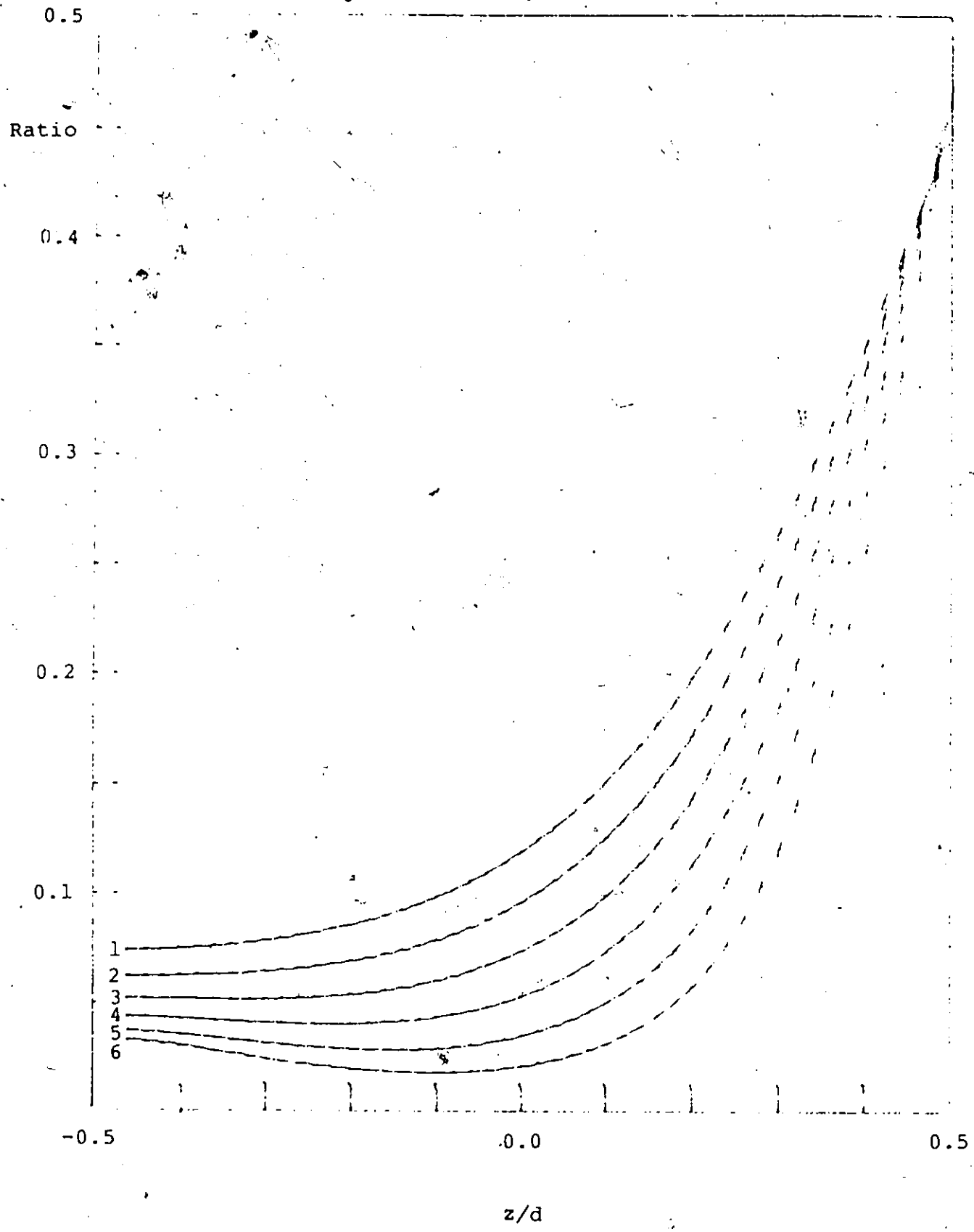

Fig. 9: Reduced field at the origin site of an hexagonal lattice, as a function of normal distance z, for various values of r_0.

Curve 1: $r_0 = 1.5 \times 10^{-8}$ cm

Curve 2: $r_0 = 3.0 \times 10^{-8}$ cm

Curve 3: $r_0 = 4.5 \times 10^{-8}$ cm

Curve 4: $r_0 = 6.0 \times 10^{-8}$ cm

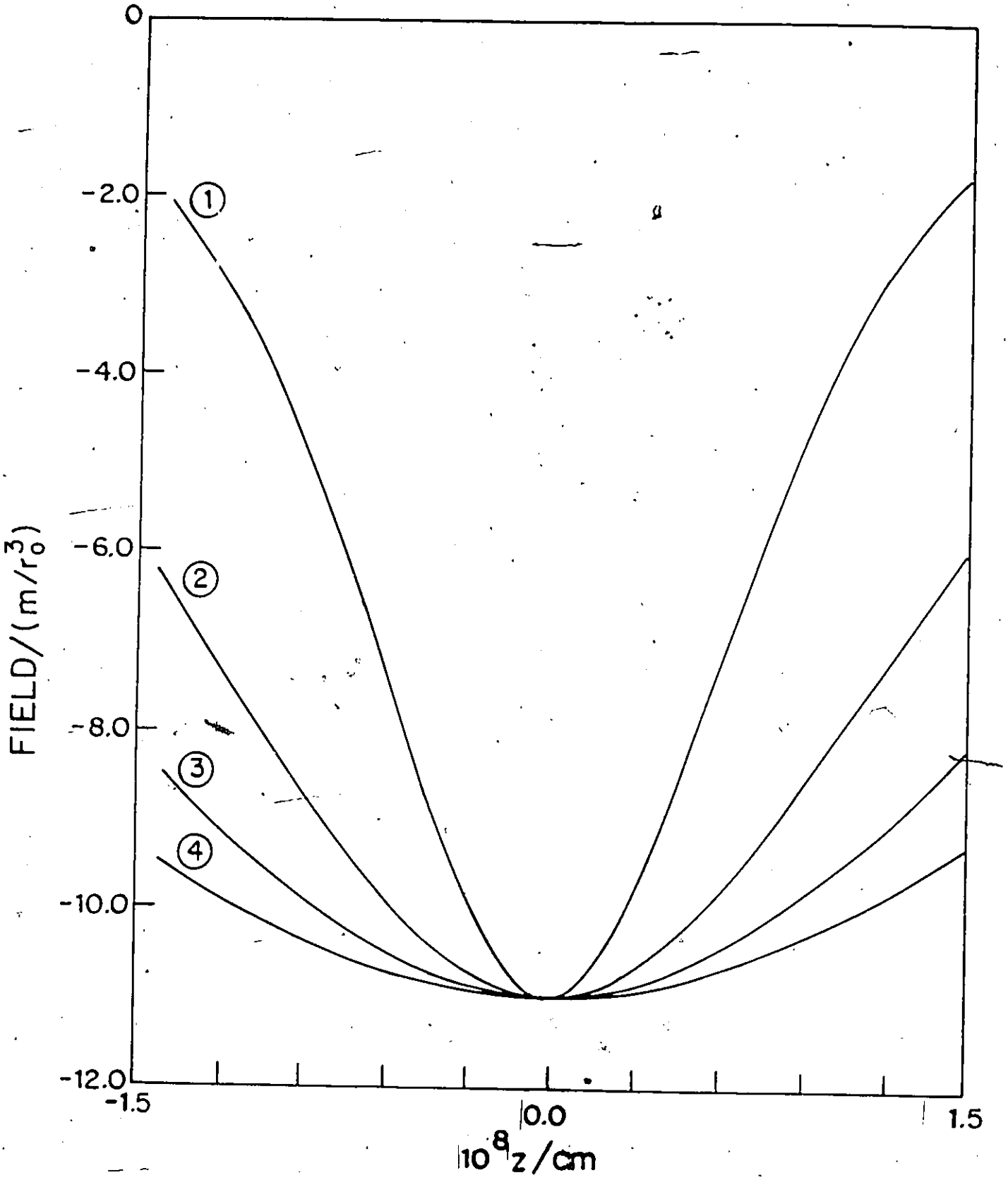
0
-2.0
-4.0
-6.0
-8.0
-10.0
-12.0
FIELD/(m/r$_o^3$)
①
②
③
④
-1.5
0.0
1.5
10^{8}z/cm

van der Hoff and Benson [15] and Topping [56]. The discrepancy is probably due to the fact that in the present work, the calculation was carried out in single precision, using an approximating polynomial to evaluate the modified Bessel functions arising from the series transformation.

The calculation described in this section thus provides an interesting and useful check on the correctness of the summation procedure.

3.6 Effective Field and Potential Experienced by Adsorbed Species

In addition to the average field $E_1=4\pi(q_M+q_{ion}-q_{dip})$, which corresponds to the macropotential, the ions and dipoles in the surface layer will contribute fields given respectively by $b_1\theta$ and $b_2\langle s\rangle(1-\theta)$, according to the MFA. It is thus possible to define an effective field E_{eff} by

$$E_{eff} = E_1 + b_1\theta + b_2(1-\theta)\langle s\rangle \qquad [74]$$

The corresponding potential experienced by the adsorbed species may be defined as

$$V_{eff} = \Delta\phi_1.s/d + b_3\theta + b_4(1-\theta)\langle s\rangle \qquad [75]$$

where the macropotential term is multiplied by the fraction s/d of the interfacial potential difference obtaining at the i.H.p.; for the calculations of isotherms to be presented shortly, z_1 will be assumed equal to s, so that s/d=1/2.

A question which immediately arises from such a treatment of long-range electrostatic interactions experienced by a given species, concerns the effect exerted by the polarization of species located at shorter distances. For example, if an ion at the origin is interacting with its nearest ionic neighbour at a

distance of, say, $10r_0$, how do the dipoles in between these two ions affect this interaction energy? This question is answered automatically in the treatments which assume a constant dielectric constant ε_1 for the solvent molecules in the adsorbed layer - the interaction energy is simply attenuated by the factor $1/\varepsilon_1$. This in turn suggests that some account should be taken of the dielectric anisotropy caused by the intense field exerted by ions at close range.

In the present work, however, polarization of the solvent dipoles is to be calculated explicitly, i.e. the average polarization of all the molecules in the normal direction is to be determined by combining the statistical-mechanical expression dealing with the interactions, with the electrical boundary conditions at the interface. Therefore, rather than include the effects of dipoles on ion-ion interaction energy by using a constant attenuation factor, the contribution of the dipoles to the total potential experienced by the ions is included explicitly in v_{eff}. Similar remarks apply to the effective field; recalling the discussion in Chapter 2, it was noted that the iterative determination of q_{dip} was equivalent to dividing the field $4\pi q_M$ by a variable dielectric constant. Thus, in the present case, rather than attenuating E_{eff} by a constant factor $1/\varepsilon_1$, the polarization of the dipoles is to be included explicitly in a self-consistent way.

Closely related to this point is the use of a "saturation" dielectric constant, taking account of vibrational and electronic polarization effects, which has been used in many theoretical treatments of orientational polarization [1,4]. The present work

uses the equivalent procedure of including the induced polarization by using the appropriate polarizability; it is evidently somewhat arbitrary to adopt a discrete model for orientational polarization whilst retaining a continuum approximation for the other components.

An additional component to E_{eff}, which at first might appear to be necessary, is a correction for cavity- and reaction-field effects, of the type discussed in detail by Boettcher [54]. These calculations, however, are fundamentally inapplicable in the present situation because of the non-linear dielectric behaviour of the surroundings, as well as the replacement of spherical symmetry by cylindrical symmetry. In any case, these physical effects are already implicitly included in the calculations of the infinite image potentials, already discussed.

4. Partition Functions for Ions and Dipoles

(i) Adsorbed Ions

Since the total potential acting on the adsorbed ions is V_{eff}, the corresponding potential energy is $-e_0V_{eff}$, so that the partition function can be defined as

$$z_a = z_a^o.\exp(e_0V_{eff}/kT) \qquad [76]$$

(ii) Adsorbed Dipoles

A multiplicity of molecular models for the orientational polarization behaviour of adsorbed polar molecules has appeared in the literature (see a recent review by Fawcett [4]), almost exclusively in connection with the interpretation of capacitance results in the assumed absence of ionic adsorption. Given the assumption of point-dipoles rather than finite-length ones, the

least conjectural of these models appears to be that which admits a continuous range of orientations with respect to the interfacial field. The implications of this were first considered, in the electrochemical context, by Macdonald and Barlow [55], who proposed an expression of the following form for the angular potential energy:

$$U(\theta) = -(1+\cos\theta)U_0/2 - mE_1\cos\theta - (a_1+a_2\cos^2\theta) \qquad [77]$$

where the constants a_1 and a_2 depend on the the model assumed for the self-image interaction experienced by the dipole; in Chapter 4, the respective values of these constants were determined to be 5.501kT and 9.070kT, at 293K. In order to employ this expression in the present work it is necessary to replace the inner-layer field by E_{eff}. The partition function is

$$z_w = z_w^o.\exp[(U_0+\alpha E_{eff}^2)/2kT]$$
$$\times \int_0^{\pi}\exp[(mE_{eff}/kT+U_0/2kT)\cos\theta+(a_1+a_2\cos^2\theta)/kT].2\pi\sin\theta d\theta$$
$$=2\pi z_w^o\exp[(U_0+\alpha E_{eff}^2)/2kT]\int_{-1}^{1}\exp[(mE_{eff}/kT+U_0/2kT)y+(a_1+a_2y^2)/kT]dy \qquad [78]$$

where the last form has been obtained with the substitution $y=\cos\theta$, $dy=-\sin\theta d\theta$.

5. Adsorption Isotherms and Capacitance Expressions

The procedure used to set up the adsorption isotherms for a substitutional process of the form 2 is essentially the same as before, but with the partition functions defined as in the previous section. The calculation of the differential capacitance is rather more complicated with the inclusion of the mean field effects; in addition to the dependence of E_1 on q_M, q_{ion} and q_{dip}, it is necessary to allow for the additional dependence of E_{eff} and V_{eff} on θ and $\langle s \rangle$, expressed by eqns. 74 and 75. Thus,

the derivatives of quantities $x(E_{eff})$ and $y(V_{eff})$ with respect to q_M are

$$dx/dq_M = (dx/dE_{eff})(dE_{eff}/dq_M)$$

$$dy/dq_M = (dy/dV_{eff})(dV_{eff}/dq_M) \qquad [79]$$

Observing that $(1-\theta)\langle s\rangle N_w m = q_{dip}$, the derivatives of the effective field and potential are as follows:

$$dE_{eff}/dq_M = 4\pi(1+dq_{ion}/dq_M - dq_{dip}/dq_M) - (b_1/N_w e_0 d)dq_{ion}/dq_M + (b_2/N_w m)dq_{dip}/dq_M \qquad [80]$$

$$dV_{eff}/dq_M = (d/2).4\pi(1+dq_{ion}/dq_M - dq_{dip}/dq_M) - (b_3/N_w e_0 d)dq_{ion}/dq_M + (b_4/N_w m)dq_{dip}/dq_M \qquad [81]$$

The equations from which the unknown derivatives dq_{ion}/dq_M and dq_{dip}/dq_M may be determined are derived as before by differentiation of the isotherm and polarization function with respect to q_M, substituting the results 84 and 85 where appropriate.

5.1 Mean Field Approximation

As a first correction to the complete neglect of the interactions in the argument presented in section 1, it is of interest to examine the consequences of assuming all interactions to be equivalent to a mean potential or field. With this approximation, the only dependence of the chemical potentials of the adsorbed species on θ and $\langle s\rangle$ is through E_{eff} and V_{eff}. The equilibrium expression for the 1:1 substitutional adsorption reaction is therefore identical to that given by eqn. 3, except that the partition functions are defined as in section 4:

$$\theta/(1-\theta) = K_{eq}.(a_{A^-}/a_{H2O}).z_a(V_{eff})/z_w(E_{eff}) \qquad [82]$$

In order to determine θ it is necessary to combine this

equation with the other conditions satisfied by the unknowns E_1 and <s>. The polarization function corresponding to the partition function z_w is, applying the standard statistical-mechanical definition,

$$\langle s \rangle = kT(\partial \ln z_w / \partial E_{eff}) \qquad [83]$$

whence

$$\langle s \rangle = \alpha E_{eff}/m + \left[\frac{\int_{-1}^{1} y \exp[(mE_{eff}/kT+U_0/2kT)y+(a_1+a_2y^2)/kT]dy}{\int_{-1}^{1} \exp[(mE_{eff}/kT+U_0/2kT)y+(a_1+a_2y^2)/kT]dy}\right] \qquad [84]$$

in which the induced dipole moment has been divided by m to make <s> of the order of unity. The field E_1 must satisfy the electroneutrality condition (cf. eqn. 6):

$$E_1/4\pi + (1-\theta)N_w m = 2A\sinh[(V-E_1 d)e_0/2kT] \qquad [85]$$

It is therefore required to find the values of θ, <s> and E_1 which satisfy these equations simultaneously, for given applied potential V.

Equivalently, the problem could be formulated as the simultaneous determination of q_M, q_{ion} and q_{dip}; in this case, the isotherm would be combined with the expressions for q_{dip} and q_M, viz.

$$q_{dip} = N_w m(1-\theta)\langle s \rangle \qquad [86]$$

(where <s> is in turn defined by eqn. 84) and

$$q_M = -q_{ion} + 2A\sinh[(V-E_1 d)e_0/2kT] \qquad [87]$$

It is worth remarking that the numerical solution of these equations is very difficult, even with judicious scaling of the variables to ensure that the residuals are of similar magnitudes. The convergence behaviour of the system 82,86,87 is even more froward than that of 82,84,85. This is to be contrasted with the

situation described in Chapter 2, where it was observed that the solution of simultaneous non-linear equations for q_M and q_{dip} (with an appropriate choice of initial estimates) actually converged more rapidly than the equivalent single equation for $\Delta\phi_1$. In the present case, the Jacobian matrix is exceedingly ill-conditioned, with the determinant reaching vanishingly small values unless the initial estimate of the solution is unrealistically accurate. Consequently, the equations resist solution by the conventional Newton-Raphson iteration in three variables, and even by a sophisticated published subroutine which combines this technique with the method of steepest descents [57]. The following procedure was therefore developed:

(i) For an assumed value of E_1, the values of θ and $\langle s \rangle$ satisfying the isotherm and polarization equations were determined by solving eqns. 82 and 84. This was achieved by solving eqn. 84 for $\langle s \rangle$, for each value of θ using the Newton-Raphson method, which, for equations of the form

$$x = f(a-bx)$$

(where a and b are constants and f varies sigmoidally with its argument), has excellent convergence properties. This procedure was incorporated into a graphical bisection routine to find θ satisfying eqn. 82, written in the form

$$\theta - K/(1+K) = 0 \qquad [88]$$

where K represents the right-hand member of eqn. 82.

(ii) The value of E_1 was then selected so as to satisfy eqn. 85, using Mueller's method (graphical bisection combined with inverse parabolic extrapolation [58]).

In order to simplify the algebra involved in determining the

expressions for the differential capacitance, it is convenient to introduce the following notation for the integral occurring in z_w, and its first two derivatives with respect to E_{eff}:

$$P_1(E_{eff}) = \int_{-1}^{1} \exp[(mE_{eff}/kT+U_0/2kT)y+(a_1+a_2y^2)/kT]dy \quad [89a]$$

$$dP_1/dE_{eff} = (m/kT)\int_{-1}^{1} y \exp[(mE_{eff}/kT+U_0/2kT)y+(a_1+a_2y^2)/kT]dy$$

$$\equiv (m/kT)P_2(E_{eff}) \quad [89b]$$

$$d^2P_1/dE_{eff}^2 = (m/kT)^2\int_{-1}^{1} y^2 \exp[(mE_{eff}/kT+U_0/2kT)y+(a_1+a_2y^2)/kT]dy$$

$$\equiv (m/kT)^2P_3(E_{eff}) \quad [89c]$$

From the definitions of the partition functions, one therefore obtains

$$kT(\partial \ln z_w/\partial E_{eff}) = \alpha E_{eff} + m.P_2/P_1 \quad [90]$$

$$kT(\partial^2 \ln z_w/\partial E_{eff}^2) = \alpha + (m^2/kT)[P_3/P_1 - P_2^2/P_1^2] \quad [91]$$

$$\partial \ln z_a/\partial V_{eff} = e_0/kT \quad [92]$$

Differentiation of the equation for q_{dip} results in

$$dq_{dip}/dq_M = (1-\theta)N_w kT(\partial^2 \ln z_w/\partial E_{eff}^2).dE_{eff}/dq_M$$

$$- N_w kT(\partial \ln z_w/\partial E_{eff}).d\theta/dq_M$$

$$\equiv 4\pi g_1(1+dq_{ion}/dq_M-dq_{dip}/dq_M) + g_2 dq_{ion}/dq_M + g_3 dq_{dip}/dq_M \quad [93]$$

where

$$g_1 = (1-\theta)N_w[\alpha + (m^2/kT)(P_3/P_1-P_2^2/P_1^2)]$$

$$g_2 = -N_w(1-\theta)[\alpha + (m^2/kT)(P_3/P_1-P_2^2/P_1^2)]$$

$$+ [\alpha E_{eff} + mP_2/P_1]/e_0 d$$

$$g_3 = (1-\theta)[\alpha + (m^2/kT)(P_3/P_1-P_2^2/P_1^2)]b_2/m$$

The other equation is obtained by implicit differentiation of the isotherm:

$$d\theta/dq_M = \theta(1-\theta)[(\partial \ln z_a/\partial V_{eff})dV_{eff}/dq_M-(\partial \ln z_w/\partial E_{eff})dE_{eff}/dq_M]$$

whence

$$dq_{ion}/dq_M = -4\pi g_4(1+dq_{ion}/dq_M-dq_{dip}/dq_M) + g_5 dq_{ion}/dq_M$$

$$+ g_6 dq_{dip}/dq_M \qquad [94]$$

where

$$g_4 = \theta(1-\theta).(N_w e_0 d/kT)[\alpha E_{eff} + mP_2/P_1 - e_0 d/2]$$

$$g_5 = \theta(1-\theta).[b_3.e_0/kT - (\alpha E_{eff} + mP_2/P_1).b_1/kT]$$

$$g_6 = \theta(1-\theta).[(\alpha E_{eff} + mP_2/P_1).b_2/kT - b_4.e_0/kT]$$

The solution of the simultaneous equations 93 and 94, which can be arranged in the form

$$(4\pi g_1+g_2)dq_{ion}/dq_M + (-4\pi g_1+g_3-1)dq_{dip}/dq_M = -4\pi g_1 \qquad [95]$$

$$(4\pi g_4+g_5-1)dq_{ion}/dq_M + (-4\pi g_4+g_3)dq_{dip}/dq_M = 4\pi g_4 \qquad [96]$$

is

$$dq_{ion}/dq_M = \begin{vmatrix} -4\pi g_1 & -4\pi g_1+g_3-1 \\ 4\pi g_4 & -4\pi g_4+g_6 \end{vmatrix} \Big/ \begin{vmatrix} 4\pi g_1+g_2 & -4\pi g_1+g_3-1 \\ 4\pi g_4+g_5-1 & -4\pi g_4+g_6 \end{vmatrix}$$

$$dq_{dip}/dq_M = \begin{vmatrix} 4\pi g_1+g_2 & -4\pi g_1 \\ 4\pi g_4+g_5-1 & 4\pi g_4 \end{vmatrix} \Big/ \begin{vmatrix} 4\pi g_1+g_2 & -4\pi g_1+g_3-1 \\ 4\pi g_4+g_5-1 & -4\pi g_4+g_6 \end{vmatrix} \qquad [97]$$

and as before, the reciprocal inner-layer differential capacitance is given by eqn. 8.

The differential capacitance for a 1:1-substitutional adsorption reaction, of the type exemplified in eqn. 2, is shown in Fig. 10, as a function of V, together with the corresponding variation of $\langle s \rangle$ and θ. The most conspicuous feature of the capacitance curve is the complete suppression of the "hump" behaviour evident in the capacitance curves presented earlier; the numerical values of C are also much lower.

The near-constancy of the capacitance for negative V can be rationalized by considering the calculation of the capacitance in the assumed absence of ionic adsorption. Application of the results of Chapter 2, using $E_{eff} = E + b_2\langle s \rangle$, yields the expression

Fig. 10: Ionic coverage, reduced average dipole moment and differential capacity according to the Mean Field Approximation. $K_{eq} = 10^6$, $c_{A^-} = 0.01$ mol/l, inert electrolyte concentration 0.1 mol/l.

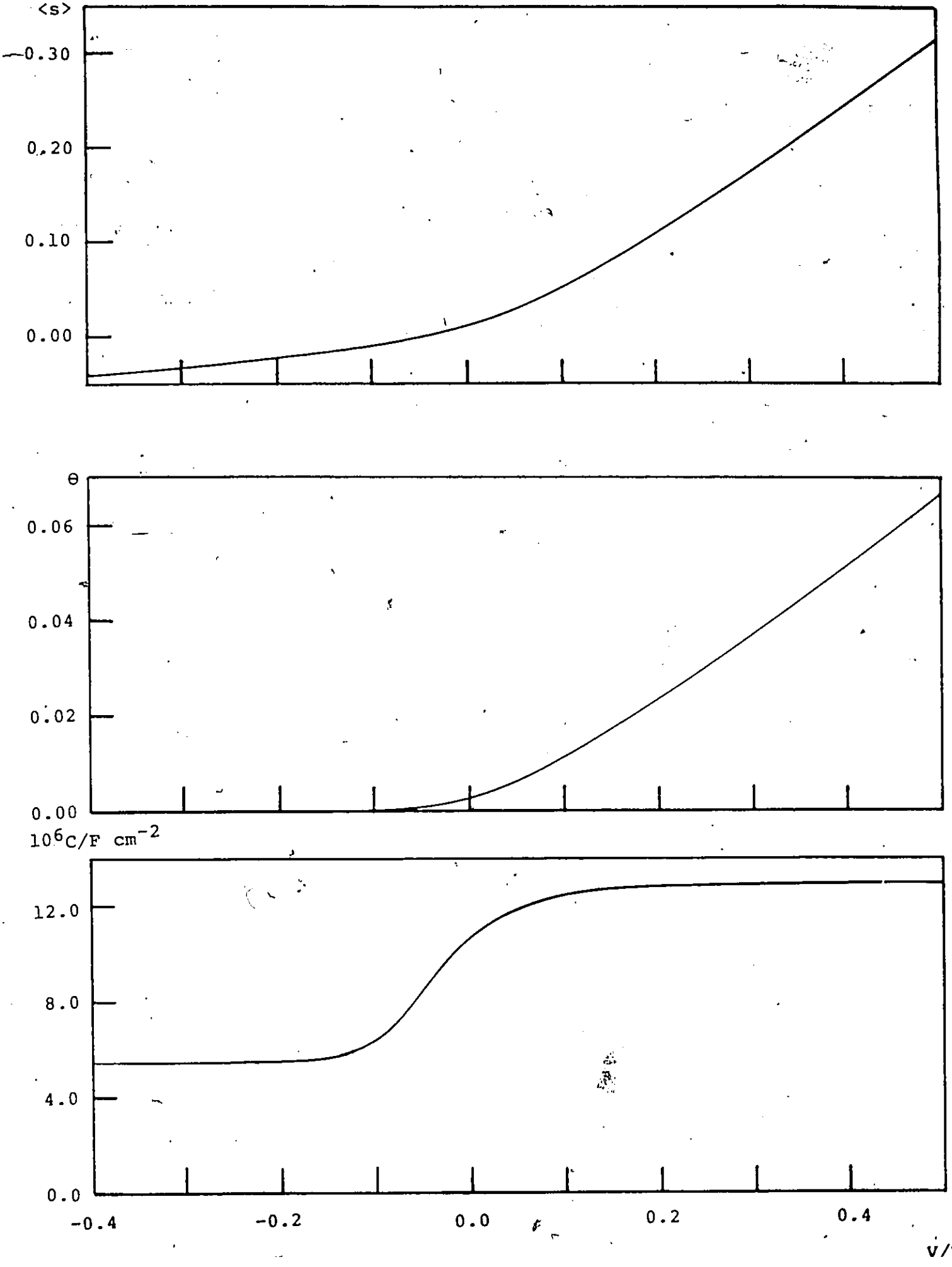
<s>
0.30
0.20
0.10
0.00
θ
0.06
0.04
0.02
0.00
10^6C/F cm^{-2}
12.0
8.0
4.0
0.0
-0.4
-0.2
0.0
0.2
0.4
V/V

$$1/C_1 = 4\pi d.\frac{1 - [P_3/P_1 - P_2^2/P_1^2]b_2m/kT}{1 + 4\pi N_w\alpha + (4\pi N_w m^2 - b_2m/kT)[P_3/P_1 - P_2^2/P_1^2]} \quad [98]$$

for the reciprocal inner-layer capacitance. The total capacitance for this model is shown in Fig. 11; the curve calculated with $b_2 = 0$ exhibits the capacitance "hump" present in the results of Chapter 2, but with b_2 defined by eqn. 71, this "hump" disappears completely. This is in qualitative agreement with the trend shown by capacitance calculations using the BDM theory [1] with increasing values of Uc/kT (cf. Chapter 2, Fig. 6b). The mean field interaction energies due to ions and dipoles are respectively $b_1m/kT = 175kT$ and $b_2m/kT = -44.83$ at 293K; the second quantity, which corresponds to -Uc/kT, is seen to be many times the values of $Uc/kT \approx 5$ required to "flatten" the capacitance curves according to the BDM theory in the absence of specific ionic adsorption.

The very large values of the corresponding components of the effective potential due to ions ($b_3e_0/kT = -837.6$) and dipoles ($b_4e_0/kT = 166.7$) result in much lower ionic coverages. In contrast to Section 1, however, these small coverages do not cause large values of C, since C depends on the rate at which θ and $\langle s \rangle$ vary with q_M, and not simply on their actual values.

While Fig. 10 does not resemble experimental behaviour, the calculations of this section nevertheless illustrate that the widely-used dipole-lattice model for the compact double layer does not perform any better (even with no ionic adsorption), when full account is taken of dipolar discreteness and imaging, in the manner described earlier.

Fig. 11: Double layer capacitance according to the Mean Field Approximation, with no ionic specific adsorption.

Curve 1: $b_2 = 0$

Curve 2: b_2 given by eqn. 71

$c = 0.1$ mol/l

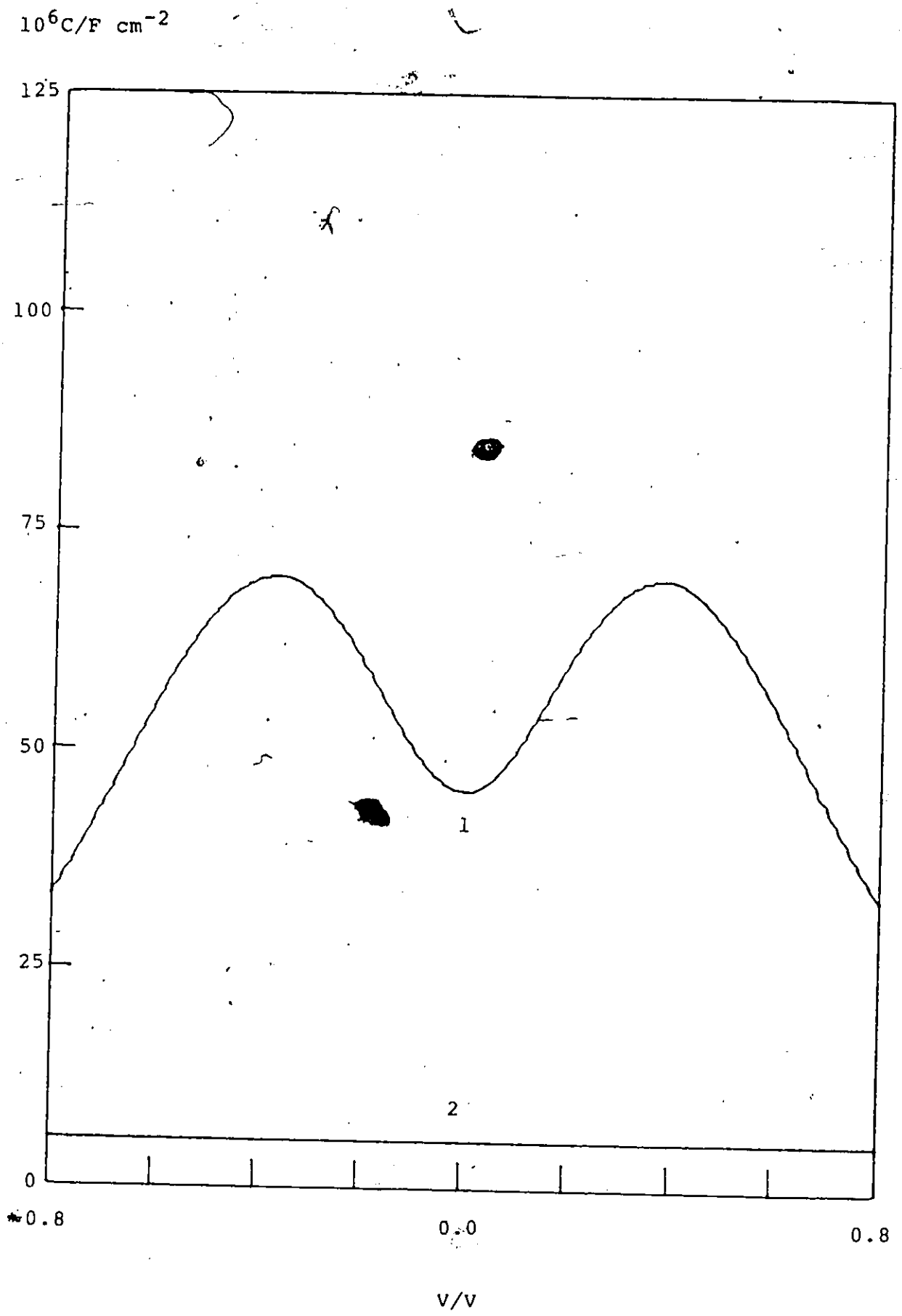
10^6C/F cm^{-2}
125
100
75
50
25
0
-0.8
0.0
0.8
V/V
1
2

5.2 Quasi-Chemical Approximation

This section will examine the consequences of incorporating a first approximate correction to the random-distribution assumption implicit in the MFA. Specifically, the nearest neighbours of a given species will be determined using the pairwise free-energies of interaction derived in Chapter 4; the MFA will be retained to account for the long-range effects of the remaining ions and dipoles.

The application of this approximation requires the modification of the constants b_{1-4} used in the definition of the effective field and potential, by subtraction of the field and potential due to the nearest-neighbours (6 for the hexagonal lattice used in the present work). These fields and potentials are defined by Fourier-Bessel integral representations, as discussed earlier.

(i) Potential due to ions

The potential due to an ion of charge $(-e_0)$ located at the origin is given by

$$(-e_0)([\rho^2+z^2]^{-1/2} + \int_0^\infty [f_1(k)e^{kz}+f_2(k)e^{-kz}]J_0(k\rho)dk) \quad [99]$$

where f_1 and f_2 are defined by eqns. 42. With $\varepsilon_1 = 1$, $\varepsilon_2 = \varepsilon = 78$, $z = 0$ and $\rho = r_0$, this expression becomes, after transforming with the substitution $u = k\rho$,

$$(-e_0/r_0)(1 + \int_0^\infty [f_1(u/r_0)+f_2(u/r_0)]J_0(u)du) \quad [100]$$

Evaluating the integral numerically and multiplying by 6, the total potential due to nearest neighbours in the limit of $\Theta = 1$ is

$$(-6e_0/r_0)[1 - 0.39491] = 3.63054.(-e_0/r_0) \quad [101]$$

The required modified mean potential constant b_3' is therefore given by

$$b_3' = b_3 - 3.63054.(-e_0/r_0) \qquad [102]$$

$$= (-e_0/r_0)[4.40603 - 3.63054]$$

$$= (-e_0/r_0).0.77549$$

(ii) Field due to ions

Differentiation of eqn. 98 leads to

$$(-e_0/r_0)(z/[\rho^2+z^2]^{-1/2} + \int_o^\infty [f_2(k)e^{kz} - f_1(k)e^{-kz}]kJ_0(k\rho)dk) \qquad [103]$$

and with the previous values of the parameters,

$$(-e_0/r_0^2)\int_o^\infty [f_2(u/r_0) - f_1(u/r_0)]kJ_0(u)du = -0.40387.(-e_0/r_0^2) \qquad [104]$$

The modified constant b_1' is therefore

$$b_1' = b_1 - 6(-e_0/r_0^2).(-0.40387) \qquad [105]$$

$$= [-7.22527 + 6 \times 0.40387](-e_0/r_0^2)$$

$$= -4.80205.(-e_0/r_0^2)$$

(iii) Potential due to dipoles

The potential due to a dipole of moment $m\langle s\rangle$ is

$$m\langle s\rangle(z/[\rho^2+z^2]^{-1/2} + \int_o^\infty [F_1(k)e^{kz} + F_2(k)e^{-kz}]kJ_0(k\rho)dk) \qquad [106]$$

where F_1 and F_2 are defined by eqns. 64. Similar manipulations provide

$$0.20773.(m\langle s\rangle/r_0^2) \qquad [107]$$

so that the modified constant b_4' may be defined by

$$b_4' = b_4 - 6 \times 0.20773(m/r_0^2) \qquad [108]$$

$$= [6.88346 - 1.24638](m/r_0^2)$$

$$= 5.63708(m/r_0^2)$$

(iv) Field due to dipoles

This is given by

$$m\langle s\rangle(3z^2/[\rho^2+z^2]^{-5/2} - [\rho^2+z^2]^{-3/2}$$

$$+ \int_o^\infty [F_2(k)e^{-kz} - F_1(k)e^{kz}]k^2J_0(k\rho)dk) \qquad [109]$$

$$= (m\langle s\rangle/r_0^3)[-1 + 0.48422]$$

$$= -0.51578.(m\langle s\rangle/r_0^3)$$

The constant b_2 is therefore modified to

$$b_2' = b_2 - 6 \times (-0.51578).(m/r_0^3) \qquad [110]$$

$$= [-14.53603 + 6 \times 0.51578](m/r_0^3)$$

$$= -11.44135(m/r_0^3)$$

which, quite fortuitously, is seen to be not too different from the effective coordination number for a dipole lattice with no imaging.

It is again of interest to consider the inner-layer capacitance predicted according to this dipole model in the absence of ionic adsorption. The counterpart of eqn. 98 is

$$1/C_1 = \qquad [111]$$

$$4\pi d \frac{1 - [P_3/P_1 - P_2^2/P_1^2 + 3\zeta''_{ww}/\zeta_{ww} - 3\zeta'^2_{ww}/\zeta^2_{ww}]b_2 m/kT}{1 + 4\pi N_w \alpha + (4\pi N_w m^2/kT - b_2 m/kT)[P_3/P_1 - P_2^2/P_1^2 + 3\zeta''_{ww}/\zeta_{ww} - 3\zeta'^2_{ww}/\zeta^2_{ww}]}$$

and in Fig. 12, the total capacity is compared for $b_2'=0$ and b_2' given by eqn. 110. Interestingly, there is not much difference between this pair of capacitance curves and that in Fig. 11; the field-dependent interaction partition function results, as expected, in slightly lower values of C, but with the additional inclusion of the mean field due to non-nearest neighbours, the "hump" behaviour is again entirely absent. Thus, even with the more realistic explicit treatment of the nearest-neighbour polarization free energy, the capacitance curve bears no resemblance either to experiment or to predictions of existing models that attempt to explain experimental behaviour in terms of molecular polarization in a dipole lattice.

Fig. 12: Double layer capacitance with no ionic specific adsorption, and nearest-neighbour interactions given by the interaction partition function ζ_{ww}, with and without non-nearest-neighbour Mean Field effect.

Curve 1: $b_2' = 0$

Curve 2: b_2' given by eqn. 97

c = 0.1 mol/l

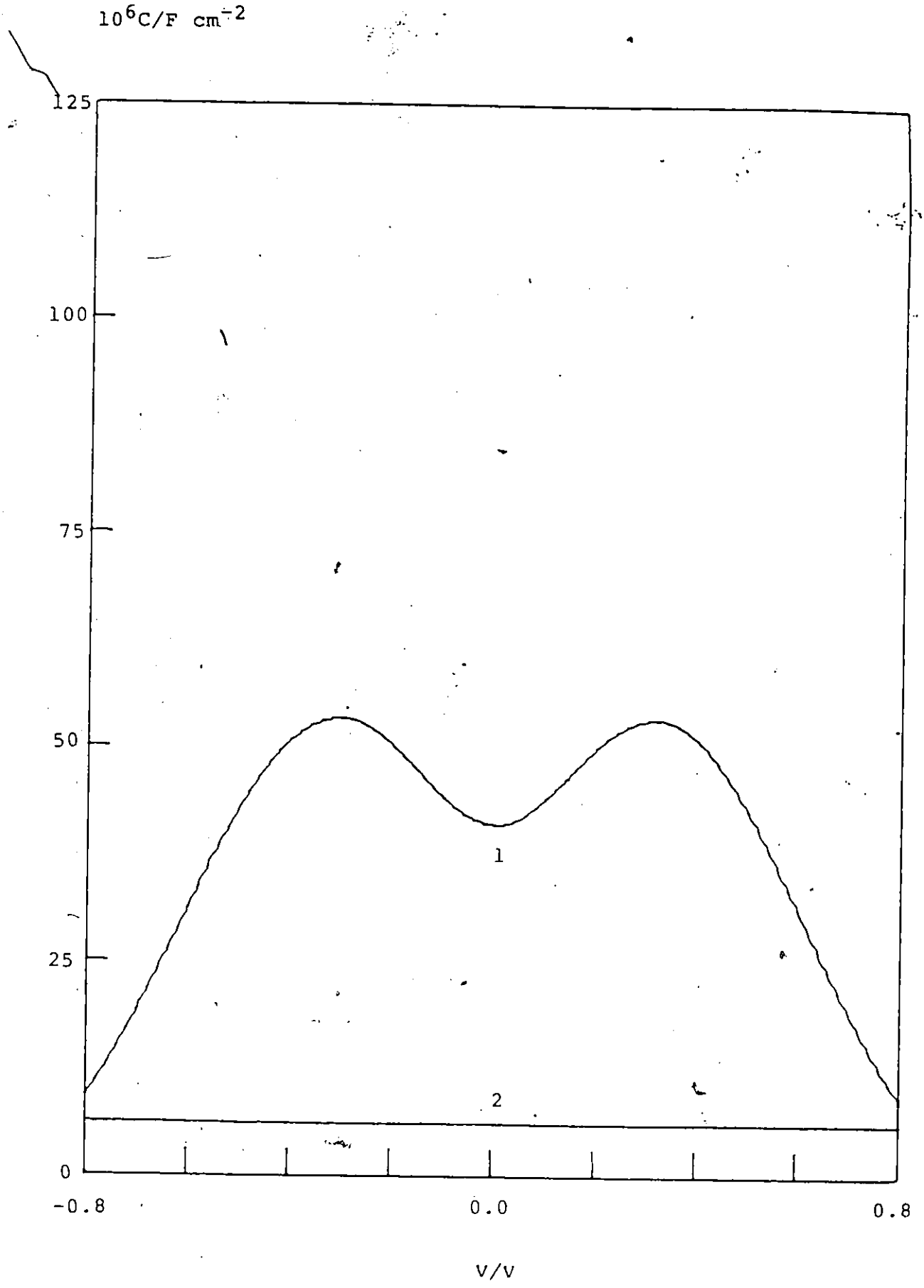
10^6C/F cm^{-2}
125
100
75
50
25
0
-0.8
0.0
0.8
V/V
1
2

According to the quasi-chemical approximation (QCA) for a two-dimensional two-component lattice, the number of species of each kind adjacent to a given site is determined by the relative magnitudes of the pairwise free energies of interaction. The relevant isotherm is, from Chapter 4,

$$K(a_{A^-}/a_{H2O}).z_a\zeta_{aa}^3/z_w\zeta_{ww}^3 = (1-\theta)^2(\delta-1+2\theta)^3/\theta^2(\delta+1-\theta)^3 \quad [112]$$

where

$$\delta^2 = 1 + 4\theta(1-\theta)(G-1); \quad G = \zeta_{aa}\zeta_{ww}/\zeta_{a\cdot w}^2$$

and the quantities ζ are the partition functions corresponding to the interaction free energies u between water dipoles (ww), ions (aa), and water dipoles and ions (aw) (defined respectively by eqns. 10, 36 and 34 of Chapter 4):

$$\zeta_{ww} = \exp(-u_{ww}/kT)$$

$$\zeta_{aa} = \exp(-u_{aa}/kT)$$

$$\zeta_{aw} = \exp(-u_{aw}/kT)$$

Application of this isotherm to the description of the adsorption of ions (bearing whole electronic charges) encounters serious problems, resulting from the enormous positive values of u_{aa}, the pairwise interaction energy between ions, relative to u_{aw} and u_{ww}. Specifically, because the corresponding Boltzmann factor $\exp(-u_{aa}/kT)$ is vanishingly small, the term $\delta-1+2\theta$ in the numerator of the isotherm becomes approximately $[1-4\theta(1-\theta)]^{1/2}-1+2\theta = 0$, so that the corresponding chemical potential term (that of the ions) becomes singular. It is, however, possible to derive an approximate form of the isotherm, by noting that δ may be written in the form

$$\delta^2 = (1-2\theta)^2[1 + 4\theta(1-\theta)G/(1-2\theta)^2] \quad [113]$$

Fig. 13: Solution of the equation

$\theta(1-\theta)^5/(1-2\theta)^6 = K$

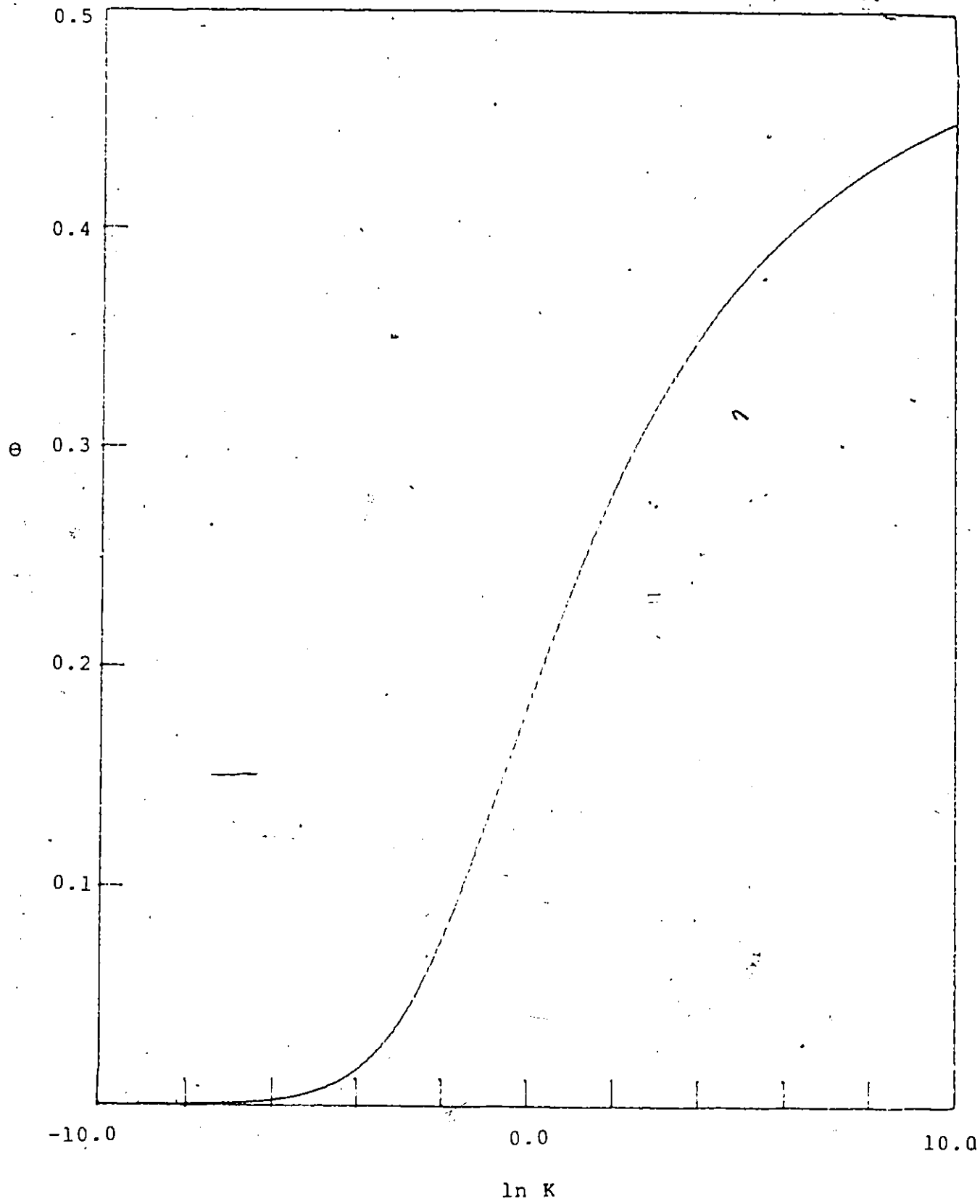

Taking the square root and expanding,

$$\delta \approx (1-2\theta)[1 + 2\theta(1-\theta)G/(1-2\theta)^2 + \ldots.]$$

$$= 1 - 2\theta + 2\theta(1-\theta)G/(1-2\theta)^2 \qquad [114]$$

Therefore

$$\delta - 1 + 2\theta \approx 2\theta(1-\theta)G/(1-2\theta) \qquad [115]$$

$$\ln(\delta - 1 + 2\theta) \approx \ln(2G) + \ln[\theta(1-\theta)/(1-2\theta)]$$

The chemical potential balance condition for the reaction 2 may be written, as in Chapter 5,

$$[\mu^{\circ}_{A^-} - RT\ln(z^{\circ}_w) - \mu^{\circ}_{H2O} + RT\ln(z^{\circ}_a)] + RT\ln(z_a\zeta^3_{aa}/z_w\zeta^3_{ww})$$

$$+ RT\ln(a_{A^-}/a_{H2O}) = 3RT\ln[(\delta-1+2\theta)/(\delta+1-2\theta)] - 2RT\ln[\theta/(1-\theta)] \qquad [116]$$

With the approximation, the right-hand member of eqn. 116 is

$$RT\ln[\theta(1-\theta)^5/(1-2\theta)^6] + 3RT\ln(G) \qquad [117]$$

since $\delta+1-2\theta$ is approximately $2(1-2\theta)$. The desired approximate isotherm is therefore

$$K_{eq}c_{A^-}\cdot z_a\zeta^3_{aa}/z_w\zeta^3_{ww}$$

$$= G^3\theta(1-\theta)^5/(1-2\theta)^6 \qquad [118]$$

or, recalling the definition of G,

$$\theta(1-\theta)^5/(1-2\theta)^6 = K_{eq}c_{A^-}\cdot\zeta^6_{aw}/\zeta^6_{ww} \qquad [119]$$

This isotherm is different from those considered earlier in that the maximum value of θ which it predicts is 1/2; the solution of this equation

$$\theta(1-\theta)^5/(1-2\theta)^6 = K \qquad [120]$$

as a function of K is shown in Fig. 13. Physically, this is because, owing to the extremely small value of $\exp(-u_{aa}/kT)$, there is virtually zero probability that two adsorbed ions will be adjacent. The maximum coverage which permits configurations with no "aa" pairs is evidently 1/2. Intuitively, however, one

would expect that for the hexagonal lattice under consideration, the limiting coverage would be that in which every ion were to be surrounded by 6 water molecules, corresponding to $\theta=1/3$. This inconsistency seems to arise from the fundamental assumption, inherent in the quasi-chemical approximation, that the pairs may be considered to be independent of one another.

When the polarization and interaction partition functions contained in the isotherm are expressed in terms of an effective potential and field defined by

$$V_{eff} = (1/2).4\pi d(q_M+q_{ion}-q_{dip}) + b_3'\theta + b_4'\langle s\rangle(1-\theta)$$

$$E_{eff} = 4\pi(q_M+q_{ion}-q_{dip}) + b_1'\theta + b_2'\langle s\rangle(1-\theta) \qquad [121]$$

it is found that the isotherm unfortunately cannot be solved for θ by the method described earlier.

It is, nevertheless, possible to obtain some insight into the physical implications of the model by considering the values of the field-dependent terms of the equilibrium constant. The value of K_{eq} must be chosen to be extremely small (of the order of 10^{-50}) to compensate for the very large values assumed by the term $(\zeta_{aw}/\zeta_{ww})^6$. This seems more reasonable on consideration of the chemical potential terms which occur in K_{eq}, in particular $\mu^o_{A^-}$. The ions in solution are stabilized by a very large, negative free energy of hydration, which, for a primary coordination number of 6, may be estimated by the approximate formula

$$-6me_0/r_0^2 = -145.3kT \text{ at } 293K \qquad [122]$$

This is to be regarded as an upper limit, since no account is taken of the Born solvation energy and interactions involving

quadrupoles and induced dipoles. The factor $\exp[\mu^{o}_{A^-}/kT]$ in the expression for K_{eq} is therefore at most $10^{-63.1}$.

However, the importance of this factor in determining the overall value of K_{eq} is also dependent on the value of standard chemical potential of adsorbed ions, μ^{o}_{a}. A major contribution to this quantity arises from the self-image energy (-8.197kT) which is very much reduced (from $-e_0^2/r_0 = -192.1kT$) by the inclusion of secondary dielectric-conductive imaging. The value of the standard chemical potential of ions in the adsorbed layer relative to that in the solution is more importantly determined by the degree of "independence" attributed to the adsorbed ions and dipoles. In other words, instead of an adsorbed lattice composed of ions and dipoles as assumed here, an intuitively more appropriate model would assume the ions to be partially hydrated, with the water molecules in the primary hydration "disc" being unable to contribute to the polarization of the lattice. In order to treat such a model using the lattice formalism retained here, the additional effect of packing species of different sizes on the lattice would have to be considered.

The results of Chapter 4 may be used to determine whether this approach would be more suitable. In the solution, the ions may be considered to be hydrated because the ion-solvent interaction energies are very much larger than the interaction energies among solvent molecules. In the adsorbed layer, however, the "independence" of these hydrated ions is determined by the relative values of the interaction energies between adsorbed ions and dipoles (u_{aw}), and the orientational potential energy of the adsorbed dipoles (which includes the self-image interaction

energy as well as that arising from polarization by the electrode and the non-nearest-neighbour mean field; cf. eqn. 42 of Chapter 4). Noting the values of the imaging constants a_1 (5.501kT) and a_2 (9.070kT) and u_{aw} as given in Figs. 7a and 7b of Chapter 4 (facing page 95), it is seen that the orientational energy of the dipoles would be typically 1/2 or 1/3 of u_{aw}, and could easily exceed u_{aw} for moderately large values of mE_{eff}/kT. Therefore, for adsorbed ions, the interaction energy with adsorbed dipoles does not seem to provide sufficiently large stabilization to justify the treatment of hydrated ions as independent entities, except, perhaps, in the vicinity of the p.z.c..

In connexion with the likely errors of the present work, the remarks at the end of Chapter 5, concerning the likely direction of the errors in the previous lattice-gas treatment of the adatom-adsorption isotherm, can be expected to apply a fortiori here, in view of the much larger interaction energies resulting from the presence of fully-charged ions. The consequence of combining the two errors in ζ_{aw} and ζ_{ww} is that the ratio of the two functions, when raised to the sixth power, becomes extremely large, implying that such interactions are possibly more important than they in fact are. The usefulness of this particular approach to the ion-adsorption lattice-statistics problem thus seems to be limited by the approximations used in the derivation of the pairwise interaction partition functions. The most unambiguous method of investigating this possibility would be to carry out a Monte-Carlo simulation; this, as noted before, would be extremely difficult, because for each value of θ

the energy of the lattice would have to be averaged (at least in principle) over all polarization states of the molecules as well as all arrangements of the dipoles and ions on the two-dimensional lattice.

6. Conclusions

The objective of this chapter has been to investigate the implications of a purely electrostatic treatment of ionic adsorption at electrodes, using the conventional lattice model for the adsorbed layer.

Attention was first directed to establishing the relationship between q_M and the charge densities q_{ion} and q_{dip} respectively associated with ionic adsorption and molecular polarization, in order to derive the expression for the differential capacitance.

Comparison was then made of the various theoretical approaches to the calculation of ionic discreteness-of-charge effects, and calculations of the corresponding dipolar discreteness potentials and fields were presented and discussed.

The use of a mean field approximation to describe all the interactions experienced by ions and dipoles in the adsorbed layer leads to the prediction of much lower capacitance than that encountered experimentally, together with almost complete suppression of the "capacitance hump" expected to result from molecular polarization. This latter result is also obtained for capacitance calculations in the assumed absence of ionic adsorption, when the mean-field constants appropriate for dielectric-conductive imaging of dipoles are used in the arguments of the polarization functions.

APPENDIX

1. Evaluation of the Lattice Sums

The convergence of the series in the expressions arising from the foregoing mean-field treatment of the electrostatic interactions may be established by standard methods, e.g. the integral test [61]. This states that an infinite series of positive terms converges if the integral between zero and infinity of the summand, with respect to the summation variable, is finite. However, the numerical evaluation of these series is complicated by the fact that they converge very slowly. For example, consider the direct evaluation of the sum

$$\sum_1^\infty \sum_{-\infty}^{\infty} 1/[a_-^2+(m-k/2)^2]^{3/2} \qquad [A.1]$$

where $a_-^2 = (z/r_0)^2 + 3k^2/4$. If k=1 and z=0, and summation of the series is to be ceased when the leading term is about 10^{-9}, it is seen that satisfaction of this condition requires that m be about 1000. For larger values of k, fewer terms will be required, but the overall result may be quite inaccurate owing to accumulation of round-off error.

Of the divers analytical methods available for the summation of slowly-convergent infinite series, those based on Laplace- and Fourier-Transformation seem to be the most readily applied.

The Laplace Transform Method has been discussed and applied at length by Wheelon [59]. Briefly, it involves the identification of the summand f(m) as the Laplace Transform of some other function, with the summation variable as the Laplace transformation parameter. This permits the transformation of the series into an improper integral which, in favourable cases, may in turn be evaluated in closed form. Specifically,

$$\sum_1^\infty f(m) = \sum_1^\infty \int_0^\infty e^{-mt} G(t)dt$$
$$= \int_0^\infty \sum_1^\infty e^{-mt} G(t)dt$$
$$= \int_0^\infty dt\ G(t)/(e^t-1) \qquad [A.2]$$

assuming that the order of integration and summation can be interchanged.

The Poisson Summation Formula [60] is

$$\sum_{-\infty}^{\infty} f(m) = \sum_{-\infty}^{\infty} \int_{-\infty}^{\infty} \exp(2\pi inx) f(x)dx \qquad [A.3]$$
$$= F(0) + 2\sum_1^\infty F(2n\pi)$$

where

$$F(t) = \int_{-\infty}^{\infty} f(x)\cos(tx)dx$$

The problem thus reduces to the evaluation of an improper integral, which is in turn effected by means of complex contour integration. The utility of this result lies in the fact that a slowly-varying function f(m) has a rapidly-varying Fourier cosine transform F(t). It can thus be applied to transform a series requiring, e.g., the evaluation of several hundred terms for a convergent estimate, into a second infinite series, in which all but the first few terms are entirely negligible.

Of these two techniques, the Laplace Transform Method has proved to be the more popular, possibly because the Laplace transform of a given function is frequently easier to evaluate than the Fourier cosine transform, and exists under less restrictive concitions.

The Laplace transform of a function G(t) exists [10] if there exist constants M and c such that $|G(t)| \leq Me^{ct}$, and the function is sectionally continuous for $t \geq 0$. If the constant c is negative, then the Laplace transform defined by

$$\int_0^\infty e^{-mt}G(t)dt \qquad [A.4]$$

exists for all $m \geq 0$. With these conditions, it is also possible to derive the Poisson Summation Formula from the integral A.2, by the following heuristic argument.

Since [61]

$$\sum_{-\infty}^{\infty} 1/(n^2+z^2) = (\pi/z)\coth(\pi z) \qquad [A.5]$$

and

$$\coth(z/2) = 1 + 2/(e^z-1) \qquad [A.6]$$

the denominator of the integral in eqn. A.2 admits the expansion

$$1/(e^t-1) = 1/t - 1/2 + 2\sum_1^\infty t/(t^2+4n^2\pi^2) \qquad [A.7]$$

Therefore

$$\int_0^\infty dt\ G(t)/(e^t-1) = \int_0^\infty (1/t-1/2)G(t)dt + 2\sum_1^\infty \int_0^\infty dt\ tG(t)/(t^2+4n^2\pi^2) \qquad [A.8]$$

The general term in this expansion may be transformed as follows:

$$\begin{aligned}\int_0^\infty dt\ tG(t)/(t^2+4n^2\pi^2) &= \int_0^\infty G(t)\left[\int_0^\infty e^{-xt}\cos(2\pi nx)dx\right]dt \\ &= \int_0^\infty \cos(2\pi nx)\left[\int_0^\infty e^{-xt}G(t)dt\right]dx \\ &= \int_0^\infty f(x)\cos(2\pi nx)dx \qquad [A.9]\end{aligned}$$

This transformation is useful in determining certain types of Laplace transforms and definite integrals involving Bessel functions (see, e.g., ref. 12) but it appears not to have been applied specifically to the summation of slowly-convergent series.

If it be supposed further that f(m) is an even function, defined for m=0, then

$$\int_0^\infty f(x)\cos(2\pi nx) = (1/2)F(2n\pi) \qquad [A.10]$$

and the first term of the right-hand member of eqn. A.8 may be identified as

$$\int_0^\infty (1/t-1/2)G(t)dt = (F(0) - f(0))/2 \qquad [A.11]$$

Therefore,

$$\sum_1^\infty f(m) = \int_0^\infty dtG(t)/(e^t-1) = -f(0)/2 + F(0)/2 + 2\sum_1^\infty F(2n\pi)/2 \qquad [A.12]$$

which is clearly equivalent to eqn. A.3.

The summands in the infinite series which are to be evaluated clearly satisfy the conditions for the validity of the foregoing argument, so that the Laplace Transform Method and the Poisson Summation Formula are in this case entirely equivalent. As will be seen presently, this equivalence permits a more computationally efficient evaluation of certain of the lattice sums for small values of z.

For irrational functions such as those occurring in the sums, the integrals can be reduced to Bassett's integral formula [11,12]:

$$\int_{-\infty}^{\infty} (x^2+a^2)^{-p-1/2}\cos(tx)dx = \pi^{1/2}(t/2a)^p K_p(at)/\Gamma(p+1/2) \qquad [A.13]$$

where K_p is the modified Bessel function of the second kind, of order p, Γ is the Gamma function, Re(a)>0, and Re(p)>-1/2. For the case under consideration, it is necessary to evaluate

$$F(t) = \int_{-\infty}^{\infty} [a^2+(x-k/2)^2]^{-p-1/2}\cos(tx)dx \quad (p=0,1,2)$$

This can be written as the sum of two integrals

$$F(t) = \int_0^\infty [a^2+(x-k/2)^2]^{-p-1/2}\cos(tx)dx + \int_0^\infty [a^2+(x+k/2)^2]^{-p-1/2}\cos(tx)dx \qquad [A.14]$$

The first integral may be transformed with the substitution u=x-k/2, which results in

$$\int_0^\infty [a^2+(x-k/2)^2]^{-p-1/2}\cos(tx)dx = \qquad [A.15]$$

$$\int_0^\infty [a^2+u^2]^{-p-1/2}\cos[t(u+k/2)]du + \int_{-k/2}^\infty [a^2+u^2]^{-p-1/2}\cos[t(u+k/2)]du$$

Similarly the second integral becomes

$$\int_0^\infty [a^2+(x+k/2)^2]^{-p-1/2}\cos(tx)dx = \qquad [A.16]$$

$$\int_0^\infty [a^2+u^2]^{-p-1/2}\cos[t(u-k/2)]du - \int_0^{k/2} [a^2+u^2]^{-p-1/2}\cos[t(u-k/2)]du$$

Since

$$\int_{-k/2}^0 [a^2+u^2]^{-p-1/2}\cos[t(u+k/2)]du$$

$$= \int_0^{k/2} [a^2+u^2]^{-p-1/2}\cos[t(u-k/2)]du \qquad [A.17]$$

the required expression for F(t) is

$$F(t) = 2\cos(tk/2)\int_0^\infty [a^2+u^2]^{-p-1/2}\cos(tu)du \qquad [A.18]$$

$$= 2\cos(tk/2).\pi^{1/2}(t/2a)^p K_p(at)/\Gamma(p+1/2)$$

The modified Bessel functions of the second kind $K_p(x)$ decay exponentially to zero with increasing x, but possess logarithmic singularities at x=0. Therefore, the first term in the right hand side of eqn. A.3 cannot be calculated by means of eqn. A.18 and the integrals must be determined separately.

Before proceeding to the details of the calculation of the lattice sums involved in the present work, it is of interest to consider the relationship between the use of the Poisson Summation Formula and the method of Mackenzie [16], applied by van der Hoff and Benson [15] and Barlow and Macdonald [14]. Since the discussion given by van der Hoff and Benson first considered the simplest of Topping's lattice sums [56], viz. that for a square dipole lattice,

$$-S_T^S(0) = 2\sum_1^\infty \sum_{-\infty}^\infty (m^2+k^2)^{-3/2} + 2\sum_1^\infty m^{-3} \qquad [A.19]$$

it seems appropriate to do likewise here. Application of the Poisson Summation Formula to the summation over m gives

$$\sum_{-\infty}^\infty (m^2+k^2)^{-3/2} = F(0) + 2\sum_1^\infty F(2n\pi) \qquad [A.20]$$

where

$$F(0) = \int_{-\infty}^\infty dx/(x^2+k^2)^{3/2}$$

$$= 2/k^2$$

$$F(t) = \int_{-\infty}^{\infty} dx\, \cos(tx)/(x^2+k^2)$$

$$= (2t/k)K_1(tk) \qquad (t\neq 0)$$

Putting $t = 2n\pi$, $n=0,1,2,\ldots$, and performing the summation over k, one obtains

$$-S_T^s = 2\sum_1^{\infty} m^{-3} + 2\sum_1^{\infty} k^{-2} + 16\pi \sum_1^{\infty}\sum_1^{\infty} K_1(2n\pi k)n/k \qquad [A.21]$$

The first two terms on the right-hand side are Riemann zeta functions, with the values [62]

$$\sum_1^{\infty} k^{-2} = \pi^2/6 \qquad [A.22]$$

$$\sum_1^{\infty} m^{-3} \approx 1.2020569$$

This transformed sum is identical to that obtained by van der Hoff and Benson [15] using a considerably less direct method. Numerically evaluating the above expression,

$$-S_T^s(0) = 9.033590 \qquad [A.23]$$

which compares favourably with the values 9.0336217 and $9.033617 < -S_T^s(0) < 9.033629$ given in refs. 15 and 56 respectively.

In order to evaluate the corresponding sum for an hexagonal lattice, van der Hoff and Benson used a counting scheme rather different from that used in the present work. The summation was decomposed into two sums for a rectangular lattice:

$$-S_T^h(0) = 2\sum_1^{\infty}\sum_{-\infty}^{\infty} (m^2+3k^2)^{-3/2} + 2\sum_1^{\infty} m^{-3}$$

$$+ 2\sum_0^{\infty}\sum_{-\infty}^{\infty} [3(k+1/2)^2+(m+1/2)^2]^{-3/2} \qquad [A.24]$$

It involves considerably less work, however, to write

$$-S_T^h(0) = 2\sum_1^{\infty}\sum_{-\infty}^{\infty} [(m-k/2)^2+3k^2/4]^{-3/2} + \sum_1^{\infty} m^{-3} \qquad [A.25]$$

Proceeding as before,

$$\sum_{-\infty}^{\infty} [(m-k/2)^2+a^2]^{-3/2} = F(0) + 2\sum_1^{\infty} F(2n\pi); \; a^2 = 3k^2/4 \qquad [A.26]$$

where in this case

$$F(0) = 2/a^2$$

$$F(t) = 2\cos(tk/2).(t/a)K_1(at) \qquad (t\neq 0)$$

Therefore

$$-S_T^h(0) = 8\pi^2/9 + 2\zeta(3) + (16\pi/a)\sum_1^\infty\sum_1^\infty K_1(2n\pi a).n(-1)^{kn}/k \qquad [A.27]$$

$$\approx 11.03419$$

which is again in satisfactory agreement with the values quoted earlier. The use of the alternative counting procedure with the Poisson Summation Formula results in the value 11.03418. In the following work, the sums for the hexagonal lattice will be evaluated directly using the form $k^2-km+m^2 = (m-k/2)^2+3k^2/4$, since the other method evidently requires twice as much work and does not succeed in eliminating the inconvenient factors of $\sqrt{3}/2$ arising from the hexagonal geometry.

2.1 Potential due to Ions and Primary Images

The expression

$$2\sum_1^\infty\sum_{-\infty}^\infty([(m-k/2)^2+a_-^2]^{-1/2} - [(m-k/2)^2+a_+^2]^{-1/2});$$

$$a_\pm^2 = 3k^2/4+(z+s\pm s)^2/r_0^2 \qquad [A.28]$$

is composed of two series which, for large values of the indices, behave approximately like harmonic series and are therefore divergent. By application of the integral test, however, the difference of these two sums is readily shown to be convergent.

(i) Summation with respect to m

This may be carried out using eqn. A.3, using

$$F(0) = 2\int_0^\infty(1/[u^2+a_-^2]^{1/2}-1/[u^2+a_+^2]^{1/2})du$$

$$= 2\ln(a_+/a_-)$$

$$F(t) = 2\int_0^\infty dx\ \cos(tx)([(x-k/2)^2+a_-^2]^{-1/2}-[(x-k/2)^2+a_+^2]^{-1/2})$$

$$= 2[K_0(a_-t) - K_0(a_+t)]\cos(tk/2) \quad (t\neq 0) \qquad [A.29]$$

(ii) Summation with respect to k

The Bessel functions in the expression for F(t) ($t\neq 0$) tend

to zero so quickly that, for all values of k, all but the first few terms will be entirely negligible, permitting the summation with respect to k to be carried out directly. The series of F(0) terms, however, converges very slowly with respect to k, and moreover does not lend itself to a second application of the Poisson Summation Formula.

From the definition of $a_{\pm}$, the expression for F(0) may be written as

$$F(0) = -\ln(1 + 4z^2/3k^2r_0^2) + \ln(1 + 4(z+2s)^2/3k^2r_0^2) \qquad [A.30]$$

so that the series of F(0) terms becomes

$$\sum_1^\infty F(0) = \sum_1^\infty [\ln(1 + 4(z+2s)^2/3r_0^2k^2) - \ln(1 + 4z^2/3r_0^2k^2)] \qquad [A.31]$$

This series is readily evaluated by noting that the application of the Weierstrass Factorization Theorem [60,61] to the function sinh y/y gives the infinite product

$$\sinh y/y = (1+y^2/\pi^2)(1+y^2/4\pi^2)(1+y^2/9\pi^2)\ldots. \qquad [A.32]$$

On taking logarithms and putting $y=2\pi(z+s\pm s)/r_0\sqrt{3}$, there results

$$\sum_1^\infty F(0) = \ln\left[\frac{\sinh 2\pi(z+2s)/r_0\sqrt{3}}{\sinh 2\pi z/r_0\sqrt{3}}\right] + \ln[z/(z+2s)] \qquad [A.33]$$

Noting that for $t=2n\pi$, $\cos(tk/2)=(-1)^{kn}$, the final expression for the lattice sum in eqn. A.28 is

$$2\sum_1^\infty\sum_{-\infty}^\infty (1/[(m-k/2)^2a_-^2]^{1/2} - 1/[(m-k)^2+a_+^2]^{1/2}) = \qquad [A.34]$$

$$2\ln\left[\frac{\sinh 2\pi(z+2s)/r_0\sqrt{3}}{\sinh 2\pi z/r_0\sqrt{3}} \cdot \frac{z}{z+2s}\right] + 8\sum_1^\infty\sum_1^\infty (-1)^{kn}[K_0(2n\pi a_-) - K_0(2n\pi a_+)]$$

(iii) Summation of k=0 terms

The sum over m for k=0 is clearly of the same form as that already considered. Consequently, rearranging from the corresponding sum between $\pm\infty$.

$$\sum_1^\infty (1/[m^2+z^2/r_0^2]^{1/2} - 1/[m^2+(z+2s)^2/r_0^2]^{1/2})$$
$$= -[r_0/z - r_0/(z+2s)] + 2\ln[(z+2s)/z]$$
$$+ 4\sum_1^\infty (K_0[2n\pi.z/r_0] - K_0[2n\pi.(z+2s)/r_0]) \qquad [A.35]$$

The efficiency of this transformation decreases markedly as z becomes close to zero; the terms $K_0[2n\pi.z/r_0]$ become very large and many in number. For such values of z, it is therefore preferable to use the Laplace Transform Method:

$$\sum_1^\infty (1/[m^2+z^2/r_0^2]^{1/2} - 1/[m^2+(z+2s)^2/r_0^2]^{1/2})$$
$$= \int_o^\infty dt[J_0(A_1t)-J_0(B_1t)]/(e^t-1);\ A_1 = z/r_0,\ B_1 = (z+2s)/r_0 \qquad [A.36]$$

To evaluate this integral conveniently, it is first necessary to integrate by parts:

$$\int_o^\infty dt[J_0(A_1t)-J_0(B_1t)]/(e^t-1) = \int_o^\infty [A_1J_1(A_1t)-B_1J_1(B_1t)]\ln(1-e^{-t})dt \qquad [A.37]$$

and apply the substitutions $u=A_1t$, $u=B_1t$ to each integral in turn:

$$\int_o^\infty A_1J_1(A_1t)\ln(1-e^{-t})dt = \int_o^\infty J_1(u)\ln(1-e^{-u/A_1})du \qquad [A.38]$$

$$\int_o^\infty B_1J_1(B_1t)\ln(1-e^{-t})dt = \int_o^\infty J_1(u)\ln(1-e^{-u/B_1})du \qquad [A.39]$$

Therefore, one obtains the alternative representation of the series in A.35:

$$\sum_1^\infty (1/[m^2+z^2/r_0^2]^{1/2} - 1/[m^2+(z+2s)^2/r_0^2]^{1/2})$$
$$= \int_o^\infty J_1(u)\ln[(1-e^{-u/A_1})/(1-e^{-u/B_1})]dt \qquad [A.40]$$

The limit of this integral as $A_1 \to 0$ is far easier to evaluate than the corresponding limit of eqn. A.35.

The potential due to ions and primary images may therefore

be represented by

$$\Phi_1 = (-e_0/r_0)T_0 \qquad [A.41]$$

where

$$T_0 = 2\ln\left[\frac{\sinh 2\pi(z+2s)/r_0\sqrt{3}}{\sinh 2\pi z/r_0\sqrt{3}} \cdot \frac{z}{z+2s}\right]$$

$$+ 8\sum_1^\infty\sum_1^\infty(-1)^{kn}[K_0(2n\pi a_-) - K_0(2n\pi a_+)]$$

$$+ 2\int_0^\infty J_1(u)\ln[(1-e^{-u/A_1})/(1-e^{-u/B_1})]du$$

and the integral has the alternative form A.35.

2.2 Potential due to Secondary Ionic Images

The series occurring in the second component of the expression for the constant b_3 are clearly of the same form as those considered in Section 2.1. The details of the transformation may therefore be omitted, and one has

$$2\sum_1^\infty\sum_{-\infty}^\infty([(m-k/2)^2+p_+^2]^{-1/2}-[(m-k/2)^2+q_+^2]^{-1/2}$$

$$+[(m-k/2)^2+p_-^2]^{-1/2}-[(m-k/2)^2+q_-^2]^{-1/2}) = \qquad [A.42]$$

$$2\ln\left[\frac{\sinh[2\pi(2jd+2s+z)/r_0\sqrt{3}]\sinh[2\pi(2jd-2s-z)/r_0\sqrt{3}]}{\sinh[2\pi(2jd+z)/r_0\sqrt{3}]\sinh[2\pi(2jd-z)/r_0\sqrt{3}]}\right]$$

$$+ 2\ln\left[\frac{(2jd+z)(2jd-z)}{(2jd+2s+z)(2jd-2s-z)}\right]$$

$$+ 8\sum_1^\infty\sum_1^\infty(-1)^{kn}[K_0(2n\pi p_+)-K_0(2n\pi q_+)+K_0(2n\pi p_-)-K_0(2n\pi q_-)]$$

and

$$2\sum_1^\infty(1/[m^2+(2jd+z)^2/r_0^2]^{1/2} - 1/[m^2+(2jd+2d+z)^2/r_0^2]^{1/2}$$

$$+ 1/[m^2+(2jd-z)^2/r_0^2]^{1/2} - 1/[m^2+(2jd-2s-z)^2/r_0^2]^{1/2})$$

$$= r_0/(2jd+2s+z) - r_0/(2jd+z) + r_0/(2jd-2s-z) - r_0/(2jd-z)$$

$$+ 2\ln\left[\frac{(2jd+z)(2jd-z)}{(2jd+2s+z)(2jd-2s-z)}\right]$$

$$+ 4\sum_1^\infty (K_0[2n\pi(2jd+z)/r_0] + K_0[2n\pi(2jd-z)/r_0]$$

$$- K_0[2n\pi(2jd+2s+z)/r_0] - K_0[2n\pi(2jd-2s-z)/r_0]). \quad [A.43]$$

In this case, it is not necessary to use the Laplace Transform Method to construct an alternative representation, since the constants in each square root term are never zero for the values of z being considered (and for which the solution is valid in the first place). On adding the transformed series A.42 and A.43, the logarithmic terms involving ratios of linear factors cancel, and the result can be written

$$r_0/(2jd+2s+z)+r_0/(2jd-2s-z)-r_0/(2jd+z)-r_0/(2jd-z) + T_j \quad [A.44]$$

where

$$T_j = 2\ln\left[\frac{\sinh[2\pi(2jd+2s+z)/r_0\sqrt{3}]\sinh[2\pi(2jd-2s-z)/r_0\sqrt{3}]}{\sinh[2\pi(2jd+z)/r_0\sqrt{3}]\sinh[2\pi(2jd-z)/r_0\sqrt{3}]}\right]$$

$$+ 8\sum_1^\infty\sum_1^\infty(-1)^{kn}[K_0(2n\pi p_+)-K_0(2n\pi q_+)+K_0(2n\pi p_-)-K_0(2n\pi q_-)]$$

$$+ 4\sum_1^\infty (K_0[2n\pi(2jd+z)/r_0] + K_0[2n\pi(2jd-z)/r_0]$$

$$- K_0[2n\pi(2jd+2s+z)/r_0] - K_0[2n\pi(2jd-2s-z)/r_0])$$

Calculation of the secondary image potential thus reduces to the summation of the two series

$$- \sum_1^\infty \beta^j T_j$$

$$+ \sum_1^\infty \beta^j [r_0/(2jd+2s+z)+r_0/(2jd-2s-z)-r_0/(2jd+z)-r_0/(2jd-z)] \quad [A.45]$$

The first of these series converges very rapidly and can therefore be evaluated directly; the second requires application of the Laplace Transform Method, as follows.

It is possible to write

$$\sum_1^\infty \beta^j [r_0/(2jd+2s+z) + r_0/(2jd-2s-z)]$$

$$= (r_0/2d)\sum_1^\infty e^{-jC}[1/(j+B_2) + 1/(j-B_2)] \qquad [A.46]$$

where $C = -\ln \beta$ and $B_2 = (2s+z)/2d$. Since

$$1/(j+B_2) + 1/(j-B_2) = 2j/(j^2-B_2^2) \qquad [A.47]$$

the general term of the series may be identified as the Laplace transform (with parameter j) of the function G(t) defined by

$$G(t) = 0 \qquad (t<C)$$

$$= 2\cosh B_2(t-C) \qquad (t \geq C) \qquad [A.48]$$

Therefore

$$\sum_1^\infty \int_0^\infty e^{-jt}G(t)dt = \int_C^\infty dt\ 2\cosh B_2(t-C)/(e^t-1)$$

$$= \int_0^\infty du\ 2\cosh(b_2u)/(e^{u+C}-1) \qquad [A.49]$$

Clearly, the same procedure may be applied to the other series, so that, defining $A_2 = z/2d$,

$$\sum_1^\infty \beta^j[r_0/(2jd+2s+z)+r_0/(2jd-2s-z)-r_0/(2jd+z)-r_0/(2jd-z)]$$

$$= (r_0/d)\int_0^\infty du[\cosh B_2u \mp \cosh A_2u]/(e^{u+C}-1) \qquad [A.50]$$

The final expression for the constant b_3 is therefore

$$b_3 = \Phi_1 + \Phi_2$$

$$= (-e_0/r_0)[T_0 + \sum_1^\infty \beta^j T_j + (r_0/d)\int_0^\infty du[\cosh B_2u - \cosh A_2u]/(e^{u+C}-1)] \qquad [A.51]$$

where T_0 and T_j are defined by eqns. A.41 and A.44 respectively.

3.1 Field due to Ions and Primary Images

The field corresponding to the potential evaluated in the previous two sections is obtained by differentiation, which requires application of the following identities:

$$da_\pm/dz = (z+s\pm s)/r_0^2 a_\pm \qquad [A.52]$$

$$dp_\pm/dz = \pm(2jd\pm z)/r_0^2 p_\pm \qquad [A.53]$$

$$dq_\pm/dz = \pm(2jd\pm 2s\pm z)/r_0^2 q_\pm \qquad [A.54]$$

$$(d/dz)\ln(\sinh az) = a \coth z \qquad [A.55]$$

$$(d/dz)K_0(az) = -\,a\,K_1(az) \qquad [A.56]$$

The field due to the ions and the primary images is

$$-\partial\Phi_1/\partial z = (-e_0/r_0^2).T_0' \qquad [A.57]$$

where

$$T_0' = (4\pi/\sqrt{3}).(\coth[2\pi z/r_0\sqrt{3}] - \coth[2\pi(z+2s)/r_0\sqrt{3}]) + r_0^2/(z+2s)^2 - r_0^2/z^2$$
$$+ 16\pi\sum_1^\infty\sum_1^\infty(-1)^{kn}n[K_1(2n\pi a_-).z/r_0a_- - K_1(2n\pi a_+).(z+2s)/r_0a_+]$$
$$+ 8\pi\sum_1^\infty n(K_1[2n\pi z/r_0] - K_1[2n\pi(z+2s)/r_0])$$

The last two lines are also the result of applying the Poisson Summation Formula to the series

$$2\sum_1^\infty([m^2+z^2/r_0^2]^{-1/2}.z/r_0 - [m^2+(z+2s)^2/r_0^2]^{-1/2}.(z+2s)/r_0) \qquad [A.58]$$

In contrast to the corresponding potential, the series in this expression are individually convergent; however, as before, the above transformation is not well-behaved for small values of z. The alternative Laplace transform representation of the first series is

$$\sum_1^\infty[m^2+z^2/r_0^2]^{-3/2}.z/r_0 = \sum_1^\infty\int_0^\infty e^{-mt}tJ_1(tz/r_0)dt$$
$$= (1/A_1^2)\int_0^\infty du\, ue^{-u/A_1}J_1(u)/(1-e^{-u/A_1}) \qquad [A.59]$$

This tends to zero as z approaches 0, and may be accurately evaluated by Gauss-Laguerre quadrature.

3.2 Field due to Secondary Ionic Images

By similar manipulations, it follows that

$$-\partial\Phi_2/\partial z = (-e_0/r_0^2)[\sum_1^\infty\beta^jT_j'$$
$$- (r_0^2/2d^2)\int_0^\infty du\, u[\sinh B_2u - \sinh A_2u]/(e^{u+C}-1)] \qquad [A.60]$$

where

$$T_j' = (4\pi/\sqrt{3})[\coth(2\pi(2jd+z)/r_0\sqrt{3}) - \coth(2\pi(2jd+2s+z)/r_0\sqrt{3})$$
$$- \coth(2\pi(2jd-z)/r_0\sqrt{3}) + \coth(2\pi(2jd-2s-z)/r_0\sqrt{3})] +$$

$$16\pi\sum_1^\infty\sum_1^\infty(-1)^{kn}n[K_1(2n\pi p_+).(2dj+z)/r_0p_+ - K_1(2n\pi q_+).(2jd+2s+z)/r_0q_+$$
$$-K_1(2n\pi p_-).(2jd-z)/r_0p_- + K_1(2n\pi q_-).(2jd-2s-z)/r_0q_-]$$
$$+ 8\pi\sum_1^\infty(K_1[2n\pi(2jd+z)/r_0] - K_1[2n\pi(2jd+2s+d)/r_0]$$
$$- K_1[2n\pi(2jd-z)/r_0] + K_1[2n\pi(2jd-2s-z)/r_0])$$

The final expression for the constant b_1 is therefore

$$b_1 = (-e_0/r_0^2)[T_0' + \sum_1^\infty\beta^jT_j'$$
$$- (r_0^2/2d^2)\int_0^\infty du\ u[\sinh B_2u - \sinh A_2u]/(e^{u+C}-1)] \qquad [A.61]$$

where T_0' and T_j' are defined by eqns. A.57 and A.60 respectively.

4.1 Potential due to Dipoles and Primary Images

Each of the lattice sums appearing in the expression for b_4 is also included in the expressions for the field due to ions and images.

$$2\sum_1^\infty\sum_{-\infty}^\infty[(m-k/2)^2+a_\pm^2]^{-3/2}.(z+s\pm s)/r_0$$
$$+ 2\sum_1^\infty[m^2+(z+s\pm s)^2/r_0^2]^{-3/2}.(z+s\pm s)/r_0$$
$$= (4\pi/\sqrt{3})\coth[2\pi(z+s\pm s)/r_0\sqrt{3}]$$
$$- r_0^2/(z+s\pm s)^2$$
$$+ 16\pi\sum_1^\infty\sum_1^\infty(-1)^{kn}nK_1(2n\pi a_\pm).(z+s\pm s)/r_0a_\pm$$
$$+ 8\pi\sum_1^\infty nK_1[2n\pi(z+s\pm s)] \qquad [A.62]$$

The potential due to dipoles and their primary images is given by the sum of these two series, not the difference as for the ionic field expressions:

$$\Psi_1 = (m/r_0^2)U_0 \qquad [A.63]$$

where

$$U_0 = (4\pi/\sqrt{3})(\coth[2\pi z/r_0\sqrt{3}] + \coth[2\pi(z+2s)/r_0\sqrt{3}])$$
$$- [r_0^2/(z+2s)^2 + r_0^2/z^2]$$
$$+ 16\pi\sum_1^\infty\sum_1^\infty(-1)^{kn}n[K_1(2n\pi a_+).(z+2s)/r_0a_+ + K_1(2n\pi a_-).z/r_0a_-]$$
$$+ 8\pi\sum_1^\infty n(K_1[2n\pi(z+2s)/r_0] + K_1[2n\pi z/r_0])$$

4.2 Potential due to Secondary Dipolar Images

Again, some of the results of the foregoing analysis may be applied again here, but when the dielectric image series is constructed, the summation with respect to j will be different, because of the addition (instead of subtraction) of the series.

$$2\sum_1^\infty\sum_{-\infty}^{\infty}[(m-k/2)^2+p_\pm^2]^{-3/2}.(2jd\pm z)/r_0$$
$$+\ 2\sum_1^\infty[m^2+(2jd\pm z)^2/r_0^2]^{-3/2}.(2jd\pm z)/r_0$$
$$=(4\pi/\sqrt{3})\coth[2\pi(2jd\pm z)/r_0\sqrt{3}]$$
$$+\ 16\pi\sum_1^\infty\sum_1^\infty(-1)^{kn}nK_1(2n\pi p_\pm).(2jd\pm z)/r_0p_\pm$$
$$-\ r_0^2/(2jd\pm z)^2+8\pi\sum_1^\infty nK_1[2n\pi(2jd\pm z)/r_0] \qquad [A.64]$$

$$2\sum_1^\infty\sum_{-\infty}^{\infty}[(m-k/2)^2+q_\pm]^{-3/2}.(2jd\pm 2s\pm z)/r_0$$
$$+\ 2\sum_1^\infty[m^2+(2jd\pm 2s\pm z)^2/r_0^2]^{-3/2}.(2jd\pm 2s\pm z)/r_0$$
$$=(4\pi/\sqrt{3})\coth[2\pi(2jd\pm 2s\pm z)/r_0\sqrt{3}]$$
$$+\ 16\pi\sum_1^\infty\sum_1^\infty(-1)^{kn}nK_1(2n\pi q_\pm).(2jd\pm 2s\pm z)/r_0q_\pm$$
$$-\ r_0^2/(2jd\pm 2s\pm z)^2+8\pi\sum_1^\infty nK_1[2n\pi(2jd\pm 2s\pm z)/r_0] \qquad [A.65]$$

Subtracting the the sum of the two series A.65 from the sum of the two series A.64 provides

$$U_j + 2r_0^2[1/(2jd-2s-z)^2+1/(2jd+2s+z)^2-1/(2jd-z)^2-1/(2jd+z)^2]$$

where

$$U_j=(4\pi/\sqrt{3})[\coth(2\pi(2jd+z)/r_0\sqrt{3})+\coth(2\pi(2jd-z)/r_0\sqrt{3})$$
$$-\coth(2\pi(2jd+2s+z)/r_0\sqrt{3})-\coth(2\pi(2jd-2s-z)/r_0\sqrt{3})]$$
$$+\ 16\pi\sum_1^\infty\sum_1^\infty(-1)^{kn}n[K_1(2n\pi p_+).(2dj+z)/r_0p_+ + K_1(2n\pi p_-).(2jd-z)/r_0p_-$$
$$-\ K_1(2n\pi q_+).(2jd+2s+z)/r_0q_+ - K_1(2n\pi q_-).(2jd-2s-z)/r_0q_-]$$
$$+\ 8\pi\sum_1^\infty n(K_1[2n\pi(2jd+z)/r_0]+K_1[2n\pi(2jd-z)/r_0]$$
$$-\ K_1[2n\pi(2jd+2s+z)/r_0]-K_1[2n\pi(2jd-2s-z)/r_0]) \qquad [A.66]$$

and as before the evaluation of the secondary image potential

$$\Psi_2=(m/r_0^2)[\sum_1^\infty\beta^jU_j \qquad [A.67]$$

$$+ \sum_1^\infty \beta^j r_0^2[1/(2jd-2s-z)^2+1/(2jd+2s+z)^2-1/(2jd-z)^2-1/(2jd+z)^2]$$

reduces to the summation of the second, slowly-convergent series of reciprocal quadratic terms. This can be written

$$(r_0/2d)^2\sum_1^\infty e^{-jC}[1/(j+B_2)^2 + 1/(j-B_2)^2 - 1/(j+A_2)^2 - 1/(j-A_2)^2] \quad [A.68]$$

using the previous notation. Observing that

$$e^{-jC}/(j\pm A_2)^2 = \int_o^\infty G_a(t)e^{-jt}dt \quad [A.69]$$

$$e^{-jC}/(j\pm B_2)^2 = \int_o^\infty G_b(t)e^{-jt}dt \quad [A.70]$$

where

$$G_a(t) = 0 \qquad (t<C)$$

$$= (t-C)\exp[\pm A_2(t-C)] \qquad (t\geq C)$$

and

$$G_b(t) = 0 \qquad (t<C)$$

$$= (t-C)\exp[\pm B_2(t-C)] \qquad (t\geq C)$$

the series may be transformed to

$$\sum_1^\infty e^{-jC}/(j\pm A_2)^2 = \int_o^\infty du\ ue^{\pm A_2 u}/(e^{u+C}-1) \quad [A.71]$$

$$\sum_1^\infty e^{-jC}/(j\pm B_2)^2 = \int_o^\infty du\ ue^{\pm B_2 u}/(e^{u+C}-1) \quad [A.72]$$

The final expression for the constant b_4 is therefore

$$b_4 = (m/r_0^2)[U_0 + \sum_1^\infty \beta^j U_j \quad [A.73]$$

$$+ (r_0^2/2d^2)\int_o^\infty du\ u[\cosh B_2 u - \cosh A_2 u]/(e^{u+C}-1)]$$

where U_0 and U_j are defined by eqns. A.63 and A.66 respectively.

5.1 Field due to Dipoles and Primary Images

The deduction of the fields corresponding to the potentials calculated in Sections 4.1 and 4.2 requires the following identities in addition to eqns. A.52 - A.56:

$$(d/dz)K_1(az) = -(a/2)[K_0(az)+K_2(az)] \quad [A.74]$$

$$K_2(az) = K_0(az) + 2K_1(az)/az \quad [A.75]$$

$$(d/dz)\coth(az) = -a\ \mathrm{cosech}^2(az) \quad [A.76]$$

$$(d/dz)[K_1(2n\pi a_{\pm}).(z+s\pm s)/r_0 a_{\pm}] \qquad [A.77]$$

$$= K_1(2n\pi a_{\pm})/r_0 a_{\pm} - 2n\pi.K_2(2n\pi a_{\pm}).(z+s\pm s)^2/r_0{}^3 a_{\pm}{}^2$$

Accordingly, the field due to dipoles and primary images is

$$-\partial\Psi_1/\partial z = (m/r_0 3)U_0' \qquad [A.78]$$

where

$$U_0' = (8\pi^2/3)(\mathrm{cosech}^2[2\pi z/r_0\sqrt{3}] + \mathrm{cosech}^2[2\pi(z+2s)/r_0\sqrt{3}]$$

$$- 16\pi\textstyle\sum_1^\infty\sum_1^\infty(-1)^{kn}n[K_1(2n\pi a_+)/a_+ + K_1(2n\pi a_-)/a_-]$$

$$+32\pi^2\textstyle\sum_1^\infty\sum_1^\infty(-1)^{kn}n^2[K_2(2n\pi a_+).(z+2s)^2/r_0{}^2 a_+{}^2 + K_2(2n\pi a_-).z^2/r_0{}^2 a_-{}^2]$$

$$- 2r_0{}^3[1/(z+2s)^3 + 1/z^3]$$

$$+ 8\pi^2\textstyle\sum_1^\infty n^2(K_2[2n\pi(z+2s)/r_0] + K_2[2n\pi z/r_0]$$

$$+ K_0[2n\pi(z+2s)/r_0] + K_0[2n\pi z/r_0])$$

The series of k=0 terms has an alternative Laplace transform representation which follows from the differentiation of the corresponding expressions for the ionic field and dipole potential:

$$\textstyle\sum_1^\infty([m^2+z^2/r_0{}^2]^{-5/2}.3z^2/r_0{}^2 - [m^2+z^2/r_0{}^2]^{-3/2})$$

$$= \textstyle\int_0^\infty dt\ t[J_1(A_1 t)/A_1 - tJ_0(A_1 t)]/[e^t-1]$$

$$= (1/A_1{}^3)\textstyle\int_0^\infty du\ ue^{-u/A_1}[J_1(u)-uJ_0(u)]/[1-e^{-u/A_1}] \qquad [A.79]$$

and the Poisson Summation Formula may be retained for the series involving $(z+2s)/r_0$.

5.2 Field due to Secondary Dipolar Imaging

The counterparts of eqn. A.77 for use in the secondary-image series are

$$(d/dz)[K_1(2n\pi p_{\pm}).(2jd\pm z)/r_0 p_{\pm}] \qquad [A.80]$$

$$= \pm[K_1(2n\pi p_{\pm})/r_0 p_{\pm} - K_2(2n\pi p_{\pm}).2n\pi(2jd\pm z)^2/r_0{}^3 p_{\pm}{}^2]$$

$$(d/dz)[K_1(2n\pi q_{\pm}).(2jd\pm 2s\pm z)/r_0 q_{\pm}] \qquad [A.81]$$

$$= \pm[K_1(2n\pi q_{\pm})/r_0 q_{\pm} - K_2(2n\pi q_{\pm}).2n\pi(2jd\pm 2s\pm z)^2/r_0{}^3 q_{\pm}{}^2]$$

Therefore, the final expression for the field at the origin due to a lattice of adsorbed dipoles, and all induced dipoles induced by them, is

$$b_2 = (m/r_0^3)[(r_0^3/4d^3).\int_0^\infty du\ u^2(\sinh B_2u-\sinh A_2u)/(e^{u+C}-1) + U_0' + \sum_1^\infty \beta^j U_j'] \qquad [A.82]$$

where U_0' is defined in eqn. A.78, and

$$\begin{aligned}U_j' = {} & (8\pi^2/3)[\operatorname{cosech}^2(2\pi(2jd+z)/r_0\sqrt{3}) - \operatorname{cosech}^2(2\pi(2jd-z)/r_0\sqrt{3}) \\ & + \operatorname{cosech}^2(2\pi(2jd+2s+z)/r_0\sqrt{3}) + \operatorname{cosech}^2(2\pi(2jd-2s-z)/r_0\sqrt{3})] \\ & + 32\pi^2\sum_1^\infty\sum_1^\infty(-1)^{kn}n^2[K_2(2n\pi p_+).(2jd+z)^2/r_0^2p_+^2 \\ & - K_2(2n\pi p_-).(2jd-z)^2/r_0^2p_-^2 - K_2(2n\pi q_+).(2jd+2s+z)/r_0^2q_+^2 \\ & + K_2(2n\pi q_-).(2jd-2s-z)^2/r_0^2q_-^2] \\ & - 16\pi\sum_1^\infty\sum_1^\infty(-1)^{kn}n[-K_1(2n\pi p_+)/p_+ + K_1(2n\pi p_-)/p_- \\ & + K_1(2n\pi q_+)/q_+ - K_1(2n\pi q_-)/q_-] \\ & + 8\pi^2\sum_1^\infty n^2(K_2[2n\pi(2jd+z)/r_0] + K_0[2n\pi(2jd+z)/r_0] \\ & - K_2[2n\pi(2jd+2s+z)/r_0] - K_0[2n\pi(2jd+2s+z)/r_0] \\ & - K_2[2n\pi(2jd-z)/r_0] - K_0[2n\pi(2jd-z)/r_0] \\ & + K_2[2n\pi(2jd-2s-z)/r_0] + K_0[2n\pi(2jd-2s-z)/r_0])\end{aligned}$$

5.3 Generalization of Topping's Lattice Sum

The sum $S_T^h(z)$ given by eqn. 72 is simply the dipolar term of $-\partial\Psi/\partial z$ as given by eqn. A.78. Therefore

$$\begin{aligned}S_T^h(z) = {} & (8\pi^2/3)\operatorname{cosech}^2[2\pi z/r_0\sqrt{3}] - 2r_0^2/z^2 \\ & - 16\pi\sum_1^\infty\sum_1^\infty(-1)^{kn}nK_1(2n\pi a_-)/a_- \\ & + 32\pi^2\sum_1^\infty\sum_1^\infty(-1)^{kn}n^2K_2(2n\pi a_-).z^2/r_0^2a_- \\ & - 2r_0^3/z^3 + 2r_0^2/z^2 \\ & + 8\pi^2\sum_1^\infty n^2(K_2[2n\pi z/r_0] + K_0[2n\pi z/r_0])\end{aligned} \qquad [A.83]$$

The last two lines of this expression have the alternative Laplace transform representation A.79, and so tend to $-2\zeta(3)$ as z approaches zero. Also, in this limit, a_-^2 approaches $3k^2/4$ and

the singular parts of the first two terms cancel; this is easily seen by considering the hyperbolic cotangent for small values of its argument:

$$\coth(x) \approx 1/x + x/3 \qquad [A.84]$$

Differentiating and changing sign:

$$\mathrm{cosech}^2(x) \approx 1/x^2 - 1/3 \qquad [A.85]$$

Therefore, as z tends to zero,

$$(8\pi^2/3)\mathrm{cosech}^2(2\pi z/r_0\sqrt{3}) - 2r_0^2/z^2$$
$$\approx (8\pi^2/3)[3r_0^2/4\pi^2z^2 - 1/3] - 2r_0^2/z^2$$
$$= -8\pi^2/9 \qquad [A.86]$$

and the expression A.83 reduces to A.27.

REFERENCES

1. J.O'M. Bockris, M.A.V. Devanathan and K. Mueller
   Proc. Roy. Soc. Lond. **A274**: 55 (1963)
2. B.B. Damaskin and A.N. Frumkin
   Electrochim. Acta **19**: 173 (1974)
3. R. Parsons
   J. Electroanal. Chem. **59**: 229 (1975)
4. W.R. Fawcett
   J. Phys. Chem. **82**: 1385 (1978)
5. J.O'M. Bockris and A.K.N. Reddy
   "Modern Electrochemistry" (Plenum N.Y., 1972) v. 2
6. H. Wroblowa and K. Mueller
   J. Phys. Chem. **73**: 3528 (1969)
7. H. Wroblowa, Z. Kovac and J.O'M. Bockris
   Trans. Faraday Soc. **61**: 1523 (1965)
8. A.N. Frumkin
   Phys. Z. Sowjetunion **4**: 259 (1933)
9. D. Henderson
   Progr. Surf. Sci. **13**: 197 (1982)
10. E. Kreyszig
    "Advanced Engineering Mathematics" (3ed., Wiley 1972)
11. G.N. Watson
    "A Treatise on the Theory of Bessel Functions" (C.U.P. 1922)
12. A. Gray, G.B. Mathews and T.M. Macrobert
    "A Treatise on Bessel Functions and their Application to Physics" (2ed., Macmillan 1952)
13. N.F. Mott and R.J. Watts-Tobin
    Electrochim. Acta **4**: 79 (1961)

14. C.A. Barlow, Jr, and J.R. Macdonald
J. Chem. Phys. **43**: 2575 (1965)

15. B.M.E. van der Hoff and G.C. Benson
Can. J. Phys. **31**: 1087 (1950)

16. J.K. Mackenzie
Thesis, University of Bristol (1950)

17. J.R. Macdonald and C.A. Barlow, Jr
J. Chem. Phys. **44**: 202 (1966)

18. B.V. Ershler
Zh. Fiz. Khim. **20**: 679 (1946)

19. S. Levine, G.M. Bell and D. Calvert
Can. J. Chem. **40**: 518 (1962)

20. C.A. Barlow and J.R. Macdonald
J. Chem. Phys. **40**: 1535 (1964)

21. P.P. Ewald
Ann. Phys. **54**: 519,557 (1917)

22. S. Levine, K. Robertson, G.M. Bell and J. Mingins
J. Electroanal. Chem. **47**: 395 (1973)

23. J.R. Macdonald and C.A. Barlow, Jr
Can. J. Chem. **43**: 2985 (1965)

24. F.H. Stillinger, Jr
J. Chem. Phys. **35**: 1584 (1961)

25. F.P. Buff and F.H. Stillinger, Jr
J. Chem. Phys. **39**: 1911 (1963)

26. H.D. Hurwitz
J. Chem. Phys. **48**: 1541 (1968)

27. C.A. Croxton

"Liquid State Physics" (C.U.P. 1972)

28. V.A. Kir'yanov
Elektrokhimiya **6**: 1173 (1970)

29. V.A. Kir'yanov, V.S. Krylov and B.B. Damaskin
Elektrokhimiya **6**: 553 (1970)

30. V.S. Krylov and V.A. Myamlin
Elektrokhimiya **13**: 210 (1971)

31. V.S. Krylov, V.A. Kir'yanov and I.F. Fishtik
Elektrokhimiya **16**: 340 (1980)

32. V.S. Krylov, V.A. Kir'yanov and I.F. Fishtik
J. Elektroanal. Chem. **109**: 115 (1980)

33. V.A. Myamlin and V.S. Krylov
Elektrokhimiya **13**: 1581 (1977)

34. V.S. Krylov
Elektrokhimiya **14**: 1315 (1978)

35. V.S. Krylov
Elektrokhimiya **4**: 763 (1968)

36. J.R. Macdonald and C.A. Barlow, Jr
J. Electrochem. Soc. **113**: 978 (1966)

37. J.O'M. Bockris and M.A. Habib
J. Res. Inst. Catal., Hokkaido Univ. **23**: 47 (1975)

38. F.B. Buff and N.S. Goel
J. Chem. Phys. **51**: 4983,5363 (1963)

39. J.R. Clay, N.S. Goel and F.P. Buff
J. Chem. Phys. **56**: 4245 (1972)

40. S. Levine and K. Robinson
J. Electroanal. Chem. **41**: 159 (1973)

41. K. Robinson and S. Levine

J. Electroanal. Chem. **47**: 395 (1973)

42. D.C. Grahame

J. Chem. Phys. **18**: 903 (1950)

43. F.H. Stillinger, Jr and J.G. Kirkwood

J. Chem. Phys. **33**: 1282 (1960)

44. D.M. Newns

J. Chem. Phys. **50**: 4572 (1969)

45. M.A. Vorotyntsev

Elektrokhimiya **16**: 1350 (1980)

46. M.A. Vorotyntsev, A.A. Kornyshev and A.I. Rubinshtein

Elektokhimiya **16**: 73 (1980)

47. A.A. Kornyshev, A.I. Rubinshtein and M.A. Vorotyntsev

Phys. Stat. Solidi **b84**: 125 (1977)

48. N.D. Lang and W. Kohn

Phys. Rev. **B7**: 3541 (1973)

49. J.-P. Badiali. M.-L. Rosinberg and J. Goodisman

J. Electroanal. Chem. **150**: 25 (1983)

50. W. Schmickler

J. Electroanal. Chem. **150**: 19 (1983)

51. W. Schmickler

J. Electroanal. Chem. **157**: 1 (1983)

52. A.N. Frumkin

Z. Phys. Chem. **116**: 466 (1925)

53. C.A. Barlow, Jr and J.R. Macdonald

Adv. Electrochem. Electrochem. Eng. **6**: 1 (1968)

54. C.J.F. Boettcher

"Theory of Electric Polarization" (2ed., Elsevier 1972) v.1

55. J.R. Macdonald and C.A. Barlow, Jr
J. Chem. Phys. **36**: 3062 (1962)

56. J. Topping
Proc. Roy. Soc. Lond. **A114**: 67 (1927)

57. M.J.D. Powell, in P. Rabinowitz (ed.)
"Numerical Methods for Nonlinear Algebraic Equations"
(Gordon and Breach Science Publishers, London, 1970)

58. Digital Equipment Corporation
"Subroutine RTMI", Scientific Subroutines Package (1975).

59. A.D. Wheelon
"A Short Table of Summable Series and Integrals Involving
Bessel Functions", (Holden-Day 1968)

60. W. Rudin
"Real and Complex Analysis" (2ed., McGraw-Hill 1974)

61. M.R. Spiegel
"Theory and Problems of Complex Variables", Schaum's Outline
Series (McGraw-Hill 1974)

62. M. Abramowitz and I.A. Stegun
"Handbook of Mathematical Functions" (Dover, N.Y. 1965)

63. D.C. Grahame
Z. Elektrochem. **62**: 264 (1958)

SUMMARY OF ORIGINAL CONTRIBUTIONS

Electrostatically consistent procedures have been devised for the calculation of capacitance behaviour of electrode-solution interfaces, according to the widely-assumed primitive model of the double layer, resulting from the adsorption of ions and neutral molecules. These considerations have led to a clarification of the supposed polarization "catastrophe", noted by Cooper and Harrison and subsequently identified in a number of treatments of double layer capacitance, but avoided in the earlier analysis by Macdonald and Barlow.

A new theory of interactions among charged and polarized species adsorbed at a metal surface has been developed. By calculation of effective pairwise interaction free energies and application of approximations from lattice-gas theory, the treatment permits inclusion of short-range ordering effects implicitly ignored by existing approaches based on mean-field approximations.

The field and potential due to an adsorbed dipole of arbitrary orientation, with infinite dielectric-conductive imaging, have been calculated using Fourier-Bessel transforms. The corresponding effective coordination numbers for an infinite two-dimensional lattice of such dipoles have also been determined, and permit the calculation of long-range electrostatic interactions amongst adsorbed ions and dipoles without the use of dielectric continuum approximations inherent in existing treatments.